REGULATION OF CALCIUM RELEASE CHANNELS (RyR2) IN HEALTHY AND FAILING HUMAN HEARTS

Kafa Walweel
M. Sc

A thesis submitted in fulfilment
of the requirements for the degree of
Doctor of Philosophy
April 2014

School of Biomedical Sciences and Pharmacy
University of Newcastle

Statement of Originality

This thesis contains no material which has been accepted for the award of any other degree or diploma in any university or other tertiary institution and, to the best of my knowledge and belief, contains no material previously published or written by another person, except where due reference has been made in the text. I give consent to this copy of my thesis, when deposited in the University Library, being made available for loan and photocopying subject to the provisions of the Copyright Act 1968.

…….

School of Biomedical Sciences and Pharmacy
University of Newcastle

Statement of Collaboration

I hereby certify that the work embodied in this thesis has been done in collaboration with other researchers, or carried out in other institutions. I have included as part of the thesis a statement clearly outlining the extent of collaboration, with whom and under what auspices.

1) The gating parameters of RyR2 from sheep heart in Chapter 3 are given by **Dr. Derek R. Laver** (University of Newcastle, Australia).

2) The gating parameters of RyR2 from rat heart in Chapter 3 are given by **Dr. Jaio Li** (University of Newcastle, Australia).

3) **Dr. Nicole A. Beard** (The Australian National University, Australia) did the biochemical experiments in Chapter 4.

…….

School of Biomedical Sciences and Pharmacy

University of Newcastle

Statement of Authorship

I hereby certify that the work embodied in this thesis contains a published paper/s/scholarly work of which I am a joint author. I have included as part of the thesis a written statement, endorsed by my supervisor, attesting to my contribution to the joint publication/s/scholarly work.

- Hyun-Seok Hwang , Florentin R Nitu, Yi Yang, **Kafa Walweel**, Laetitia Pereira, Christopher N Johnson, Michela Faggioni, Walter J Chazin, Derek R Laver, Alfred L George, Jr., Razvan L Cornea, Donald M Bers, Björn C Knollmann (2014) "Divergent Regulation of RyR2 Calcium Release Channels by Arrhythmogenic Human Calmodulin Missense Mutants." Circ Res 114 (7): 1114-24

…….

School of Biomedical Sciences and Pharmacy

University of Newcastle

Dedication

To my parents, who always stood behind me and knew I would succeed. Who taught me invaluable lessons in life. Gone now but never forgotten. I will miss them always and love them forever. Thanks for all you did.

Acknowledgement

First and foremost, I would like to express my sincere gratitude to my primary supervisor A/Prof Derek Laver for the continuous support of my PhD study and research, for his patience, motivation, enthusiasm, and immense knowledge. He has been a tremendous mentor for me. His guidance helped me in all the time of research and writing of this thesis. The good advice and friendship of Derek has been invaluable on both an academic and a personal level, for which I am extremely grateful. I feel very grateful towards Derek, who so kindly and generously extended my scholarship in the final stages of my PhD.

I would like to express the deepest appreciation to my second supervisors Prof Dirk vanHelden and Dr Mohammad Imtiaz who gave me a lot of advice about my PhD study. I am very grateful to Dr Nicole Beard (Australian National University) particularly since she introduced me the biochemical techniques in her lab, and also contributed to the western blot experiments in this thesis. I would like to sincerely thank my colleague Dr Jiao Li who kindly introduced me the biochemical techniques and gave me a lot of advice on western blot technique. I would like also to thank Dr Rick Thorne and Dr Liz Milward who kindly provided a space in their labs for my western blot experiments. In addition, a thank you to Mr Paul Johnson for his assistance in single channel experiments.

It would not have been possible to write this doctoral thesis without the help and support of the kind people around me, to only some of whom it is possible to give particular mention here. Above all, I would like to thank my husband Mohammad for his personal support and great patience at all times. My brothers and sisters have given me their unequivocal support throughout, as always, for which my mere expression of thanks likewise does not suffice. Never forget the most important thing of all, my children who make my life even happier. I feel very fortunate to have such a lovely

family. Last, but by no means least, I thank my friends elsewhere for their support and encouragement.

List of Publications

Journal articles

- Hyun-Seok Hwang , Florentin R Nitu, Yi Yang, **Kafa Walweel**, Laetitia Pereira, Christopher N Johnson, Michela Faggioni, Walter J Chazin, Derek R Laver, Alfred L George, Jr., Razvan L Cornea, Donald M Bers, Björn C Knollmann (2014) "Divergent Regulation of RyR2 Calcium Release Channels by Arrhythmogenic Human Calmodulin Missense Mutants." Circ Res 114 (7): 1114-24

- **K. Walweel**, J. Li, P. Molenaar, M.S. Imtiaz, A. Quail, C.G. dos Remedios, N.A. Beard, A.F. Dulhunty, D.F. vanHelden, D.R. Laver (2014) "Regulation of human RyR2 by Ca^{2+} and Mg^{2+} in the cytoplasm and in the lumen of the sarcoplasmic reticulum." (J Gen Physiol 144 (3): 263-71)

- **K. Walweel**, N.A. Beard, P. Molenaar, M.S. Imtiaz, A.F. Dulhunty, D.F. vanHelden, D.R. Laver "Ryanodine channel function (RyR2) in healthy and failing human hearts." (Manuscript in preparation).

Conference oral presentations

2008 **Walweel, K.**, Flaifel, M., Abdulla, M., Khoury, F., Qunais, E., Abu Ghalyun, Y "A comparative study of the physiological, histochemical, and ultrastructural properties of the gastrocnemius muscle in two species of frogs: Rana bedriagae and Bufo viridis." Middle Eastern Biodiversity Congress Aqaba-Jordan, 20-23 October 2008

2012 Received an invitation to give a presentation at Gordon conference (Oral presentation by D.R. Laver). **K. Walweel**, N. Beard, D.F. vanHelden, M. Imtiaz, P. Molenaar, Angela Dulhunty and D.R. Laver "Regulation of RyR2 from failing and non-failing human heart." 3-9 June 2012 in Switzerland.

2012 **K. Walweel**, J. Li, N. Beard, D.F. vanHelden, M. Imtiaz, P. Molenaar, and D.R. Laver "Regulation of human RyR2 by intracellular Ca^{2+} and Mg^{2+}." Abstract selected for oral presentation on the 2nd Dec at the AuPS meeting in Sydney.

Conference poster presentations

2010 **K. Walweel**, D.F. vanHelden, and D. R. Laver "Role of Phosphorylation in the Ca^{2+} Regulation of Ca^{2+} Release Channels in Skeletal Muscle." Abstract selected for Poster presentation on the 29th Nov at the AuPS/ASB meeting in Adelaide.

2011 **K. Walweel**, J. Li, D.F. vanHelden, M. Imtiaz, P. Molenaar and D.R. Laver "Regulation of RyRs by intracellular Ca^{2+} and Mg^{2+} compared in sheep, rat, and human heart." Abstract selected for Poster presentation on the 3rd Dec at the AuPS meeting in Perth.

2012 **K. Walweel**, N. Beard, D.F. vanHelden, M. Imtiaz, P. Molenaar, and D.R. Laver "Regulation of RYR2 from failing and non-failing human heart by intracellulCa^{2+} and Mg^{2+}." Abstract selected for Poster presentation at Gordon conference (3-9 June) in Switzerland.

2013 **K. Walweel**, N. Beard, D.F. vanHelden, M. Imtiaz, P. Molenaar, and D.R. Laver "Regulation RyR2 macromolecular complex in failing and healthy human hearts." Abstract selected for Poster presentation at ISHR World Congress conference (30th of June to the 4th of July) in San Diego, USA.

2013 **K. Walweel**, N. Beard, D.F. vanHelden, M. Imtiaz, P. Molenaar, and D.R. Laver **"**Inhibition of RyR2 from failing and non-failing human hearts by calmodulin." Abstract selected for Poster presentation on the 8rd Dec at the AuPS meeting in Geelong.

Abbreviations

βAR	β-adrenergic receptors
ADP	adenosine diphosphate
apoCaM	apocalmodulin
AMP	adenosine monophosphate
AMP-PCP	5'-adenylyl (beta, gamma-methylene) diphosphonate
AVN	atrioventricular node
BAPTA	1, 2-bis [o-aminophenoxy] ethane-*N*, *N*, *N*', *N*'- tetraacetic acid
CaCaM	Ca^{2+}/calmodulin
CaM	calmodulin
CaMKII	Ca^{2+}/calmodulin dependent protein kinase II
CFTR	cystic fibrosis transmembrane conductance regulator
CICR	calcium-induced calcium release
CPVT	Catecholaminergic Polymorphic Ventricular Tachycardia
CSQ2	calsequestrin
CsMS	cesium methanesulfonate
DHPR	dihydropyridine channel
DR	divergent region
DTT	dithiothreitol
EDMD	Emery Dreifuss muscular dystrophy
FKBP	FK506-binding proteins
FRET	fluorescence-resonance-energy-transfer
fSR	free SR
H-89	PKA inhibitor
HF	heart failure
HRP	horseradish peroxidase
$I_{Ca,L}$	L-type Ca^{2+} current (long-lasting)
$I_{Ca,T}$	T-type Ca^{2+} current (transient)
ICM	Ischaemic cardiomyopathy
I_f	funny current

I_k	outward current
I_{Na}	inward current
JN	junctin
jSR	junctional SR
KN-93	CaMKII inhibitor
LQT	long QT
LTCC	L-type Ca^{2+} channel
mM	millimolar (mmol/l)
ms	millisecond
NaF	sodium fluoride
NaN_3	sodium azide
NCX	Na^+/ Ca^{2+} exchanger
nM	nanomolar (nmol/l)
PBS	phosphate buffered saline
PC	phosphatidylcholine
PDE4D3	type 4 phosphodiesterase
PE	phosphatidylethanolamine
PKA	cyclic AMP-dependent protein kinase
PKC	protein kinase C
PKG	cyclic GMP-dependent protein kinase
PKI	protein kinase inhibitor
PLB	phospholamban
pM	picomolar
PMSF	phenylmethanesulfonyl fluoride
PP1	protein phosphatase 1
PP2A	protein phosphatase 2A
pS	picosiemens
ROS	reactive oxygen species
RyR	ryanodine receptor
s	second
s^{-1}	1/second
SAN	sinoatrial node

SERCA2a	sarcoplasmic/endoplasmic reticulum Ca^{2+}-ATPase
SR	sarcoplasmic reticulum
TES	N-tris [Hydroxymethyl] methyl-2-aminoethanesulfonic acid
TRD	triadin
w/v	weight/volume
w/w	weight/ weight
$\Delta[Ca^{2+}]_I$	Ca^{2+} transient
µl	microliter
µM	micromolar (µmol/l)

Contents

Chapter 1- General introduction

1.1 Introduction 1

1.2 Electrophysiology of the heart 1

1.3 Cardiomyocyte organelles involved in excitation contraction coupling (ECC) 6

1.3.1 Cardiac sarcolemmal channels, pumps and exchangers 6

1.3.2 The dyad junctions 8

1.4 Structure of RyR2 macromolecular complex 9

1.4.1 Structure and Isoforms 9

1.4.2 Interdomain interactions 9

1.4.3 Regulatory proteins 13

1.4.3.1 FK506 binding proteins (Calstabins) 13

1.4.3.2 Luminal proteins, Calsequestrin, Junctin and Triadin 13

1.4.3.3 Calmodulin 15

1.4.3.4 Kinases and phosphatases 16

1.5 Calcium handling in cardiac myocytes during excitation-contraction coupling 18

1.6 Ca^{2+} leak, sparks and waves 21

1.7 Adrenergic stimulation of ECC- signalling pathway (Fight or Flight response) 22

1.8 Modulation (regulation) of Ca^{2+} release channels by intracellular Ca^{2+}, Mg^{2+} and adenine nucleotides 26

1.9 Models of HF 30

1.10 Structural remodelling of dyad junctions in HF 31

1.11 Ca^{2+} handling alteration in HF 31

1.12 Molecular mechanisms of RyR2 dysfunction in HF 32

1.12.1 RyR2 hyperphosphorylation 33

1.12.2 The role of FKBP12.6 (Calstabin) loss in RyR2 dysfunction 37

1.12.3 RyR2 oxidation, phosphorylation, FKBP12.6 loss and domain unzipping in HF 39

1.12.4 Intracellular Mg^{2+} deficiency 40

1.12.5 Increased RyR2 sensitivity to luminal Ca^{2+} 41

1.13 Therapeutic strategies that target RyR2 dysfunction in HF 42

1.13.1 β-blockers 42

1.13.2 Free radical scavengers 43

1.13.3 JTV19 as a RyR2 stabilizer 43

1.13.4 Flecainide 44

1.14 Aims and Hypothesis 44

1.14.1 Hypothesis: 44

1.14.2 Aims 45

The first specific aim 45

The third specific aim 45

The fourth specific aim 45

Chapter 2- Methods

2.1 Source of heart tissue 46

2.2 Preparation of SR Vesicles 48

2.3 Single channel recording 48

2.3.1 Planar lipid bilayer 48

2.3.1.1 Membrane formation and vesicle fusion 50

2.3.1.2 Amplification and filtering 52

2.3.1.3 Bathing solutions 53

2.3.2 Chemicals and solutions 53

2.3.2.1 Calibration of Ca^{2+} electrode 55

2.3.3 Advanced perfusion methods 57

2.4 Biochemical assays 57

2.4.1 Materials 57

2.4.2 Antibodies 59

2.4.3 SDS PAGE 59

2.4.4 Western blot and immunoprobing 60

2.4.4.1 Western blot 60

2.4.4.2 Immunoprobing 60

2.4.4.3 Determining total protein 61

2.4.4.4 Reprobing PVDF membranes 61

2.4.5 Co-immunoprecipitation 62

2.4.6 In-vitro phosphorylation and dephosphorylation assays 63

2.5 Data analysis 64

2.5.1 Analysis of ion channel recordings 64

2.5.2 Statistics 65

Chapter 3- Regulation of human RyR2 by Ca^{2+} and Mg^{2+} in the cytoplasm and in the lumen of the sarcoplasmic reticulum

3.1 Introduction 68

3.2 Materials and Methods 71

3.2.1 Heart tissue & single-channel measurements 71

3.2.2 Statistics 71

3.3 RESULTS 72

3.3.1 Cytoplasmic Ca^{2+} regulation 72

3.3.2 Luminal Ca^{2+} regulation 77

3.3.3 Cytoplasmic Mg^{2+} regulation 80

3.3.4 Luminal Mg^{2+} regulation 80

3.3.5 Ca^{2+}/Mg^{2+} regulation among species 85

3.3.6 Ca^{2+} activation in the presence of [Mg^{2+}] 89

3.4 Discussion 92

3.4.1 Mechanisms for Ca^{2+} and Mg^{2+} regulation of RyR2 92

3.4.2 The importance of luminal Mg^{2+} 95

3.4.3 Role of RyR2 regulation in the Calcium Release Units (CRUs) 95

Chapter 4- Ryanodine channel function (RyR2) in healthy and failing human hearts

4.1 Introduction 98

4.2 Materials and Methods 102

4.2.1 *Human heart tissue & single-channel measurements* 102

4.2.2 Statistics 102

4.3 Results 103

4.3.1 RyR2 regulation by intracellular Ca^{2+} 103

4.3.2 RyR2 regulation by intracellular Mg^{2+} 111

4.3.3 Protein expression levels 116

4.3.4 RyR2 phosphorylation 119

4.3.5 FKBP, PP1 and PP2A 123

4.4 Discussion 127

4.4.1 RyR2 complex remodelling in HF 128

4.4.2 Mechanisms for RyR2 variability 130

4.4.3 Ca^{2+}/ Mg^{2+} regulation of RyR2 from failing hearts 131

Chapter 5- Inhibition of RYR2 from healthy and failing human hearts by calmodulin (CaM)

5.1 Introduction 134

5.2 Materials and methods 137

5.2.1 Human heart tissue & single-channel measurements 137

5.2.2 In-vitro Phosphorylation of the RyR2 channel 137

5.3 Results 138

5.3.1 CaM inhibits RyR2s from failing human heart 138

5.3.2 CaM had no effect on RyR2s from healthy human heart 143

5.3.3 CaM inhibition of human RyR2 is potentiated by phosphorylation 145

5.4 Discussion 149

Chapter 6-General Discussion

6.1 Key findings and hypothesis 151

6.1.1 Relevance of animal RyRs to human RyRs. 151

6.1.2 Are animal heart models good for failing human heart? 154

6.1.3 Do different forms of HF exhibit variations in RyR2 remodelling? 155

6.1.4 Has RyR2 from CF heart undergone remodelling? 156

6.2 Future directions 156

6.2.1 Test the hypothesis that regulation of RyR2 by CaM is potentiated by adrenergic stimulation or RyR2 remodeling in HF. 156

6.2.2 Role of FKBP12.6 in HF. 158

Abstract

Heart failure (HF) is a complex disorder that involves changes in Ca^{2+} handling protein expression, Ca^{2+} homeostasis and tissue remodelling. A general feature of heart dysfunction associated with HF is aberrant Ca^{2+} flux across the sarcolemma and the sarcoplasmic reticulum (SR) of cardiac cells. The Ca^{2+} release channel (RyR2) activates and modulates heart function by controlling the Ca^{2+} release from the SR. The RyR2 forms a complex with many accessory proteins that regulate channel activity. The regulation of the RyR2 from human heart by intracellular Ca^{2+} and Mg^{2+} is still poorly defined. In this study single channel recordings of RyR2s were used to compare Ca^{2+} and Mg^{2+} regulation of RyR2s from patients with healthy, cystic fibrosis (CF) and failing hearts, specifically, Ischaemic cardiomyopathy (ICM) and Emery Dreifuss muscular dystrophy (EDMD, a rare inherited disorder that affects skeletal and cardiac muscle). We also compared these functional changes with remodelling of the macromolecular structural properties using Western blot.

RyR2s from healthy human hearts (n=4) were incorporated into lipid bilayers and the channel gating was measured at diastolic [Ca^{2+}]. Under these conditions, at least 90% of the channels had open probabilities (P_o) that comprised a normal distribution on a logarithmic scale with a mean P_o= 0.02 and a standard deviation of 6.3 fold. Grouping the data according to the four donor hearts revealed no significant difference between these groups in the Ca^{2+} and Mg^{2+} regulation of RyRs. Initially, a CF heart was the only source of non-failing samples. However, as the study progressed and hearts became available from healthy donors, it became clear that RyR2 from the CF heart differed from those obtained from four healthy hearts and these are now reported as a separate group.

This thesis is the first to report on the regulation by Ca^{2+} and Mg^{2+} of native RyR2 receptor activity from healthy human hearts. Human RyR2s displayed cytoplasmic Ca^{2+} activation (K_a = 6 μM) and inhibition by cytoplasmic Mg^{2+} (K_i = 10 μM at 100 nM cytoplasmic Ca^{2+}). The K_a for luminal Ca^{2+} activation was 35 μM and the K_i for luminal

Mg^{2+} inhibition was 550 μM (cytoplasmic [Ca^{2+}] = 100 nM). Modulation of RyR2 gating by luminal Ca^{2+} and Mg^{2+} only occurred when the cytoplasmic [Ca^{2+}] was less than 1 μM. In this range, luminal and cytoplasmic Ca^{2+}have a synergistic action on the RyR2 opening rate where cytoplasmic Ca^{2+} increased the luminal Ca^{2+} response. The activation response of RyR2 to luminal and cytoplasmic Ca^{2+} was strongly dependent on the Mg^{2+} concentration. Addition of physiological levels (1 mM) of Mg^{2+} raised the K_a for cytoplasmic Ca^{2+} to 25 μM and raised the K_a for luminal Ca^{2+} from below 60 μM to ~1 mM.

Single channel studies showed that RyRs from CF and failing human hearts exhibited higher activity (4-fold for CF, 5-fold for ICM, 13-fold for EDMD, and 35-fold for ICM trabecule) where cytoplasmic solutions contained diastolic concentrations of Ca^{2+} (100 nM Ca^{2+}) and 2 mM ATP and luminal solutions contained 0.1 mM Ca^{2+}, at -40mV. At high cytoplasmic Ca^{2+} concentrations (systolic [Ca^{2+}], 10-100 μM), RyR2s from healthy and failing human hearts showed similar channel activity. RyR2s from CF hearts showed similar inhibition by intracellular Mg^{2+} to healthy hearts, whereas RyR2s from failing hearts exhibited less sensitivity (10-1000 fold attenuation) to intracellular Mg^{2+} inhibition. The attenuation of Mg^{2+} inhibition and increased RyR2 activity at low [Ca^{2+}] would cause these channels to leak Ca^{2+} from the SR during diastole.

The distribution of RyR2 activity from CF, EDMD and ICM hearts compared to healthy heart was also examined. RyR2s from healthy heart showed a large variation in open probability, ranging from 0.001 up to 0.75. RyR2s from CF heart showed a similar range of open probability values but the distribution was skewed to higher open probability in CF hearts. This preliminary finding suggests that pulmonary stress associated with cystic fibrosis induces a form of HF in this group that has not previously been identified. However, RyR2s from failing hearts showed greater scatter than those from healthy hearts. Distributions of the opening rate from failing hearts showed two groups of activity. One group (low activity group consisting of 85% of RyR2 in ICM hearts and 50% of RyR2 in EDMD hearts and none from ICM trabecule) had a similar distribution to healthy hearts whilst the other high activity group, exhibited more than a 10-fold higher mean value. These differences in the proportion of high activity RyR2s compared

to those from healthy hearts suggest that a sub population of RyR2 are altered during HF.

Western Blots of RyR2s showed higher phosphorylation at PS2808 and PS2814 in both ICM and EDMD hearts. They also exhibited decreased expression levels of RyR2s and dephosphorylating enzymes, PP1 and PP2A. SERCA2a was decreased in ICM heart. CSQ2 and triadin-1 were reduced in EDMD heart. Finally, both FKBP12 and FKBP12.6 were found to be dissociated from RyR2s in failing hearts. These findings indicate that RyR2 remodelling in HF may have a role in RyR2 hyperactivity at diastolic [Ca^{2+}] and reduced sensitivity to intracellular Mg^{2+} inhibition. It has been shown that calmodulin (CaM) binds to healthy human RyR2 with high affinity, while in HF RyR2 shows decreased CaM affinity. Binding of CaM to RyR2s from mice cardiomyocytes inhibits SR Ca^{2+} release. However, no one has examined the effect of CaM on the gating of human RyR2s and how it may be affected by RyR2 remodeling in failing hearts. Importantly, this study showed that the regulatory action of CaM depends on whether RyR2s were obtained from healthy or failing hearts. Addition of CaM (0.5 μM) to the cytoplasmic bath caused a reduction (~ 35%) in the open probability of RyR2s from failing hearts. Surprisingly, RyR2s from healthy human heart were not affected by CaM addition which was also different to what is seen in commonly used animal models for RyR2 function in HF, dog and sheep. These findings suggest that animals may not provide accurate models for the RyR2 function in humans. These data also indicate that the effect of CaM binding to RyR2s depended on the phosphorylation state of the RyR2, which is different in healthy and failing hearts.

Regulation by intracellular Ca^{2+} and Mg^{2+} from human RyR2s was also compared to that seen in two commonly used animal models for RyR function, rat and sheep. Human RyR2s displayed the same regulation by cytoplasmic Ca^{2+}/ Mg^{2+} as seen in rat and sheep. However, RyR2 sensitivity to luminal Ca^{2+} and Mg^{2+} varied between species. The K_a's for luminal Ca^{2+} activation were 35 μM for human, 60 μM for sheep and 10 μM for rat whilst peak activation for human RyR2s and sheep were similar but 10-fold higher than rat RyR2s. Furthermore, human RyR2s were 10-fold less sensitive to luminal Mg^{2+} than RyR2s from rat and sheep. Together with CaM results, these

differences highlighted the importance of using RyR2s from healthy human tissues in lieu of using animal models to understand how RyR2 function is altered in HF.

Chapter 1- General introduction

1.1 Introduction

Cardiac disease is the leading cause of death in Australia with over 50,000 deaths annually, heart failure (HF) being the most prominent (Tomaselli and Zipes 2004). HF is a complex disorder that involves changes in expression of Ca^{2+} handling proteins, Ca^{2+} dynamics and tissue remodelling (George 2008). HF development involves reduction in cardiac output and increase in sympathetic nervous system activity via beta-adrenergic receptors (β-AR) which increase heart rate and cardiac contractility, thereby compensating for decreased blood pumping. Patients with HF die because of contraction failure or arrhythmia (Mozaffarian, Anker et al. 2007). A recent study on the mode of death proposed that death from arrhythmias is more likely to occur during early stage HF, whereas death is more likely to occur from contraction failure at a later stage (Mozaffarian, Anker et al. 2007). The cardiac Ca^{2+} release channel for the intracellular Ca^{2+} stores (the ryanodine receptor RyR2) has a key role in excitation-contraction coupling in the heart. The RyR2 activates and modulates heart function by controlling the Ca^{2+} release from the sarcoplasmic reticulum (SR). Abnormal regulation of RyR2s observed in failing heart may increase the propensity for sudden death and impair contractility (Marks 2001; Wehrens, Lehnart et al. 2003).

1.2 Electrophysiology of the heart

The heart is largely composed of muscle tissue. A network of conducting fibers extends from the Sinoatrial (SA) node, (located at the junction of the superior vena cava and right atrium) (Chandler, Aslanidi et al. 2011), through to the atrium to the atrioventricular (AV) node located in the septal component of the atrioventricular junction and extending onward through the bundle of His into the left and right bundle branches of the ventricles (Greener, Monfredi et al. 2011). The SA node is the pacemaker in the sinus node that generates the cardio-electrical signal that is responsible for each heart beat. The impulse that is generated from the pacemaker spreads through the atria causing them to contract then passes to the AV node. The AV node in turn sends the signal through the right and left bundle branches to the ventricles to initiate

similar periodic contractions of the ventricles (Brown, Kozlowski et al. 1997). (See Figure 1.1)

The action potential waveform varies throughout the heart due to regional variations in expression of ion channels and transporters. The cardiac action potential can be monitored by measuring the changes in voltage on the body surface and recorded as an electrocardiogram. In an electrocardiographic impulse the first small hump is known as the P wave which occurs when the atria depolarize. The next three waves constitute the QRS complex which represents the depolarization of the ventricles (see Figure 1.2).

The ventricular action potential is divided into five phases (Figure 1.2A): Phase 0 represents the initial depolarization phase due to sodium influx through voltage-activated sodium channels and the generation of an inward current (I_{Na}). Phase 1 is caused by the opening of outward potassium channels (outward potassium current), termed initial repolarisation, which influences the height and duration of the action potential plateau. Phase 2, due to slow calcium influx via L-type voltage-gated Ca^{2+}channels, leads to a delay in initial repolarisation (plateau) resulting in cardiac muscle contraction (systole). Phase 3 represents repolarisation due to the outflow of potassium ions thus giving rise to a corresponding current (I_k). Fast potassium efflux contributes to cardiac muscle relaxation. In Phase 4, I_k persists and causes the membrane potential to overshoot the resting membrane potential (after-hyperpolarization) and during this phase the membrane is refractory. Thus the myocytes do not respond to the next electrical impulse until phase 0 of the next cycle. Phases 0 and 4 are associated with diastole while phases 1-3 are associated with systole.

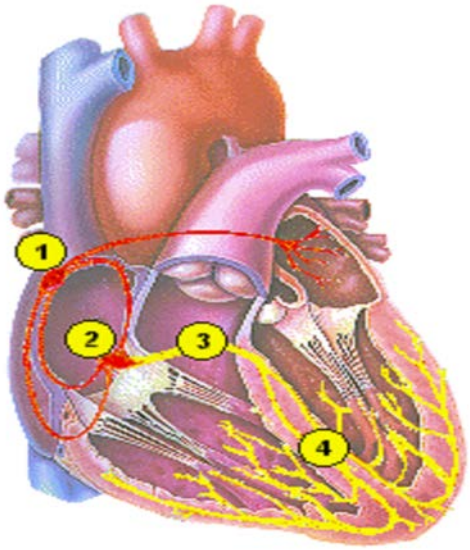

Figure 1.1: Heart conducting fibers

1. Sinoatrial node (SA node)
2. Atrioventricular node (AV node)
3. Common AV bundle
4. Right & Left bundle

A

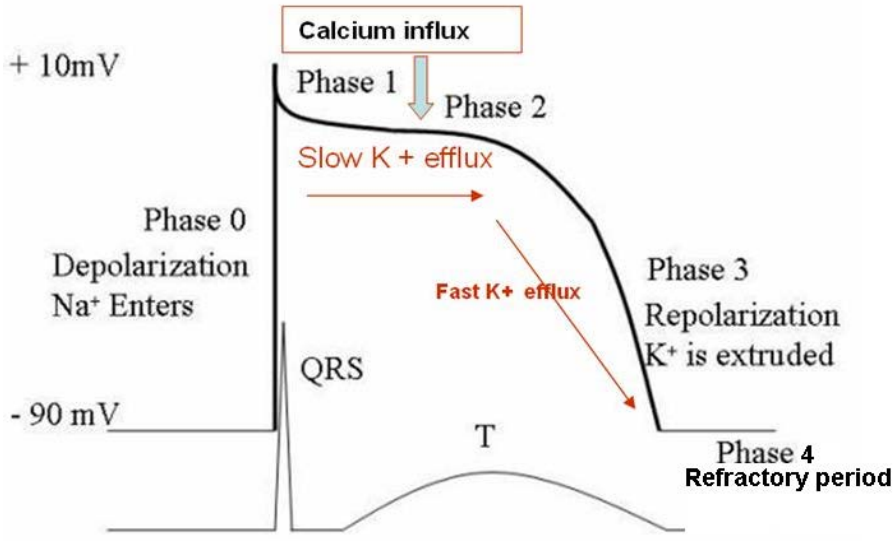

B

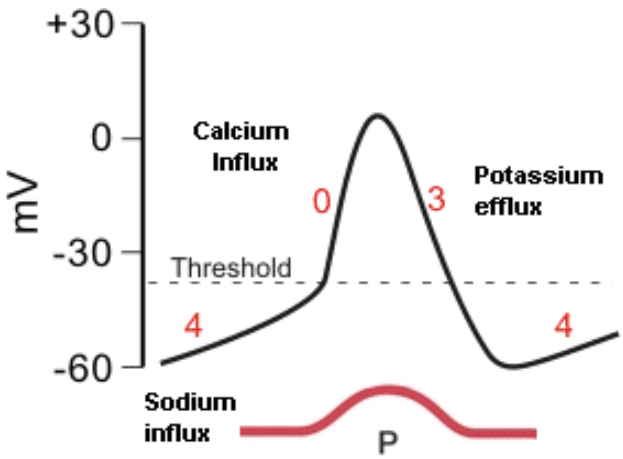

Figure 1.2: Cardiac action potential. A: Ventricular action potential (modified from www.drsvenkatesan.com). B: Sinoatrial node action potential (modified from www.cram.com).

The sinoatrial action potential is divided into three phases (Figure 1.2B): Phase 0 is due to Ca^{2+} influx (inward calcium current) which causes further depolarization. Phase 3 is repolarisation due to K^+ efflux and the generation of an outward current (I_k). Phase 4 represents sodium uptake (depolarization) via slow inward sodium currents called the funny current (I_f). The sinoatrial node lacks phases 1 and 2 (DiFrancesco 1993). The action potential of the SA node is spontaneously active and acts as the pacemaker for the heart where the AP frequency depends on the duration of phase 4. During phase 4, the net inward Na^+ current (pacemaking current) leads to continued depolarisation of the cell membrane that eventually triggers the rapid upstroke in the AP during phase 0.

In spontaneously active cardiac regions such as the sinoatrial node, the inward sodium current (I_f) is present and, together with the NCX current (see below), is responsible for the pacemaking current (Sanders, Rakovic et al. 2006; Barbuti and DiFrancesco 2008). A small amount of calcium (long-lasting ($I_{Ca,L}$)) enters through the L-type channel (LTCC) or dihydropyridine receptor (DHPR) during the plateau phase of the heart action potential. This triggers a large-scale Ca^{2+} release from the SR via ryanodine receptors in a process called calcium induced calcium release (CICR). Another voltage-dependant calcium channel involved in the flow of calcium from outside of the cell into the cytoplasm is called the transient voltage-gated calcium channel (T-type current ($I_{Ca,T}$)). In the SA node of the heart the T-type calcium channel contributes to the pacemaking (Barbuti and DiFrancesco 2008).

In ventricular myocytes, initiation and propagation of the action potential is due to the opening of voltage-gated sodium channels. In contrast to the SAN, the total amount of Ca^{2+} flux via $I_{Ca,T}$ channels is small compared to that via $I_{Ca,L}$ channels. Voltage-gated potassium channels and inward rectifier potassium channels are both located in the surface membrane of the myocytes (Barbuti and DiFrancesco 2008). Voltage-gated potassium channels have an important role in repolarisation and regulation of the duration of the action potential, whilst the inward rectifier potassium channels set the resting membrane potential by passing positive current in an inward direction (Gehrmann and Berul 2000) (Figure 1.3).

1.3 Cardiomyocyte organelles involved in excitation contraction coupling (ECC)

Cardiac ECC refers to a series of events that link the cardiac action potential (cardiac excitation) of the sarcolemma (cardiomyocyte membrane) to muscular contraction (see section 1.8).

The pumping function of the heart depends on the cardiac cell contraction and the fundamental contractile unit for contraction within the myocyte is the sarcomere. The synchronized contraction of the myocytes is a consequence of electrical signals passing from cell to cell via specialized intercellular junctions called gap junctions. Cardiac myocytes have specialized organelles such as the SR that stores and releases the Ca^{2+} and transverse tubules (sarcolemmal invaginations called t-tubules) which help in moving the action potential into the interior of the cell to ensure rapid and synchronous contraction of the cell and hence of the heart. The sarcolemma has a large number of channels, pumps and exchangers necessary for normal cardiac function (Walker and Spinale 1999).

1.3.1 Cardiac sarcolemmal channels, pumps and exchangers

Orchestration of cardiac channels, pumps and exchangers has a key role in action potential generation and maintenance of proper timing of diastole and systole.

During diastole, the low levels of cytoplasmic Ca^{2+} are maintained by transport of Ca^{2+} out of the cytoplasm. Ca^{2+} extrusion into the extracellular fluid is done mainly by the sarcolemmal sodium/calcium exchanger (NCX) in which three Na^{+} ions are exchanged for one Ca^{2+} ion in a process not requiring ATP (Zhou and Lipsius 1993) and also by the Ca^{2+} ATPase (Bers 2002; Lehnart, Wehrens et al. 2004; Wehrens, Lehnart et al. 2005; Bers 2006). Ca^{2+} is also sequestered into the SR by the SR, ATP driven Ca^{2+} pump (SERCA2a).

The sarcolemmal Na^+/H^+ exchanger is involved in controlling intracellular pH and maintaining intracellular pH at 7.3 which is necessary for cellular processes and binding of calcium to myofibril (Laver, Roden et al. 1995). Removing of Na^+ from the intracellular space is achieved by a sodium/potassium pump in a process requiring energy in the form of ATP.

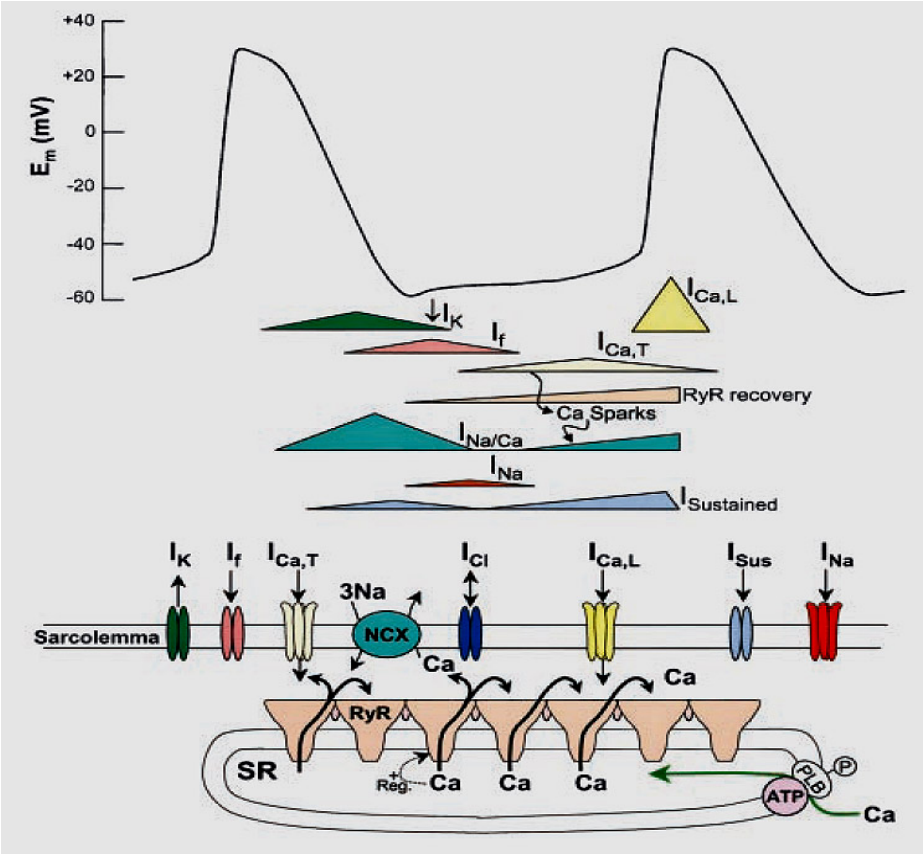

Figure 1.3: The pacemaker AP in the SA node and the timing of the currents that contribute to it. (the magnitude of the ionic currents are indicated by triangular shapes, (Bers 2002)).

1.3.2 The dyad junctions

The dyad is the synapse between the t-tubule and the sarcoplasmic reticulum. The t-tubule is approximately 125 nm in diameter (McGrath, Yuki et al. 2009) and is separated from the SR by a gap of 15 nm (dyad cleft) (Radermacher, Rao et al. 1994). Junctophilin-2 (JPH2) is an essential component of the dyadic cleft that spans the cleft from the plasma membrane (PM) to the SR and plays a key role in the development and maintenance of that space (Takeshima, Komazaki et al. 2000; Nishi, Sakagami et al. 2003). The SR, a highly specialized form of endoplasmic reticulum, is an internal membrane system in muscle. It is an extensive network of interconnected cisternae and tubules located in the cytoplasm (Franzini-Armstrong and Protasi 1997). Two distinct regions in the SR have been recognized: the junctional SR (jSR), which directly faces the t-tubules, and the free SR (fSR) which faces the myofibrils. The junctional SR in rabbit ventricular myocytes forms extended flattened cisternae (~26 nm thick with an average diameter about 592 nm) that surrounds the t-tubule at the dyad (Brochet, Yang et al. 2005). EM micrographs show that the jSR contains an electron dense material, which is formed by calsequestrin (Ca^{2+} binding protein). Each jSR cisternae carries a number of RyRs particles, depending on species, that permit flux of Ca^{2+} from the lumen of the jSR into the dyad cleft. Ca^{2+} uptake into the SR is mediated by the Ca^{2+} ATPase molecules (SERCA2a) located throughout the junctional and free SR (Tijskens, Jones et al. 2003).

The Ca^{2+} stored in and released from the SR plays a key role in cardiac rhythm contractility. The total amount of calcium stored in the SR has been estimated to be in the range of 1.5–3 mmol/l of SR volume (Bers 2001). Most of the Ca^{2+} in the SR (50 to 90%) is bound to Ca^{2+} buffering proteins such as calsequestrin (CASQ) (Shannon and Bers 1997; Shannon, Ginsburg et al. 2000) which substantially increases the Ca^{2+} storage capacity of the SR (Knollmann, Chopra et al. 2006). Measurements using Ca^{2+} dyes estimate the free $[Ca^{2+}]$ in the SR ($[Ca^{2+}]_{SR}$) to be about 1 to 1.5 mM during diastole and ~0.3 mM during systole (Shannon, Guo et al. 2003).

1.4 Structure of RyR2 macromolecular complex

1.4.1 Structure and Isoforms

There are three RyR isoforms found in mammals. RyR1 is predominant in skeletal muscle (Marks, Tempst et al. 1989) and RyR2 is predominant in cardiac muscle (Nakai, Imagawa et al. 1990). RyR3 was first cloned from rabbit brain but is expressed along with either RyR1 or RyR2 in many organs (Hakamata, Nakai et al. 1992). The N-terminal of the ryanodine channel, comprising about 80% of the RyR polypeptide chain, forms a bulky cytoplasmic domain that acts as a scaffold and largely modulates the channel function (Marks, Marx et al. 2002). This cytoplasmic domain was originally recognized as the "foot" structure in electron micrographs (Franzini-Armstrong and Jorgensen 1994). The remaining 20% of the RyR polypeptide chain (C-terminal region) forms the transmembrane channel pore regions. Most of the differences in amino acid composition between RyR isoforms are concentrated in three regions called the divergent region (DR), DR1, DR2 and DR3 (Sorrentino and Volpe 1993) (Figure 1.4).

RyR2 is a macromolecular complex consisting of four monomers (MW 565 kDa per monomer), each of which is associated with regulatory polypeptides that regulate the channel function. These peptides include: the channel-stabilizing subunit called FKBP12.6 (calstabin2), protein kinases (PKA and CaMKII), protein phosphatases (PP1 and PP2a) (Marx, Gaburjakova et al. 2001), and a cAMP-specific type 4 phosphodiesterase (PDE4D3). These peptides bind to each ryanodine channel monomer via specific anchoring proteins shown in Figure 1.5A (Mohler and Wehrens 2007). On the luminal side, the RyR2 is associated with Ca^{2+} buffering proteins such as calsequestrin (CSQ2), and the transmembrane proteins triadin (TRD) and junctin (JN) which mediate RyR2 interactions with CSQ2.

1.4.2 Interdomain interactions

Mutations of the N-terminal and central domain of RyRs exhibit the same type of functional modification (channel dysfunction) which makes the channel hyperactive and very sensitive to agonists (ligands). Based on these observations, Ikemoto and Yamamoto (Ikemoto and Yamamoto 2002) introduced the interdomain interaction

concept which proposed that the N-terminal (residues 590-639) and the central domain (residues 2460-2495) of RyR2 interact with each other (zipped state) to stabilize the channel in the closed state. Defects in these interactions (unzipping) either by mutation, as in Catecholaminergic Polymorphic Ventricular Tachycardia (CPVT), or by use of synthetic domain peptides such as DPc10 (binding to the Gly2459-Pro2494 region of the human RyR2 zipper domain), activate the ryanodine channels, especially at a low calcium concentration.

Addition of DPc10 to ryanodine channels was found to induce the unzipped state as evidenced by fluorescently labelled SR (methylcoumarin acetate (MCA)) and DPc10 (Oda, Yano et al. 2005). A recent study confirmed and extended those of previous studies suggesting that the proposed interactions between the NH2-terminal and central regions of RyR2 are likely to take place between domains 5 and 6 (Figure 1.5B) (Wang, Chen et al. 2007).Weakening of the interdomain interaction would lead to destabilization of the channel and increase of the open probability during diastole (Uchinoumi, Yano et al. ; Yamamoto, El-Hayek et al. 2000; Lehnart, Wehrens et al. 2005; Oda, Yano et al. 2005; Yano, Okuda et al. 2005; Yano 2008; Kobayashi, Yano et al. 2009). It has been proposed that destabilization of the zipped state of the interacting domains (5 and 6) may be a key mechanism for the development of heart disease including HF (Uchinoumi, Yano et al. ; Wang, Chen et al. 2007).

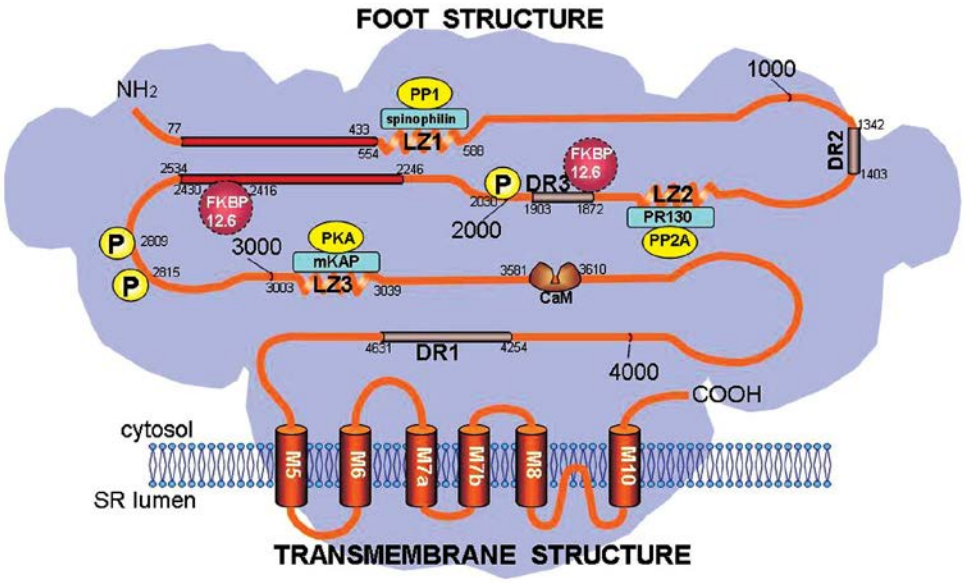

Figure 1.4: The RyR2 cytoplasmic domain known as the foot structure (Yano 2008).

A **B**

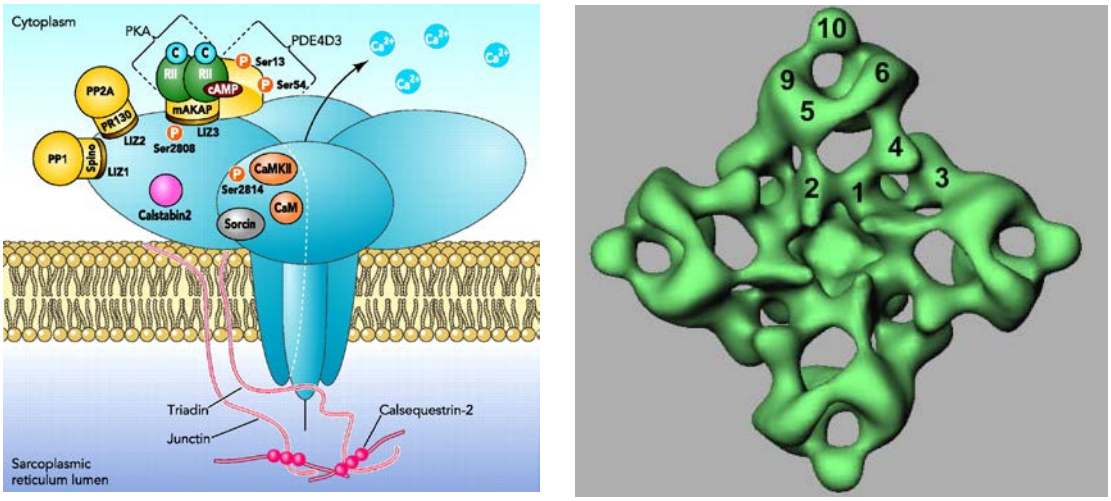

Figure 1.5: **A**: Schematic illustration of the RyR2 macromolecular complex: Calmodulin (CaM), FKBP12.6 (Calstabin2), protein kinases (PKA and CaMKII), phosphatases (PP1 and PP2A), and phosphodiesterase 4D3 (PDE4D3) bind to the cytoplasmic region of the RyR. Both junctin and triadin, which anchor calsequestrin to the RyR depending on the SR Ca^{2+} concentration, bind to the intraluminal portion of RyR2 (Mohler and Wehrens 2007). **B**: three-dimensional reconstruction of RyR2 (Yano 2008).

1.4.3 Regulatory proteins

1.4.3.1 FK506 binding proteins (Calstabins)

FK506 binding protein (FKBP) or FK506-binding immunophilin protein (Brilliantes, Ondrias et al. 1994) exists in two isoforms with molecular weights of 12.0 kDa and 12.6 kDa, respectively. FKBP12.6 has approximately 85% sequence homology with FKBP12 (Sewell, Lam et al. 1994). They bind tightly to the cytoplasmic domain of the RyR at amino acids 2416-2430 (Bers 2004). The stoichiometry of binding is one FKBP per RyR subunit (4 FKBP molecules per RyR tetramer) (Marks 1997). In cardiac muscle FKBP12 and FKBP12.6 are both present (Jayaraman, Brillantes et al. 1992; Timerman, Ogunbumni et al. 1993; Timerman, Onoue et al. 1996). In most species, including human, the amount of FKBP12 expressed in cardiomyocytes is 10 times higher than that of FKBP12.6 (Bers 2004). However, FKBP12.6 is preferentially associated with RyR2 due to its higher affinity (Timerman, Onoue et al. 1996). FK506 or rapamycin (immunosuppressant) has been shown to dissociate FKBP12.6 from RyRs. Loss of FKBP12.6 from RyRs by the addition of FK506 or rapamycin leads to increased channel activity (Ma, Bhat et al. 1995).

1.4.3.2 Luminal proteins, Calsequestrin, Junctin and Triadin

CSQ2 is an intra-SR Ca^{2+}-binding protein localized at the junctional membrane of the SR (Jorgensen and Campbell 1984). Cardiac CSQ2 is highly acidic with more than 37% (119 residues) of the total amino acids composed of Asp and Glu. Each CSQ2 molecule can bind to ~20 Ca^{2+} ions (Mitchell, Simmerman et al. 1988) with low affinity (Beard, Laver et al. 2004; Gyorke and Terentyev 2008). When Ca^{2+} binds to CSQ2, the shape of the CSQ2 molecule changes (Park, Park et al. 2004). Cardiac CSQ2 is found in a soluble form (monomer) at low Ca^{2+} concentrations, however increasing the Ca^{2+} concentration causes the CSQ2 protein to polymerize and precipitate. CSQ2 polymerization involves both front-to-front and back-to-back contacts via the N- and C-terminal regions of the protein (Wang, Trumble et al. 1998; Park, Park et al. 2004). Under such conditions, two thirds of the total bound Ca^{2+} associated with Ca^{2+}-CSQ2 aggregates, whilst one third is associated with the soluble form of CSQ2 (Tanaka, Ozawa et al. 1986; Park, Park et al. 2004).

Calsequestrin has functions as both a Ca^{2+} buffer/storage site and as a RyR2 modulator. It has been shown that CSQ2 can regulate RyR2 activity directly via protein-protein interactions involving triadin and junctin. CSQ2 controls the RyR2 open probability in a luminal Ca^{2+} -dependent manner and it has been argued that this may serve as a luminal Ca^{2+} sensor (Gyorke, Hester et al. 2004; Terentyev, Viatchenko-Karpinski et al. 2007). Data from mice with gene-targeted knock-out (ablation of CSQ2) suggested that CSQ2 has a role in protecting the heart against premature spontaneous SR Ca^{2+} release and triggered arrhythmia. However, loss of CSQ2 doesn't impair contractile function (Knollmann 2009). At low luminal Ca^{2+} concentrations CSQ2 prevents RyR2 activation by binding tightly to triadin and junctin. This inhibition is relieved by the binding of Ca^{2+} to CSQ2, and as the concentration rises (Gyorke, Hester et al. 2004) the Ca^{2+} binding disrupts the interaction of CASQ to triadin and junctin thereby removing the inhibitory effect of CSQ2 on RyR2.

Triadin and junctin are integral membrane proteins in the junctional SR and interact with each other, calsequestrin and the RyR. Whilst three cardiac triadin isoforms exist (35, 40, and 92KD) triadin-1 is the most abundant form representing more than 95% of the total amount of triadin in cardiac myocytes (Kobayashi and Jones 1999). Triadin (TRD) and junctin (JCN) exhibit similar domain structures composed of a short cytoplasmic N-terminal segment, single membrane spanning domain, and a long, highly positively charged C-terminus. The luminal domains of triadin and junctin are composed of long stretches of alternating positively and negatively charged residues known as KEKE motifs, which have been proposed to be involved in protein-protein interactions (interactions between TRD and JCN and also with CSQ2 and RyR2) (Kobayashi, Alseikhan et al. 2000). Studies in CSQ2 null mice suggested that the presence of CSQ2 is important to stabilize the heterotrimeric complex of CSQ2, TRD and JCN, which is important for the structural organization of the SR (Knollmann, Chopra et al. 2006). However, ablation of TRD causes a 50% reduction in the contacts between the plasma membrane and the SR and a 50% reduction in the extent of the junctional SR, which impaired EC-coupling and contractility at the level of the myocyte (Chopra, Yang et al. 2009).

1.4.3.3 Calmodulin

Calmodulin (CaM) is a Ca^{2+} binding protein that binds to larger proteins and acts as a Ca^{2+} sensor. CaM influences RyR2-mediated Ca^{2+} release by a direct interaction (binding) with the RyR and by phosphorylation of the RyR through CaMKII (Ai, Curran et al. 2005). CaM is a 148 amino acid protein arranged in two globular heads each of which is composed of 2 binding EF-hands: I and II for the N-terminal lobe, and III and IV for the C-terminal lobe (Figure 1.6). Ca^{2+}-binding domains I and II in the N-terminal lobe have a 10-fold lower Ca^{2+} affinity (10^{-5} M) than those in the C-terminal lobe (10^{-6} M) (Black, Tikunova et al. 2000). The Ca^{2+}-free calmodulin is named apocalmodulin (apoCaM), whilst the Ca^{2+}-bound calmodulin is named Ca^{2+}/calmodulin (CaCaM, four Ca^{2+} bound). Three-dimensional reconstructions of the RyR2 based on cryo-electron microscopy (Huang, Liu et al. 2013) showed that the effects of CaM on RyR2s are mediated via binding to a single binding domain comprising amino acid residues 3581–3612 and 4261–4286 (corresponding to 3614–3643 and 4302–4328 in RyR1). Each RyR2 subunit can bind with nanomolar affinity (5.5 ± 2.2 nM in the presence of 100 μM Ca^{2+} ; 54 ± 34 nM in the presence of ≤10 nM Ca^{2+}) to 1 CaCaM or 1 ApoCaM (Balshaw, Yamaguchi et al. 2002). CaCaM and ApoCaM bind to and dissociate from RyR2 on a time scale of seconds to minutes (Tripathy, Xu et al. 1995). In cardiac muscle, CaM inhibits the RyR2 channel opening at low and high [Ca^{2+}] (maximal effect observed at low micromolar to submicromolar Ca^{2+} concentrations (Xu and Meissner 2004)) Since CaCaM is the predominant form at low micromolar [Ca^{2+}], this finding suggests that CaCaM is a more potent inhibitor of RyR2s than apoCaM.

The binding of intracellular CaM, (~45 nM ir

release in cardiomyocytes (Xu and Meissner 2004) due to its ability to inhibit RyR2 channel opening. Single channel studies of RyR2s in lipid bilayers have found that CaM inhibits RyR2 activity with an IC_{50} of 100 nM (Xu and Meissner 2004). During the process of RyR2 isolation from the heart and their incorporation into lipid bilayers, the macromolecular complex stays mostly intact (Marks, Marx et al. 2002) with the exception of CaM which can dissociate from the RyR2 complex. Most single channel studies do not include this important regulatory molecule in the RyR2 complex, but in the cell, CaM is abundant and is associated with the RyR (Xu and Meissner 2004).

1.4.3.4 Kinases and phosphatases

PKA (protein kinase A) binds to the RyR2 via an A kinase anchoring protein (mAKAP). CaMKII also co-immunoprecipitates with RyR2s, but the binding site has not yet been identified. CaMKII is expressed as the δ isoform in heart (Edman and Schulman 1994) and has three domains: an amino-terminal catalytic domain, a central regulatory domain and a carboxyl-terminal association domain responsible for oligomerization (Bronstein, Farber et al. 1993). Protein phosphatase 1 (PP1) and protein phosphatase 2A (PP2A) are anchored to the RyR2 via spinophilin and PR130, respectively. mAKAP, spinophilin and PR130 interact with the leucine zipper in the cytosolic domain of the RyR2 which in turn target PKA, PP1 and PP2A to the channel complex. These kinases and phosphatases have a role in determining the level of RyR2 phosphorylation. Ser^{2808} (close to the regulatory subunit of PKA) on the RyR2 is the target site of PKA phosphorylation (Marx, Reiken et al. 2000). CaMKII, in the presence of CaM, can mediate RyR2 phosphorylation at S^{2814} (Wehrens, Lehnart et al. 2004).

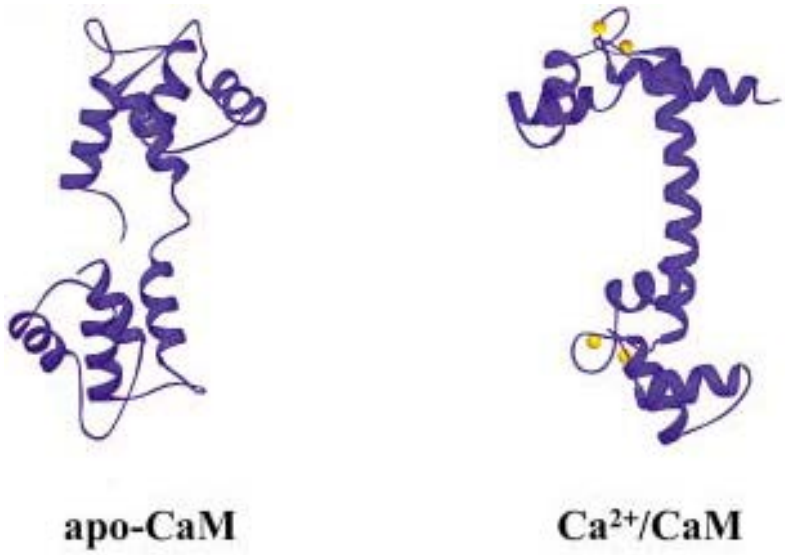

Figure 1.6: Ribbon presentations of CaM (Apo-CaM) and CaM in complex with Ca^{2+} (CaCaM). CaM is coloured blue and Ca^{2+} ions are yellow. The N-terminal lobe of CaM is orientated to the top and the C-terminal lobe to the bottom of the Figures (Vetter and Leclerc 2003).

1.5 Calcium handling in cardiac myocytes during excitation-contraction coupling

Ca^{2+} release and uptake from the SR as well as its transport between mitochondria, intracellular and extracellular spaces, play a key role in heart contraction and relaxation (Tanaka, Dinenno et al. 2000) (Figure 1.7). The ECC process in heart myocytes begins with the action potential (AP), which activates the LTCC Ca^{2+} current (I_{Ca} in Figure 1.7) allowing Ca^{2+} to enter the cell. The rise in cytoplasmic Ca^{2+} ($[Ca^{2+}]_i$) triggers Ca^{2+} release from the SR by activation of Ca^{2+} release channels via a cytoplasmic activation site in a process called CICR. The Ca^{2+} released from the SR contributes between 60-95% of the cytoplasmic Ca^{2+} during ECC depending on the species (Lehnart, Maier et al. 2009). The binding of cytosolic Ca^{2+} to the myofilament protein troponin C activates muscle contraction. During diastole, $[Ca^{2+}]_i$ falls and the heart muscle relaxes as Ca^{2+} is either sequestered by the SR via SERCA2a, sequestered into mitochondria or extruded from the cell by the NCX (Bers 2002). These mechanisms serve a fundamental role in the large changes in free $[Ca^{2+}]$ in the cytoplasm ($[Ca^{2+}]_i$ ~ 0.1 to 1 μM) and SR lumen ($[Ca^{2+}]_L$ ~ 1 to 0.3 mM) between diastole and systole, respectively (Ginsburg, Weber et al. 1998; Bers 2002).

The main calcium release channels in the SR are the ryanodine receptors (RyR2). These channels can be activated by Ca^{2+} in the cytoplasm and lumen (see below). In ventricles, the rise in $[Ca^{2+}]_i$ during ECC causes activation of RyR2s and triggers Ca^{2+} release from the SR. In the SA node the SR Ca^{2+} load contributes to pacemaking by activating RyRs via luminal-facing Ca^{2+} binding sites. After 20 ms of activation, the RyR2 closes, Ca^{2+} release terminates and $[Ca^{2+}]_i$ declines. The decline in $[Ca^{2+}]_i$ is mediated by the SERCA2a, the NCX, the sarcolemmal Ca-ATPase and the mitochondrial Ca^{2+} uniporter. Under normal conditions, SERCA2a takes up ~70% of the Ca^{2+} involved in the Ca^{2+} release whereas nearly 30% is extruded from the cell via NCX, and ~1% each via sarcolemmal Ca-ATPase and the mitochondrial Ca^{2+} uniporter (Bers 2002).

Since the cell and its Ca^{2+} stores are closed compartments, there must be a balance in Ca^{2+} uptake and release by these compartments over the course of the heartbeat.

Therefore, the uptake and release fluxes are interdependent. The main transporter routes for Ca^{2+} across the sarcolemma are NCX for extrusion and LTCC for uptake. In the SR the SERCA and RyR2 serve as the uptake and release mechanisms. The concept is that the SR Ca^{2+} content can act to regulate itself such that the amount of released Ca^{2+} from the SR must be balanced by the amount of Ca^{2+} taken back up by SERCA2a (Bhogal and Colyer 1998; Eisner, Choi et al. 2000). By using channel modulators such as caffeine and tetracaine, Eisner and his colleagues have shown that the mechanism of SR Ca^{2+} release in cardiac myocytes exhibits this ability, a process they have called autoregulation.

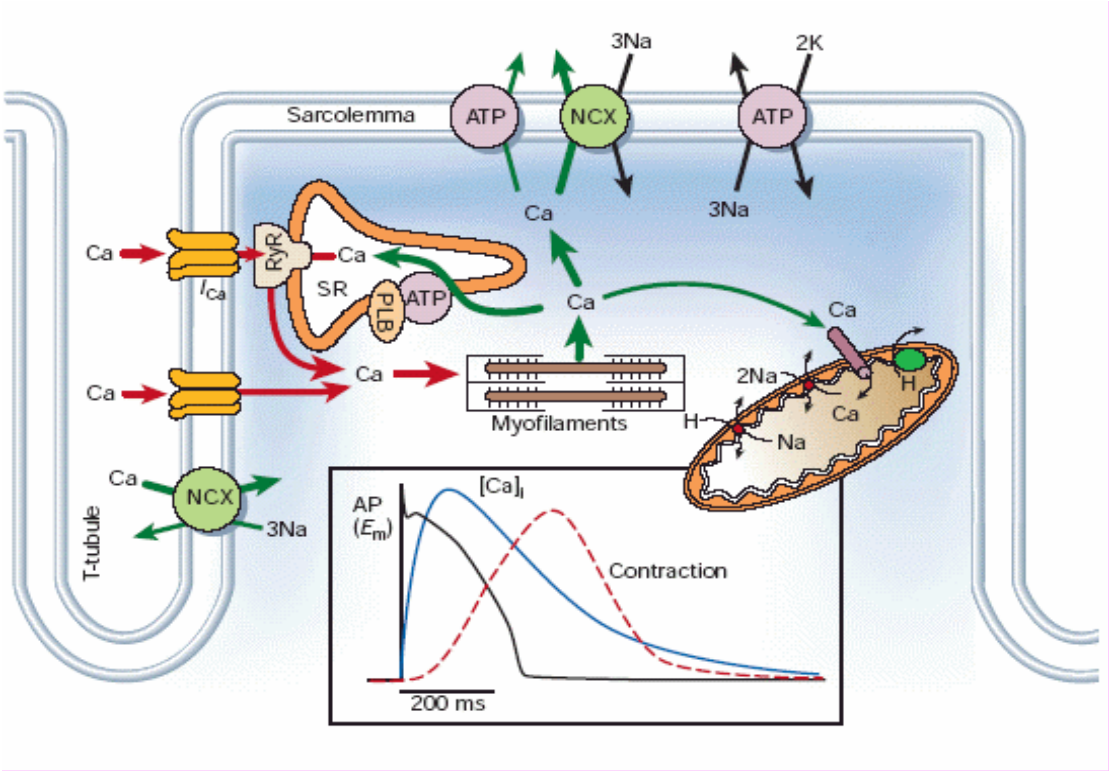

Figure 1.7: Excitation contraction coupling in the ventricular myocyte. NCX, Na^+/Ca^{2+} exchange; ATP, ATPase; PLB, phospholamban; SR, sarcoplasmic reticulum (Bers 2002)

1.6 Ca^{2+} leak, sparks and waves

Three Ca^{2+} release phenomena have been observed in cardiomyocytes: Ca^{2+} leak, sparks and waves. Ca^{2+} leak is a spatially uniform, relatively slow release of Ca^{2+} from the SR that is present during diastole. It is believed to be due to the opening of single RyRs in the SR membrane. Activation of RyR2s by elevated luminal Ca^{2+} leads to increased SR Ca^{2+} leak (Schiefer, Meissner et al. 1995; Berridge 1997). Increased SR Ca^{2+} leak has a key role in several pathological states such as HF (Bers, Eisner et al. 2003).

Ca^{2+} sparks are brief, localised SR Ca^{2+} release events, so named because they appear as bursts of light in the presence of fluorescent Ca^{2+} indicators seen under confocal microscopy (Cheng, Lederer et al. 1993). Sparks are believed to be due to synchronised opening of ~ 6-30 RyRs in a junction between the SR and t-tubule membranes (Cheng and Lederer 2008). Their fluorescence rising phase corresponds to the time that the RyRs are open and releasing Ca^{2+} during the ECC process. It is confined to regions of around 2.0 µm in diameter and lasts for about 20 ms (Cheng and Lederer 2008). The frequency of spark occurrence increases with increased luminal and cytoplasmic [Ca^{2+}].

Several mechanisms have been proposed for spark termination, including feed-back inhibition by elevated cytoplasmic Ca^{2+} release (Wang, Stern et al. 2004); deactivation of RyRs caused by a decrease in SR luminal Ca^{2+} (luminal-Ca^{2+}-dependent deactivation) (Brochet, Yang et al. 2005; Huertas and Smith 2007), and intrinsic changes occurring within the RyR2 such as adaptation and inactivation (Cheng, Fill et al. 1995; Sitsapesan, Montgomery et al. 1995; Laver and Lamb 1998). Recent studies have shown that spark termination is due to a decay in the CICR that occurs as the jSR is depleted of Ca^{2+} (Guo, Gillespie et al. 2012; Cannell, Kong et al. 2013), a process dubbed 'induction decay' (Laver, Kong et al. 2013). According to this mechanism, the rate of termination of RyR activity will depend on RyR sensitivity to Ca^{2+} in the dyad cleft and the time course of jSR depletion.

Ca^{2+} waves (Ca^{2+} transients) are global, propagating Ca^{2+} release events initiated by Ca^{2+} sparks. Propagation of Ca^{2+} waves throughout the cell occurs by salutatory

propagation between neighbouring Ca^{2+} release sites by CICR (Wier 2007). About 10^4 sparks are released during systole within a few tens of milliseconds in a single cardiac myocyte to form Ca^{2+} transients of ~1 µM in the bulk cytoplasm. Ca^{2+} release occurs through RyRs and wave termination occurs by closure of RyRs and removal of Ca^{2+} from the cytoplasm via SERCA2a and NCX. The relationship between I_{Ca} and the amount of calcium released from the SR is called 'Ca^{2+} gain' which is defined as the ratio of total Ca^{2+} released through RyRs relative to that entering through L-type Ca^{2+} channels (Wier 2007). Ca^{2+} leak and sparks are the predominate forms of Ca^{2+} release in diastole whereas in systole Ca^{2+} waves predominate

1.7 Adrenergic stimulation of ECC- signalling pathway (Fight or Flight response)

Cardiac output is increased by stimulation of β-adrenergic receptors (β-AR) by adrenaline and noradrenaline. This is part of the classic 'fight or flight' response activated by stress and exercise to increase cardiac output required to meet the body's increased metabolic demands. Noradrenaline binds to the β_1-AR which is the most abundant β-AR in the human heart, approaching 75% of the total receptors, whereas adrenaline binds to both β_1- and β_2-AR (Caron and Lefkowitz 1993; Brodde and Michel 1999). In human heart, β_1-ARs activates the Gsα-protein resulting in synthesis and accumulation of cAMP and activation of protein kinase A (Frick, Hariharan et al.); β_2-ARs couple to both the 'stimulatory' Gsα -protein and 'inhibitory' Giα-protein signaling (Lohse, Engelhardt et al. 2003). Gsα signaling activates the second messenger PKA which in turn modulates different targets involved in ECC, including 1) LTCC's (increases the Ca^{2+}influx pathway), 2) phospholamban (PLB; inhibits SERCA2a unless phosphorylated), 3) RyRs (activates the Ca^{2+} release channel) and 4) troponin I (increases Ca^{2+} sensitivity of contraction) (Bers 2002) (Figure 1.8). These phosphorylation events are orchestrated to increase cardiac contractility. However, the Giα signaling pathway inhibits adenylyl cyclase activity and decreases the cAMP level which results in a large decrease in myocardial force and may contribute to the development of cardiac pathology (Rockman, Koch et al. 2002).

In humans, β_1- and β_2-ARs-Gsα-protein couplings accelerate relaxation of cardiac myocytes via phosphorylation of PLB and troponin I, which increase the activity of the SERCA2a and dissociation of Ca^{2+} from the myofilaments, respectively. Increasing the rate of SR Ca^{2+} uptake contributes to increasing the SR Ca^{2+} load which in turn increases RyR2 activity, thus phosphorylation of PLB would tend to accelerate both contraction (inotropic) and relaxation (lusitropic) of cardiac myocytes. Phosphorylation of PLB occurs at two sites; Ser 16 by PKA (Frick, Hariharan et al.) and Thr 17 by Ca^{2+}/calmodulin-dependent protein kinase II (CaMKII) (Koss and Kranias 1996; Kaumann, Bartel et al. 1999; Molenaar, Savarimuthu et al. 2007). Unlike human, other mammals do not accelerate relaxation via β_2-ARs-Gsα-protein coupling because of simultaneous β_2-ARs-Giα-protein coupling, but instead hasten relaxation via β_1-ARs-Gsα-protein coupling (Kaumann, Sanders et al. 1996; Zheng, Zhu et al. 2005; Molenaar, Savarimuthu et al. 2007).

β-AR agonists, via PKA phosphorylation of LTCC's, cause a 2- to 4-fold increase in I_{Ca} in ventricular myocytes by shifting the voltage-dependence of activation and inactivation to more negative potentials (Hartzell 1988). Increased I_{Ca} accompanied with greater availability of SR Ca^{2+}, greatly enhances the Ca^{2+} transient amplitude and thus increases the rate of contraction (Bers 2002). Phosphorylation of RyRs during adrenergic stimulation has been shown to increase RyR2 activity (Li, Imtiaz et al. 2013). PKA phosphorylation of RyRs has been reported to increase the amplitude and duration of Ca^{2+} sparks (Shen 2006). The RyR2 is phosphorylated at Ser^{2808} by PKA (Witcher, Kovacs et al. 1991; Rodriguez, Bhogal et al. 2003; Wehrens, Lehnart et al. 2004; Xiao, Zhong et al. 2006). Ser^{2815} is phosphorylated by CaMKII (Wehrens, Lehnart et al. 2004) and Ser^{2030} is phosphorylated by PKA (Xiao, Zhong et al. 2006). There are conflicting reports in the literature as to how RyRs are phosphorylated *in situ*. One study found that β-adrenergic stimulation is linked to modulation of RyR2s via phosphorylation of Ser^{2030} (Xiao, Zhong et al. 2006), whereas two other studies found it was linked to Ser^{2808} (corresponds to Ser^{2808} in human) (Marx, Reiken et al. 2000; Yano, Okuda et al. 2005). Moreover, there is no consensus on the effects of phosphorylation on RyR2 activity. Some groups found phosphorylation increased RyR2 activity (Hain, Onoue et al. 1995; Marx, Reiken et al. 2000) whilst others reported decreases in RyR2 activity (Lokuta, Rogers et al. 1995; Valdivia, Kaplan et al. 1995). In view of the

controversy surrounding the effects of PKA-dependent phosphorylation on the RyR2 activity, Carter *et al.* (Carter, Colyer et al. 2006) examined RyR2 activity at three different levels of Ser^{2808} phosphorylation. Endogenous phosphorylation of this site in non-stimulated sheep heart was 75% of maximum and this was associated with significantly less RyR2 activity than seen with RyRs that were dephosphorylated by PP1 or maximally phosphorylated by PKA. These findings indicate that 75% of maximum phosphorylation at Ser^{2808} represents the RyR2 phosphorylation level at rest (a basal level of RyR2 activity). These results are in accord with the idea that prolonged or maintained maximum phosphorylation of RyR2s at Ser^{2808} results in pathological alteration of cellular Ca^{2+} handling mechanisms. In addition, recent experiments have proposed that up-regulation of Ca^{2+} release could occur as a result of an increased sensitivity to $[Ca^{2+}]_L$ (Xiao, Tian et al. 2007).

CaMKII has also been shown to activate the RyR2 at high cytosolic Ca^{2+} and is associated with phosphorylation of the same ECC proteins as PKA (MacQuaide, Dempster et al. 2007). PKA activation through β-AR stimulation increases pacemaking frequency and increases cytosolic Ca^{2+}. Both of these actions are known to activate CaMKII which further phosphorylates the RyR2 (Wehrens, Lehnart et al. 2004; Bers 2006; Venetucci, Trafford et al. 2007). However, distinguishing their precise roles and the importance of phosphorylation of RyR2 by PKA and CaMKII is not yet known (Wehrens, Lehnart et al. 2004; Bers 2006; Sipido 2007; Venetucci, Trafford et al. 2007; Yamaguchi and Meissner 2007).

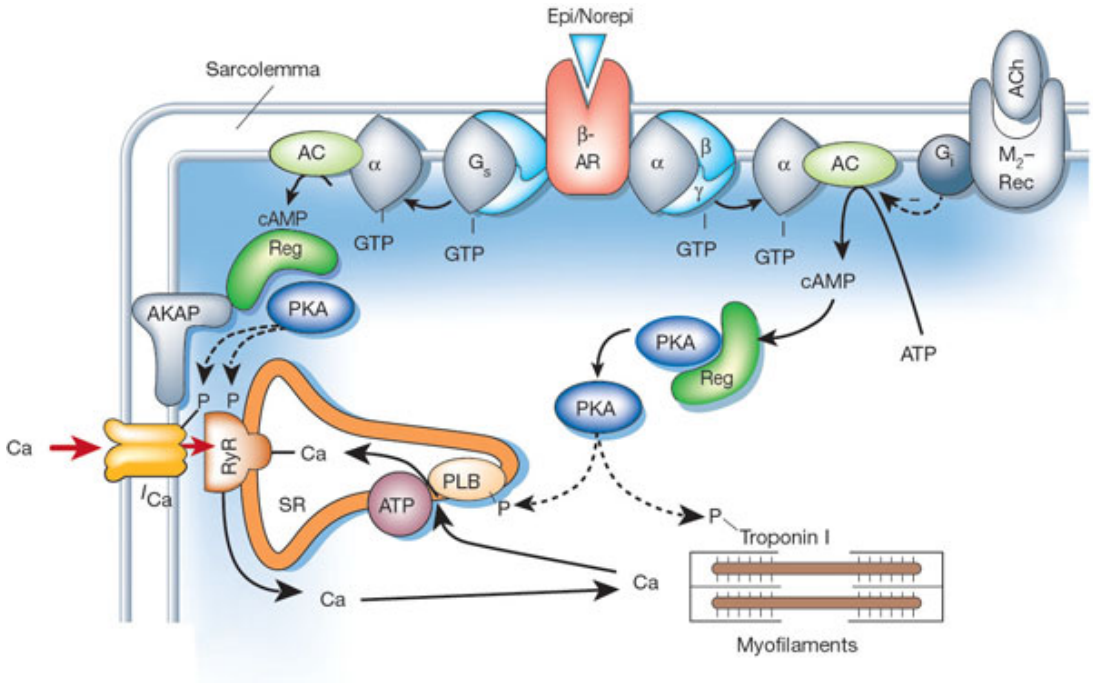

Figure 1.8: β-adrenergic stimulation and phosphorylation targets relevant to ECC. AC, adenylyl cyclase; ACh, acetylcholine; AKAP, A kinase anchoring protein; β-AR, β-adrenergic receptor; M_2-Rec, M_2-muscarinic receptor; PLB, phospholamban; Reg, PKA regulatory subunit; SR, sarcoplasmic reticulum (Bers 2002).

1.8 Modulation (regulation) of Ca^{2+} release channels by intracellular Ca^{2+}, Mg^{2+} and adenine nucleotides

RyR2s are exposed to continually changing Ca^{2+} concentrations in the cytoplasm and SR lumen during the ECC cycle, and these changes have a key role in RyR2 regulation (Soeller and Cannell 2004). The main physiological regulators of RyR2s are Ca^{2+}, Mg^{2+}, and ATP (Meissner 1994). Ca^{2+} release measurements from skeletal and cardiac SR vesicles showed that micromolar concentrations of cytoplasmic Ca^{2+} strongly activate RyRs (Meissner 1986; Meissner and Henderson 1987). Single channel recordings have shown that RyR2s are activated by ~1 µM $[Ca^{2+}]_C$ and inhibited by >1 mM Ca^{2+} and /or Mg^{2+} (intracellular $[Mg^{2+}]$ =1 mM) (Meissner 1994; Laver, Baynes et al. 1997). RyR2 open probability (P_o) exhibited the characteristic bell-shaped Ca^{2+}-dependence with activation at µM Ca^{2+} and inhibition at mM Ca^{2+} (Laver, Roden et al. 1995). Luminal Ca^{2+} activation was first identified in sheep RyR2s (Sitsapesan and Williams 1994) and is partly attributed to a luminal facing Ca^{2+} activation site (Ching, Williams et al. 2000; Laver 2007) and, under certain conditions, to the flux of luminal Ca^{2+} to the cytoplasmic activation site (Tripathy and Meissner 1996; Laver 2007). The P_o showed a bell-shaped dependence on luminal Ca^{2+} due to the combined action of Ca^{2+} activation and inactivation mechanisms (Laver and Honen 2008).

So far, four different Ca^{2+} dependent mechanisms have been identified in RyR2s, which in turn are controlled by four Ca^{2+}/ Mg^{2+} sites on each RyR2 subunit (Figure 1.9). RyR2 activation is mediated by Ca^{2+} binding to sites that are accessible to either the cytoplasmic or luminal sides of the channel. One high-affinity cytoplasmic facing Ca^{2+} binding site on each subunit (A-site) is believed to cause channel activation by cytoplasmic Ca^{2+} (Zahradnik, Gyorke et al. 2005), and a lower affinity site in the SR luminal side of the channel causes activation by luminal Ca^{2+}. In addition, there is evidence for two Ca^{2+} inactivation sites located on the cytoplasmic face (Laver 2007). RyR2 inhibition at 1 mM Ca^{2+} has been attributed to low-affinity inhibitory sites (I1-site) on the RyR (Laver, Baynes et al. 1997; Meissner 2002). A-site and I1-site together produce the bell-shaped cytoplasmic $[Ca^{2+}]$ dependence of RyR2 activity. Recently, Laver (Laver 2007) has identified a high-affinity (1 µM) cytoplasmic facing site (I2-site) on each RyR subunit that accounts for a cytoplasmic Ca^{2+}-inhibition phenomenon

in single channel recordings of RyR2. Early lipid bilayer studies reported that luminal Ca^{2+}-activated RyR (Sitsapesan and Williams 1994; Sitsapesan and Williams 1995; Sitsapesan and Williams 1997) either by Ca^{2+} binding to the luminal activation site (L-site) on RyR (Sitsapesan and Williams 1997; Gyorke and Gyorke 1998; Laver 2009) or by flux of luminal Ca^{2+} (feed-through) to the cytoplasmic Ca^{2+} activation and inhibition sites (A- and I2-sites, respectively?) (Tripathy and Meissner 1996; Xu and Meissner 1998; Laver 2007; Laver 2009). A publication by Laver *et al.* (Laver 2007) later found that both mechanisms are involved in luminal regulation of RyR2.

Intracellular Mg^{2+} interacts with Ca^{2+} binding sites on many enzymes and transport proteins involved in ECC. Mg^{2+} is a strong inhibitor of RyR2s which inhibits by competing for Ca^{2+} at activation sites. However, unlike Ca^{2+}, binding of Mg^{2+} to activation sites does not cause channel opening. The competitive inhibition by Mg^{2+} plays a key role in shaping the cytoplasmic and luminal [Ca^{2+}] dependencies of RyR activity in the cell (Laver and Honen 2008). Because of competition with Ca^{2+}, Mg^{2+} is a stronger inhibitor of the RyR in diastole than in systole. Previous studies, using sheep RyR2s, found that the two independent mechanisms produced inhibition by cytoplasmic Mg^{2+}: 1) Mg^{2+} is a competitive antagonist at the cytoplasmic Ca^{2+} activation site (A-site) and this mechanism determines the EC_{50} for Mg^{2+} inhibition at a cytoplasmic Ca^{2+} concentration of less than 10 μM, and 2) at higher Ca^{2+} concentrations, the EC_{50} for Mg^{2+} is determined by Mg^{2+} binding to a low affinity Mg^{2+}/Ca^{2+} inhibition site (I_1-site). Binding of either Ca^{2+} or Mg^{2+} to the I1-site causes channel inactivation (Laver, Baynes et al. 1997). Luminal Mg^{2+} inhibits by competing with luminal Ca^{2+} for the L-site. This has the effect of increasing the half-maximal activation concentration for luminal Ca^{2+}, thus affecting RyR sensitivity to luminal Ca^{2+} (Laver and Honen 2008). In addition, Mg^{2+} blocks Ca^{2+} conduction by binding to Ca^{2+} sites in the pore (Valdivia, Kaplan et al. 1995). According to the rate-based ion conduction model of Tinker *et al*. (Tinker, Lindsay et al. 1992), the presence of intracellular Mg^{2+} causes a 50% reduction in the Ca^{2+} flow through the open RyR.

Intracellular Mg^{2+} is a cofactor for SERCA2a, increasing its activity at micromolar Ca^{2+} concentrations but lowering its activity at submicromolar concentrations by competing

with Ca^{2+} for transport sites (Krause 1991). Mg^{2+} also has a small inhibiting effect on the LTCC (The peak L-type calcium current is inhibited by free Mg^{2+}) (White and Hartzell 1988) and the NCX (Mg^{2+} acts at a site that regulates both forward and reverse mode NCX activities and does not compete with Ca^{2+} for binding). Reduction in $[Mg^{2+}]_i$ appears to enhance the I_{NCX} at both low and high diastolic Ca^{2+} concentrations (Wei, Quigley et al. 2002).

ATP activates the RyR2 in the presence of Ca^{2+} but it cannot open the channel in the absence of Ca^{2+}. Studies using [^{3}H]ryanodine binding and single channel recordings have shown that millimolar levels of ATP (K_a = 0.22 mM) (Kermode, Williams et al. 1998) activate RyRs (Meissner and Henderson 1987). It has been shown that by-products of ATP hydrolysis, such as ADP and AMP, are less effective activators (Kermode, Williams et al. 1998). The same authors demonstrated that phosphate can also activate and interact with RyR2 via a different mechanism (not by binding to ATP binding site). The mode of action of ATP in RyR2 activation is to stabilize channel open conformations (Laver 2007). Concentrations of ATP above optimum (~ 2 mM), leads to a reduction in P_o, for example up to 50% at 5 mM. One possible mechanism could be the binding of ATP to low-affinity inactivation sites (Kermode, Williams et al. 1998). ATP also has been detected to increase the luminal Ca^{2+} dependence of the RyR2 opening rate without altering the Ca^{2+} binding affinity of the L-site (Laver 2007).

At the begining of diastole, $[Ca^{2+}]_i$ is at subactivating levels (~ 100 nM). Under these conditions, the A- and L-sites of the RyRs are mostly occupied by Mg^{2+} ($[Mg^{2+}]$ is 1mM which is 20-fold higher than the EC_{50} for the A & L-sites). Therefore, RyRs are mostly closed in diastole. Since RyR2 has activating sites on both the cytoplasmic and luminal sides of the protein, any channel openings that do occur in diastole can arise from Ca^{2+} elevations in either the SR or cytoplasm. During the course of diastole, the SERCA2a pump sequesters Ca^{2+} into the SR, thus increasing the luminal Ca^{2+} and activating the channel via the L-site. Also, during cell depolarisation and ECC (systole), depolarisation of the t-tubule causes DHPRs to increase cytoplasmic Ca^{2+} to ~50-100 μM in the dyad (Soeller and Cannell 1997) and stimulate the channel via the

cytoplasmic activation site (A-site). In the presence of Mg^{2+}, the EC_{50} for Ca^{2+} activation is 50 µM with a maximum open probability of 0.5.

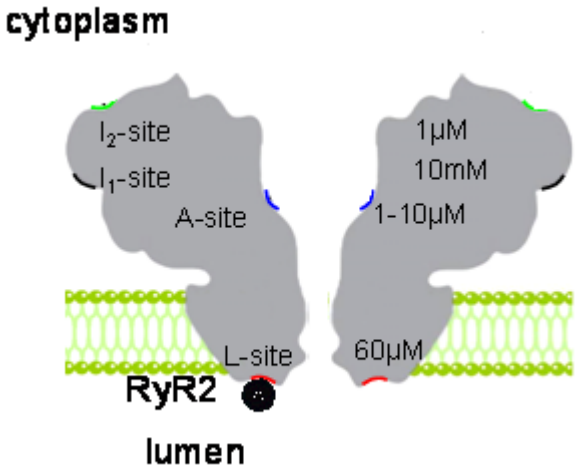

Figure 1.9: An illustration of the four Ca^{2+} binding sites on each RyR2 subunit that regulate channel opening (A, L, I1 & I2 sites). The affinities of each site (Ca^{2+}, Mg^{2+}) are tagged to the corresponding sites on the right. The cytoplasmic facing A, I1 & I2 sites respond to Ca^{2+} (Park, Kim et al. 2005) from the DHPR. As the SR refills during diastole, Ca^{2+}ions in the SR lumen bind to the luminal L-site and can trigger channel openings independently of the DHPR. The subsequent efflux of Ca^{2+} during systole regulates the cytoplasmic Ca^{2+} activation (A-site) and inhibition sites (I2-site). Thus, during diastole the RyR2 is triggered primarily by luminal Ca^{2+} at the L-site whereas during systole it is triggered mainly by cytoplasmic Ca^{2+}at the A-site (Laver 2009).

1.9 Models of HF

Experimental animal models of HF are often needed to address specific questions not easily answered in patients. Choosing a species for an experimental model of HF not only depends on the scientific question addressed but also on other factors such as accessibility and reproducibility of the model and ethical considerations. These models include: rapid ventricular pacing (created in dogs, sheep and pigs), ventricular pressure and volume overload, ischemic cardiomyopathy, arteriovenous shunt, supravalvular stenosis, chronic heart block, myocardial infarction and repetitive transmyocardial direct current (DC) shock (Marín-García 2010). The most commonly used animals in HF models are rat, mouse, dog and rabbit. Rat and mouse models are relatively inexpensive, and because of their short gestation period, a large sample size can be produced in a relatively short period of time. However, there are limitations to the use of rats and mouse as models of human HF because of the differences in myocardial function compared to human heart. Firstly, rat and mouse myocardium action potential is very short and lacks a plateau phase (Bers 1991). Secondly, in rats and mouse, removal of intracellular Ca^{2+} ($[Ca^{2+}]_i$) is mediated more by SERCA2a and less by the Na^+/Ca^{2+}-exchanger than it is in humans (Bers 1991). Thirdly, unlike human myocardium, α-myosin heavy-chain isoform predominates in rat and mouse myocardium (Swynghedauw 1986). However, mouse models have more benefit than rat because of the availability of a great number of transgenic and knockout strains, which could make the animal model an invaluable tool to study the pathogenesis of HF and to identify novel therapeutic targets (Richard D. Patten and Monica R. Hall-Porter 2009).. Mouse models also have lower housing costs compared with rats. On the other hand, dog and other large animal models of HF more accurately model human left ventricle (LV) function and chamber volumes. Furthermore, in dog, the excitation–contraction coupling process is similar to that in human myocardium and the b-myosin heavy-chain isoform predominates in both (Lompre, Mercadier et al. 1981). Rabbit myocardium exhibits interesting similarities to human myocardium (Bers 1991; Hasenfuss, Mulieri et al. 1991) and is less expensive than dog.

1.10 Structural remodelling of dyad junctions in HF

Crossman *et al*. (Crossman, Ruygrok et al. 2010) examined the organization of t-tubules, L-type calcium channels (LTCC) and RyRs using high resolution fluorescent imaging. They showed that the disruption of t-tubule architecture in failing human heart cells was associated with a small loss of RyR clusters and displacement of LTCC location (~30%) from RyRs. Song *et al.* (2006) found a similar loss of colocalization (~20%) between RyRs and LTCC's associated with t-tubule reorganizing in diseased cells. These findings showed that remodelling of the t-tubular architecture and a decrease in colocalization between LTCC's and RyRs in the failing human heart may contribute to calcium handling abnormalities seen in HF (Crossman, Ruygrok et al. 2010). These studies also showed substantial changes in the organisation of the sarcoplasmic reticulum, t-tubules and their junctional microdomains. A decrease in expression levels of SERCA2a, LTCC (Guo, Chapman et al. 2003; Hu, Shen et al. 2010) and a 35% decrease in RyR2 (Go, Moschella et al. 1995) has been reported in human HF.

1.11 Ca^{2+} handling alteration in HF

Three abnormalities in intracellular calcium transport mechanisms have been demonstrated in HF: 1) down regulation of SR Ca^{2+}-ATPase (SERCA2a), 2) up regulation of Na^{+}/Ca^{2+} exchanger (NCX), and 3) increased SR Ca^{2+} leak via RyR2s (Bers, Eisner et al. 2003). Changes in expression level of SERCA2a (~50% reduction in mRNA levels) and NCX (41-50% increase in mRNA levels) have been reported in human HF (Studer, Reinecke et al. 1994). These Ca^{2+} transport dysfunctions enhance Ca^{2+} extrusion to the extracellular space and decrease SR Ca^{2+} uptake (Hobai and O'Rourke 2001). Low luminal Ca^{2+} ($[Ca^{2+}]_L$) is a marker for HF and treatments that raise $[Ca^{2+}]_L$ generally tend to restore cardiac function in failing hearts (Bers, Eisner et al. 2003). Decreased SR Ca^{2+} content decreases the amplitude of intracellular Ca^{2+} transients ($\Delta[Ca^{2+}]_i$). As the latter has a key role in the cardiac force development (Maier, Zhang et al. 2003), these findings suggest that the reduction in the amount of Ca^{2+} released from SR into the cytosol will account for the reduced contractile force

generated by the failing heart (Kubalova, Terentyev et al. 2005). $[Ca^{2+}]_i$ transients in HF rise more slowly as a consequence of low SR Ca^{2+} content and reduction in potassium outward current, which contributes to the prolonged AP duration. $[Ca^{2+}]_i$ decline is also slow due to reduced Ca^{2+} uptake into the SR via SERCA2a (Bers 2006).

Jiang and his colleagues (Jiang, Lokuta et al. 2002) suggested that abnormal Ca^{2+} uptake by SERCA2a, rather than Ca^{2+} release by RyR2s, contributed to reduced and slow Ca^{2+} transients in HF. They showed 44% reduction in SERCA2a function in canine HF, and 30% reduction in SERCA2a level in human HF, whilst RyRs from canine and human HF exhibited no major structural or functional changes compared with control. Moreover, Holmberg and Williams have showed that the properties of RyR2 from failing human hearts are identical with those previously reported for sheep and canine RyRs (no normal control heart was used in this study), which suggest that other factors may contribute to abnormal Ca^{2+} release from the SR (Holmberg and Williams 1992). However, the latter findings conflict with several studies using different models of HF including human, which showed that RyRs become highly active in HF and lack regulation by intracellular Ca^{2+}. Increased diastolic SR Ca^{2+} leak as a consequence of high RyR activity would tend to deplete SR Ca^{2+} load reduction and increase diastolic $[Ca^{2+}]_i$ (Shannon, Pogwizd et al. 2003) (See below). Thus, it is still not clear how RyR activity changes in HF and, as yet, it is still not understood how RyRs from failing and healthy human hearts are regulated by Ca^{2+} and Mg^{2+}.

1.12 Molecular mechanisms of RyR2 dysfunction in HF

The cause of RyR2 channel dysfunction is highly controversial and may involve many mechanisms. Reduction in the amount of bound FKBP12.6, PP1, PP2A, and phosphodiesterase 4D3 (PDE4D3) in the RyR2 complex has been reported in human HF (Marx, Reiken et al. 2000). Direct modulation of RyR2 via PKA hyperphosphorylation, a consequence of the loss of phosphatases, leads to dissociation of the regulatory protein FKBP12.6 from the RyR2 complex and changes the channel stoichiometry (see section 12). Loss of FKBP12.6 from RyR2 leads to destabilization of the channel and increases diastolic Ca^{2+} leak (Marx, Reiken et al. 2000; Yano, Ono et al.

2000). Another hypothesis reported in RyR2 remodelling involves defective interdomain interaction (unzipping state) in response to oxidation associated with RyR2 hyperphosphorylation (Oda, Yano et al. 2005; Yano, Okuda et al. 2005).

1.12.1 RyR2 hyperphosphorylation

HF is accompanied by increased sympathetic nerve system activity, increased levels of noradrenaline and chronic activation of β-ARs with hyperadrenergic state (Braunwald and Chidsey 1965; Bristow, Ginsburg et al. 1982; Cohn, Levine et al. 1984; Kinugawa, Ogino et al. 1996). Chronic activation of β_1-ARs in HF is characterized by an adaptive, down-regulation and desensitization of β_1-ARs (Brodde 1991; Brodde and Leineweber 2004). β_2-ARs are less affected, and in some cases, β_2-ARs function in HF is preserved (Brodde 1991; Molenaar, Savarimuthu et al. 2007). Decreased β_1-AR density reduces the inotropic effect of noradrenaline mediated through β_1-AR in HF. Moreover, the amount and activity of Gi-protein is increased in HF, thus suppressing receptor-mediated activation of adenylyl cyclase and inhibiting Ca^{2+} release (Gong, Sun et al. 2002). Accordingly, β-adrenergic stimulation is impaired in human HF. β-AR blockers improve failing heart function by reducing the effect of catecholamines on AR in the heart (Shin and Johnson 2007), reducing Ca^{2+} release and increasing $[Ca^{2+}]_L$ in diastole. Several recent studies demonstrated the effect of β-adrenergic stimulation on cardiomyocytes from healthy and failing hearts in terms of contraction and relaxation. The effects of adrenergic stimulation on key proteins such as cAMP, PLB, troponin I, and C-protein involved in the β-adrenergic stimulation pathway, were measured (Kilts, Gerhardt et al. 2000; Molenaar, Bartel et al. 2000; El-Armouche, Zolk et al. 2003; Molenaar, Savarimuthu et al. 2007). Although the effects of phosphorylation during combined β_1- and β_2-AR stimulation on RyR2 activity have been measured in non-failing rat hearts (Li, Imtiaz et al. 2013), it is not known if β_1- and β_2-AR stimulation each has a different effect on RyR2 function in human, nor how they are altered in HF.

Although it is agreed that increased RyR2 phosphorylation in HF is important in pathological Ca^{2+} signalling, research groups are divided on the phosphorylation mechanism and whether RyR2 phosphorylation causes dissociation of FKBP12.6 from RyR2 (Bers, Eisner et al. 2003; Dulhunty, Beard et al. 2007). Several recent studies

demonstrated the role of PKA in RyR2 hyperphosphorylation in HF (Kushnir, Betzenhauser et al. ; Lehnart, Wehrens et al. 2005; Wehrens, Lehnart et al. 2006). PKA hyperphosphorylation of RyR2 has been detected in different failing hearts including human (Reiken, Gaburjakova et al. 2003). Wehrens *et al.* (Wehrens, Lehnart et al. 2006) have used a knock-in-mouse with a Ser^{2808} mutation site (RyR2-S2808A) in which the RyR2 cannot be PKA phosphorylated, to show the importance of Ser^{2808} in HF. They found that the channel was no longer phosphorylated by PKA, suggesting that Ser^{2808} is the major PKA phosphorylation site. Moreover, they demonstrated that the channel had normal levels of FKBP12 associated with RyR2 and the mice did not develop HF symptoms. However, other groups reported no changes in Ser^{2808} phosphorylation in HF using the paced dog model (Jiang, Lokuta et al. 2002; Xiao, Jiang et al. 2005) and a different residue, Ser^{2030}, showed increased phosphorylation by PKA in response to β-adrenergic receptor stimulation (Xiao, Zhong et al. 2006) (Figure 1.10).

It has been proposed that reduction in PP1 and PP2A levels in the RyR2 macromolecular complex (from human failing heart (Marx, Reiken et al. 2000), paced dog model (Marx, Reiken et al. 2000; Yano, Ono et al. 2000), and rabbit model (Ai, Curran et al. 2005)) rather than increased PKA activity appear to be responsible for the RyR2 hyperphosphorylation and the formation of 'leaky' channels (Marks 2003). In addition, reduction in PDE4D3 (metabolises cAMP) levels in human HF leads to an increase in the level of cAMP (activates PKA) which in turn results in RyR2 hyperphosphorylation via PKA. Moreover, PDE4D3-deficient mice have been shown to develop cardiomyopathy (Lehnart, Wehrens et al. 2005).

However, several more recent investigations proposed that CaMKII rather than PKA was important for RyR2 modulation and developing HF (Belevych, Terentyev et al. ; van Oort, McCauley et al. 2010). High levels of CaMKII expression and activity have been reported in animals and patients (Hoch, Meyer et al. 1999; Hagemann, Bohlender et al. 2001; Ai, Curran et al. 2005; Curran, Hinton et al. 2007). In animal models of HF, several recent studies demonstrated that increased CaMKII activity was associated with increased SR Ca^{2+} leak (Ai, Curran et al. 2005; Bers 2006; Guo, Zhang et al. 2006; van Oort, McCauley et al. 2010). This leak was prevented by CaMKII inhibition (using KN-

93 inhibitor) but not by PKA inhibition (using H-89) and that such inhibition can stop the progression to HF (Ling, Zhang et al. 2009; Sag, Wadsack et al. 2009). A knock-in mouse model of constitutive hyperphosphorylation of S^{2814} has shown direct evidence for enhanced RyR2 open probability using single channel recordings in planar lipid bilayers (van Oort, McCauley et al. 2010). Recent investigations have shown that the excessive diastolic Ca^{2+} release 'leak' via CaMKII hyperphosphorylated RyR2, leads to excess Ca^{2+} sparks (van Oort, McCauley et al. 2010), increased plasma membrane afterdepolarizations (Bers and Guo 2005) and lethal ventricular arrhythmias (Bell, Curl et al. 2012). However, other recent studies showed that CaMKII might not have an equal role in all types of HF. Toischer *et al.* (Toischer, Rokita et al. 2010) detected differences in the molecular signalling of HF development in mice with elevated afterload due to transverse aortic constriction (TAC) and elevated preload with aortocaval shunt. They found that activation of CaMKII is involved in the development of HF following TAC, but not in preload with aortocaval shunt. Wehrens and his co-workers have shown that increased RyR2 phosphorylation via CaMKII has a key role in HF progression in non-ischaemic forms of HF in both human and mice (Respress, van Oort et al. 2012). In contrast, the importance of CaMKII oxidation in developing arrhythmias and HF has been shown in ischemia-reperfusion injury (Bell, Curl et al. 2012). Additional mechanisms that involve CaMKII activation include beta-adrenergic stimulation (Gao, Singh et al. 2011) and possible molecular cross-talk between CaMKII and PKA that affects RyR2 function (Valverde, Tortelote et al. 2005). As yet, precise roles for PKA and CaMKII phosphorylation of RyR2s in HF are not clearly determined.

HF also involves defects in phosphorylation of other proteins involved in ECC during adrenergic stimulation. Increased LTCC activity (phosphorylation contributed to adrenergic responsiveness) as a consequence of decreased LTCC density has been reported in failing human heart (Chen, Piacentino et al. 2002). PLB hypophosphorylation has been shown in HF, which may account for decreased SR Ca^{2+} uptake (Dash, Frank et al. 2001; Reiken, Lacampagne et al. 2003; Bers 2006). One possible mechanism of PLB hypophosphorylation may be an increased PLB dephosphorylation rate via PP1 (Pathak, del Monte et al. 2005).

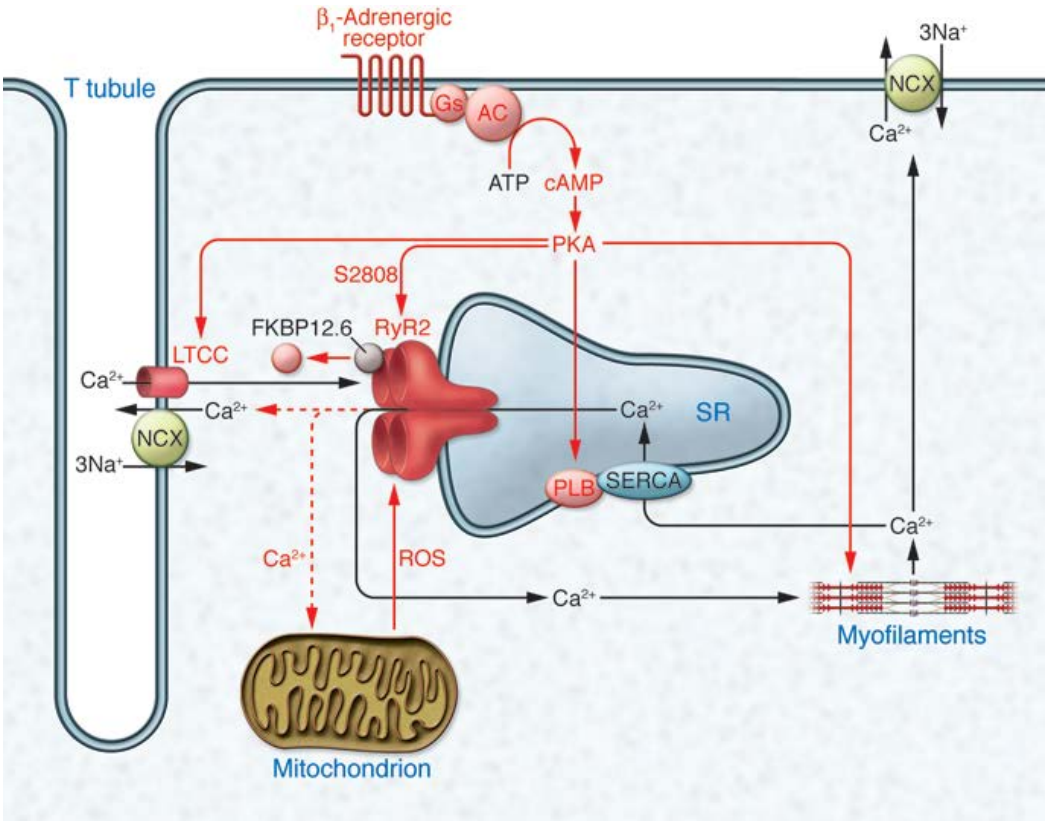

Figure 1.10: The leaky RyR2 hypothesis: According to Marks and colleagues, catecholamines control excitation contraction coupling gain not only at the level of LTCCs and PLB, but also at the level of RyR2 by phosphorylation at S^{2808}. The latter reduces RyR2 affinity for the stabilizing accessory protein, FKBP12.6, and increases its open probability. In HF, sustained catecholamine stimulation leads to hyperphosphorylation, leaky RyR2, spontaneous Ca^{2+} release and, via NCX, spontaneous depolarisations (Eschenhagen 2010).

1.12.2 The role of FKBP12.6 (Calstabin) loss in RyR2 dysfunction

In addition to stabilizing RyR2 channel function, two bilayer studies from one group suggest that FKBP12.6 may act as a mediator of "coupled gating" between adjacent RyRs (Marx, Gaburjakova et al. 2001). Coupled gating means that the opening and closing of one RyR2 regulate the gating of neighbours via protein-protein interactions. Removal of FKBP12.6 from coupled RyRs leads to functional uncoupling that can be restored by the addition of FKBP12.6. (Marx, Gaburjakova et al. 2001). It has been shown that FK506 treated cardiomyocytes exhibits an alteration in Ca^{2+} spark amplitude and duration (Xiao, Valdivia et al. 1997) which is consistent with the idea that FK506 dissociates FKBP from the RyR2 which in turn activates the RyR2 and causes channel uncoupling. Addition of FKBP12.6 to FK506 treated channels decreases the RyR2 open probability and restores normal gating properties (Marx, Reiken et al. 2000). Two major changes within the RyR2 complex may contribute to FKBP12.6 dissociation from the RyR2: either a change in the binding affinity to FKBP12.6 or a reduction in FKBP12.6 concentration. Using surface plasmon resonance to measure the binding interaction between RyR2 and FKBP12.6, Jones *et al.* (Jones, Reynolds et al. 2005) found that the affinity of closed RyR2 for FKBP12.6 is higher than open RyR2. These findings indicate that a conformational change within the RyR2 when phosphorylated, which favours the open channel conformation, reduces FKBP12.6 affinity for the RyR2 channel (Jones, Reynolds et al. 2005) (the hyperphosphorylation hypothesis discussed below). It has been argued that FKBP12.6 binding to RyR2 has an important role in minimizing Ca^{2+} release from the SR during diastole (Wehrens, Lehnart et al. 2003). Dissociation of FKBP12.6 from RyR2 has been reported to increase RyR2 activity (Ahern, Junankar et al. 1994; Kaftan, Marks et al. 1996).

Measuring the ratio of [^{3}H]ryanodine and [^{3}H]dihydro-FK506 binding sites provides an estimate of the molar ratio of FKBP per RyR2 which is about 3.6 in normal SR vesicles (~ 4 FKBP/RyR2) (Yano, Ono et al. 2000; Guo, Cornea et al. 2010). Failing heart exhibits a reduction (~ 38%) in the molar ratio of FKBP per RyR2 (1.6 molar ratios ~ 2 to 3 FKBP molecules have been lost) (Yano, Ono et al. 2000; Ai, Curran et al. 2005).

The hyperphosphorylation hypothesis, proposed by Marx *et al.* (Marx, Reiken et al. 2000), states that PKA mediated hyperphosphorylation of the RyR2 is responsible for

dissociation of the regulatory protein FKBP12.6 from the RyR2 complex and that this leads to increased opening of the channel and increased diastolic Ca^{2+} leak (Marx, Reiken et al. 2000). Single channel studies of RyR2s from human and dog failing myocardium tissues revealed that RyR2s from these failing hearts exhibited the same alterations in single channel properties as the PKA phosphorylated RyR2. These alterations included increased RyR2 open probability, increased sensitivity to Ca^{2+}–induced activation and increased presence of subconductance states that were similar to those seen during dissociation of FKPB from PKA phosphorylated channels (Marx, Reiken et al. 2000). The loss of FKBP12.6 from RyR2 via PKA hyperphosphorylation in HF may result in the loss of coupled gating of RyR2s which in turn may result in the defective closure of RyR2 channels and SR Ca^{2+} depletion (Marx, Gaburjakova et al. 2001). On the other hand, one study using human and canine failing hearts showed no difference in Ca^{2+} sensitivity of RyRs between failing and non-failing hearts and channel gating was the same in control and failing heart RyR2 (Jiang, Lokuta et al. 2002).

Although FKBP12.6 association with RyR2 is reduced in HF (50% in paced dog (Marx, Reiken et al. 2000), 65% in human (Marx, Reiken et al. 2000), and 38% in rabbit (Ai, Curran et al. 2005)), the role of FKBP12.6 in RyR2 modulation remains highly controversial. It has been shown that the expression of RyR2 in HF does not differ from control, although the expression of FKBP12.6 associated with RyR2 was significantly decreased in HF (~ 49% reduction) (Hu, Shen et al. 2010). However, recent studies demonstrated that phosphorylation at Ser^{2808} did not cause FKBP12.6 dissociation from the RyR2 (Xiao, Sutherland et al. 2004), and the constitutive phosphorylation of Ser^{2808} by mutations (S^{2808D}) failed to dissociate FKBP12.6 from the RyR2 complex (Jiang, Lokuta et al. 2002; Stange, Xu et al. 2003; Xiao, Sutherland et al. 2004; Xiao, Jiang et al. 2005; Yano 2005; Benkusky, Weber et al. 2007; Guo, Cornea et al. 2010; Shan, Betzenhauser et al. 2010). In addition, Guo *et al*. (Guo, Cornea et al. 2010) have found that the quantity of FKBP12.6 is much lower than RyR2 and therefore only a small portion of RyR2 molecules (about 15%) are bound to FKBP12.6. Moreover, they found that FKBP12 is more abundant than FKBP12.6 and does not dissociate from RyR2 complex as a consequence of PKA phosphorylation. Together, these results suggest that the FKBP12.6 binding to RyR2 is not affected by PKA phosphorylation of S^{2808} on

RyR2s. However, this finding leaves the possibility that binding of FKBP12.6 to the RyR2 complex has a small role in RyR2 modulation in failing and non-failing hearts (Houser 2010). Shan *et al.* (Shan, Betzenhauser et al. 2010) used RyR2-S2808D+/+ mice, mimics of constitutive PKA hyperphosphorylation, to explore the role of chronic PKA phosphorylation of RyR2 in HF pathogenesis. They detected a modest (~20%) depletion of FKBP12.6 from RyR2-S2808D$^{+/+}$ in 6-week-old mice whereas depletion of FKBP12.6 in 1-year-old RyR2-S2808D$^{+/+}$ mice was complete. These data suggest that other changes of the RyR2 combined with PKA phosphorylation to cause FKBP12.6 depletion from RyR2s. RyR2-S2808D+/+ mice also developed age-dependent cardiomyopathy and elevation in oxidation and nitrosylation levels. Taken together, these findings indicated that PKA phosphorylation of oxidized and/or nitrosylated RyR2 causes FKBP12.6 depletion from the RyR2 complex.

1.12.3 RyR2 oxidation, phosphorylation, FKBP12.6 loss and domain unzipping in HF

Changing the phosphorylation status of RyR2s is not the only modification that could modulate RyR2s in failing heart (Oda, Yano et al. 2005; Yano, Okuda et al. 2005). In addition to many phosphorylation sites, the RyR2 also contains about 84 free thiols (Xu, Eu et al. 1998) and several cysteine residues that are susceptible to modulation by redox modifications, including disulfide crosslinking, S-nitrosylation, and S-glutathionylation (Sun, Xin et al. 2001). Reactive oxygen species (ROS) produced during the development of HF might be created by mitochondrial Ca^{2+} overload during Ca^{2+} sequestration from the cytosol as a consequence of SR Ca^{2+} uptake down-regulation (Ide, Tsutsui et al. 1999). Growing evidence suggests that modification of RyR2s by oxidative stress contributed to abnormal Ca^{2+} handling associated with HF (Belevych, Terentyev et al. ; Gyorke and Carnes 2008). One possible mechanism for this modulation is a conformational change in the RyR2 since defective interdomain interaction associated with abnormal Ca^{2+} leak already takes place in HF (Yano, Okuda et al. 2005; Shan, Betzenhauser et al. 2010). Using co-immunoprecipitation assays, Zissimopoulos *et al.* (Zissimopoulos, Docrat et al. 2007) found that oxidation of RyR2 by the oxidizing agent H_2O_2, reduces the binding of FKBP12.6 to the channel by 25-

50%. Furthermore, Wehrens *et al*. (Wehrens, Lehnart et al. 2005) showed a reduced FKBP12.6 binding affinity in RyR2 channels harbouring mutations in the N-terminal and central domain for CPVT. RyRs from pacing-induced failing dog hearts exhibit domain unzipping (detected by the increase in the accessibility of labelled RyR2 to a fluorescence quencher) coupled with FKBP12.6 dissociation and Ca^{2+} leak. Inhibition of FKBP12.6 dissociation in these experiments by S107 rescued cardiac function (Shan, Betzenhauser et al. 2010) indicating a critical role of FKBP12.6 in preventing Ca^{2+} leak and domain unzipping.

It has been suggested that phosphorylation at S^{2808} alone is not sufficient to dissociate FKBP12.6 from the RyR2 but that it needs oxidation of the channel plus phosphorylation (Eschenhagen 2010). Shan *et al.* (Shan, Betzenhauser et al. 2010) proposed that oxidation of the RyR2, associated with PKA hyperphosphorylation, accounts for reduced binding of FKBP12.6 to the RyR2 complex. Depletion of FKBP12.6 from RyR2s is age-dependent which can be explained by the progressive age-dependent oxidation of RyR2 (Shan, Betzenhauser et al. 2010), suggesting that HF is an age-dependent disease and most likely to occur in elderly people. Taken together; domain unzipping, hyperphosphorylation, and FKBP12.6 dissociation from the RyR2 complex, play a key role in ryanodine channel dysfunction in HF (Yano, Okuda et al. 2005).

1.12.4 Intracellular Mg^{2+} deficiency

Abnormalities in Mg^{2+} metabolism and deficiency states play a key role in the aetiology of many heart diseases including HF (Chakraborti, Chakraborti et al. 2002). Deficiencies of intracellular Mg^{2+} ions can lead to abnormalities in myocardial membrane potential, which then cause cardiac arrhythmias (Chakraborti, Chakraborti et al. 2002). A number of studies have reported a reduction in cardiac Mg^{2+} concentrations in patients with HF compared to healthy controls (Haigney, Wei et al. 1998; Chakraborti, Chakraborti et al. 2002). Since Mg^{2+} is a competitive inhibitor at Ca^{2+} activation sites, reduction in intracellular Mg^{2+} causes an increase in Ca^{2+} release from the SR. Also, a reduction in the intracellular free Mg^{2+} may contribute to the unstable

repolarisation and prolonged APs (Haigney, Wei et al. 1998). Haigney *et al.* (Haigney, Wei et al. 1998), using a paced dog experimental model, showed a 50% decrease in $[Mg^{2+}]_i$ compared with control dogs. Given the role of Mg^{2+} in preventing Ca^{2+} release during diastole, a 50% reduction in $[Mg^{2+}]_i$ could contribute to aberrant Ca^{2+} release in HF. Low intracellular $[Mg^{2+}]$ induces an increase in intracellular $[Ca^{2+}]$ from 50 to 200 nM, and formation of reactive oxygen species (Chakraborti, Chakraborti et al. 2002). Increased intracellular $[Ca^{2+}]$ activates NCX activity (NCX up-regulation) as presented by increased outward I_{NCX} (Wei, Quigley et al. 2002). Marks and his co-workers have found that mutant RyR2 from familial polymorphic ventricular tachycardia (FPVT) showed less sensitivity to Mg^{2+} inhibition associated with a significant gain-of-function defect (Lehnart, Wehrens et al. 2004). These data suggest that reduced Mg^{2+} sensitivity might play a role in RyR2 dysfunction. It has been also shown that phosphorylation of RyRs either by PKA or CaMKII can overcome Mg^{2+} block of RyR2 (Hain, Onoue et al. 1995). As RyR2 is hyperphosphorylated in HF, it is quite possible that Mg^{2+} sensitivity is affected.

1.12.5 Increased RyR2 sensitivity to luminal Ca^{2+}

The frequency of spontaneous Ca^{2+} release events (Ca^{2+} sparks and waves) in isolated quiescent myocytes is increased as a result of elevations in SR Ca^{2+} load under stressful conditions such as, β-adrenergic stimulation (Cheng, Lederer et al. 1996). Some studies showed that the reduction in SR Ca^{2+} load in HF does not prevent an increase in the Ca^{2+} release frequency because of chronic phosphorylation of the RyR2 (Maier, Zhang et al. 2003; Kubalova, Terentyev et al. 2005; Song, Pi et al. 2005), suggesting that phosphorylation modulates RyR2s by increasing its sensitivity to luminal calcium (Wehrens, Lehnart et al. 2003; Wehrens, Lehnart et al. 2004; Wehrens, Lehnart et al. 2004; Kubalova, Terentyev et al. 2005; Xiao, Tian et al. 2007). One study that used single channel measurements of RyR2 function using a canine model of chronic tachypacing, induced HF to demonstrate increased sensitivity of RyRs to luminal Ca^{2+} (Kubalova, Terentyev et al. 2005). They compared the sensitivities of RyR channels, from normal and failing canine hearts, to luminal Ca^{2+} using the lipid bilayer technique. Single-channel recordings made at different luminal Ca^{2+} concentrations and in the

presence of Mg^{2+} and ATP, showed that RyR sensitivity to luminal Ca^{2+} is higher in HF (a shift towards lower concentrations in comparison with controls). The chronic hyperadrenergic state accompanying HF may have a role in increased sensitivity of RyR2 to luminal Ca^{2+}.

1.13 Therapeutic strategies that target RyR2 dysfunction in HF

HF therapies targeted to the RyR rely on the hypothesis that defective interdomain interaction (unzipping of domain binding regions) in RyR2s is a key point in the progression of heart disease. According to this hypothesis, a drug that could reduce SR Ca^{2+} leak by modulating (stabilizing) RyR2s, rather than blocking the channel, will prevent the progression of HF (George and Lai 2007; Shannon and Lew 2009). Some drugs such as beta-blockers, antioxidants, and JTV519 (K201), have already been developed to stabilize RyR2-dependent Ca^{2+} leak.

1.13.1 β-blockers

Large clinical trials in the mid-1990s showed that treatment with β-blocker drugs enhances heart contractility (restoring cardiac function) and reduces mortality in patients with failing heart (Packer, Bristow et al. 1996; Packer, Coats et al. 2001; Yano 2005). Several researchers have reported that β-blockers restore normal RyR2 channel function, decrease the hyperadrenergic effect and PKA-mediated hyperphosphorylation, restore the RyR2 zipped state and inhibit diastolic Ca^{2+} leak via RyR2s (Reiken, Gaburjakova et al. 2001; Reiken, Wehrens et al. 2003). One possible mechanism of β-blockade may be a reduction in RyR2 open probability and sensitivity to luminal Ca^{2+} (enhanced SR accumulation) and a decrease in heart rate (Cheng, George et al. 2007). It has been shown that bisprolol and carvedilol β-blockers are very effective in slowing the progression of HF and reducing arrhythmia (McGavin and Keating 2002; Poole-Wilson, Swedberg et al. 2003; Hori, Sasayama et al. 2004). A recent study has shown that the anti-arrhythmic effect of carvedilol is via reducing the open duration of the

RyR2 (Zhou, Xiao et al. 2011). Propranolol has been shown to reduce RyR2 hyperphosphorylation and restore FKBP12.6 binding levels in a paced dog model (Reiken, Gaburjakova et al. 2001). Same effect has been achieved using human heart muscle strips treated with carvedilol, metoprolol or atenolol (Reiken, Wehrens et al. 2003). However, unacceptable side effects such as bradycardia may be a drawback to β-blocker treatment (White, Yanowitz et al. 1995).

1.13.2 Free radical scavengers

Free radical scavengers, a promising therapeutic strategy in HF, prevent the development of HF via correction of several problems within the RyR2 associated with failing heart (Yano, Okuda et al. 2005). As described above, ROS scavengers reduce ROS and redox-dependent Ca^{2+} leak by restoring the zipped state of RyR2s, prevention of FKBP12.6 dissociation from the channel, decrease in PKA phosphorylation and enhancement of the channel function in HF (Choudhary and Dudley 2002; Mochizuki, Yano et al. 2007; Terentyev, Gyorke et al. 2008).

1.13.3 JTV19 as a RyR2 stabilizer

A new compound, JTV519 (1,4-benzothiazepine derivative), was recently found to improve contractility by stabilizing domain interactions (zipped state) in RyR2s (Yano, Kobayashi et al. 2003). The JTV519-binding site has been identified close to the central domain in the zipper region within domain 2114-2149 (Yamamoto, Yano et al. 2008). Binding of JTV519 to this site strongly stabilized the channel in the zipped state to prevent Ca^{2+} leak even though much of the FKBP12.6 would already have been dissociated from the RyR2 in HF (Lehnart, Wehrens et al. 2004; Oda, Yano et al. 2005; Yamamoto, Yano et al. 2008). JTV519 inhibited both the FK506-induced Ca^{2+} leak in normal heart and the spontaneous Ca^{2+} leak in failing heart (Yano, Kobayashi et al. 2003). Inhibition of Ca^{2+} leak was not due to rebinding of FKBP12.6 to RyR2 but to stabilizing the domain interaction (Oda, Yano et al. 2005). Phosphorylation levels in HF also returned toward the levels seen in normal heart following JTV519 treatment (Yano, Kobayashi et al. 2003). It has been shown that JTV519 action is not mediated by

rebinding of FKBP12.6 to the RyR2. The amount of RyR2-FKBP12.6 bound remained the same in the presence or absence of JTV519 (Oda, Yano et al. 2005), suggesting that changing the FKBP12.6 binding site as a consequence of RyR2 conformational change in HF, prevented rebinding of FKBP12.6 to the RyR2 (Zissimopoulos, Docrat et al. 2007). These findings suggest that the action mode of JTV519, like that of FKBP12.6, is to stabilize the interactions between domains and prevent SR Ca^{2+} leak.

1.13.4 Flecainide

Flecainide is a sodium channel blocker that also inhibit the opening of RyR2 in the SR (Anderson, Gilbert et al. 1989) . Flecainide has been used as antiarrhythmic drug to treat a variety of cardiac arrhythmias including atrial fibrillation and ventricular tachycardia (Apostolakis, Oeff et al. 2013). Flecainide prolongs the refractory period (Seipel, Abendroth et al. 1981) by inducing 'post-repolarization refractoriness' rather than by prolongation of the action potential (Neuss and Schlepper 1988). However, the toxicity effect of flecainide has put a limitation in its use as a treatment, which could be demonstrated by prolongation of the PR interval and widening of the QRS duration on the surface ECG (Winkelmann and Leinberger 1987). Moreover, Flecainide has a very high affinity for lung tissue, which is associated with drug-induced interstitial lung disease (Pesenti, Lauque et al. 2002; Camus, Fanton et al. 2004).

1.14 Aims and Hypothesis

1.14.1 Hypothesis: The response of the RyR2 to remodelling during HF critically depends on ionic conditions including altered intracellular [Ca^{2+}] and [Mg^{2+}].

RyR2 dysfunction resulting from pathological phosphorylation in HF is due to differences in (a) intracellular [Ca^{2+}] and [Mg^{2+}], (b) the response of RyR2 to changes in these ion concentrations and (c) change in RyR2 structure, including phosphorylation, and RyR association with co proteins.

1.14.2 Aims

The first specific aim in this thesis was to present a detailed analysis of the regulation of healthy human RyR2s by intracellular Ca^{2+} and Mg^{2+}. This study presents the first measurements of the concentration dependencies of human RyR2 regulation by luminal and cytoplasmic Ca^{2+} and Mg^{2+}. A theoretical model of Ca^{2+} and Mg^{2+} regulation of sheep RyR2 was used as a framework to understand how Ca^{2+} and Mg^{2+} regulate RyR2s in healthy human heart and how it may differ from that of established experimental animal models such as sheep and rat hearts.

The second specific aim was to determine if aberrant Ca^{2+} signalling in human HF can be understood in terms of the same RyR2 regulation mechanisms (*i.e.* phosphorylation and Ca^{2+}/Mg^{2+} regulation) identified in healthy human heart. How much would altered intracellular Ca^{2+} and Mg^{2+} alone account for mis-regulation of RyR2s in failing human heart?

The third specific aim is to determine how the human RyR2 complex is remodelled during HF.

The fourth specific aim was to understand how CaM regulates RyR2 in healthy and failing human hearts.

Chapter 2- Methods

2.1 Source of heart tissue

Human tissues were obtained with approval from the Human Research Ethics Committees of both the University of Newcastle (approval number H-2009-0369) and the University of Sydney (approval number #09-2009-12146). Table 2.1 summarizes the characteristics of donor hearts (failing and non-failing human hearts) used in this study. Non-failing human left ventricle tissue was obtained from 'unused' donor hearts. These hearts were collected at the site of organ donation by the St Vincent's Hospital (Darlinghurst) surgical team following the declaration of brain death by the transplant coordinator. The hearts were flushed with ice-cold cardioplegia, packaged under sterile conditions, transported by the Australian Red Cross Blood Service and delivered to the Bosch Institute. These hearts were not required for orthotopic heart transplantation for a range of reasons, such as tissue incompatibility. Transmural sections of left ventricle free wall (~1 gm) were snap frozen in liquid nitrogen (-196°C) not more than four hours, and usually within three hours.

One heart was harvested from a patient with cystic fibrosis (an autosomal recessive genetic disorder affecting most critically the lungs) undergoing combined heart-lung transplantation at The Prince Charles Hospital (The Prince Charles Hospital Health Service District Human Research Ethics Committee approval EC28114). Echocardiography showed normal left and right ventricular size and function (left ventricular ejection fraction 55%), normal atrial size and normal valves. This patient was not being medicated for any cardiac conditions.The heart was designated for transplant but no suitable recipient was found on the day of explant.

Hearts were also obtained from a patient with Emery Dreifuss Muscular Dystrophy with cardiomyopathy (a condition that chiefly affects skeletal and cardiac muscle) and two patients with Ischaemic cardiomyopathy at the time of explantation. Failing heart tissue was obtained from explanted hearts from patients with terminal HF undergoing heart transplantation (at The Prince Charles Hospital). Tissue was snap frozen in liquid N_2 within 40 min of explantation.

Table 2.1

Sample		Sex	Age	Aetiology	Source
Healthy hearts	6.008	M	40	Stroke	U Syd
	6.028	F	62	Not recorded	U Syd
	7.012	M	19	Motor cycle accident	U Syd
	6.048	F	54	Subarachnoid haemorrhage	U Syd
Cystic fibrosis heart	CF	F	30	Cystic fibrosis	TPCH
Failing hearts	EDMD	M	25	EDMD	TPCH
	ICM	M	58	ICM	TPCH
	ICM Trabecule	*	*	ICM	TPCH

Table 2.1 Characteristics of patients. U Syd patients were brain dead, TPCH patient underwent heart-lung transplantation. LV- left ventricle, RV- right ventricle, *age and sex of patient are not indicated because the SR vesicles were obtained from 15 patients, U Syd (University of Sydney), TPCH (The Prince Charles Hospital).

2.2 Preparation of SR Vesicles

Heart muscle was minced and homogenized in a Waring blender (4 ✕ 15 sec bursts at high speed) in homogenizing buffer containing 0.3 M sucrose, 10 mM imidazole, 0.5 mM dithiothreitol (DTT), 3 mM sodium azide, and 20 mM NaF; pH 6.9, plus the protease inhibitors, 0.5 mM phenylmethylsulfonylfluoride (PMSF), 1 µg/ml leupeptin, 1 µg/ml pepstatin A, 1 mM benzamidine. NaF was used to prevent ongoing activity of phosphatases during RyR isolation. The homogenate was further homogenised by 10 manual strokes of a loose glass/glass Dounce homogenizer. The homogenate was centrifuged at 8,000 g for 20 minutes using a Beckman Optima L-100XP ultracentrifuge to sediment cell debris and connective tissue. The supernatant was then centrifuged at 170,000 g for 30 minutes to collect the cell microsomes. The resultant pellet was resuspended with homogenizing buffer containing 0.65 M KCl using a glass/glass Dounce homogenizer, incubated for 30 minutes on ice and then centrifuged at 8,000 g for 15 minutes to sediment myosin. The supernatant was centrifuged at 170,000 g for 1 hour and the pellet, containing SR vesicles, was resuspended in storage buffer (homogenizing buffer + 0.65 M KCl), snap-frozen in liquid nitrogen and stored at -80°C.

2.3 Single channel recording

2.3.1 Planar lipid bilayer

The bilayer rig was comprised of apparatus to support the lipid membrane, high gain amplification of signals, shielding from electromagnetic interference and mechanical vibration, mechanisms for stirring and changing solutions, signal filtering, data acquisition hardware and software, data analysis software, and a means to archive acquired data. A schematic representation of the bilayer setup and current recording system is shown in Figure 2.1.

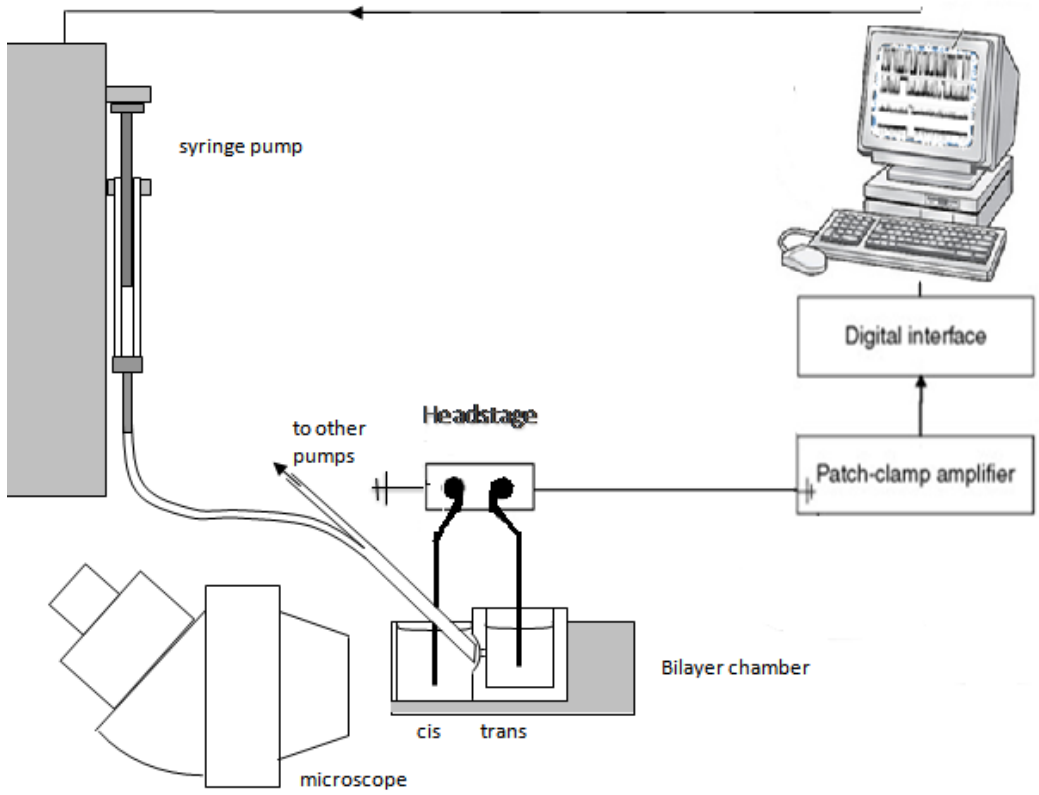

Figure 2.1: Cartoon diagram of the bilayer setup and current recording system. The bilayer chamber consisted of *cis* and *trans* baths separated by a partition on which the bilayer was formed. A Delrin cup formed the inner compartment and contained the *trans* bath. The outer compartment (*cis* bath) was made from either glass or Delrin. A hole formed by spark discharge was punched into the side of the inner chamber to produce the support for the bilayer. The bevelled PVC nozzle of the perfusion tube was positioned over the bilayer using a micromanipulator. The nozzle was connected via quartz tubing (300 µm i.d.) and micro manifold (2 µl dead space) to 8 glass syringes with Teflon pistons. The bath partition near the bilayer aperture had a large portion of the lateral wall machined away to provide adequate access for the perfusion tube and flow solution. The bilayer membrane and perfusion tube were viewed under a 10–40× binocular microscope. Electrical connection with the bath was made using silver chloride coated silver wire. The *cis* chamber was electrically grounded to prevent the tubing leading to the flow nozzle, the reservoir and the solution they contained, from becoming a source of electrical interference. Voltage was controlled and current recorded with an Axopatch 200B amplifier (Axon Instruments). During the experiments the bilayer current and voltage were recorded at a bandwidth of 5 kHz. (Modified from (Laver 2009)).

2.3.1.1 Membrane formation and vesicle fusion

In 1976, Millar and Racker (Miller and Racker 1976) discovered that the SR vesicles isolated from muscle could be fused and incorporated into an artificial lipid bilayer. Artificial lipid bilayers were formed from phosphatidylethanolamine and phosphatidylcholine (8:2 wt/wt) in n-decane (a hydrophobic solvent, 50 mg/ml). The lipid was applied to an aperture in a Delrin cup using a glass rod with a small (1-2 mm) ball formed on the end with a Bunson burner. This produced a thick lipid film separating the two baths. The bilayer can be observed either visually by using the microscope (the lipid film will be bright as a consequence of light reflection (Figure 2.2) or electrically by measuring the bilayer capacitance (measured by the amplitude of a rectangular current signal in response to a triangular voltage wave). The capacitance value is up to 200 pS for fully-formed lipid bilayers depending on the area of the bilayer across the aperture. The geometry of the aperture is important to the stability of the painted membrane. If the hole diameter is small then the membrane formed will be mechanically robust and the electrical noise is reduced, whereas, a larger hole diameter increases electrical noise and is mechanically more fragile. The probability that a vesicle will fuse to the membrane is inversely proportional to the membrane size.

Electrical connections into each chamber were made with silver chloride coated silver electrodes to transduce ionic currents in the electrolyte solution to an electron current within the wire. This was done by utilizing a reversible oxidation/reduction reaction between the silver in the electrode and Cl- ions in the bath. The chemical reaction is:

$$Cl^{-} + Ag^{+} \longrightarrow AgCl + e^{-}$$

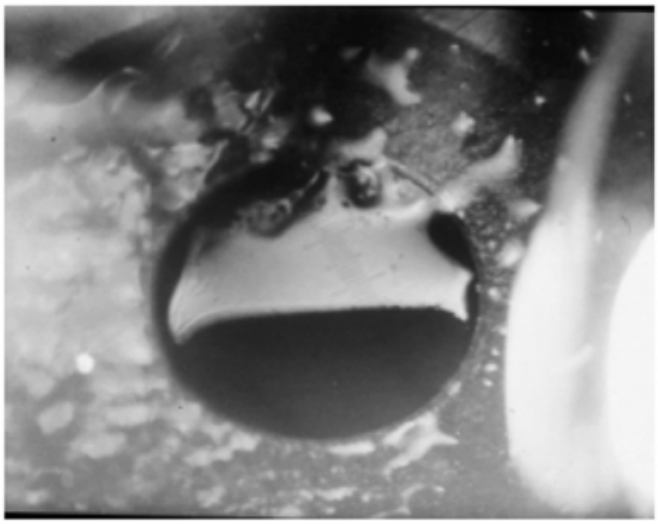

Figure 2.2: A photograph of a lipid bilayer (bottom half of aperture) during its formation from a thick lipid film (top half). The lipid film was spread across an aperture (approximately 100 μm diameter) in a Delrin septum. The thick lipid film strongly reflects the incident light, whereas the bilayer, which shows the black background, is totally transparent. The bilayer portion of the film spreads across the entire aperture in a few seconds, leaving a region of thick film at the periphery (Laver 2001).

This chemical reaction is associated with a voltage difference between the silver and the electrolyte that depends on the Cl- concentration. Differences in these potentials at each electrode produced an offset voltage on the lipid bilayer. This offset voltage was nulled in the signal detection amplifier (see below).

The bilayer chambers were mounted above a magnetic stirrer to provide stirring of the cis bath to facilitate fusion of SR vesicles. The bilayer apparatus was enclosed in a copper, mesh Faraday cage to isolate the high impedance electronics from external electrical noise. The bilayer apparatus was mounted on a vibration isolation table to provide long-term mechanical stability for the lipid bilayer.

RyRs from failing and non-failing human hearts were incorporated into the artificial lipid bilayer simply by adding ion channel proteins (1-10 μg/ml) to the *cis* bath and stirring (using magnetic stirrer) until channel activity indicated vesicle fusion with the bilayer (detected by conductance changes in the bilayer membrane). The *cis* bath faces the cytoplasmic side of the membrane and the *trans* bath faces the SR luminal side.

2.3.1.2 Amplification and filtering

Bilayer experiments were carried out on either of two workstations. Control of the bilayer potential and recording of unitary currents was done using either an Axopatch 200B amplifier (Axon Instruments Pty, Ltd CA) or a Warner Instruments bilayer amplifier (BC525C). Electrical potential differences are expressed as cytoplasmic potential relative to the luminal potential (at virtual ground).

The channel currents were recorded during the experiments using a 50 kHz sampling rate and 5 kHz low pass filtering. The recordings were stored on computer disk using a data interface (either Data Translation DT301 or DT3001) under the control of in-house software written in Visual Basic by Dr D.R. Laver (University of Newcastle, Australia). Before analysis the current signal was re-digitized at 5 kHz and low pass-filtered at 1 kHz with a Gaussian digital filter.

2.3.1.3 Bathing solutions

During vesicle fusion the *cis* solution contained 250 mM Cs^+ (230 mM cesium methane sulfonate ($CsCH_3O_3S$), 20 mM CsCl), 1.0 mM $CaCl_2$ and 500 mM mannitol, whilst the *trans* solution contained 50 mM Cs+ (30 mM $CsCH_3O_3S$, 20 mM $CsCl_2$) and 0.1 mM $CaCl_2$. The osmotic potential gradient between *cis* and *trans* solutions and the mM concentrations of Ca^{2+} in the *cis* bath promoted vesicle fusion (Cohen and Niles 1993).

Cesium methane sulfonate was used as the principal salt in the bathing solution in order to prevent current signals from other ion channels interfering with ryanodine receptor recordings. After vesicle fusion and prior to single channel recording, the [$CsCH_3O_3S$] in the *trans* solution was increased to 230 mM by adding an aliquot of 4M $CsCH_3O_3S$ to the *trans* bath (*i.e.*, producing 250 mM Cs^+ in both *cis* and *trans* baths). During recordings, the composition of the *trans* solution was altered by means of aliquot additions of stock solutions and the *cis* solution was exchanged (using advanced perfusion apparatus, see below) for mannitol free solutions with specified free Ca^{2+} and Mg^{2+}, peptides, kinases and phosphatases.

2.3.2 Chemicals and solutions

Lipids, used for planar lipid bilayers, were obtained in chloroform from Avanti Polar Avanti Polar Lipids (Alabama, United States). Cesium salt, used in both *cis* and *trans* chambers, was obtained from Aldrich chemical Company. $CaCl_2$ and $MgCl_2$, were from BDH Chemicals, and TES and ATP were obtained from Sigma.

All solutions were pH buffered using 10 mM TES (N-tris[hydroxymethyl] methyl-2-aminoethanesulfonic acid (ICN Biomedicals) titrated to pH 7.4 using CsOH (ICN Biomedicals). pH was maintained above 7.0, because pH lower than this is known to inhibit channel activity (Laver et al. 2000).

Since RyR activity is sensitive to small changes in redox potential (Feng, Liu et al. 2000; Marinov, Olojo et al. 2007), solutions were buffered to a redox potential of -232 mV (cytoplasmic level) using a combination of oxidized and reduced glutathione disulfide (GSSG (0.2 mM) and GSH (4 mM)). GSH and GSSG are the main intracellular redox buffers (Sies 1999). The ratio of redox buffer was calculated (Hwang, Sinskey et al. 1992; Laver and van Helden 2011) using the Nernst equation to eliminate experimental variations in RyR2 activity.

In this study, Cs^+ was used as the main current carrier because it has a higher conductance (500 ± 12 pS) in the RyR than Ca^{2+} (110 ± 10 pS) (Smith, Imagawa et al. 1988; Tinker and Williams 1992) and therefore increases the current signal and the signal to noise ratio in the recordings.

Some single channel studies use grossly supra-physiological luminal Ca^{2+} (50 mM Ca^{2+}) so that Ca^{2+} is the main current carrier in experiments (Marx, Reiken et al. 2000). The rationale is that Ca^{2+} is the physiological ion. The estimate for free [Ca^{2+}] in the SR ($[Ca^{2+}]_{SR}$) to be about 1 to 1.5 mM during diastole (Shannon, Guo et al. 2003). Therefore, using high concentrations of luminal Ca^{2+} (~50 fold higher than physiological level) in studying Ca^{2+} regulation of RyR2s so far removed from the physiological range of [Ca^{2+}] is problematic.

RyRs are highly permeable to K^+ (Smith, Imagawa et al. 1988). Therefore given the high [K^+] in the cell, K^+ will carry most of the current in vivo. Cs^+ was used as a surrogate for K^+ because it frees the constraints on the Ca^{2+} concentrations used in the studies of Ca^{2+} regulation of RyR2s. In addition, CsMS salt also reduces interfering signals from K^+ and Cl^- channels (Cs^+ blocks K^+ channels (Coronado, Kawano et al. 1992)) located in SR vesicles. Cs^+ is likely to be a good surrogate for K^+ because the Ca^{2+}-dependence of [^{3}H] ryanodine binding indicates that Ca^{2+} regulation of RyR is the same in both K^+ and Cs^+ solutions (Meissner, Rios et al. 1997). The use of Cl^- in both cis and trans solutions stabilises junction potentials between the solutions and the AgCl-coated silver electrodes. Cl^- concentrations were set at 20 mM which is similar to levels present in the cell. The concentration of Cl^- in the solutions is not sufficient to induce openings of Cl^- channels.

Several Ca^{2+} chelators were used to buffer free Ca^{2+} in this study. Free Ca^{2+} buffered using 4.5 mM BAPTA (1,2-bis(o-aminophenoxy) ethane- *N*,*N*,*N*',*N*'-tetraacetic acid obtained (Invitrogen); free [Ca^{2+}] < 1 μM), dibromo BAPTA (up to 2 mM; free [Ca^{2+}] between 1-10 μM) (Harrison and Bers 1987) or sodium citrate (up to 6 mM; free [Ca^{2+}] between 10-50 μM in the absence of Mg^{2+}). Free Ca^{2+} was titrated with $CaCl_2$. Because all solutions applied in the *cis* bath contained ATP (2 mM, ATP chelates Ca^{2+} and Mg^{2+}), free levels of Mg^{2+} (added as $MgCl_2$) were calculated using estimates of ATP purity and effective Mg^{2+} binding constants that were determined previously under our experimental conditions (Laver, O'Neill et al. 2004). Under given conditions of ATP (mM), BAPTA (mM), ionic strength, pH and temperature, free [Mg^{2+}] in the *cis* solution was calculated using Bound And Determined software (Brooks and Storey 1992) which were based on the equations established by Marks P.W. and Maxfield F.R (Marks and Maxfield 1991).

2.3.2.1 Calibration of Ca^{2+} electrode

A Ca^{2+} electrode (Radiometer) was used in our experiments to determine the purity of Ca^{2+} buffers and Ca^{2+} stock solutions as well as free [Ca^{2+}] when [Ca^{2+}] was > 100 nM. A standard $CaCl_2$ solution (100 mM, Fluka) was used to calibrate the Ca^{2+} meter and buffer stock solutions. The calibration of the Ca^{2+} electrode and BAPTA stock solutions was done by titrating $CaCl_2$ standard solutions with BAPTA solutions (a highly selective Ca^{2+} buffer and less sensitive to changes in pH, developed by Tsien in 1980 (Tsien 1980)). The titration was monitored by the Ca^{2+} electrode (Figure 2.3A) and the equivalence point, where the concentration of BAPTA is equal to the concentration of Ca^{2}, indicates a precise estimate of the concentration of the BAPTA stock. The titration curve was also used to calculate the calibration curve for the Ca^{2+} electrode (Figure 2.3B). A subsequent titration, using the calibrated BAPTA solution, was used to calibrate an experimental Ca^{2+}- stock solution.

A

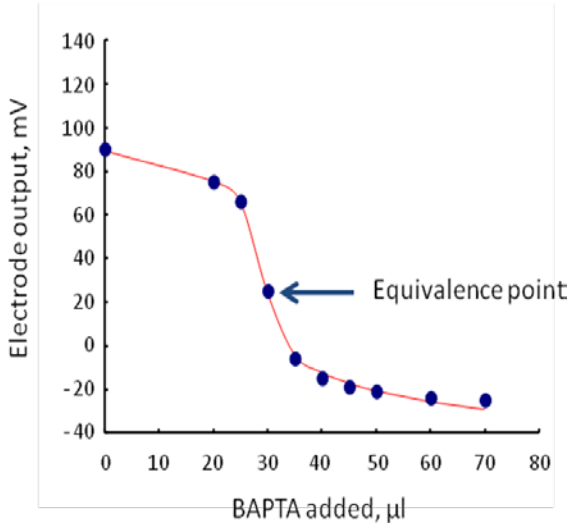

B

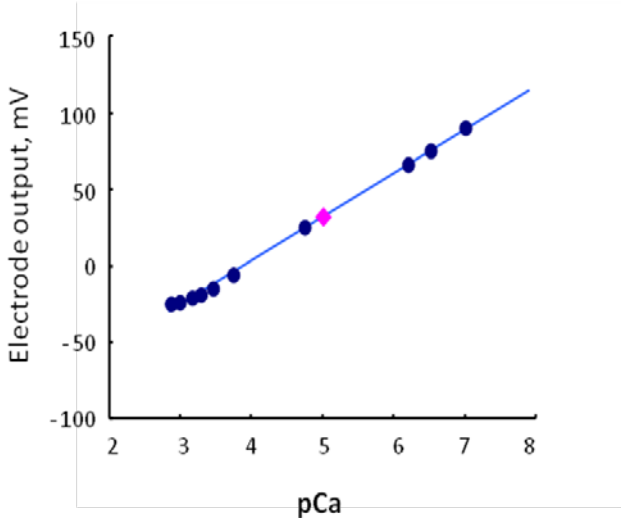

Figure 2.3: Calibration of Ca^{2+} electrode. (A) The measured electrode potential (blue circles) is plotted against the amount of BAPTA added to the *cis* solution initially containing a1 mM Ca^{2+} standard. The theoretical red line shows the electrode potential calculated from the electrode calibration and the dependence of free Ca^{2+} on [$BAPTA_{total}$] and [$Ca^{2+}{}_{total}$]. The concentration of free calcium was calculated using the following quadratic equation:

$$\left[X^{2+}\right] = \frac{-\left([Anion]_T + K_{app} - [X]_T\right) + \sqrt{\left([Anion]_T + K_{app} - [X]_T\right)^2 + 4K_{app}[X]_T}}{2}$$

Where X is Ca^{2+} and the anion is BAPTA in our titration. **(B)** The linear relationship between the electrode potential (blue circles) and Ca^{2+} standards (pCa (–log[Ca^{2+}], M)) is shown by the blue line.

2.3.3 Advanced perfusion methods

The perfusion apparatus consisted of 8 plastic micro-syringes (1 ml-volume) driven by syringe pumps under computer control (Figure 2.4). These syringes were connected with a PVC tube, where the nozzle was positioned in close proximity to the bilayer. Solutions in the syringes flowed over the bilayer by a pressure-driven syringe injection system which could produce solution changes at the nozzle within 1 s. This system allowed flexibility in manipulating the experimental conditions. The response of channels to a variety of substances in the cytosolic and luminal baths could readily be examined. This also allowed measurement of channel function under steady-state conditions or when solutions were rapidly and transiently altered. This design permitted quite sophisticated experimental protocols to obtain detailed information about mechanisms determining channel conductance and gating.

2.4 Biochemical assays

2.4.1 Materials

The mini protein system, Western blot apparatus, TGX pre-poured gels, electrophoresis buffer and protein standards for electrophoresis were obtained from Bio-Rad (Gladesville, Australia). The Novex BOLT electrophoresis system, bis/tris gels, bis/tris and electrophoresis buffer were obtained from Life Technologies (Mulgrave, Australia). Readymatic developer and fixer were obtained from Kodak Dental (Stuttgart, Germany). Immobilon-P PVDF membrane was obtained from Millipore (Billerica, USA). Western blot filter paper and chemiluminescent substrate were obtained from Thermo Scientific (Rockford, USA).

Figure 2.4: Advanced Perfusion system. The apparatus contained 8 plastic syringes, with Teflon pistons, which combined into a micro manifold (2 µl dead space) and connected to a PVC tube via its other side. The bevelled PVC nozzle of the perfusion tube was positioned over the bilayer using a micromanipulator. Once the syringe is selected through the computer, the piston presses down on the syringe and the solution flows through the tube and micro manifold thus perfusing the lipid bilayer.

2.4.2 Antibodies

Antibodies were purchased from the following suppliers: anti-RyR2 phospho-Ser^{2808} (anti pS^{2808}), anti-RyR2 phospho-Ser^{2814} (anti pS^{2814}), anti-RyR2 phospho-Ser^{2030} (anti-pS^{2030}), Anti-SERCA 2A (Badrilla, UK); Anti-RyR PAB17291 (Abnova), Anti-CSQ2 (Thermoscientific), Anti-FKBP 12/12.6 (R&D Biosystems), anti-PP2a (Merck), anti-PP1 (Abcam), anti-triadin-1, anti-NCX, anti-mouse IgG and anti-rabbit IgG (Santa Cruz). Anti-junctin antibody was produced against a small N-terminal peptide and raised in rabbits by IMVS pathology (Adelaide, SA, Australia). All gels and PAGE buffers were obtained from Bio-rad, PVDF membrane was obtained from Millipore, ECL plus chemiluminescence reagent were obtained from GE Healthcare, and the PP1 reaction kit was obtained from New England Biolabs. All other chemicals were obtained from Sigma-Aldrich (Castle Hill, Australia).

2.4.3 SDS PAGE

SDS Polyacrylamide gel electrophoresis was performed under denaturing conditions according to Laemmli (Laemmli 1970) using either the Biorad mini protein electrophoresis (Bio-rad) or the Novex BOLT electrophoresis system (Life Technologies, Mulgrave, Australia).Proteins were separated on 4-15 % TGX precast polyacrylamide gels (for the Bio-rad system) or on 8% or 4-12% bis-tris precast polyacrylamide gels for the BOLT system. SR vesicles/purified RyR2s were diluted in Milli-Q water and sample buffer (1:1 vol/vol) (200 mM Tris-HCl, 8% sodium dodecyl sulphate (SDS), 40 mM EDTA, 40% glycerol, 0.588 M 2-Mercaptoethanol and 0.08% bromophenol blue, pH 6.8) so that 2.5-10 µg of SR was loaded per lane. Standards (5 µL of Bio-rad Dual Colour Protein Standard) and protein samples were loaded onto the gel, with the order of samples randomized routinely as to minimize bias. Running buffer contained 50 mM MOPS, 50 mM Tris base, 0.1% SDS and 1 mM EDTA. Gels were run at a constant voltage of 200 V for approximately 25-40 min (depending on system), or until the dye front reached the end of the gel.

2.4.4 Western blot and immunoprobing

2.4.4.1 Western blot

Western blot was completed according to the method of Towbin *et al.* (Towbin, Staehelin et al. 1992) using a Bio-Rad transfer system (Gladesville, Australia). After electrophoresis, the gel was equilibrated in transfer buffer (in mM: 37 Tris, 140 glycine and 20% methanol pH ~8.2) for 15 minutes at 4 °C. Other components of the blot sandwich were equilibrated for 30 min at 4 °C in transfer buffer, including fibre pads, filter paper and a PVDF membrane. The hydrophobic PVDF membrane was activated first by exposure to 100% ethanol for one minute prior to equilibration in transfer buffer. The gel was placed gently on top of the PVDF membrane, which was sandwiched between filter paper and fibre pads. The blot sandwich was clamped inside a trans blot cassette and partially submersed in cold transfer buffer so that no components were allowed to dry out. The cassette was clamped into the trans blot holder in the blot tank filled with transfer buffer that contained an ice pack and stir bar. Buffer was constantly stirred during protein transfer to ensure an even temperature. Proteins were transferred at 100 V for 60 min and then ~150 V so that the current was 0.5 -0.6 A for the final 30 min of transfer. Increasing the current assisted in transferring the high molecular weight RyR monomer. Post transfer, the gels were stained in Coomassie blue (0.1% Coomassie Brilliant Blue, 40% ethanol and 10% glacial acetic acid) for 1 hour, followed by destaining in 40% ethanol and 10% glacial acetic acid for 4 hrs, to assess efficiency of transfer.

2.4.4.2 Immunoprobing

The PVDF membrane was blocked in 3% BSA in phosphate buffered saline for 1 hour with rotation to prevent non-specific binding. Following a wash step (15 min in TPBS – PBS + 0.05% Tween-20), membranes were exposed to a primary antibody solution, (containing appropriate antibodies in TPBS) overnight with rotation and at 4 °C. Antibody dilutions were optimized for human samples. Blots were washed in 5-10 mls TPBS 5 times, then incubated with appropriate horseradish peroxidase (HRP) conjugated secondary antibody in TPBS for 2 hours at room temperature. Blots were washed again twice in 5-10 mls TPBS followed by one wash in PBS.

HRP-conjugated secondary antibodies were visualized using an enhanced chemiluminescence method. After removal of excess secondary antibody solution (see above), the membrane was exposed to SuperSignal West Pico Chemiluminescent Substrate for 1 – 2 min. Membranes were exposed to autoradiographic medical X-ray Film (Fujifilm, Tokyo, Japan) in a hypercassette (Amersham International, Buckinghamshire, England) for 30 s^{-1} min, before being developed using sequential 1 minute washes of film developer and fixer. Films were imaged on a Biorad Chemidoc using the Bio-Rad Image Lab software (Bio-Rad) (Gladesville, Australia), and quantified using the associated Quantity One software.

2.4.4.3 Determining total protein

Protein expression levels were normalized against all SR protein. Total protein was determined either via the TGX statins-free gel system or post-coomassie blue staining. In the majority of experiments, we used the statins-free gel system, which allows total protein loaded onto a gel to be visualized and captured on the Biorad Chemidoc, prior to Western blot. Samples were subject to SDS Page and then loaded onto the Biorad ChemiDoc system for visualization. Band densities (for total SR protein) were analyzed using Quantity One software. In a small number of cases, it was necessary to normalize our data against protein detected using the coomassie blue stain (see SDS Page and coomassie blue stain described above).

2.4.4.4 Reprobing PVDF membranes

In the experiments where the RyR2 single residue phosphorylation was measured, the results were normalized against total RyR2 protein. In many experiments, RyR2 phosphorylation at S^{2808} and S^{2814} was measured (using antibodies specific for the phosphorylated RyR2 S^{2808} residue) and normalized to total RyR2 protein loaded onto the gel and transferred by Western blot. To do this, two methods were used. After probing for PS2080 or PS814, samples were reprobed with a second primary antibody against RyR2 (anti-RyR2 PAB17291). This was achieved by incubating the PVDF membrane at 50 °C for 30 min in PBS with 2 % SDS and 0.7 % β-mercaptoethanol (v/v)

to 'strip' the primary and secondary antibodies. PVDF membranes were washed at least 12 times for 5 mins each wash in PBS to completely remove the incubation solution. The membranes were then ready for immunoprobing with the second primary antibody (see section 4.2.4.2). Membrane stripping is a relatively harsh method and it is possible that this could remove protein from the membrane or undermine the second antibody's ability to bind to the target protein. To test for this possibility, we reversed the order of probing with the first and the second primary antibody (i.e., anti-RyR2 was probed for first, and anti-PS2080 or PS2814 was probed for after membrane stripping). No difference in immuno-decoration or in the relative amount of phosphorylated RyR residue was found. The stains-free TGX gels were used in some experiments, which allowed visualization of RyR2 protein on the gel prior to Western blot and immunoprobing, and as such, negated the use of membrane stripping and reprobing. The calculated relative levels of RyR phosphorylation at S^{2808} or S^{2814} using this method were no different to those calculated using the membrane stripping methodology.

2.4.5 Co-immunoprecipitation

Co–immunoprecipitation of the RyR2 complex (or the FKBP-protein complexes) was achieved using a Pierce Co-IP kit and anti-RyR2 PAB17291 or anti-FKBP antibodies, following the manufacturer instructions.

The protocol is outlined below. For each Co-IP, the following were prepared. Fifty µl amino-linked resin was rehydrated and loaded into a pierce spin column and washed with 200 µl coupling buffer. After the wash step, resin was centrifuged at 1000 x g for 1 minute and the supernatant discarded. In all wash steps listed from here on, the washing solution was added to the upper chamber of the spin column, left for 1 minute and then centrifuged at 1000 x g for 1 minute. Twenty five µg of antibody was diluted in coupling buffer (to 200 µl) and sodium cyanoborohydride, and coupled to the resin by rotation for 2 hours at room temperature. The supernatant was removed by centrifugation (1000 x g for 1 minute). The resin was quenched by washing in quench buffer followed by a wash step in 200 µl coupling buffer. After 6 washes in 150 µl washing solution, the antibody-coupled resin was ready for Co-IP.

SR samples (50-200 µg) were lysed in IP Lysis/Wash Buffer and solubilized with the addition of 0.2% triton X-100. Samples were pre-cleared over prepared resin, in the absence of antibody. The resultant supernatant (the pre-cleared sample) was used for all Co-IPs. Pre-cleared samples were added to the antibody-coupled resin and incubated overnight with rotation at 4 °C. The unbound flow-through was collected by centrifugation (1000 x g for 1 minute) and the resin was washed 5 times with 200 µl of IP Lysis/Wash Buffer. The Co-IP samples were briefly washed with 10 µl of Elution Buffer and then eluted from the antibody-coupled resin by incubating with 40 µl of elution buffer for 5 minutes at room temperature, followed by collection of sample by centrifugation for 1 minute at 1000 x g. To show specificity for the RyR for the anti-RyR antibody, the following controls were performed (data not shown).

1. Solubilized SR vesicles (containing RyR2 and FKBPs) was pre cleared with control agarose resin, to control for non-specific binding of proteins to the resin.

2. Anti-CSQ2 and anti-FKBP IgG were unable to immunoprecipitate purified RyR2, illustrating that it was the specific RyR epitope and not a generalise IgG, which precipitated RyR2. Control blots illustrated that Anti-RyR and Anti-FKBP antibody did not substantially cross react with FKBP and RyR2, respectively.

2.4.6 In-vitro phosphorylation and dephosphorylation assays

In-vitro phosphorylation and dephosphorylation assays were conducted as previously described (Li, Imtiaz et al. 2013). PP1 activity on RyR2s from healthy and failing human hearts, was measured by incubation of the RyR2s in PP1 reaction kit (containing $MnCl_2$, NEBuffer® and 2.5 unit/µl PP1 at 30°C for 30 minutes, New England BioLabs). To measure in-vitro PKA activity on the RyR2s (maximal phosphorylation), the RyR2s were first maximally dephosphorylated by PP1 (15 minutes incubation) and then incubated with exogenous PKA in buffer containing (mM): 50 Tris-HCl (pH 7.4), 10 MgCl2, 2 ATP, 1 cAMP, 10 NaF and 0.25 g/ml PKA (Sigma Aldrich) at 30°C for 20 minutes. To measure in-vitro CaMKII effect on RyR2 phosphorylation status, RyRs were incubated in a CaMKII activating buffer containing (mM): 50 Tris-HCl (pH 7.4), 10 MgCl2, 2 ATP, 25 NaF, 2.5 CaCl2 and 62.5 µM CaM at 30°C for 20 min. The CaMKII activation buffer did not contain any exogenous CaMKII because endogenous

CaMKII is known to be associated with and phosphorylate the RyR2 in vitro (Witcher, Kovacs et al. 1991; Bers 2004; Currie, Loughrey et al. 2004). During these incubations, S^{2808} and S^{2814} phosphorylation was measured by sequentially probing (and stripping, see above) membranes with anti-pS^{2808}, anti-pS^{2814} and C3-33 antibodies. To measure the specificity of antibody binding for phosphorylated S^{2808} and S^{2814}, blot densities were normalised to that for maximal phosphorylation by PKA and CaCaM. In each case, the reactions were stopped by adding LDS sample buffer (Invitrogen). Assays were conducted as previously described (Li, Imtiaz et al. 2013). Maximal PP1, PKA and endogenous CaMKII phosphorylation and dephosphorylation of RyR2s was determined on healthy heart samples.

2.5 Data analysis

2.5.1 Analysis of ion channel recordings

Single channel parameters, open probability (P_o), mean open time (T_o) and mean closed time (T_c), were measured using a threshold discriminator at 50% of channel amplitude (Figure 2.5). These parameters were measured from single channel records using Channel3 software (N.W. Laver, nic@niclaver.com). Opening rate was determined from mean closed times (k_o=1/T_c).

For bilayer experiments with multi-channel recordings, P_o was calculated from the time-averaged current divided by the unitary current and the number of channels (n). Similarly, T_o and T_c could also be calculated from mean open and closed times from experiments with several RyR recordings ($T_o(n)$ and $T_c(n)$) provided that multiple openings were rare: $T_o = T_o(n)$ and $T_c = T_c(n)$ x n. The number of channels was determined by the number of current levels in the recording during periods of strong activation, which was usually achieved by turning off the local perfusion and exposing the RyRs to the *cis* bath, which normally contained 5 mM Ca^2.

During the experiments, a voltage of -40 mV(+40 mV physiological convention) was applied to the *trans* chamber whilst the voltage in the *cis* chamber was set at virtual ground in order to minimise electrical noise originating from the perfusion tubes and

magnetic stirrer. Thus the membrane potential difference is recorded as $V=V_{luminal}-V_{cytoplasmic}$. However, in this thesis the bilayer potential difference is always expressed using the standard physiological convention where $V= V_{cytoplasmic} -V_{luminal}$.

2.5.2 Statistics

Unless otherwise stated, all data are presented as means ± standard errors of the mean (SEM). Significance was calculated by Student's *t* test on normal distributions where $p<0.05$ was considered significant (*), and $p < 0.01$ was considered highly significant (**).

Hill equations were fitted to the dose-response data (Ca^{2+}/Mg^{2+} concentration dependencies of RyR2 open probability (P_o) for Ca^{2+} activation and Ca^{2+}/ Mg^{2+} inhibition) by the method of least squares. The Hill curve was fitted with the experimental data by adjusting three parameters: P_{max}, K_a/K_i, and H_a/H_i.

Hill equation for activation of RyR2s P_o by Ca^{2+} is:

$$P_o = \frac{(P_{\max} - P_{\min})\left(\left[Ca^{2+}\right]/K_a\right)^{Ha}}{\left(1+\left(\left[Ca^{2+}\right]/K_a\right)^{Ha}\right)} + P_{\min}$$

Hill equation for inhibition of RyR2 P_o by Ca^{2+} is:

$$P_o = \frac{(P_{\max} - P_{\min})}{\left(1+\left(\left[Ca^{2+}\right]/K_i\right)^{H_i}\right)}$$

Hill equation for inhibition of RyR2 P_o by Mg^{2+} is:

$$P_o = \frac{(P_{\max} - P_{\min})}{\left(1+\left(\left[Mg^{2+}\right]/K_i\right)^{H_i}\right)}$$

P_{max} is the open probability of a maximally activated RyR2 channel, P_{min} is the open probability of a minimally activated RyR2 channel. K_a and K_i are the Ca^{2+} and Mg^{2+} concentrations for half activation and inhibition of RyR2 P_o, respectively, representing ion binding affinities. H_a and H_i are the corresponding Hill coefficients of activation and inhibition, respectively, which indicate the minimum number of ions (Ca^{2+}or Mg^{2+}) which bind cooperatively to produce either channel activation or inhibition.

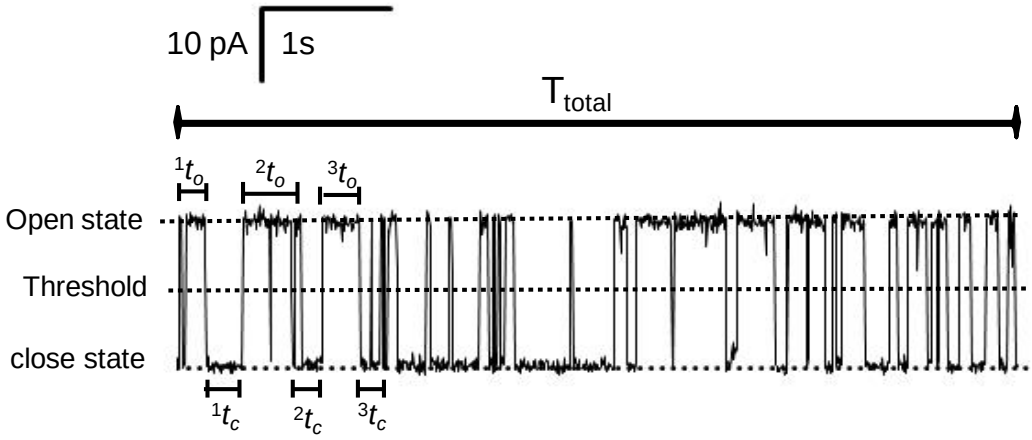

Figure 2.5: Single-channel recording analysis. Channel openings are upward current jumps from the base line (considered as channel closure) at positive 40 mV. Threshold, defines opening and closing events of the channel, set at half of maximal current amplitude.
t_o is the open dwell time, t_c is the time interval between two openings, T_{total} is the total time of analysed record.

The mean gating parameters of the RyR2 were calculated according to the following equations where n is the number of events:

Open probability (P_o) = $({}^1t_o + {}^2t_o + {}^3t_o \ldots\ldots + n\, t_o)/T_{total}$

Mean open duration (T_o; ms) = $({}^1t_o + {}^2t_o + {}^3t_o \ldots\ldots + n\, t_o)/n$

Mean closed duration (T_c; ms) = $({}^1t_c + {}^2t_c + {}^3t_c \ldots\ldots + n\, t_c)/n$

Opening rate (k_o; events/s) = $1/\, T_c$

Chapter 3- Regulation of human RyR2 by Ca^{2+} and Mg^{2+} in the cytoplasm and in the lumen of the sarcoplasmic reticulum

3.1 Introduction

The cardiac ryanodine receptor (RyR2), an intracellular Ca^{2+} release channel, plays a key role in excitation contraction coupling (ECC) in heart. Depolarisation of the sarcolemma opens voltage-dependent L-type Ca^{2+} channels (dihydropyridine receptors - DHPRs), which allows Ca^{2+} to enter the cell. The subsequent increase in cytoplasmic Ca^{2+} activates RyR2, which releases Ca^{2+} from the sarcoplasmic reticulum (SR). The Ca^{2+} released from the SR contributes between 60 - 95% of the cytoplasmic Ca^{2+} during ECC, depending on the species (Lehnart, Maier et al. 2009; Zima, Bovo et al. 2010). The RyR2s together with the DHPRs form a functional unit (couplon) that modulates heart function by controlling the Ca^{2+} release from the SR (Franzini-Armstrong, Protasi et al. 1999).

Intracellular Ca^{2+}, Mg^{2+} and ATP are allosteric regulators of RyR2 (Meissner and Henderson 1987; Meissner 1994; Laver and Honen 2008) which play an important role in determining normal cardiac contraction and rhythmicity (Meissner 1994; Bers 2002), and their disruption can lead to sudden cardiac death. Ca^{2+} in the SR lumen and cytoplasm activate RyR2 whereas Mg^{2+} (free concentration of ~1 mM in cytoplasm and lumen (Meissner 1994)) is a channel inhibitor. During diastole, cytoplasmic and SR luminal Ca^{2+} concentrations are ~100 nM and 1 mM, respectively (Ginsburg, Weber et al. 1998; Bers 2001). During systole, clusters of RyR2s release Ca^{2+} into the confined region between the SR and sarcolemma/T-tubule membrane known as the dyadic cleft. Computer simulations of Ca^{2+} release estimate that cytoplasmic Ca^{2+} concentration near the RyR2 peaks at ~200 μM and that luminal Ca^{2+} declines to ~200 μM (Laver, Kong et al. 2013).

Single channel studies of RyR2 isolated from animal hearts (*e.g.* sheep, rat and dog) have provided valuable insights into the regulation of RyR2 by intracellular Ca^{2+}, Mg^{2+} and ATP (Sitsapesan and Williams 1997; Gyorke, Gyorke et al. 2002; Laver 2005; Laver 2007; Gyorke and Terentyev 2008). These studies provide evidence for four different Ca^{2+} dependent mechanisms, controlled by four Ca^{2+}/ Mg^{2+} sites on each RyR2 subunit (Laver 2010). RyR2 can be activated by Ca^{2+} binding to either the cytoplasmic

side of the channel with ~ 2 μM affinity (A-site, (Smith, Coronado et al. 1986; Hymel, Inui et al. 1988; Sitsapesan and Williams 1994)) or to the luminal side of the channel with ~ 0.1 mM affinity (L-site, (Sitsapesan and Williams 1994; Laver 2007)). Identification of a luminal Ca^{2+} activation site was complicated by the possibility that Ca^{2+} from the luminal side of the membrane could pass through the RyR2 pore and activate the RyR2 via the site responsible for cytoplasmic Ca^{2+} activation. Functional characterization of the L-site was made possible by considering RyR2 activity in terms of open and closed times rather than open probability. One could distinguish the action of luminal and cytoplasmic RyR2 Ca^{2+} activation sites by considering only the properties of channel closed events when Ca^{2+} was not flowing through the channel. In this study, I also consider RyR2 mean open and closed times when interpreting RyR2 gating mechanisms.

Two mechanisms for cytoplasmic Ca^{2+} inhibition of RyR2 have been identified. Channels inhibited by mM concentrations of cytoplasmic Ca^{2+} at the I_1-site (Meissner 1986; Laver, Roden et al. 1995) and partially inhibited by μM concentrations at the I_2-site (Laver 2007). Mg^{2+} inhibits RyR2 by competing with Ca^{2+} at the A-site (Smith, Coronado et al. 1986) and the L-site (Laver and Honen 2008) where, unlike Ca^{2+}, Mg^{2+} binding does not opening. Mg^{2+} also inhibits RyR2 because it acts as a surrogate for Ca^{2+} at the I_1-site (Laver, Baynes et al. 1997)

Interest in the function of human RyR2 has been spurred by the recent understanding that heart dysfunction associated with HF is generally associated with aberrant Ca^{2+} fluxes across the sarcolemma and SR of cardiac cells (Bers, Eisner et al. 2003). Although the regulation of human RyR2 by intracellular Ca^{2+} and Mg^{2+} is central to our understanding of SR Ca^{2+} fluxes, its regulation characteristics are still poorly defined. Two groups (Marx, Reiken et al. 2000; Jiang, Lokuta et al. 2002) have made single channel recordings of human RyR2 isolated from human heart. They only presented RyR2 single channel recordings under one experimental condition (spot measurement). Only one study has examined cytoplasmic Ca^{2+} activation and this was done using recombinant human RyR2 (Wehrens, Lehnart et al. 2004). Here I present the first analysis of RyR2 isolated from human heart and its regulation by intracellular Ca^{2+}

and Mg^{2+}. I note differences in the way human RyR2 is regulated by Ca^{2+} and Mg^{2+} compared to RyR2 from sheep and rat heart.

3.2 Materials and Methods

3.2.1 Heart tissue & single-channel measurements

SR vesicles containing RyRs from non-failing human, rat and sheep heart muscle were incorporated into artificial lipid bilayers and channel gating was measured by single channel recording. RyR2s open and closed times were measured in the presence of various concentrations of cytoplasmic and luminal Ca^{2+} and Mg^{2+} in the presence of cytoplasmic ATP (2 mM). See chapter 2 sections 2.1, 2.2 & 2.3 for details.

3.2.2 Statistics

Unless otherwise stated, all human data are presented as arithmetic mean ± standard error of the mean (SEM) and compared to sheep and rat data from previous studies (Laver and Honen 2008; Cannell, Kong et al. 2013; Li, Imtiaz et al. 2013) (sheep and rat data have previously been presented as arithmetic mean ± standard errors). Hill equations were fitted to the arithmetic individual experimental values of Ca^{2+}/Mg^{2+} concentration dependencies of RyR2s P_o, k_o and T_o for Ca^{2+} activation and Ca^{2+}/ Mg^{2+} inhibition. Significance was calculated using Student's *t* test on normal distributions. $p<0.05$ was considered significant (*), and $p < 0.01$ was considered highly significant (**).

3.3 RESULTS

Single channel recordings of human RyR2 shown in Figure 3.1 A were made in the presence of cytoplasmic solutions containing 100 nM Ca^{2+} (diastolic [Ca^{2+}]) and 2 mM ATP and luminal solutions containing 0.1 mM Ca^{2+}, at -40 mV. These recordings were measured in the absence of cytoplasmic Mg^{2+} because RyR2 activity is too low to be reliably measured in the presence of physiological [Mg^{2+}]. The gating kinetics of the cardiac RyRs were found to differ between individual channels from the same heart. 90% of the channels had open probabilities (P_o) that comprised a normal distribution on a logarithm scale (Figure 3.1B) with a mean P_o= 0.02 and a standard deviation of 6.3 fold. Similar distributions were seen for the opening rate, k_o (Figure 3.1C) and mean open time, T_o (Figure 3.1 D). Human RyR2s incorporated into lipid bilayers had a caesium ion conductance of 575 ± 5 pS (n = 6) in symmetric 250 mM CsCl ([Ca^{2+}] < 1 μM) which is close to values of 525 ± 10 pS (n = 6) for sheep RyRs and 460 ± 10 pS (n = 6) for rat RyR2s obtained under the same conditions. Grouping the data from the four donor hearts (see Table 2.1 for source information) revealed no significant differences between these groups in the Ca^{2+} and Mg^{2+} regulation of their RyRs. Therefore, in the analysis of the concentration dependencies of cytoplasmic and luminal Ca^{2+} and Mg^{2+} regulation of RyR2s, the data were pooled from all heart samples.

3.3.1 Cytoplasmic Ca^{2+} regulation

RyR2s were strongly activated by 1-100 μM cytoplasmic Ca^{2+} (Figure 3.2A). The half-activating cytoplasmic Ca^{2+}concentration (K_a) for P_o ranged from 4-6 μM (filled and open circles in Figure 3.2B, Table 3.1). The cytoplasmic Ca^{2+} response also depended on luminal [Ca^{2+}]. At sub μM cytoplasmic [Ca^{2+}], increasing luminal [Ca^{2+}] from 1 nM to 0.1 mM caused an increase in open probability and this increase became negligible at higher cytoplasmic [Ca^{2+}] (Figure 3.2B, *c.f.* open and filled circles). Hill equations were fitted to the P_o data (curves in Figure 3.2 B; these and other Hill parameters are given in Table 3.1, see section 2.4.2). Increasing luminal Ca^{2+} increased the basal P_o of RyR2s at low cytoplasmic [Ca^{2+}] (P_{min}) from 10^{-4} to 2 x 10^{-2} but had no significant effect on the half-activating concentration or maximal activation (K_a for P_o ranged from 4-6 μM and

P_{max} ~0.9). Activation of P_o by luminal and cytoplasmic Ca^{2+} was associated with increases in both the opening rate (k_o), (Figure 3.2C) and mean open time (T_o, Figure 3.2D).

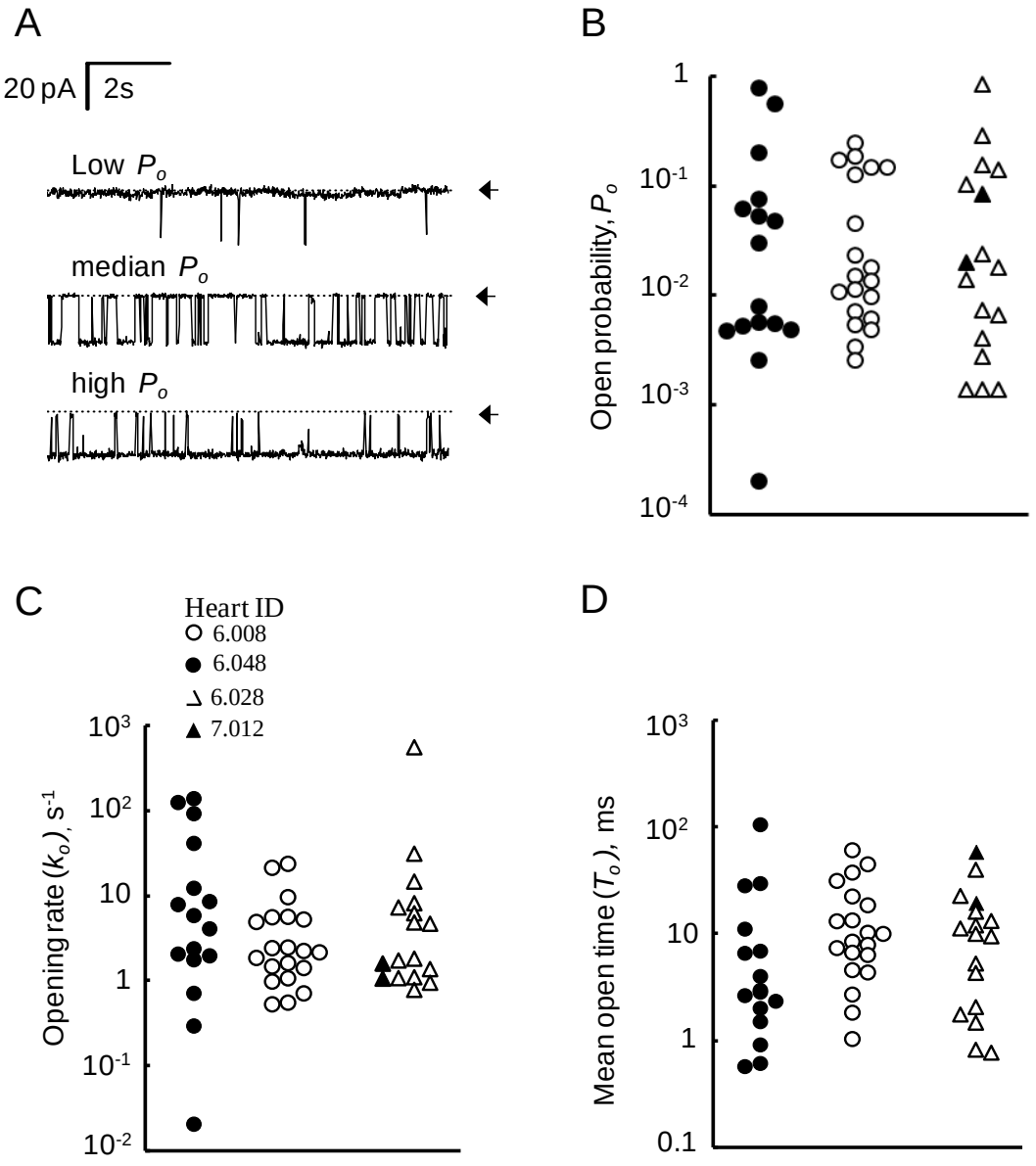

Figure 3.1: Data for individual RyR2s from non-failing human hearts (A) Single channel recordings of RyR2s showing variation in channel activity. Channel recordings were taken in the presence of cytoplasmic pCa 7 (*i.e.* 100 nM Ca^{2+}) and luminal pCa 4 (diastolic [Ca^{2+}]) in the presence of 2 mM ATP in the cytoplasm at -40 mV. Channel openings are downward current jumps from the baseline (arrows). **(B)** P_o distribution at diastolic [Ca^{2+}] of individual RyRs from four non-failing hearts identified in the legend in C and Table 2.1 **(C) & (D)** Corresponding opening rate (k_o) and mean open time (T_o), respectively.

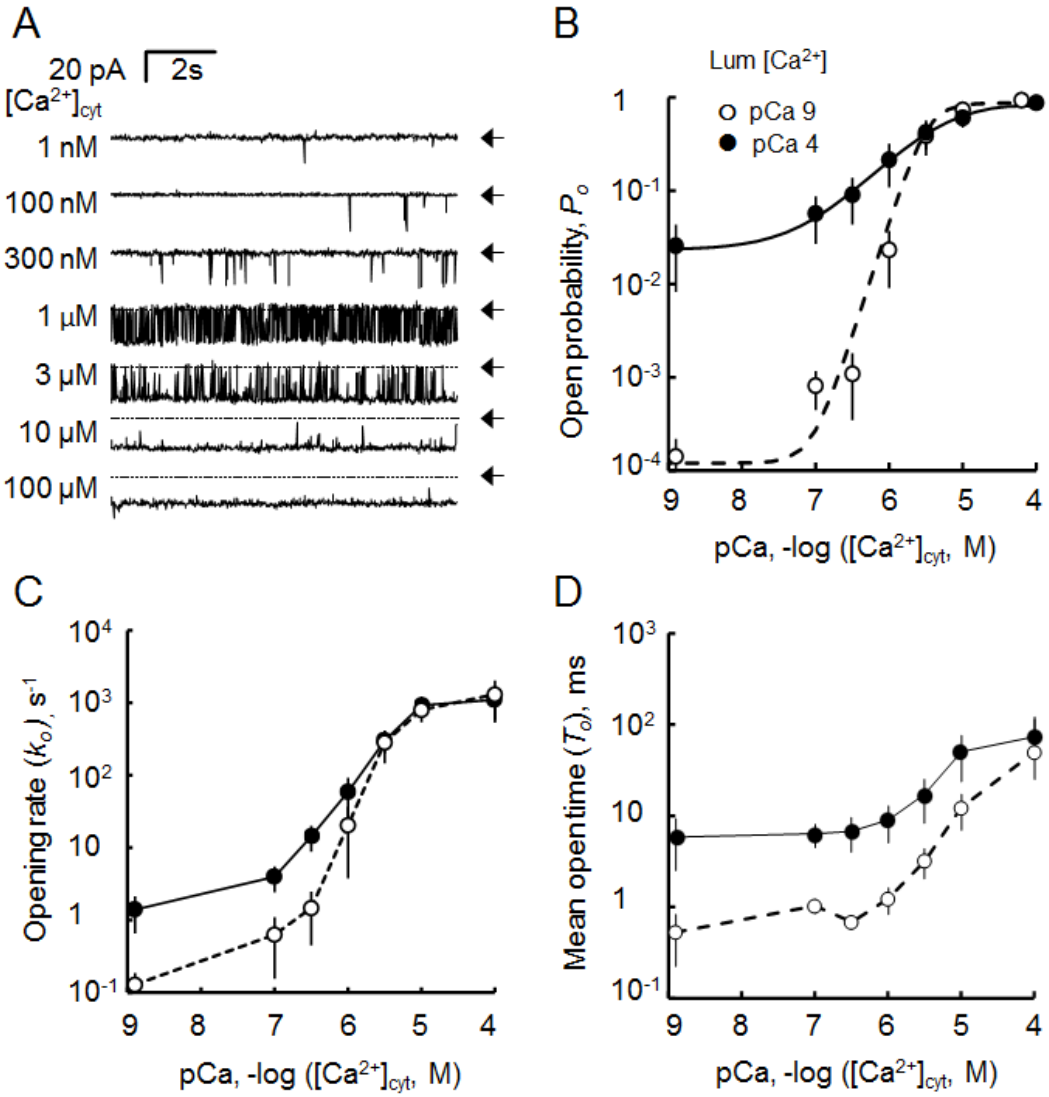

Figure 3.2: RyR2 activation by cytoplasmic Ca^{2+}. (A) Single channel recordings of RyR2 from healthy human heart with cytoplasmic [Ca^{2+}] indicated at the left of each trace. Channel recordings were taken at luminal pCa 4 in the presence of 2 mM ATP in the cytoplasm. Membrane potential is at -40 mV and channel openings are downward current jumps from the baseline (arrows). **(B)** Cytoplasmic Ca^{2+}-dependence of RyR2 P_o was measured at luminal pCa 9 and pCa 4. **(C) & (D)** Corresponding opening rate (k_o) and mean open time (T_o), respectively. Data points show the mean ± SEM pooled from 2-7 readings. The solid and dashed curves in B show Hill fits to the data. Lines in C & D have no theoretical significance. The number of experiments and the Hill parameters are listed in Table 3.1.

Table 3.1

$[Ca^{2+}]_L$ pCa	P_{max}	$P_{min} \times 10^3$	K_a, μM	H_a	n
9	0.9 ± 0.4	0.14 ± 0.02	4 ± 1	2.5 ± 0.4	2-5
4	0.9 ± 0.4	20 ± 5.0	6 ± 1	1 ± 0.5	5-10

Table 3.1 Summary of the Hill Fit Parameters for cytoplasmic Ca^{2+} activation (P_o) of human cardiac RyRs

3.3.2 Luminal Ca^{2+} regulation

The effects of luminal Ca^{2+} were investigated in more detail by measuring the luminal Ca^{2+}-dependence of P_o, T_o and k_o at 1 nM and 100 nM cytoplasmic Ca^{2+} (Figure 3.3). Representative traces from one experiment (Figure 3.3A) illustrate the action of luminal Ca^{2+}-activation of the RyR2 in the presence of cytoplasmic pCa 7 and 2 mM ATP in the cytoplasm. In the virtual absence of both luminal and cytoplasmic (1 nM) Ca^{2+}, RyR2s had a mean P_o of 10^{-4}, which increased to a maximum of 10^{-2}, upon raising luminal [Ca^{2+}] to 0.1 mM (Figure 3.3B, open circles at luminal pCa=4). The overall level of luminal Ca^{2+} activation (from pCa 9 to 4) was magnified 10-fold by increasing cytoplasmic [Ca^{2+}] from pCa 9 to pCa 7 (Figure 3.3B, *c.f.* open and filled circles). Upon raising luminal [Ca^{2+}] from pCa 9 to pCa 4, at -40 mV the P_o increased to a maximum of 10^{-1} with a K_a of 35 μM (Figure 3.3B, filled circles). At +40 mV, the K_a for luminal Ca^{2+} activation increased from 35 μM to 75 μM and the maximum P_o decreased ~ 10-fold (Figure 3.3B, *c.f.* filled circles and open squares at luminal pCa=4).

Luminal Ca^{2+} activation is mediated by increases in both k_o and T_o. The k_o has a similar hyperbolic dependence on luminal [Ca^{2+}] at positive and negative 40 mV (Figure 3.3C, squares and filled circles). The dependence of T_o on luminal Ca^{2+}-dependence shifted to higher concentrations when the voltage was switched form -40 mV to +40 mV (Figure 3.3D). The amplifying effect of cytoplasmic Ca^{2+} on luminal activation on P_o was mediated mainly by changes in the RyR2 opening rate (Figure 3.3D, open and filled circles).

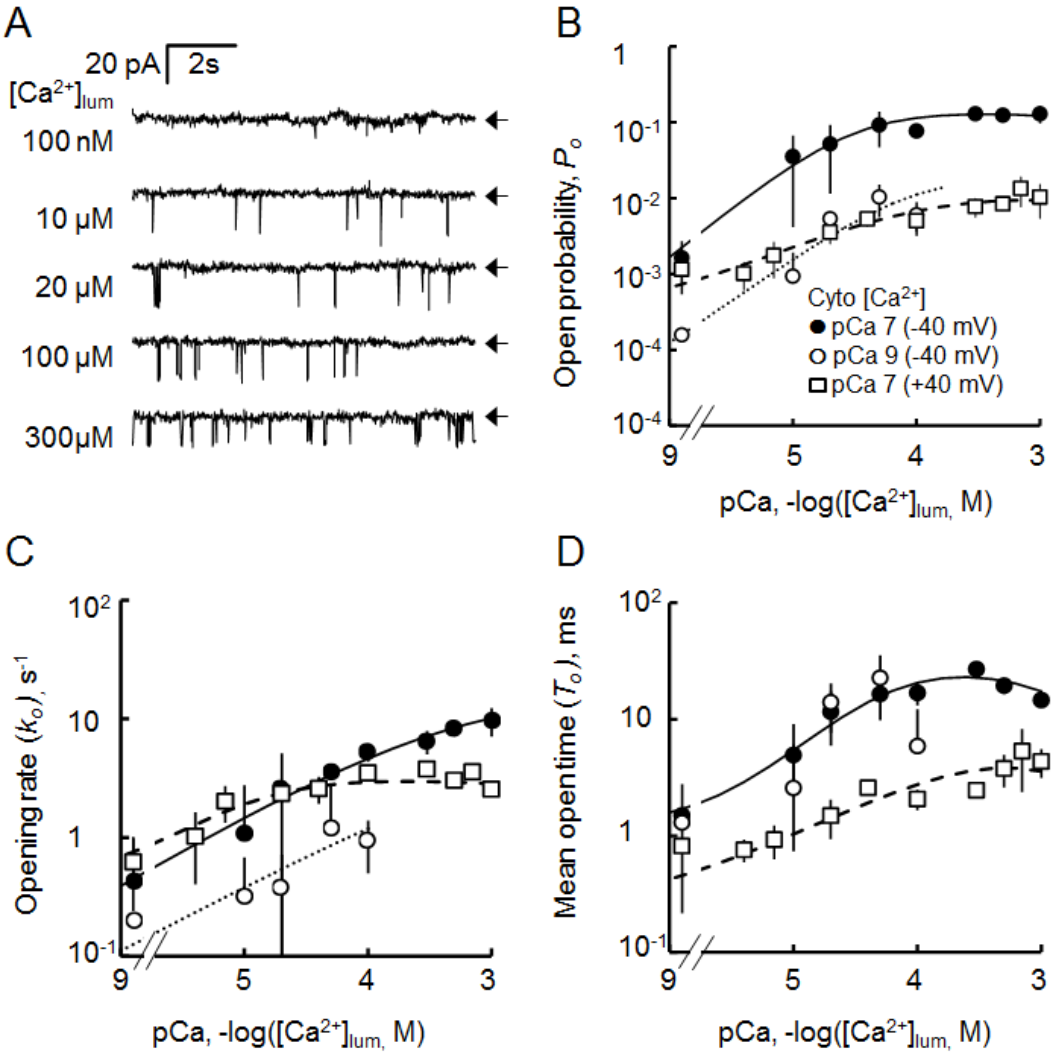

Figure 3.3: RyR2 activation by luminal Ca^{2+}. (A) Single channel recordings of RyR2s from healthy human heart with luminal [Ca^{2+}] indicated at the left of each trace. Channel recordings were taken in the presence of 100 nM Ca^{2+} and 2 mM ATP in the cytoplasm at -40 mV. Channel openings are downward current jumps from the baseline (arrows). **(B)** Luminal Ca^{2+}-dependencies of RyR2 P_o were measured at cytoplasmic pCa 7 and pCa 9 and also at +40 mV (pCa 7 only). **(C) & (D)** Corresponding opening rate (k_o) and mean open time (T_o), respectively. Data points show the mean ± SEM pooled from 2-33 readings. The solid and dashed curves in B-D show Hill fits to the data. The number of experiments and the Hill parameters are listed in Table 3.2.

Table 3.2

voltage	$[Ca^{2+}]_C$ *pCa*	*Gating parameter*	P_{max}	$P_{min} \times 10^3$	K_a, μ*M*	H_a	*n*
-40	7	P_o	0.14 ± 0.03	2 ± 1	35 ± 12	1.3 ± 0.2	3-17
-40	7	k_o	11 ± 2	-	120 ± 61	0.5 ± 0.3	3-17
-40	7	T_o	33 ± 8	-	60 ± 14	1.1 ± 0.2	3-17
+40	7	P_o	0.01 ± 0.003	0.9 ± 0.4	75 ± 36	1 ± 0.5	2-5
+40	7	k_o	4 ± 0.2	-	10 ± 5	1 ± 0.2	2-5

Table 3.2 Summary of the Hill Fit Parameters for luminal Ca^{2+} activation of human cardiac RyRs. Hill Fit Parameters for luminal Ca^{2+} activation at 1 nM cytoplasmic Ca^{2+} were very hard to get because of small n value (n=3).

3.3.3 Cytoplasmic Mg^{2+} regulation

The inhibitory effects of cytoplasmic Mg^{2+} at cytoplasmic [Ca^{2+}] of pCa 7 and pCa 4 were measured because previous studies using sheep RyR2s (Laver, Owen et al. 1997) showed that Mg^{2+} inhibition under these two conditions was determined by different and independent mechanisms. At cytoplasmic pCa 7, Mg^{2+} is a competitive antagonist at the cytoplasmic Ca^{2+} activation site (A-site) but at pCa 4, Mg^{2+} inhibits by binding to the low affinity, cytoplasmic Mg^{2+}/Ca^{2+} inhibition site (I_1-site). At cytoplasmic pCa 7, (Figure 3.4B, circles), RyR2s were strongly inhibited by micromolar cytoplasmic Mg^{2+} (Figure 3.4A). Increasing luminal [Ca^{2+}] from pCa 4 (filled circles) to pCa 3 (open circles) had no effect on Mg^{2+} concentrations for half-inhibition (K_i) of P_o (~10 μM, Figure 3.4B; Hill parameters given in Table 3.3). Mg^{2+} inhibition was associated with decreases in k_o and T_o (Figures 3.4C and 3.4D). Although an increase in luminal Ca^{2+} increased the k_o by 3 to 4-fold, it had no significant effect on K_i (~15 μM). At cytoplasmic pCa 4 (Figure 3.4B, open triangles), RyR2s were inhibited by cytoplasmic Mg^{2+} but at 300-fold higher concentrations (K_i = 5.4 mM) than seen at pCa 7. This inhibition was primarily associated with a decrease in T_o (Figure 3.4C and D).

3.3.4 Luminal Mg^{2+} regulation

Millimolar concentrations of Mg^{2+} added to the luminal bath inhibited RyRs in the presence of cytoplasmic pCa 7 (Figure 3.5A) and the luminal [Mg^{2+}]-dependence of P_o is shown in Figure 3.5B. RyR2 sensitivity to inhibition by luminal Mg^{2+} was decreased by increasing luminal [Ca^{2+}] from pCa 4 to pCa 3. Hill fits to P_o (Figure 3.5B, curves) gave Mg^{2+} K_i values of 0.55 mM at luminal pCa4 and 1.5 mM at pCa 3. The luminal Mg^{2+}-dependencies of P_o were also reflected in changes in both T_o and k_o (Figures 3.5C and D). Alleviation of inhibition by luminal Ca^{2+} was due to increases in the K_i*'s* for both k_o and T_o.

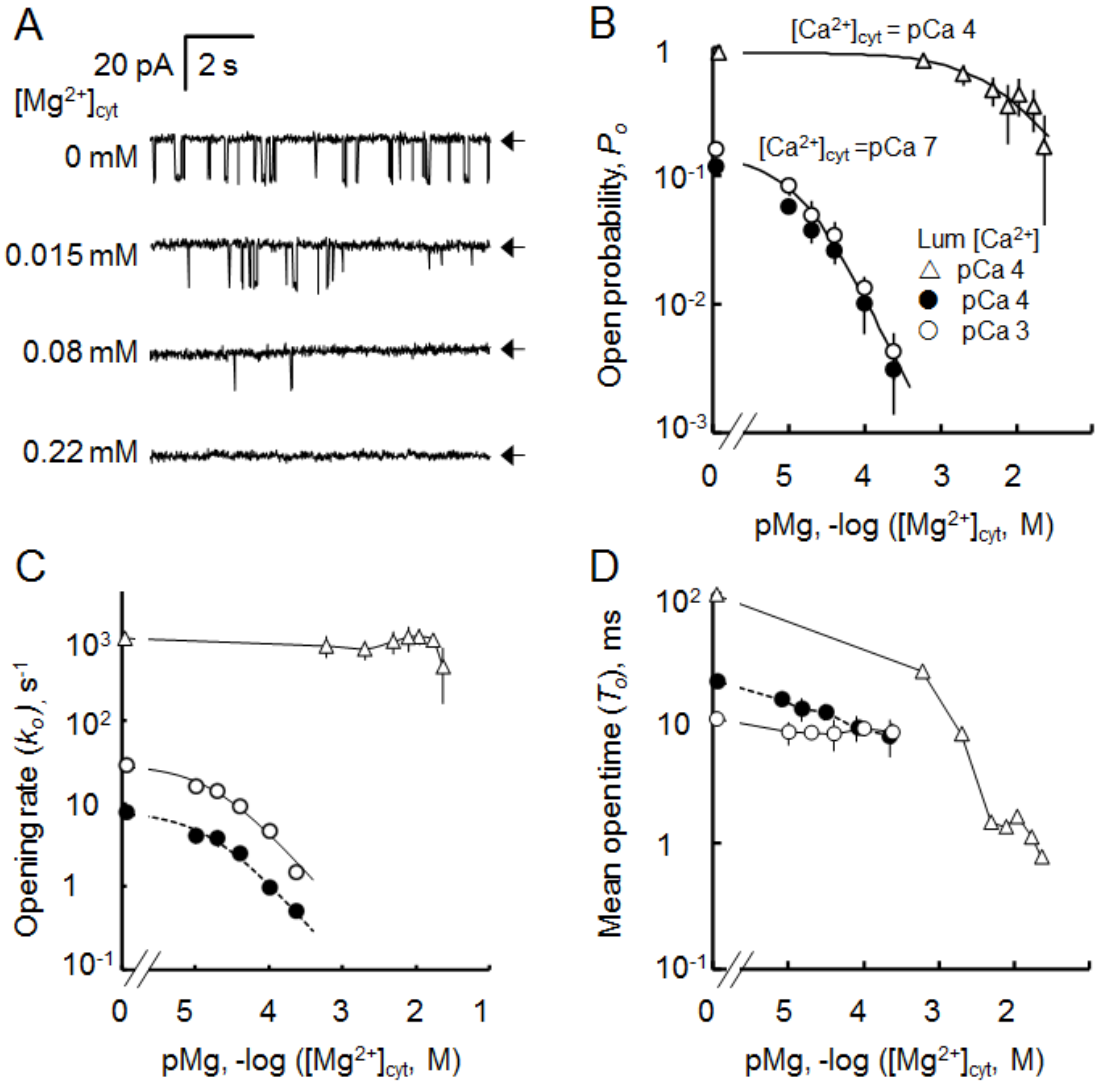

Figure 3.4: Inhibition of RyR2 by cytoplasmic Mg^{2+}. (A) Single channel recordings of RyR2 from healthy human heart with cytoplasmic free [Mg^{2+}] at the left of each trace. Channel recordings were taken at cytoplasmic pCa 7 and luminal pCa 4 in the presence of 2 mM ATP in the cytoplasm at -40 mV. Channel openings are downward current jumps from the baseline (arrows). **(B)** Cytoplasmic Mg^{2+} inhibition of RyR2 P_o was measured at luminal pCa 4 (filled circles) and pCa 3 (open circles) in the presence of cytoplasmic pCa 7. Open triangles show cytoplasmic Mg^{2+} inhibition of RyR2 P_o at cytoplasmic pCa 4 and luminal pCa 4. **(C) & (D)** Corresponding opening rate (k_o) and mean open time (T_o), respectively. Data points show the mean ± SEM pooled from 5-10 readings. The solid and dashed curves in B & C (except for open triangles in C) show Hill fits to the data for Mg^{2+} inhibition (see section 2.4.2). Lines in D have no theoretical significance. The number of experiments and the Hill parameters are listed in Table 3.3.

Table 3.3

$[Ca^{2+}]_C$ pCa	$[Ca^{2+}]_L$ pCa	Gating parameter	P_{max}	K_i, mM	H_i	n
7	4	P_o	0.03 ± 0.004	0.01 ± 0.004	1.1 ± 0.5	4
7	3	P_o	0.03 ± 0.004	0.01 ± 0.004	1.1 ± 0.5	3
7	4	k_o	3 ± 0.5	0.012 ± 0.002	1.1 ± 0.2	4
7	3	k_o	13 ± 1.2	0.017 ± 0.003	1 ± 0.2	3
4	4	P_o	0.9 ± 0.06	5.4 ± 0.8	0.85 ± 0.2	4-10

Table 3.3 Summary of the Hill Fit Parameters for cytoplasmic Mg^{2+} inhibition of human cardiac RyRs.

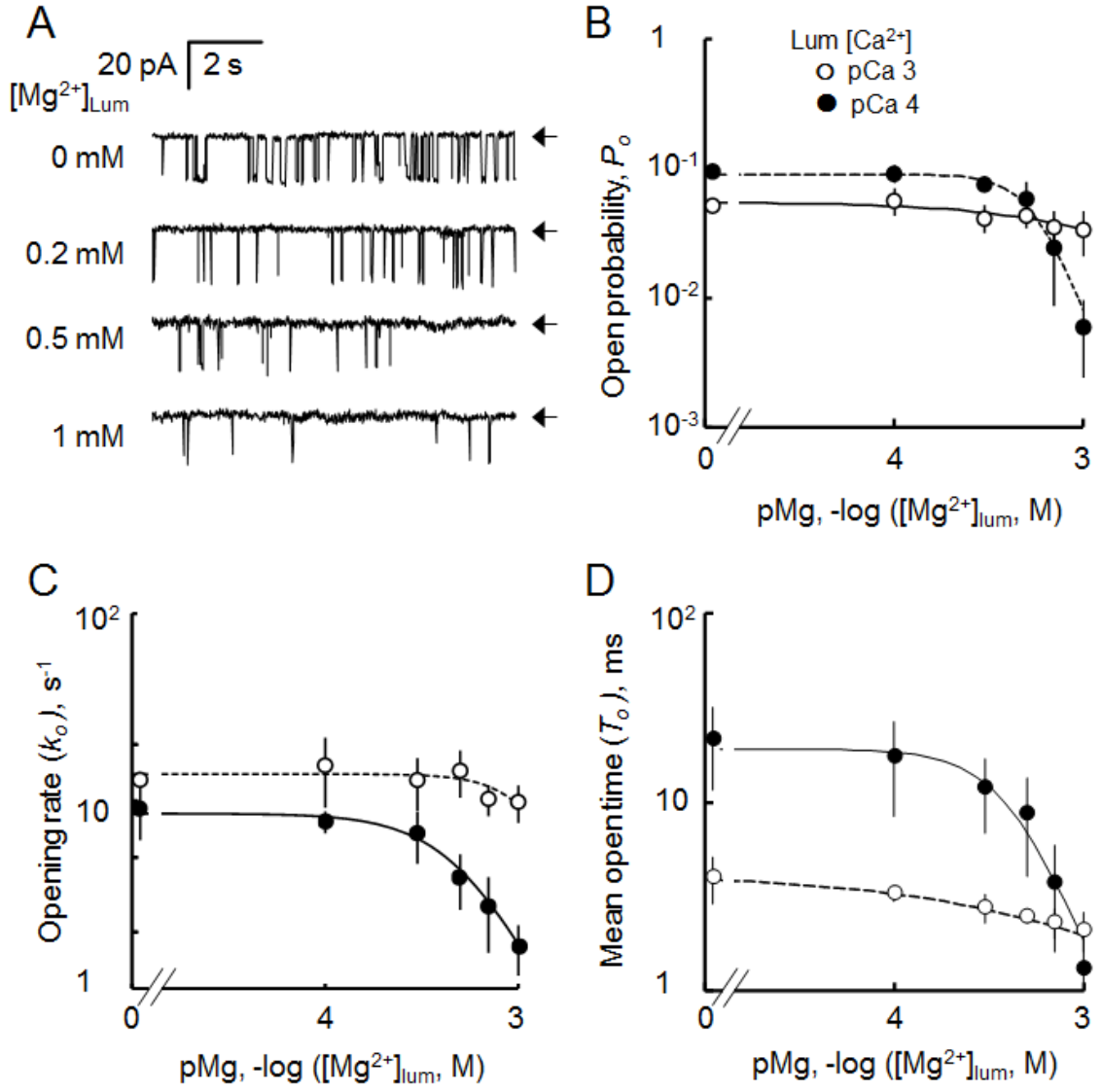

Figure 3.5: Inhibition of the RyR2 by luminal Mg^{2+}. (A) Single channel recordings of RyR2s from healthy human heart with luminal [Mg^{2+}] at the left of each trace at -40 mV. Channel recordings were taken at cytoplasmic pCa 7 and luminal pCa 4 in the presence of 2 mM ATP in the cytoplasm. Channel openings are downward current jumps from the baseline (arrows). **(B)** Luminal Mg^{2+} inhibition of RyR2 P_o were measured at luminal pCa 4 (filled circles) and pCa 3 (open circles) **(C) & (D)** Corresponding opening rate (k_o) and mean open time (T_o), respectively. Data points show the mean ± SEM pooled from 3-9 readings. The solid and dashed curves in B-D (filled circles) show Hill fits to the data. The number of experiments and the Hill parameters are listed in Table 3.4.

Table 3.4

$[Ca^{2+}]_C$ pCa	$[Ca^{2}]_L$ pCa	Gating parameter	P_{max}	K_i, mM	H_i	n
7	4	P_o	0.09 ± 0.02	0.55 ± 0.03	3.8 ± 1.8	5-6
7	4	k_o	8.6 ± 0.8	0.6 ± 0.05	2 ± 1	5-6
7	4	T_o	19 ± 1.8	0.4 ± 0.03	2.4 ± 0.6	5-6

Table 3.4 Summary of the Hill Fit Parameters for luminal Mg^{2+} inhibition of human cardiac RyRs.

3.3.5 Ca^{2+}/Mg^{2+} regulation among species

Regulation by intracellular Ca^{2+} and Mg^{2+} of human RyR2 was compared to RyR2 from rat and sheep, two commonly used animal models for RyR2 function. Activation of RyR2 from the three species by cytoplasmic Ca^{2+} alone (~1 nM luminal Ca^{2+}) showed small differences in their sensitivity to cytoplasmic Ca^{2+}. K_a values for sheep (1.4 μM) was significantly lower than that seen for human and rat (4 μM and 3.4 μM, respectively; p = 0.04; Figure 3.6A). All RyR2s could be activated by luminal Ca^{2+} (Figure 3.6B) with a bell-shaped Ca^{2+} response. However, there were differences in the luminal Ca^{2+} responses between species. RyR2 from rat exhibited peak activation that was 10-fold lower than that seen for RyR2 from human and sheep. Also, at luminal $[Ca^{2+}] \leq 10$ μM, human RyR2s were more active than those from rat and sheep. Human RyR2s showed less decline at higher luminal $[Ca^{2+}]$ than those from rat and sheep but this did not become apparent until luminal Ca^{2+} reached 10 mM. Hill fits to the data (Figure 3.6B, solid and dashed curves) give K_a values for luminal Ca^{2+} activation of 35, 60 and 10 μM for human, sheep and rat RyR2s, respectively.

RyR2 from human, sheep and rat were similarly inhibited by cytoplasmic Mg^{2+} (Figure 3.6C) in the presence of cytoplasmic pCa 7 (inhibition via the A-site). However, in the presence of cytoplasmic pCa 4, RyR2s from human were 3-fold less sensitive to cytoplasmic Mg^{2+} inhibition (p = 0.002) than those from sheep (inhibition via the I_1-site; rat RyR2 was not measured). RyR2s from human hearts showed a markedly different dependence on luminal Mg^{2+} than those from rat and sheep heart (Figure 3.6D). Hill fits to the data showed K_i values for luminal Mg^{2+} inhibition of 550, 49 and 78 μM for human, sheep and rat RyR2s, respectively (Table 3.6). Interestingly, the higher Hill coefficient for the luminal $[Mg^{2+}]$ response of human RyR2s compensated for the differences in K_i, producing similar levels of inhibition at physiological (1 mM) luminal Mg^{2+} concentration for all species.

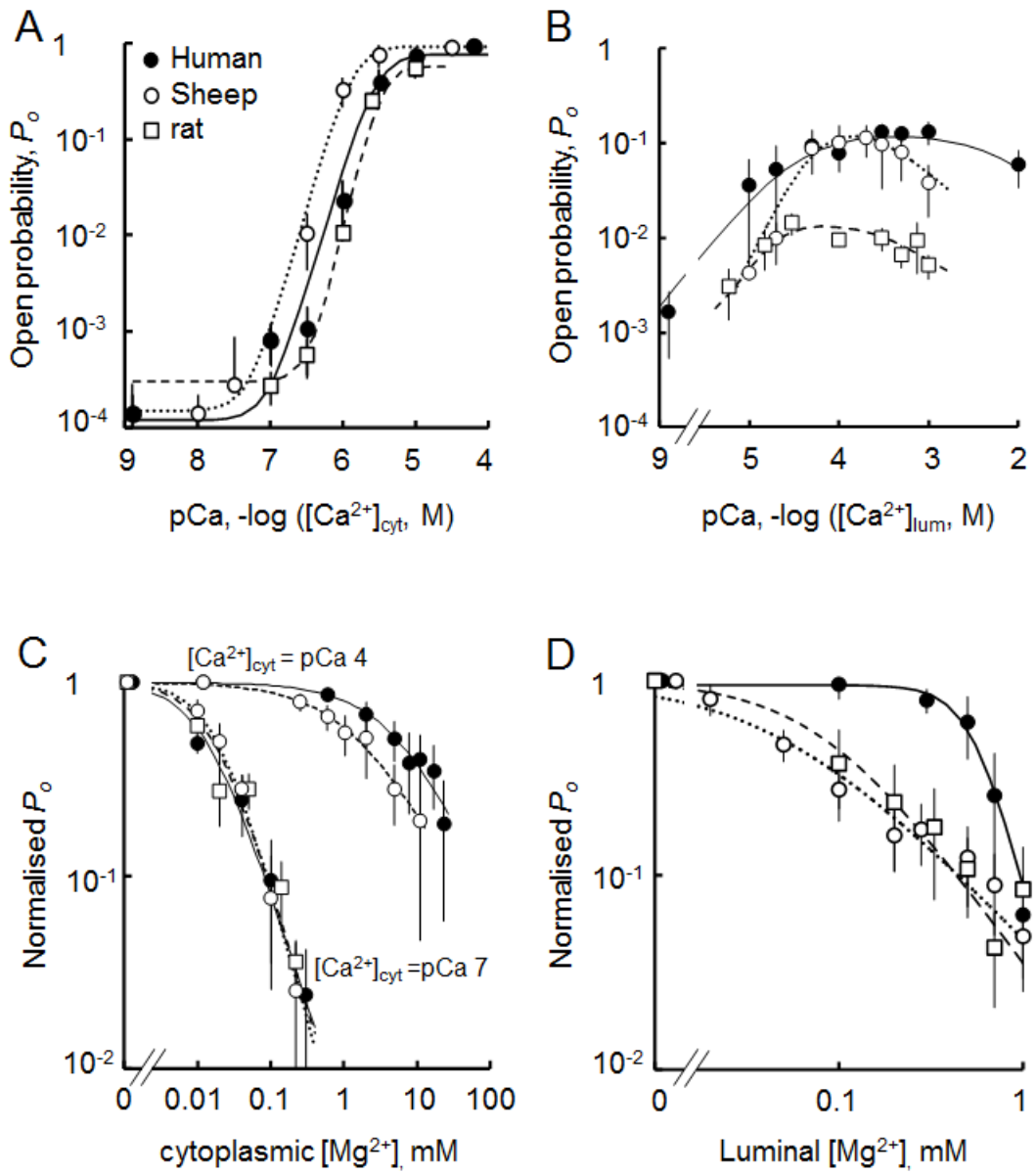

Figure 3.6: Ca^{2+} and Mg^{2+} regulation of P_o in RyR2 from human, sheep and rat. (A) Cytoplasmic [Ca^{2+}] activation in the absence (~ 1 nM) of luminal Ca^{2+} for RyR2s from human, sheep and rat as indicated in the legend (applies to all panels except B). **(B)** Luminal [Ca^{2+}] activation response of RyR2 with cytoplasmic pCa 7 **(C)** Cytoplasmic [Mg^{2+}] inhibition response of RyR2 in the presence of cytoplasmic pCa 7 and 4 (luminal pCa = 4). **(D)** Luminal [Mg^{2+}] inhibition response of RyR2s in the presence of cytoplasmic pCa 7 and luminal pCa 4. The solid and dashed curves show Hill fits to the data. The number of experiments and the Hill parameters for rat and sheep RyR2 are listed in Tables 3.5 & 3.6. Data points show the mean ± SEM. Data for sheep RyR2s in A and B were obtained from Laver and Honen (Laver and Honen 2008) and rat RyR2 data were obtained from Li *et al.* (Li, Imtiaz et al. 2013). For all RyR2 measurements, P_o values were measured in the presence of 2 mM ATP in the cytoplasm.

Table 3.5

Ca^{2+} activation	*Species*	*$[Ca^{2+}]_C$* *pCa*	*$[Ca^{2+}]_L$* *pCa*	*P_{max}*	*$P_{min} \times 10^3$*	*K_a, μM*	*H_a*	*N*
Cytoplasmic	human	-	9	0.9 ± 0.4	0.14 ± 0.02	4 ± 1	2.5 ± 0.4	2-5
Cytoplasmic	sheep	-	9	0.90 ± 0.03	0.15 ± 0.08	1.4 ± 0.3	2.6 ± 1.3	2-7
Cytoplasmic	rat	-	9	0.6 ± 0.05	0.33 ± 0.04	3.4 ± 0.3	3.2 ± 0.5	4
Luminal	human	7	-	0.14 ± 0.03	0.1 ± 0.07	35 ± 12	1.3 ± 0.2	3-17
Luminal	sheep	7	-	0.11 ± 0.06	-	60 ± 1.4	2*	4-19
Luminal	rat	7	-	0.013 ± 0.003	-	10 ± 7	2*	3-16

Table 3.5 Summary of the Hill Fit Parameters for Ca^{2+} dependence of human, sheep and rat cardiac RyRs P_o.

Table 3.6

Mg^{2+} inhibition	***Species***	***$[Ca^{2+}]_C$*** *pCa*	***$[Ca^{2+}]_L$*** *pCa*	***P_{max}***	***K_i, mM***	***H_i***	***n***
Cytoplasmic	human	7	4	0.03 ± 0.004	0.01 ± 0.004	1.1 ± 0.5	4
Cytoplasmic	sheep	7	4	0.19 ± 0.06	0.018 ± 0.003	1.4 ± 0.3	3-26
Cytoplasmic	rat	7	4	0.019 ± 0.015	0.013 ± 0.006	1.3 ± 0.7	10
Cytoplasmic	human	4	4	0.9 ± 0.06	5.4 ± 0.8	0.85 ± 0.2	4-10
Cytoplasmic	sheep	4	4	0.98 ± 0.1	1.6 ± 0.2	0.74 ± 0.3	4-7
Luminal	human	7	4	0.09 ± 0.02	0.55 ± 0.03	3.8 ± 1.8	5-6
Luminal	sheep	7	4	0.19 ± 0.1	0.049 ± 0 .004	1 ± 0.2	3-19
Luminal	rat	7	4	0.023 ± 0.011	0.078 ± 0.014	1.3 ± 0.5	7

Table 3.6 Summary of the Hill Fit Parameters for Mg^{2+} inhibition of human, sheep and rat cardiac RyRs P_o.

3.3.6 Ca^{2+} activation in the presence of [Mg^{2+}]

In order to assess the gating properties of RyR2 at physiological (systolic) concentrations of Ca^{2+} and Mg^{2+}, the dependence of RyR2 P_o for a range of cytoplasmic [Ca^{2+}] in the presence of 1 mM free Mg^{2+} and 2 mM ATP in the cytoplasm and luminal pCa 4 was measured (Cannell, Kong et al. 2013) (Figure 3.7A). The lower limit to the experimental cytoplasmic [Ca^{2+}] range was set by the minimum P_o that could be reliably measured (P_o~10^{-4}). Under these conditions, human RyR2 had a K_a for Ca^{2+} activation of 25 ± 8 μM and a maximum P_o of 0.55 ± 0.1. In the presence of 1 mM cytoplasmic Mg^{2+}, RyR2s from human and sheep have similar Ca^{2+} activation properties, whereas RyR2s from rat is 3-fold less sensitive to cytoplasmic Ca^{2+} (p= 0.002, Figure 3.7A).

The luminal Ca^{2+} activation properties of RyR2 channels from human, sheep and rat in the presence of 1 mM luminal Mg^{2+} (without cytoplasmic Mg^{2+}) are shown in Figure 3.7B. The near linear luminal Ca^{2+} dependencies of RyR P_o seen here are substantially different than the strongly saturating dependencies measured in the absence of luminal Mg^{2+} (Figure 3.3). In the presence of luminal Mg^{2+}, the RyR2 channels showed a marked variation between species with sheep exhibiting the steepest dependence on luminal Ca^{2+} followed by RyRs from human and rat. The luminal Ca^{2+} activation of human RyR2s was mediated mainly by an increase in opening rate (Figure 3.7C) whereas mean open times (Figure 3.7D) showed no significant dependence on luminal [Ca^{2+}].

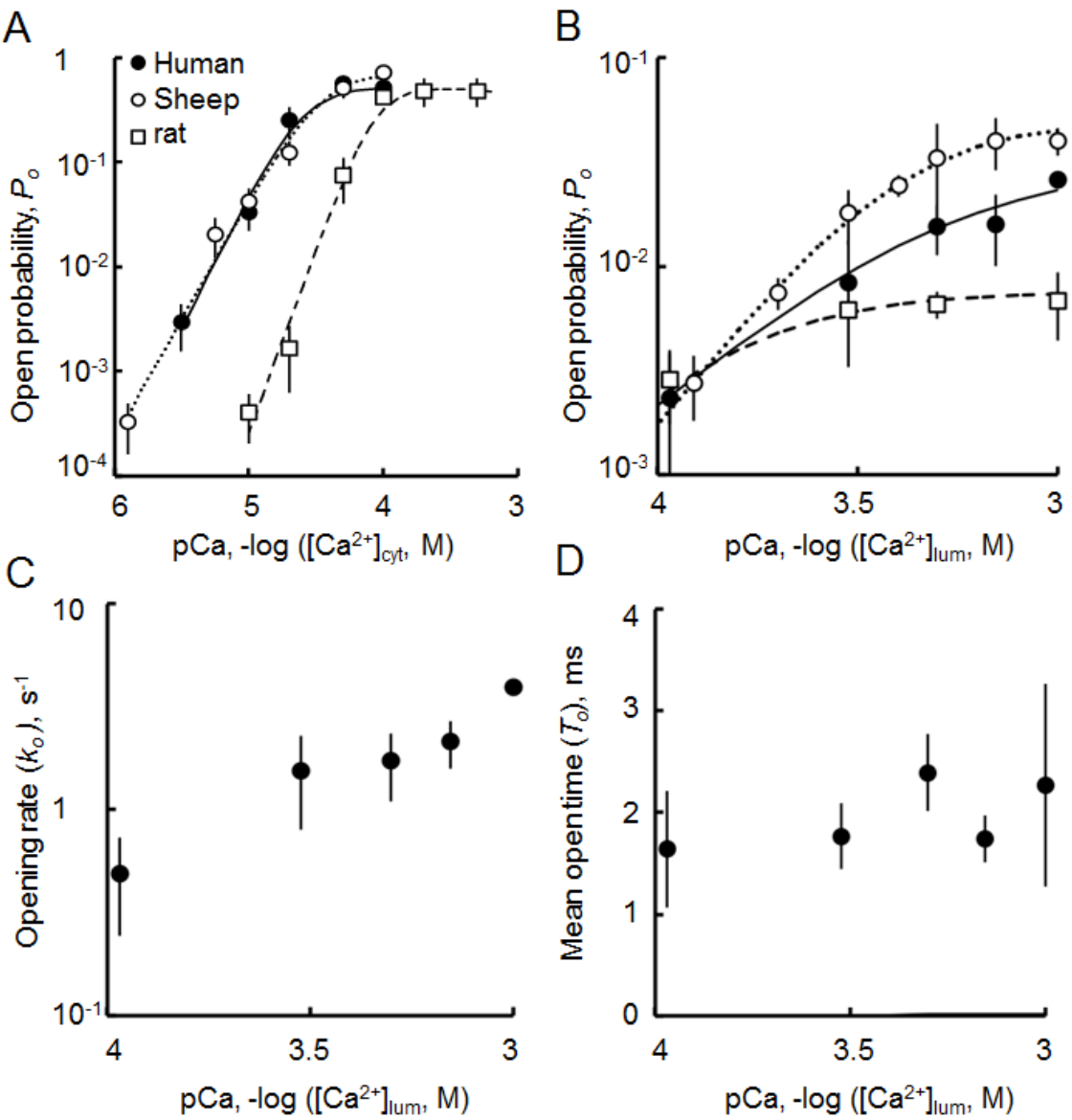

Figure 3.7: Combined Ca^{2+} and Mg^{2+} regulation of RyR2 compared in human, sheep and rat. (A) Cytoplasmic [Ca^{2+}] activation response of RyR2s in the presence 1mM free Mg^{2+} and 2 mM ATP in the cytoplasm and luminal pCa 4. RyR2 from human, sheep and rat are indicated in the legend (legend applies to all panels) **(B)** Luminal [Ca^{2+}] activation response of RyR2s in the presence of 1mM luminal Mg^{2+}, with cytoplasmic pCa 7 and 2 mM cytoplasmic ATP. **(C,D)** Corresponding values of mean opening rate and open duration for human RyR2s. Data points show the mean ± SEM. The solid and dashed curves show Hill fits to the data. The numbers of experiments and the Hill parameters for rat and sheep RyR2s are listed in Table 3.7. Data for sheep and rat RyR2s in part A were obtained from Cannell *et al.* (Cannell, Kong et al. 2013).

Table 3.7

Ca^{2+} activation	*Species*	*$[Ca^{2+}]_C$* *pCa*	*$[Ca^{2+}]_L$* *pCa*	*P_{max}*	*K_a, μM*	*H_a*	*n*
Cytoplasmic (1 mM cytoplasmic Mg^{2+})	human	-	4	0.55 ± 0.1	25 ± 8.0	2.6 ± 0.6	4-8
Cytoplasmic (1 mM cytoplasmic Mg^{2+})	sheep	-	4	0.7 ± 0.1	34 ± 5	2.2 ± 0.16	5-10
Cytoplasmic (1 mM cytoplasmic Mg^{2+})	rat	-	4	0.54 ± 0.06	88 ± 9	3.5 ± 0.4	4-7
Luminal (1 mM luminal Mg^{2+})	human	7	-	0.03 ± 0.018	-	-	3-6
Luminal (1 mM luminal Mg^{2+})	sheep	7	-	0.06 ± 0.01	400 ± 40	2.4 ± 0.5	3-6
Luminal (1 mM luminal Mg^{2+})	rat	7	-	0.007 ± 0.002	-	-	2-4

Table 3.7 Summary of the Hill Fit Parameters for Ca^{2+} dependence of human, sheep and rat cardiac RyRs P_o in presence of 1 mM Mg^{2+} (cytoplasmic or luminal).

3.4 Discussion

3.4.1 Mechanisms for Ca^{2+} and Mg^{2+} regulation of RyR2

This study presents a detailed analysis of the regulation of human RyR2s by intracellular Ca^{2+} and Mg^{2+}. This is the first report of measurements of the concentration-dependencies of native healthy human RyR2 regulation by luminal and cytoplasmic Ca^{2+} and Mg^{2+}. It was found that human RyR2s displayed the same Ca^{2+}/ Mg^{2+} regulation phenomena as seen in rat and sheep. RyR2s were activated by 1 μM cytoplasmic and luminal Ca^{2+} and inhibited by Mg^{2+} in the lumen and cytoplasm. However, the sensitivity to luminal Ca^{2+} and Mg^{2+} varied between species and RyR2s from human hearts were less sensitive to inhibition by luminal Mg^{2+} compared to that seen in sheep and rat RyR2s.

The molecular mechanism for these differences is not yet clear. They could arise from differences in the amino acid sequences of the RyR2, which share 96-98% homology between species (ExPASy: human Q92736; rat B0LPN4; and sheep Q9MZD9). However, the sensitivity for Ca^{2+} activation in isolated native human RyR2s reported here (K_a = ~ 6 μM, Table 3.1) was nearly 10-fold lower than that seen in recombinant RyR2s (K_a for cytoplasmic Ca^{2+} between 0.4 and 0.7 μM (Wehrens, Lehnart et al. 2004)). This suggests that factors other than amino acid sequence are important in determining RyR2 activity. Species-specific posttranslational modifications or differing degrees of association with co-proteins such as FKBP12/12.6 (Galfre, Pitt et al. 2012) could be responsible. For example, the adrenergic tone of rat hearts is known to affect the activity of RyRs isolated from these hearts when incorporated into artificial lipid bilayers (Li, Imtiaz et al. 2013). Therefore, it is possible that variations in adrenergic tone between species or changes in the baseline level of RyR2 phosphorylation/ oxidation during harvesting procedure could underlie the different RyR2 properties from sheep, rat and human. Unfortunately, the level of RyR2 phosphorylation/ oxidation was not measured in this study (except for the human where the level of RyR2 phosphorylation at S^{2814} and S^{2808} was measured, see chapter 4).

The cytoplasmic Ca^{2+} activation and Mg^{2+} inhibition of RyRs observed in several species has been attributed to the combined action of a high affinity Ca^{2+} activation site (Smith, Coronado et al. 1986; Hymel, Inui et al. 1988) and a low affinity divalent cation inhibition site (Meissner 1986; Laver, Roden et al. 1995; Laver, Baynes et al. 1997) located in the cytoplasm-facing domains of the RyR. These sites are referred to here as the A-site and I_1-site after the nomenclature of Balog *et al.* (Balog, Fruen et al. 2001). Mg^{2+}-inhibition that is apparent at sub-μM (diastolic) cytoplasmic Ca^{2+} occurs because Mg^{2+} binding occludes the A-site and prevents Ca^{2+} from binding and activating the RyR but unlike Ca^{2+}, Mg^{2+} does not cause the channel to open. Competition between Ca^{2+} and Mg^{2+} for the A-site reduces the potency of this form of Mg^{2+} inhibition at high (systolic) [Ca^{2+}], revealing another Mg^{2+} inhibition mechanism that is due to Mg^{2+} binding to the I_1-site. Here, RyRs from human, rat and sheep were similarly activated by cytoplasmic Ca^{2+} and inhibited by Mg^{2+} (Figures 3.6A & C), suggesting that the A- and I_1-sites could be strongly conserved between species.

At sub μM cytoplasmic [Ca^{2+}], human RyR2 P_o values were increased by raising luminal [Ca^{2+}]. Interpreting the mechanism for this phenomenon is complicated by the fact that luminal Ca^{2+} can pass through the channel and act via the cytoplasmic facing A-site (Tripathy and Meissner 1996; Laver 2007). Therefore, it is difficult to determine if luminal activation of the RyR is due to Ca^{2+} binding at the luminal or cytoplasmic facing activation sites. However, the luminal/cytoplasmic location of the activation site determining the RyR opening rate is simpler to determine because opening rate is derived from the duration of intervals where channels are closed and Ca^{2+} cannot cross the membrane. The RyR opening rate was increased by luminal Ca^{2+}, even in the virtual absence of cytoplasmic Ca^{2+} (pCa 9, Figure 3.3C), indicating a Ca^{2+} activation site (L-site) located on the luminal side of the RyR gate. An increase in cytoplasmic [Ca^{2+}] from pCa 9 to pCa 7 amplified the luminal activation of opening rate by nearly 10-fold, demonstrating a marked synergy between A- and L-site-mediated activation mechanisms. An explanation for this phenomenon has been posited in a model in which channel openings are triggered by the combined action of A- and L-sites on each of the four RyR subunits (Laver and Honen 2008; Laver 2010).

Both P_o and T_o showed bell-shaped dependencies on luminal [Ca^{2+}] (Figure 3.3B & D) due to combined actions of high affinity Ca^{2+} activation and low affinity inactivation mechanisms. Results reported here on human RyRs together with results from our previous studies on sheep RyRs, showed that the luminal Ca^{2+} sensitivity for T_o (and hence P_o) strongly depends on the electrochemical driving force for luminal Ca^{2+} through the channel suggesting that the Ca^{2+} sites that modulate open durations are on the cytoplasmic side of the RyR (Tripathy and Meissner 1996; Laver 2007). Thus, once the channel is open, feed-through of luminal Ca^{2+} to the cytoplasmic domains may further reinforce channel openings via the A-site or cause channel inactivation via either of two cytoplasmic inactivation sites: the low affinity cation site (I_1-site (Liu, Porta et al. 2010)) and the high affinity I_2-site (Laver 2007; Laver and Honen 2008).

Results here showed that a physiological concentration (1 mM) of luminal Mg^{2+} produced a 10-fold inhibition of RyR2s activity at diastolic cytoplasmic [Ca^{2+}]. The observed reduction in opening rate (Figure 3.5C) indicates that inhibition can be partly attributed to Mg^{2+} binding at a luminal site. The reduction in potency of this inhibition at higher luminal [Ca^{2+}] (*c.f.* luminal pCa 4 and pCa 3 in Figure 3.5C) indicated competition between Ca^{2+} and Mg^{2+} for this site. The simplest explanation for these properties of luminal Mg^{2+} inhibition is that Mg^{2+} inhibits by binding to and occluding the L-site from activation by Ca^{2+}. Mean open time was also decreased by luminal Mg^{2+} (Figure 3.5D) and since Mg^{2+} can also permeate the channel and bind to the cytoplasmic A-site, it is possible that the reduction in mean open time is due to interactions between luminal Mg^{2+} and cytoplasmic sites. Computational models of this process show that it can account for the kinetics of luminal Mg^{2+} inhibition of sheep RyRs (Laver and Honen 2008). Interestingly, there were substantial differences in the luminal regulation of RyR2 from human, sheep and rat (Figure 3.6C & D) where it can be seen that human RyR2s are more highly activated by luminal Ca^{2+} and less inhibited by luminal Mg^{2+}. The differences in RyR2 inhibition by luminal Mg^{2+} and activation by luminal Ca^{2+} both indicate a divergence in the properties of the L-site of RyR2s between human, rat and sheep.

3.4.2 The importance of luminal Mg^{2+}

These results show that Mg^{2+} in the cytoplasm and SR lumen will be a major determinate of how Ca^{2+} regulates RyRs. In the absence of luminal Mg^{2+}, luminal Ca^{2+} activation of RyRs is near saturation at sub-physiological luminal Ca^{2+} (pCa 4, open and filled circles in Figure 3.3B). Throughout the physiological range of luminal [Ca^{2+}] (pCa 4 to pCa 3), RyR open probability varied by only 1.7-fold at +40 mV and 2-fold at -40 mV. Thus, it would be difficult to reconcile these relatively small variations with the much larger luminal Ca^{2+} dependence of the frequency of Ca^{2+} release events in cardiomyocytes (discussed in more detail below) (Zima, Bovo et al. 2010). However, the inclusion of physiological levels of luminal Mg^{2+} in our bilayer experiments markedly increased the K_a for luminal Ca^{2+} activation from less than 100 μM to ~1 mM. Hence, RyR2 P_o and opening rate were strongly dependent on luminal Ca^{2+} showing a 10-fold increase between luminal pCa 4 and pCa 3 (Figure 3.7B and C). The increase in K_a for RyR2 opening rate is a manifestation of competition between luminal Ca^{2+} and Mg^{2+} for luminal activating sites on the RyR2 (Laver and Honen 2008). Thus, the results here indicate that Mg^{2+} in the SR lumen should markedly enhance the relative effect of SR [Ca^{2+}] on RyR activity. Therefore, luminal Mg^{2+} is likely to play an important role in the cell in shaping the dose-response of RyRs to store Ca^{2+} load during diastole.

3.4.3 Role of RyR2 regulation in the Calcium Release Units (CRUs)

Modelling studies of Ca^{2+} diffusion in the dyad cleft predict that dyad [Ca^{2+}] rises to ~0.1 mM within 500 μs of the opening of a DHPR or RyR2 (Soeller and Cannell 1997; Laver, Kong et al. 2013). The gating properties of RyR2s in the presence of dyadic [Ca^{2+}] and [Mg^{2+}] are given in Figure 3.7A where it can be seen that significant levels of RyR activation occur when [Ca^{2+}] reaches ~ 30 μM (K_a for human and sheep) or 90 μM (K_a for rat) in the cytoplasm. Therefore, RyRs have sufficient Ca^{2+} sensitivity in bilayer experiments presented here to account for CICR in the dyad and hence the generation of Ca^{2+} sparks. However, when the dyad [Ca^{2+}] falls below the K_a for RyRs, as would happen as Ca^{2+} stores deplete during Ca^{2+} release, then CICR would not be

+sustainable and Ca^{2+} sparks should terminate. Such a mechanism, dubbed 'induction decay', has been proposed as the basis for Ca^{2+} spark termination (Cannell, Kong et al. 2013). My data also suggests that modulation of RyR P_o by luminal Ca^{2+} is not likely to occur during Ca^{2+} release when cytoplasmic [Ca^{2+}]s near the RyR are high. This work here, and previous studies (Cannell, Kong et al. 2013) found that luminal Ca^{2+} did not affect RyR gating when cytoplasmic [Ca^{2+}] exceeded 1 μM.

Triggering of Ca^{2+} sparks occurs under diastolic conditions where cytoplasmic [Ca^{2+}] = 100 nM, with cytoplasmic and luminal [Mg^{2+}] =1 mM (Cannell, Kong et al. 2013). Single channel measurements of RyR2 activity under these conditions are impractical because RyR2 activity is too low. Therefore, diastolic P_o was estimated by multiplying the P_o values in Figure 3.7B (*i.e* in absence of cytoplasmic Mg^{2+}) by an inhibition factor derived from extrapolating the Hill curves for cytoplasmic Mg^{2+} inhibition. Thus, based on the K_i values and Hill coefficients for Mg^{2+} inhibition of the RyR2 for the human, rat and sheep, it was estimated that the addition of 1 mM Mg^{2+} to the cytoplasm reduces the P_o values in Figure 3.7B by a factor of ~1000 for the three species. Thus P_o for the human RyR2 is predicted to increase from 2 x 10^{-6} to 2 x 10^{-5} as store load increases from 0.1 to 1 mM.

The predicted P_o of 2 x10^{-5}, corresponding to an opening rate of 0.003 s^{-1} for RyRs under diastolic conditions (see below for calculation), predicts an upper estimate for Ca^{2+} spark frequency of 6 s^{-1} [1] which is within the range of experimental values, 1-15 s^{-1} (Cheng, Lederer et al. 1996; Zima, Bovo et al. 2010). Spark frequency is reported to have a steep dependence on luminal [Ca^{2+}], increasing 3-fold between 0.6 and 1 mM (Zima, Bovo et al. 2010) which is substantially larger than the 1.5-fold change in RyR P_o reported here over the same concentration range. This suggests that P_o is not the only determinate of spark frequency. A computational 3D model of the cardiac dyad explained the steep luminal dependence of spark frequency by increases in both RyR P_o and the probability that a single RyR opening will trigger a Ca^{2+} spark (an increased

[1] This value is calculated assuming 100 μm scan line including 110 Ca^{2+} release sites with 20 RyRs at each site and that every RyR opening triggers a spark.

Ca^{2+} flux through each RyR increases CICR) (Cannell, Kong et al. 2013). The synergistic activation of RyRs by luminal and cytoplasmic Ca^{2+} reported here, in which cytoplasmic Ca^{2+} amplifies the luminal Ca^{2+} response, is reflected in the dependence of spark frequency on luminal and cytoplasmic [Ca^{2+}] in rabbit ventricular myocytes (Zima, Bovo et al. 2010). Hence, the synergy between the A- and L-sites in determining RyR2 opening rates provides an explanation for their observed spark frequencies.

$P_o = T_o / (T_o + T_c)$, *since* $T_o << T_c$ in diastole (T_o ~6 x10^{-3} s, Figure 3.7). $P_o \sim T_o / T_c$

P_o = 2 x10^{-5}= 6 x10^{-3}/ T_c, T_c = 3 x 10^2 s

k_o = 1/ T_c = 1 /(3 x 10^2 s) = ~3 x10^{-3} s^{-1}

In summary, RyRs from all three species displayed the same Ca^{2+}/ Mg^{2+} regulation mechanisms. The cytoplasmic regulation was identical in all three species whereas the luminal based mechanisms showed up to 3-fold differences in Ca^{2+} and Mg^{2+} sensitivity. RyR2s from human hearts were less sensitive to inhibition by luminal Mg^{2+} and more sensitive to luminal Ca^{2+} compared to that seen in sheep and rat RyR2s.

Chapter 4- Ryanodine channel function (RyR2) in healthy and failing human hearts

4.1 Introduction

The ryanodine channel (RyR2), the Ca^{2+} release channel in the heart, is the key determinate of cardiac muscle force and cardiac rhythm. The RyR2 is a macromolecular complex (mw565 kDa) consisting of four monomers, each of which is associated with regulatory polypeptides that regulate the channel function (Lehnart, Wehrens et al. 2005). The N-terminal of the RyR2 acts as a scaffold for accessory proteins including FKBP12.6 (calstabin2), protein kinases (PKA and CaMKII), protein phosphatases (PP1 and PP2a) (Marx, Gaburjakova et al. 2001), and a cAMP-specific type 4 phosphodiesterase (PDE4D3) which binds to each RyR2 monomer via their specific anchoring proteins (Marks, Marx et al. 2002). Both junctin and triadin, which anchor calsequestrin, bind to the luminal portion of the channel (Bers 2004).

Heart failure (HF) is commonly the end stage of a heterogeneous group of cardiomyopathies (Maron, Towbin et al. 2006). In this study, the functional and structural remodelling of the RyR2 macromolecular complex in heart tissue from patients with Ischaemic cardiomyopathy (ICM), Emery Dreifuss Muscular Dystrophy with cardiomyopathy (EDMD) and cystic fibrosis (Pollock, McFarlane et al.) were investigated. ICM (not formally classified as a myopathy) is muscle weakness resulting from myocardial infarction or coronary artery disease, which constricts blood supply to the heart muscle. EDMD is a rare skeletal muscle dystrophy arising from mutations in either the gene encoding for lamin or emerin (Brown, Piercy et al. 2008). The autosomal dominant form of EDMD (defects in lamin) also leads to cardiac conduction defects, dilated cardiomyopathy (Brown, Piercy et al. 2008; Azibani, Muchir et al. 2014) and low-normal systolic function (Voit, Krogmann et al. 1988; Bialer, McDaniel et al. 1991). CF is an autosomal recessive genetic disorder resulting in the loss of epithelium Cl^- transport (the cystic fibrosis transmembrane conductance regulator; CFTR Cl^- transporter) resulting in reduced function of several organs including the lungs and causing increased after-load on the heart (Bright-Thomas and Webb 2002). Ischemic heart disease was found in one case of a CF patient at 48 years of age (Perrin and Serino 2010). CF is not normally associated with HF, probably due to the short life expectancy of CF patients. However, right ventricular enlargement (Burghuber, Salzer-Muhar et al. 1988; Weitzenblum 1994; Florea, Florea et al. 2000; Bright-Thomas and Webb 2002)

and reduced left ventricular filling (Jacobstein, Hirschfeld et al. 1981; Johnson, Kanga et al. 1991; Sellers, Kovacs et al. 2013) have been detected in CF, secondary to lung disease, hypoxaemia, hypercarbia and acidaemia.. Recently, it was found that loss of CFTR Cl^- transport in CF causes cardiac dysfunction independently of lung disease (Sellers, Kovacs et al. 2013), possibly because of the contribution of CFTR to maintenance of the ventricular resting membrane potential and AP duration (Kuzumoto, Takeuchi et al. 2008; Sellers, De Arcangelis et al. 2010; Sellers, Naren et al. 2012). The first investigation of structural and functional remodelling of RyR2 in CF was made in this study.

HF is a complex disorder that involves changes in expression of Ca^{2+} handling proteins, Ca^{2+} dynamics, and tissue remodelling (George 2008). In human HF, there is a down regulation of SERCA2a (Lindner, Erdmann et al. 1998; Jiang, Lokuta et al. 2002; Piacentino, Weber et al. 2003) and up regulation of the Na^+/Ca^{2+} exchanger (NCX) (Studer, Reinecke et al. 1994). Changes in expression and function of SERCA2a (decreased expression levels at both the mRNA and protein levels) have been shown in the rat model of HF (Guo, Chapman et al. 2003; Hu, Shen et al. 2010). A 35% decrease in RyR2 level has been reported in human HF (Go, Moschella et al. 1995). The resulting decline in SR calcium content causes a reduction in cardiac output and a compensating increase in sympathetic nervous system activity (Braunwald and Chidsey 1965; Bristow, Ginsburg et al. 1982; Cohn, Levine et al. 1984; Kinugawa, Ogino et al. 1996). PKA phosphorylation of most of the Ca^{2+} signaling proteins (hyperphosphorylation), including the RyR2, as a result of chronic activation of the sympathetic nervous system has been reported in HF (Kushnir, Betzenhauser et al. ; Lehnart, Wehrens et al. 2005; Wehrens, Lehnart et al. 2006). There is a considerable amount of controversy in the literature concerning the role of RyR2s in the contractile dysfunction of HF and the effects of phosphorylation on its activity (regulation by intracellular Ca^{2+} and Mg^{2+}). It has been shown that normal adrenergic stimulation of rat hearts increases RyR2 activity by increasing their activation by Ca^{2+} in the SR lumen and decreasing luminal inhibition by Mg^{2+} (Li, Imtiaz et al. 2013). However, in HF, RyRs become highly active and lack regulation by intracellular Ca^{2+} (Shannon, Pogwizd et al. 2003). Increased diastolic SR Ca^{2+} leak as a consequence of high RyR activity

would tend to deplete the SR Ca^{2+} load and increase diastolic $[Ca^{2+}]_i$ (Shannon, Pogwizd et al. 2003).

The cause of RyR2 channel dysfunction in HF is highly controversial and may involve many mechanisms. In HF, there are reductions in the amounts of bound PP1, PP2A, and PDE4D3 in the RyR2 complex (Marx, Reiken et al. 2000); each of these would lead to increased phosphorylation of the RyR2. Three phosphorylation sites on the RyR2 (Ser^{2030}, Ser^{2808} and Ser^{2815}) have been associated with regulation of RyR2. Studies have associated hyperphosphorylation at S^{2808} (Hu, Shen et al. ; Respress, van Oort et al. 2012) with the progression of HF. It has been proposed that PKA hyperphosphorylation at Ser^{2808} leads to dissociation of the regulatory protein FKBP12.6 from the RyR2 complex and changes the channel stoichiometry (Hu, Shen et al. 2010). Loss of FKBP12.6 from the RyR2 leads to destabilization of the channel and increases diastolic Ca^{2+} leak (Marx, Reiken et al. 2000; Yano, Ono et al. 2000). This is supported by single channel studies of RyR2s from human and canine failing myocardium which revealed that RyR2s from failing hearts exhibited increased open probability, sensitivity to Ca^{2+} activation and increased frequency of subconductance states (Marx, Reiken et al. 2000) which mimicked changes seen when the RyR2 was PKA phosphorylated and subsequently dissociated from FKBP12.6. On the other hand, another study also using human and canine failing hearts, did not see any of these differences in RyR2 activity from failing and non-failing hearts (Jiang, Lokuta et al. 2002). Moreover, Ser^{2808} was found not to be associated with myocardial infarction (Zhang, Makarewich et al. 2012). An alternative hypothesis proposed that RyR2 remodelling is initiated by a defective interdomain interaction (unzipping state) in response to oxidation and RyR2 hyperphosphorylation (Oda, Yano et al. 2005; Yano, Okuda et al. 2005). However, no one has examined the Ca^{2+} handling or RyR2 function in hearts from patients with CF and EDMD.

In this study, single channel recordings of RyR2s in artificial lipid bilayers were used to compare Ca^{2+} and Mg^{2+} regulation of RyR2 from healthy, CF and failing hearts, specifically, Ischaemic cardiomyopathy (ICM), Emery Dreifuss muscular dystrophy (EDMD). These functional changes were compared with remodelling of the macromolecular structural properties in healthy, CF and failing RyRs using Western

blot assays to probe RyR2 phosphorylation at S^{2808} and S^{2814}, and association of FKBP12, FKBP12.6, and phosphatases to RyR2s. The expression levels of NCX, SERCA, junctin, CSQ2 and triadin-1 were measured and compared in healthy and failing hearts. The results that are presented here help define the roles of Ca^{2+}-Mg^{2+} imbalance and changes in RyR regulation by intracellular Mg^{2+} and Ca^{2+} in CF and HF. These findings better define remodelling of the RyR complex in both. ICM and EDMD hearts that exhibited decreased expression levels of RyR2 and dephosphorylating enzymes. SERCA2a was decreased in ICM heart whilst CSQ2 and triadin-1 were reduced in EDMD heart. Finally, decreased association of both FKBP12 and FKBP12.6 have been detected in RyR2s from failing hearts. RyR2 remodelling in HF may have a role in RyR2 hyperactivity at diastolic [Ca^{2+}] and reduced sensitivity to intracellular Mg^{2+} inhibition.

4.2 Materials and Methods

4.2.1 *Human heart tissue & single-channel measurements*

Access to human heart tissue, both failing and healthy, was through collaborations with Dr. Molenaar at the University of Queensland and Dr. dos Remedios at the University of Sydney. Human RyR2s were obtained from patients with healthy, cystic fibrosis (CF) and failing hearts, specifically, Ischaemic cardiomyopathy (ICM) and Emery Dreifuss muscular dystrophy (EDMD, a rare inherited disorder that affects skeletal and cardiac muscle). Initially, CF heart samples were included among our healthy heart group. However, as the study progressed, it became clear that RyR2 from this heart differed from those obtained from five other hearts donated by healthy accident victims. SR vesicles containing RyRs from failing, CF and non-failing human hearts were incorporated into artificial lipid bilayers and channel gating was measured by single channel recordings. RyR2 open and closed times were measured in the presence of various concentrations of cytoplasmic and luminal [Ca^{2+}] and [Mg^{2+}] and cytoplasmic ATP (2 mM). See methods chapter, sections 2.1, 2.2 & 2.3.

4.2.2 Statistics

Data from Western Blot experiments are presented as arithmetic ± standard errors of the mean (SEM). RyR2 gating parameters are presented as geometric means ± 67% confidence that is given in parentheses. Geometric means were used because the distribution of gating parameters was close to normal on a logarithm scale (arithmetic mean on a logarithmic scale is equivalent to the geometric mean on a linear scale). Significance was calculated by Student's *t* test on logarithms of the data. $p<0.05$ was considered significant (*) and $p < 0.01$ was considered highly significant (**).

4.3 Results

4.3.1 RyR2 regulation by intracellular Ca^{2+}

RyR2s from healthy and failing hearts were incorporated into lipid bilayers. Figure 4.1 shows channel recordings of human RyR2 activity at -40 mV, that were taken in the presence of cytoplasmic solutions containing diastolic concentrations of Ca^{2+} (pCa 7), zero Mg^{2+} and 2 mM ATP, and luminal solutions containing 0.1 mM Ca^{2+},(unless otherwise stated, these are the experimental conditions). RyR2s from healthy human heart showed a higher unitary current compared to RyR2s from failing human hearts. The cesium ion conductance of healthy RyRs was 575 ± 5 pS (n=6), showing very little variation between individual channels, whereas, those from ICM and EDMD hearts which exhibited normal channel gating, had conductances of 505 ± 26 pS (n=7) and 500 ± 15 pS (n=7), respectively. It can also be seen from Figure 4.1 that there was considerable channel-to-channel variation in channel activity among RyRs from healthy and failing hearts (*c.f.* low medium and high P_o traces in Figure 4.1). On four occasions (from 34 experiments), RyR2s from EDMD failing heart showed abnormal channel gating (n=4, e.g. Figure 4.1, abnormal), characterised by lower conductance (304 pS) than seen with normally gated channels along with long open times and multiple conductance levels. These channels were not included in the analysis.

Figure 4.2 shows the relative values of RyR2 P_o, opening rate and mean open time compared in RyR2s from healthy human hearts, cystic fibrosis (Pollock, McFarlane et al.) and two failing human hearts (Left ventricle of a heart with Ischaemic cardiomyopathy (ICM), left ventricle of a heart from Emery Dreifuss muscular dystrophy (EDMD), and trabecule pooled from 15 hearts with ICM (ICM trabecule). Figure 4.2 shows these properties relative to the healthy group. The data show that RyR2s from CF and failing heart had higher open probabilities, opening rates and mean open times than those from healthy hearts. The absolute mean values (geometric means, see Methods) for these parameters are given in Table 4.1.

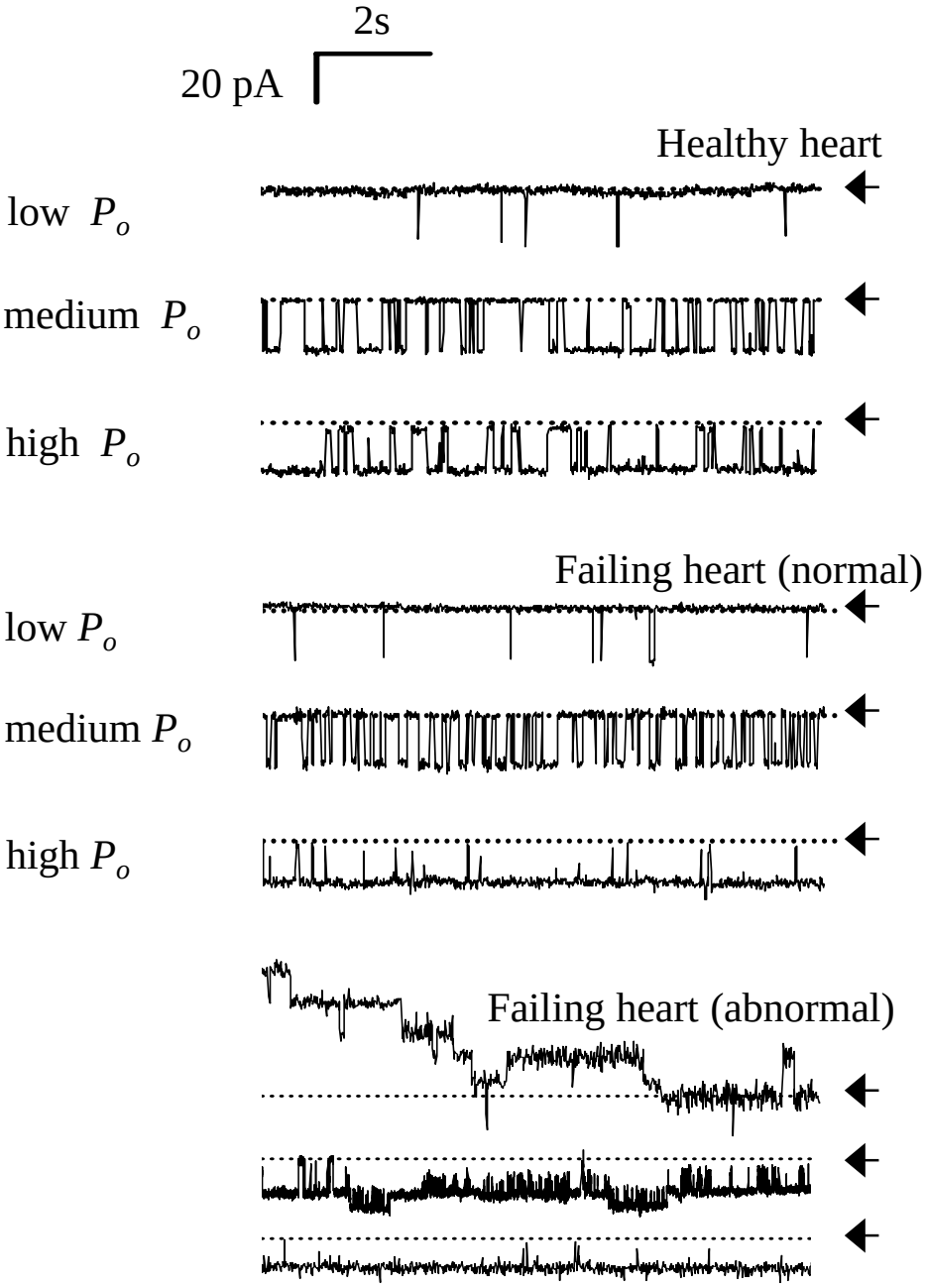

Figure 4.1: Single channel recordings of RyR2s from failing and non-failing human hearts. Channel recordings were taken at cytoplasmic pCa 7 and 0.1 mM luminal Ca^{2+} in the presence of 2 mM ATP in the cytoplasm at -40 mV. Channel openings are downward current jumps from the baseline (arrows). RyR2s were taken from healthy and failing (Emery Dreifuss muscular dystrophy (EDMD)) human hearts. Normal and abnormal indicate for channel gating.

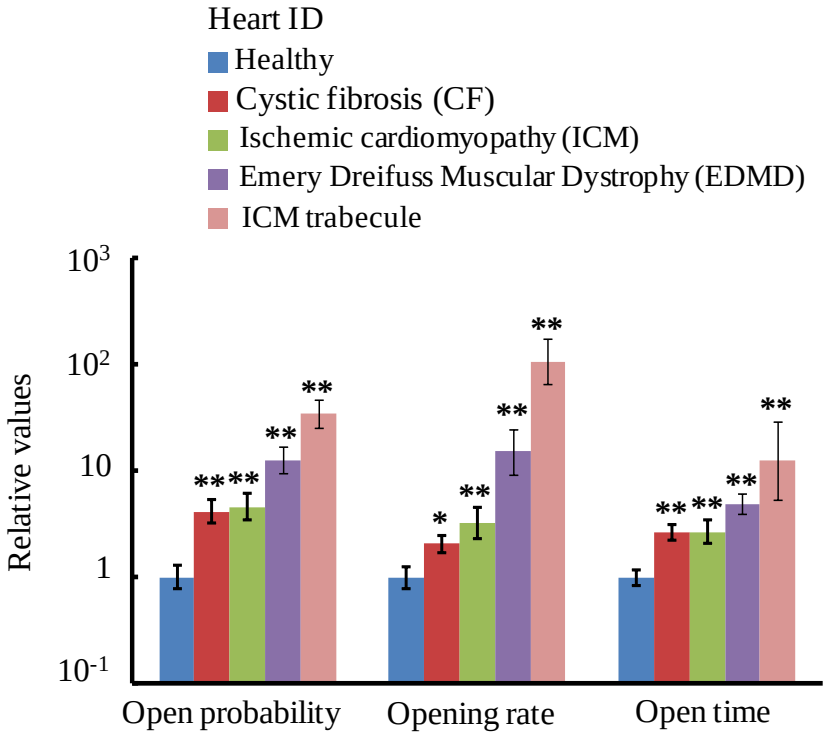

Figure 4.2: Relative values of RyR2 P_o, opening rate and mean open time. RyR2s were isolated from four healthy hearts, cystic fibrosis heart (Pollock, McFarlane et al.), the left ventricle of a failing heart with ischemic cardiomyopathy (ICM), trabecule pooled from 15 ICM hearts (ICM trabecule) and a left ventricle of a heart with Emery Dreifuss Muscular Dystrophy (EDMD). Channel activity was recorded at -40 mV were made at cytoplasmic pCa 7 and 0.1 mM luminal Ca^{2+} in the presence of 2 mM ATP in the cytoplasm. Values are expressed relative to the average calculated for healthy heart. Data are shown as geometric mean ± SEM. The number of experiments and the relative values are listed in Table 4.1. Asterisks (*) denote a significant difference in relative values compared with healthy human heart (* $p<0.05$, ** $p<0.01$).

Table 4.1

heart group	P_o	T_o, ms	k_o, s^{-1}	n
healthy	0.02 (0.014-0.026)	7 (6-8)	4 (3-5)	53
CF	0.09 (0.07-0.11)	18 (15-21)	8 (6-10)	55
ICM	0.1 (0.07-0.13)	18 (13-23)	12 (7-17)	38
EDMD	0.27 (0.2-0.34)	33 (25-41)	55 (20-90)	30
ICM trabecule	0.7 (0.4-1)	80 (40-190)	340 (230-640)	6

Table 4.1. The geometric mean values for RyR2 open probability, P_o, open duration, T_o, and opening rate, k_o. *n* is the number of experiments. Numbers in parentheses show upper and lower 67% confidence limits.

The channel-to-channel variations in RyR2 activity are shown in Figure 4.3. RyRs from healthy hearts showed a large variation in P_o, ranging from 0.001 up to 0.75. RyR2 T_o values were normally distributed on a log scale with a SD of a factor of 6. Most k_o values for RyR2s from healthy hearts lay in a normal distribution with four outlying values at the high range. RyRs P_o from the CF heart had the same range as those from healthy hearts but the distribution was skewed to higher values (Figure 4.3A, red circles). The distributions of RyR P_o from failing hearts were even more strongly skewed to higher values. Distributions of k_o from failing hearts (Figure 4.3B) showed two modes. One group (low activity group consisting of 85% ICM, 50% EDMD but none of the ICM trabecule) had a similar distribution to healthy hearts while the other, high activity group exhibited more than a 10-fold higher modal value. The distributions of T_o values were skewed to low values suggesting the presence of high and low modes in T_o (Figures 4.3C). RyR2s in the high activity group for open probability were mostly in the high activity groups for mean open time and mean opening rate. Examples of single channel recordings from these groups are shown in (Figure 4.1, *c.f.* low and high P_o traces).

The cytoplasmic Ca^{2+}-dependence of RyR2 from healthy, CF and failing hearts was examined. P_o from healthy hearts exhibited the characteristic Ca^{2+}-dependence with an EC_{50} for activation of 12 ± 4 μM Ca^{2+} (Figure 4.4: note that the fitting of the Hill equation for Ca^{2+} activation to the logarithm of RyR2 P_o is not significantly different to that shown in Table 3.1 (i.e. 6 μM, p=0.25)). At cytoplasmic pCa 7 and pCa 6.5, there was a 10-fold increase in RyR2 activity in RyR2s from CF heart compared to healthy hearts ($p<0.01$). However, the Ca^{2+}-dependent activation of RyR2 P_o from CF heart showed no significant difference in the half-activating concentration or maximal activation compared to healthy heart RyR2s (K_a for P_o is 4 ± 2 μM, p=0.2). RyR2s from failing hearts (ICM & EDMD) showed activation with significantly higher sensitivity to Ca^{2+} (EC_{50}'s ~ 1 μM, Table 4.2, $p<0.023$). The Ca^{2+} dependence of RyR2s with high P_o RyR2s were shown separately. These showed basal levels of activation at low cytoplasmic [Ca^{2+}] (P_{min}) that were ~100-fold higher than RyRs from healthy heart and were similar to fully Ca^{2+}-activated channels.

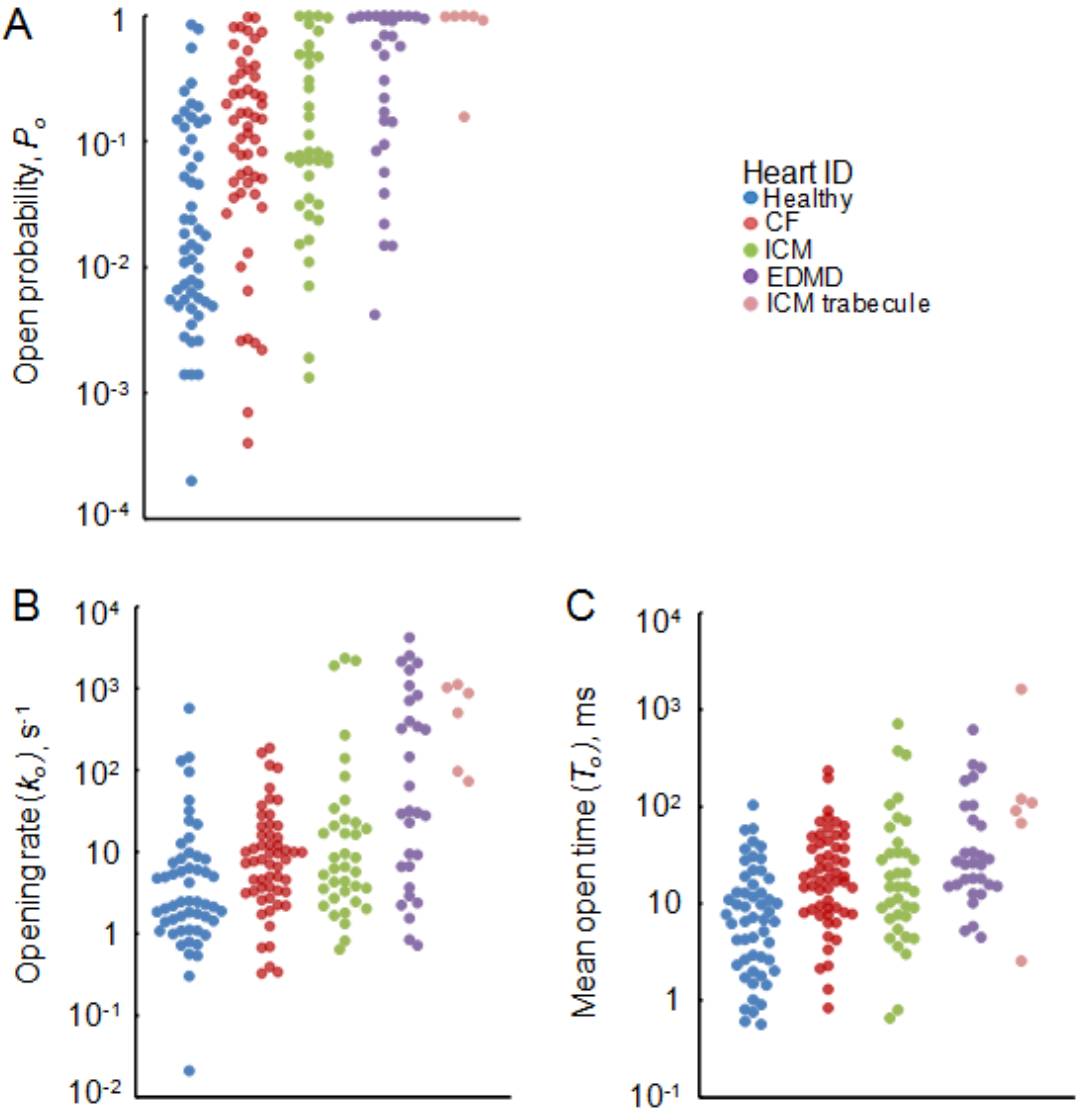

Figure 4.3: Data for individual RyR2s from failing, CF and non-failing human hearts. Channel recordings were made at -40 mV in cytoplasmic pCa 7and 0.1 mM luminal Ca^{2+} in the presence of 2 mM ATP in the cytoplasm. **(A)** P_o distribution of individual RyR2s from the same groups of RyR2s as shown in Figure 4.2. **(B) & (C)** Corresponding opening rate (k_o) and mean open time (T_o), respectively.

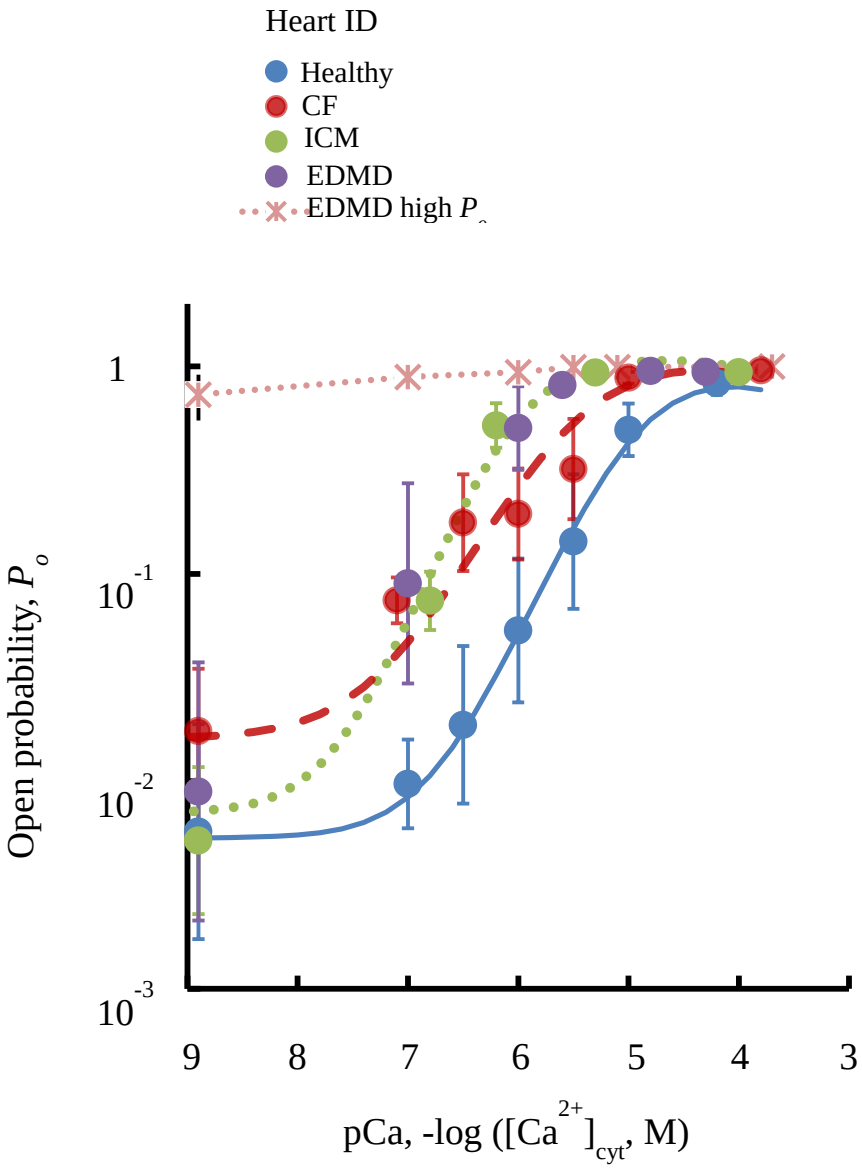

Figure 4.4: Cytoplasmic Ca^{2+} regulation of P_o *were* compared in RyR2 from healthy, CF and failing human hearts. P_o was measured at cytoplasmic pCa 7 and 0.1 mM luminal Ca^{2+} in the presence of 2 mM ATP in the cytoplasm(-40 mV). RyR2s from different human heart tissue are indicated in the legend. Data points show the geometric mean ± SEM. The solid and dashed curves show Hill fits to the data (except for EDMD high P_o, n=2-16). The number of experiments and the Hill parameters are listed in Table 4.2.

Table 4.2

heart group	$[Ca^{2+}]_L$ pCa	P_{max}	$P_{min} \times 10^3$	K_a, μM	H_a	n
healthy	4	0.94 ± 0.1	6 ± 4	12 ± 4	1.2 ± 0.6	5-9
CF	4	1 ± 0.3	20 ± 8	4 ± 2	0.8 ± 0.2	5-11
ICM	4	0.96 ± 0.02	9 ± 7	1 ± 0.2	1 ± 0.4	4-10
EDMD	4	1 ± 0.03	5 ± 3	1 ± 0.1	1.1 ± 0.5	2-5

Table 4.2. Summary of the Hill Fit Parameters for cytoplasmic Ca^{2+} activation (P_o) of human cardiac RyR2s in Figure 4.4.

4.3.2 RyR2 regulation by intracellular Mg^{2+}

The inhibitory effects of cytoplasmic Mg^{2+} on RyR2s from healthy, CF and failing human hearts were measured at cytoplasmic pCa 7 (diastolic [Ca^{2+}], Figure 4.5). Millimolar concentrations of Mg^{2+} ([Mg^{2+}] = 0.24 mM; 1 mM $MgCl_2$ + 2 mM ATP) were added to the cytoplasmic bath and the channel gating was measured before ([Mg^{2+}] = 0) and after the addition of Mg^{2+} (at physiological (1 mM) [Mg^{2+}], RyR2 P_o in healthy hearts was too low to reliably measure). At cytoplasmic pCa 7, it is known that Mg^{2+} inhibits mainly as a competitive inhibitor that binds at the cytoplasmic Ca^{2+} activation site to prevent Ca^{2+} activation of the channel (Laver, Baynes et al. 1997). RyR2s from healthy human hearts were strongly inhibited by cytoplasmic Mg^{2+} (Figure 4.5A). Addition of 1 mM $MgCl_2$ caused a ~1000-fold decrease in RyR2 P_o. RyR2s from the CF heart showed similar inhibition by cytoplasmic Mg^{2+} as healthy human hearts and this is seen in the averaged data (Figure 4.5B). RyR2s from failing human hearts exhibited substantially less inhibition by cytoplasmic Mg^{2+} than RyR2 from healthy hearts (Figure 4.5A & B).

The individual data from healthy and CF hearts showed a large variation in RyR2 sensitivity to cytoplasmic Mg^{2+} inhibition, the inhibition ranging from ~ 10-fold to complete inhibition (Figure 4.5C). None of the RyR2s from EDMD and ICM hearts showed complete inhibition by Mg^{2+}. RyR2 data from EDMD hearts appeared to be bimodally distributed suggesting two types of channel response to Mg^{2+}; one group showed similar Mg^{2+} inhibition to RyRs from healthy heart and a second group that showed a 100-fold less inhibition. All RyR2s from ICM trabecule showed very low sensitivity to Mg^{2+} inhibition. The RyR2s that showed low sensitivity to Mg^{2+} inhibition had a relatively high P_o in the absence of Mg^{2+} indicating that they belonged to the high activity group seen in Figure 4.3.

Mg^{2+} on the luminal side of the RyR2s is also known to inhibit them by competing with Ca^{2+} for luminal activation (Laver and Honen 2008). Luminal Mg^{2+} inhibition was measured at cytoplasmic pCa 7 (Figure 4.6A). Inhibition by 1 mM luminal Mg^{2+} of RyR2 from healthy, CF and failing human hearts is compared in Figure 4.6. Mg^{2+} added to the luminal bath inhibited RyR2 activity from CF and healthy human hearts by ~30 to

50-fold whereas with RyR2s from failing hearts, EDMD and ICM, luminal Mg^{2+} was much less inhibitory (Figure 4.6B). Examination of individual data in Figure 4.6C shows that ~ 40% of RyR2s from ICM and EDMD hearts showed less inhibition than any of the RyR2s from healthy and CF hearts. In several experiments, it was possible to sequentially measure the effect of luminal Mg^{2+} and cytoplasmic Mg^{2+} on the one RyR2. From these data it was possible to investigate the correlation between RyR2 inhibition by 1mM luminal Mg^{2+} and 0.24 mM cytoplasmic Mg^{2+} as shown in Figure 4.7. Interestingly, data from an individual RyR2 correlating the degree of inhibition by cytoplasmic and luminal Mg^{2+} revealed that the 2 RyRs from EDMD failing heart, which exhibited much less sensitivity to luminal Mg^{2+}, also showed less sensitivity to cytoplasmic Mg^{2+}. However, the 3 RyR2s from ICM that showed less sensitivity to luminal Mg^{2+} had normal sensitivity to cytoplasmic Mg^{2+} (Figure 4.7).

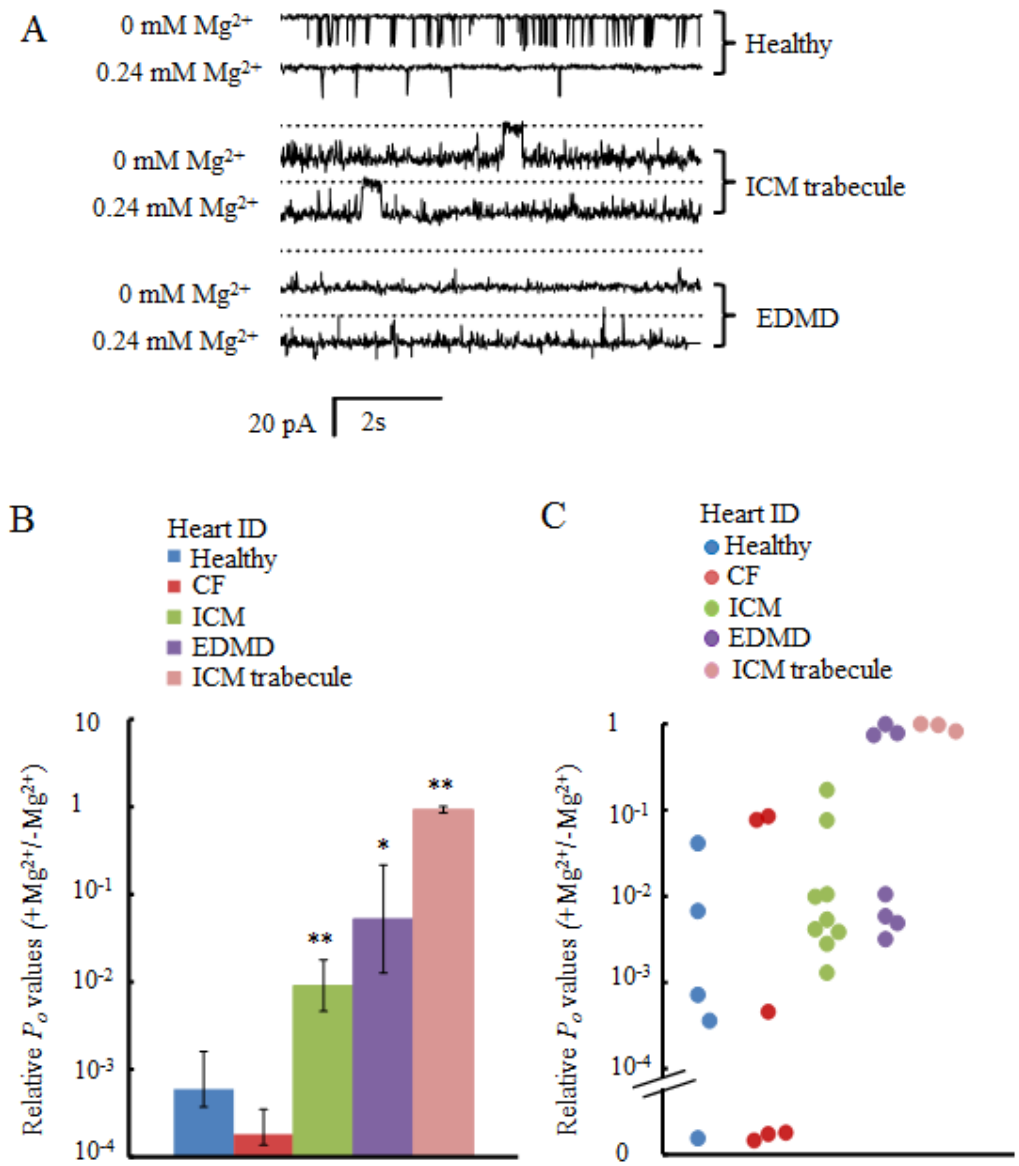

Figure 4.5: Inhibition of RyR2s from failing, CF and healthy human hearts by cytoplasmic Mg^{2+}. **(A)** Single channel recordings of RyR2 from failing and non-failing human hearts in presence or absence of 0.24 mM cytoplasmic Mg^{2+}. Openings are downward current from the baseline. Channel activity recorded at -40 mV were made in cytoplasmic pCa 7 and 0.1 mM luminal Ca^{2+} (diastolic [Ca^{2+}]) in the presence of 2 mM ATP in the cytoplasm. **(B)** Relative values of RyR2 P_o in presence of 0.24 mM cytoplasmic Mg^{2+} relative to that in the absence of Mg^{2+}. Data are shown as mean (geometric mean) ± SEM (n = 5 from healthy, 7 from CF, 9 from ICM, 7 from EDMD and 3 from ICM trabecule). Asterisks (*) denote a significant difference in relative values compared with healthy human heart (* $p<0.05$, ** $p<0.01$). **(C)** P_o distribution of individual RyRs underlying the mean data in B.

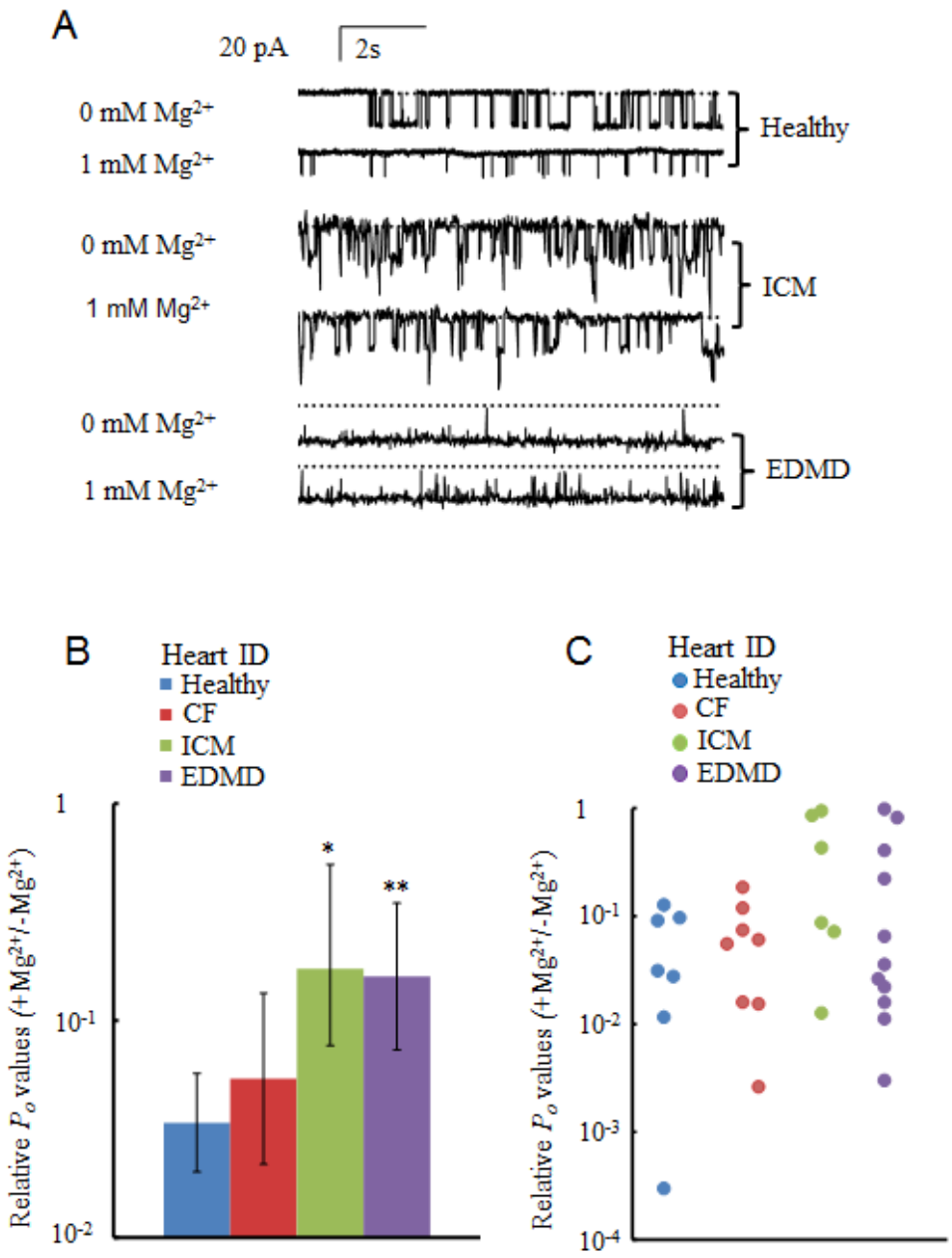

Figure 4.6: Inhibition of RyR2s from failing, CF and healthy human hearts by luminal Mg^{2+}.(A) Single channel recordings of RyR2 from failing and non-failing human hearts in presence and absence of 1mM luminal Mg^{2+}. Openings are downward current from the baseline. Channel recordings were taken at cytoplasmic pCa 7 and 0.1 mM luminal Ca^{2+} (diastolic [Ca^{2+}]) in the presence of 2 mM ATP in the cytoplasm at -40 mV. **(B)** Relative values of RyR2 P_o in presence of 1mM luminal Mg^{2+} relative to that in the absence of Mg^{2+}. Data are shown as geometric mean ± SEM (n = 7 from healthy, 8 from CF, 6 from ICM and 11 from EDMD). Asterisks (*) denote a significant difference in relative values compared with healthy human heart (* $p<0.05$, ** $p<0.01$). **(C)** P_o distribution of individual RyRs from the groups shown in B.

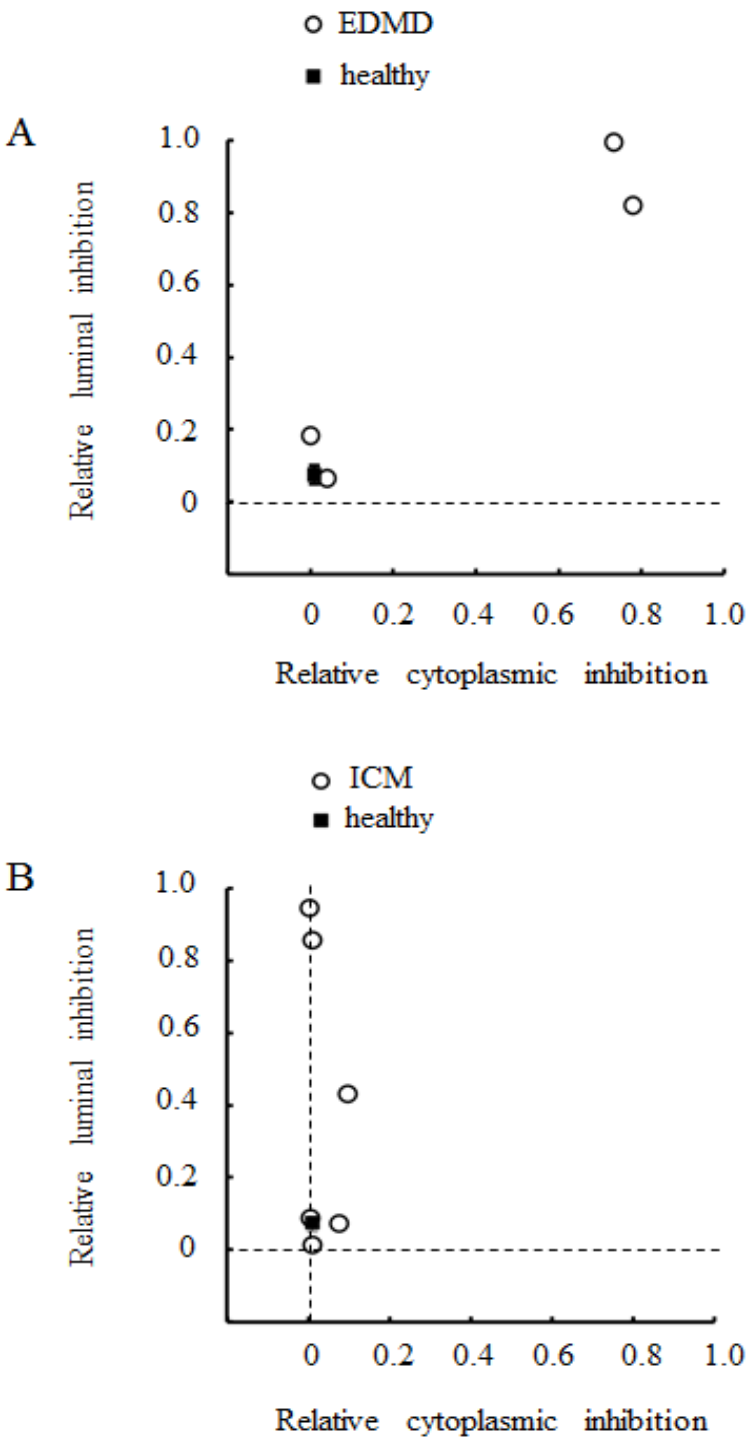

Figure 4.7: Correlation between inhibition of RyR2 by luminal and cytoplasmic Mg^{2+} in healthy and failing human hearts. The effect of luminal Mg^{2+} and cytoplasmic Mg^{2+} were measured on the one RyR2 from failing human hearts, EDMD &ICM, but not healthy **(A & B)** For each individual RyR2, the x axis shows the relative inhibition by 0.24 mM cytoplasmic Mg^{2+} and the y axis shows the relative inhibition by 1 mM luminal Mg^{2+}.

It is likely that luminal Mg^{2+} plays an important physiological role in shaping the luminal Ca^{2+} dependence of RyR2 activation in the cell (Laver and Honen 2008). Therefore, the dependence of RyR2 P_o for a range of luminal [Ca^{2+}] in the presence of 1 mM free Mg^{2+} on the luminal side of the RyR was measured. These measurements were also carried out in the presence of diastolic cytoplasmic Ca^{2+} (100 nM cytoplasmic Ca^{2+}) and 2 mM ATP in the cytoplasm (Figure 4.8). In all healthy and failing groups, increasing luminal Ca^{2+} over the physiological range of 0.1 to 1 mM produced 2-fold increases in RyR2 $P_{o,}$ which varied almost linearly with luminal [Ca^{2+}]. The absolute activity of RyR2s from CF and failing human hearts was similar and higher than those taken from healthy human hearts. Again, RyR2 receptors from ICM and EDMD failing hearts show two types of activity: RyRs that showed low activity were regulated by luminal Ca^{2+} and Mg^{2+}, whilst regulation was not evident by the group that exhibited high P_o, activity (Figure 4.8, stars and diamond).

4.3.3 Protein expression levels

To determine whether the expression level of any key Ca^{2+} handling proteins was altered in failing hearts, SR vesicles from both healthy and failing hearts were subject to quantitative Western blot. Samples (~3 µg total protein) were probed with antibodies for RyR2, NCX, SERCA2a, CSQ2, triadin-1 and junctin using both actin (Figure 4.9A & B) and total protein (Figure 4.9C) as a loading control (both controls were in agreement). In EDMD and ICM hearts, there were significant decreases in RyR2 expression to 76 ± 4% (EDMD) and 78 ± 4% (ICM) of that found in healthy human hearts (Figure 4.9D). The relative levels of protein expression from ICM ventricle (n=3) and ICM trabecule (n=4) were not significantly different from each other ($p > 0.05$) and were pooled in the analysis. A reduction in the expression levels of CSQ2 (87 ± 4%) and triadin-1 (90 ± 3%) were also seen in EDMD hearts as well as a decrease in SERCA in ICM heart to 76 ± 5%. Curiously, there was no significant reduction in SERCA in the EDMD nor were there any differences in expression levels of NCX. There were no significant differences in the expression levels of any of these proteins between healthy and CF hearts.

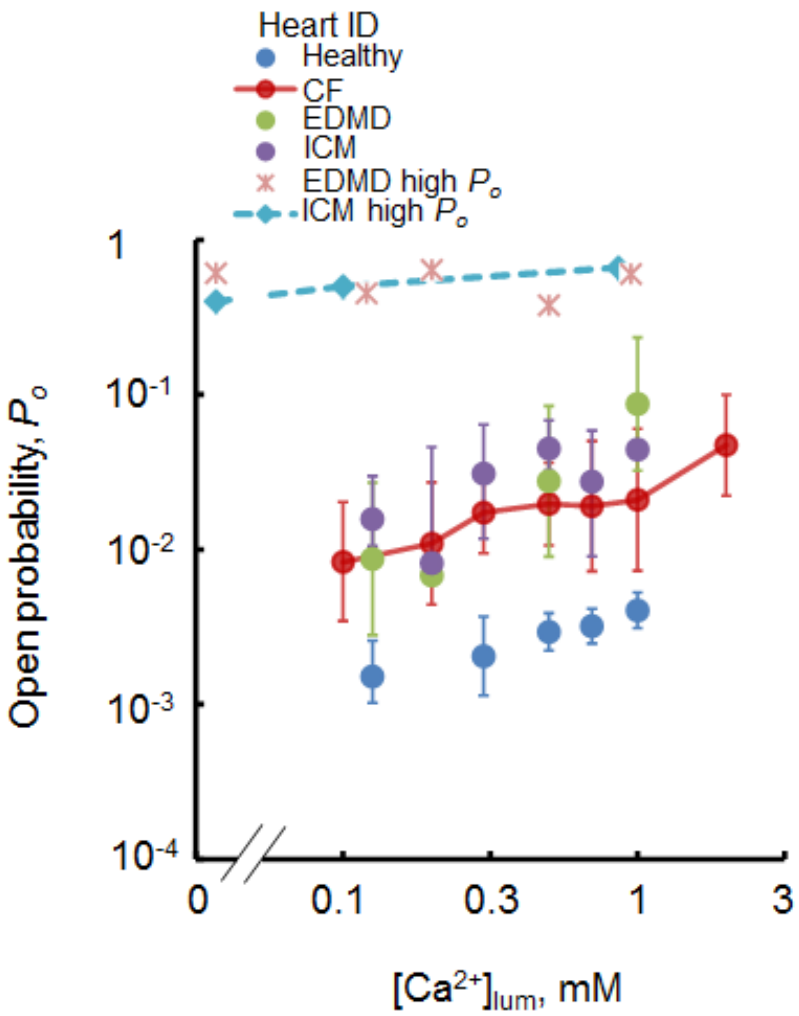

Figure 4.8: Luminal Ca^{2+} regulation of RyR2s compared in healthy, CF and failing human hearts. P_o was measured in the presence of 1mM luminal Mg^{2+} at cytoplasmic pCa 7 and 2 mM ATP. RyR2 from healthy and failing human hearts are indicated in the legend. Data points show the geometric mean ± SEM (n = 5 from healthy, 3-6 from CF, 2-4 from ICM, 2-7 from EDMD, 1-4 from EDMD abnormal and from 1-3 from ICM abnormal).

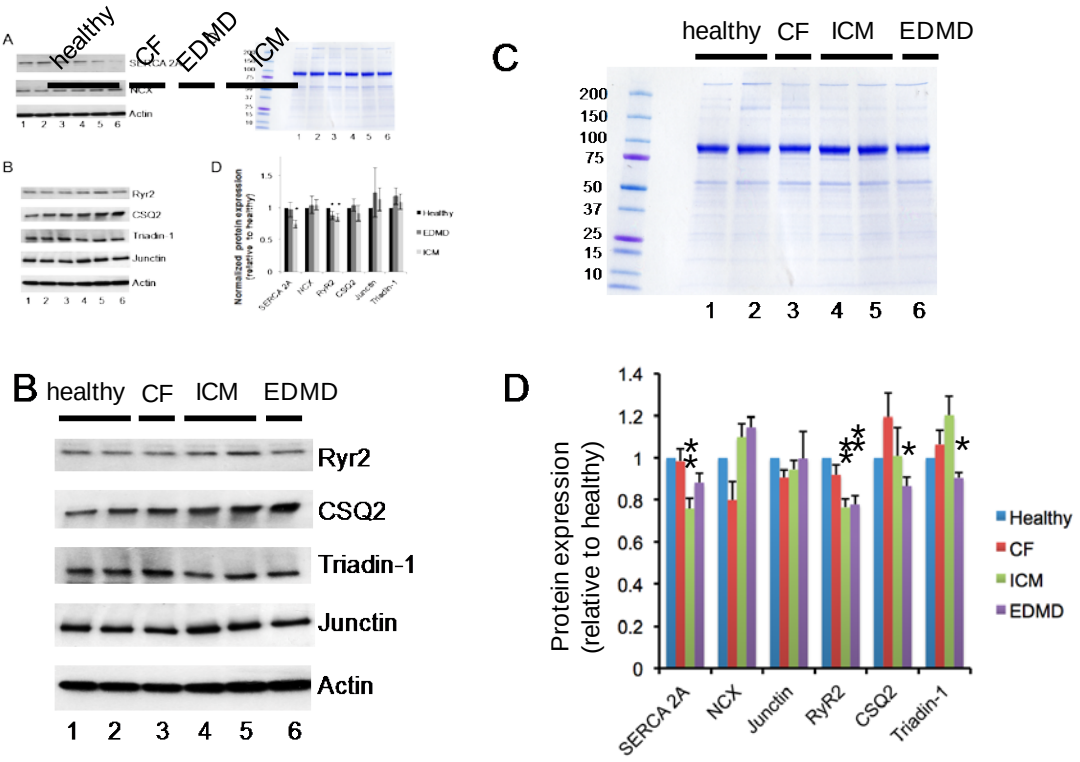

Figure 4.9: Protein expression levels in healthy, CF and failing human SR. (**A**) & (**B**) 3 mg samples of ventricular SR from two individual healthy hearts, CF, ICM and EDMD were used. All samples were separated via SDS PAGE and subject to Western Blot, prior to probing with antibodies for RyR2, SERCA2a, CSQ2, triadin-1, junctin, NCX. Actin and total protein were used as loading controls (total protein was used in this Figure). (**C**) Coomassie total protein stain of SDS Page from 4 mg of samples mentioned above. (**D**) Relative expression of target proteins. Band densities of target proteins are normalized to total protein (**C**) in each lane, and expressed relative to the densities calculated for healthy heart. Data from control and from ICM hearts were pooled. Data are shown as mean ± SEM (n = 7 from healthy, 3 from CF, 7 from ICM and 3 from EDMD). Asterisks (*) denote a significant difference in relative protein expression compared with healthy human ventricle (* $p<0.05$, ** $p<0.01$).

4.3.4 RyR2 phosphorylation

To determine the level of phosphorylation on the RyR2 at S^{2814}, S^{2808} in healthy, CF and failing human ventricles, we used semi-quantitative Western Blots and probed with phosphor-specific antibodies to these sites (Figure 4.10A & B). For loading controls, blots were stripped and re-probed with an antibody for RyR2 to calculate total RyR2 protein. The staining for the S^{2808} phosphorylation antibody was calibrated for maximal and minimal phosphorylation levels by incubating SR vesicles with either exogenous PKA (maximal) or PP1 (minimal, the method is described in section 4.2.9). After incubating healthy heart with 0.25 mg/ml PKA for 15 mins, levels of S^{2808} phosphorylation increased nearly 2-fold while levels of S^{2814} did not increase significantly, thus confirming that S^{2808} is predominantly a PKA phosphorylation site. Longer incubation times or increases in the quantity of PKA did not result in higher levels of phosphorylation (data not shown). For S^{2814}, the maximal phosphorylation controls were produced by incubating SR vesicles with substrates for endogenous CaMKII associated with the RyR2 (15 min with 62.5 μM calmodulin (CaM) and 2 mM ATP) and for minimum controls SR vesicles were incubated with PP1. There was a 1.5-fold increase in S^{2184} phosphorylation of healthy human heart post-CaM incubation and healthy heart can be considered moderately phosphorylated (Figure 4.10C).

RyR2 phosphorylation levels from each heart group were calculated relative to maximal in Table 4.3. These values are shown normalised relative to healthy heart values in Figure 4.10. RyR2s from EDMD hearts showed S^{2808} phosphorylation levels of 71 ± 3% of maximal which was significantly (30%, $p=0.04$) higher than seen in healthy hearts (See Figure 4.10D). In EDMD, S^{2814} phosphorylation was close to maximal at 83 ± 2%, which was 40% higher than that in healthy hearts.

The phosphorylation levels of S^{2808} and S^{2814} in ICM samples from ventricle and trabecule were not significantly different ($p > 0.2$) and hence the samples were pooled in the analysis. RyR2 in ICM hearts are almost fully phosphorylated at S^{2808}, with levels not significantly different ($p=0.15$) from maximal phosphorylation by PKA. S^{2808} phosphorylation was 165 ± 13% higher than in healthy hearts. The level of S^{2808} phosphorylation in the combined ICM samples was significantly higher than in the

healthy (p=0.05) and higher than in EDMD (p=0.06) hearts. In RyR2 from ICM hearts S^{2814} phosphorylation was near maximal and was 141 ± 8% higher than that found in healthy hearts.

Overall, in comparing RyR2 from ICM and EDMD hearts with those from healthy human hearts, there was a marked increase in RyR2 phosphorylation at S^{2808} and S^{2814}. By contrast, there was no significant difference in the phosphorylation state of RyR2s isolated from healthy and CF hearts (p>0.1).

In the laboratories of Derek Laver and Nicole Beard, the commercially available antibody for S^{2030} had an extremely low affinity for human RyR2. On two out of twelve occasions, only very faint immuno-decoration of both healthy and failing human RyR2 were detected using this antibody. It appeared that there was no difference in S^{2030} phosphorylation between healthy and failing samples (data not shown). On the other ten occasions, no bands were visible. Given the unreliability of this antibody, it was not possible to reliably determine S^{2030} phosphorylation in the human samples.

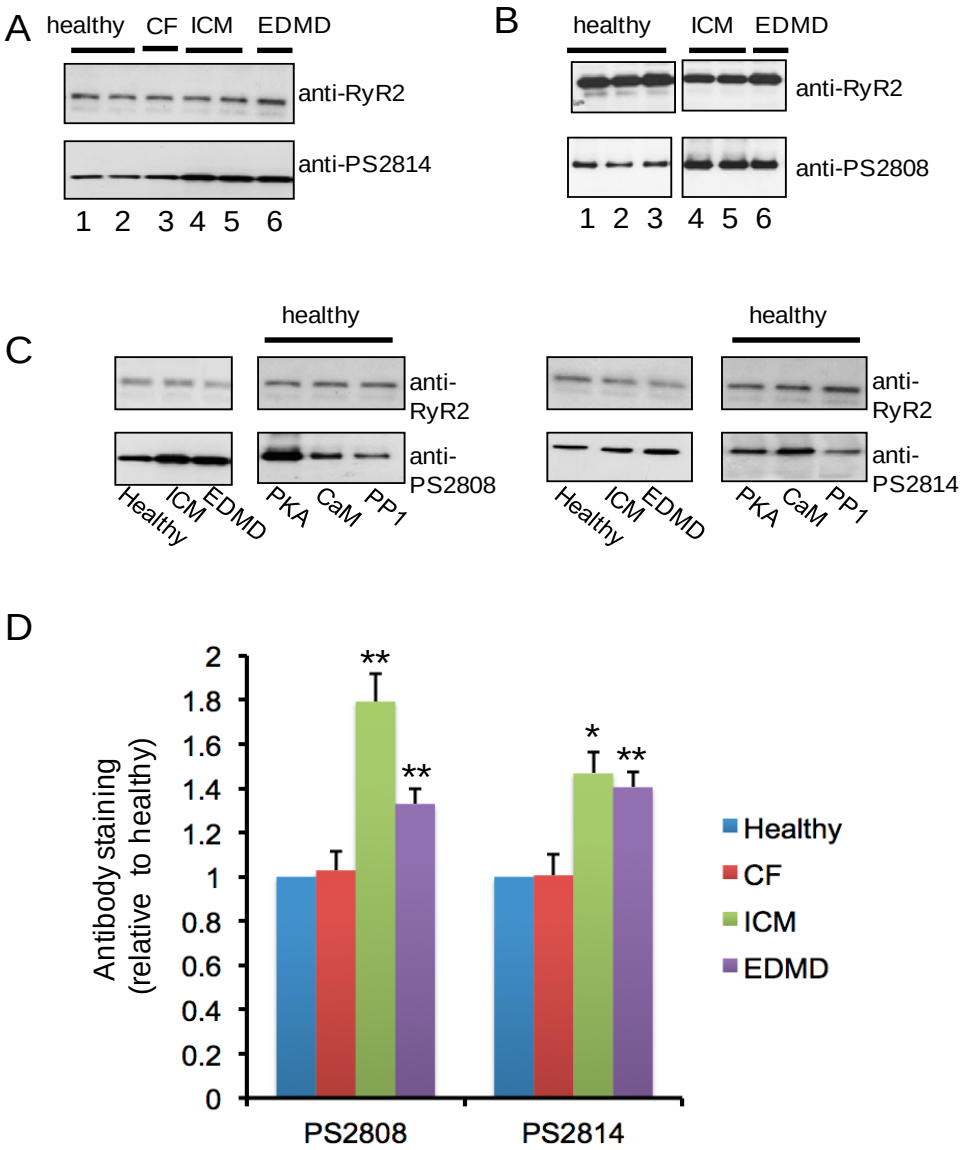

Figure 4.10: RyR2s are hyperphosphorylated at resides S^{2808} and S^{2814} in failing human heart. (A) & **(B)** show representative Western Blots of ventricular SR from three individual healthy, CF, ICM and EDMD hearts. Blots were probed with antibodies to S^{2808} and S^{2814} (PS2808 and PS2814, respectively). Blots were then stripped and re-probed with anti-RyR2 as a loading control. **(C)** Maximal phosphorylation and dephosphorylation of PS2808 and PS2814. Healthy RyR2s (7.5 µg) were treated with PKA, CaM + ATP or PP1, prior to SDS Page and Western Blot. Blots were probed with either PS2808 (n = 11 from healthy, 4 from CF, 11 from ICM and 8 from EDMD) or PS2814 (n = 8 from healthy, 3 from CF, 8 from ICM and 6 from EDMD). Blots were then stripped and re-probed with anti-RyR2. Levels of PS2814 and PS2808 for ICM and EDMD are shown for comparison. (D) Relative levels of S2808 phosphorylation and S2814 phosphorylation. Band densities were normalized to RyR2 loading in each lane relative to maximal band densities of healthy heart. Data show as mean ± SEM (* $p<0.05$, ** $p<0.01$).

Table 4.3

	PS2808 Rel to MAX (Frick, Hariharan et al.)	sem	N	ttest Rel to healthy
Healthy 7.0012	0.55	0.07	4	
Healthy 6.008	0.52	0.04	4	
CF	0.57	0.07	4	0.2
EDMD	0.71	0.03	4	0.015
ICM	0.89	0.09	4	0.05

	PS2814 Rel to MAX(CaMKII)	sem		ttest Rel to healthy
Healthy 7.0012	0.69	0.07	4	
Healthy 6.008	0.67	0.06	4	
CF	0.75	0.09	4	0.09
EDMD	0.83	0.02	4	0.03
ICM	0.96	0.05	4	0.1

Table 4.3. RyR2 phosphorylation levels relative to maximal in healthy, CF and failing hearts.

4.3.5 FKBP, PP1 and PP2A

Reduced levels of FKBP12.6 and dephosphorylating enzymes, PP1 and PP2a, associated with RyR2s have been indicated in HF. To investigate if this is occurring in the failing heart samples, RyR2s were immuno-purified from SR vesicles and probed with antibodies for these proteins.

Increased RyR2 phosphorylation in HF may be due to up-regulation of PKA/CaMKII that occurs during chronic ß-adrenergic stimulation, and/or removal of protein phosphatase (PP) 1 and 2a. The relative levels of PP1 and PP2a were determined in the immuno-precipitates using Western Blots (Figure 4.11A). There was significantly less PP1 bound to RyR2 in failing heart (67 ± 4% in ICM and 61 ± 8 % in EDMD), compared to the levels found associated in healthy samples (Figure 4.11B). Interestingly, PP2a was associated less from ICM (53± 4%) but not from EDMD (105± 2 %). However, there was no apparent change in the levels of PP1 or PP2a from RyR2s in CF hearts. Thus, dissociation of these phosphatases from the RyR2 complex in failing hearts correlates with, and could contribute to the hyperphosphorylation observed in these heart samples.

All failing heart samples had a consistently reduced quantity of the two FKBP isoforms normally associated with the RyR2 (Figure 4.12A). Whilst FKBP12.6 is traditionally considered to be the cardiac isoform of the protein, recent evidence showed a high level of FKBP12 associated with RyR2s in the heart (Zissimopoulos, Seifan et al. 2012). Consistent with this is the appearance of a double of FKBP in all human samples tested (Figure 4.12A). The anti-FKBP antibody (Ab126) used in this study recognizes both FKBP isoforms with an 80-100 fold higher affinity for FKBP12 over FKBP12.6. Molecular weight approximation was done in separate unpublished experiments (Dr. N. A. Beard, University of Canberra), where purified recombinant human FKBP12 and FKBP12.6 were loaded onto the gel adjacent to the human heart samples. The upper band detected in all human heart samples resolved at the same molecular weight as FKBP 12.6, whilst the lower band showed identical mobility as FKBP 12.6. However, it is possible that the double band seen is due to post-translation modification or breakdown of an isoform of FKPB and not to the presence of both FKPB12 and

FKPB12.6. Indeed, only Mass Spectroscopic analysis would ensure complete certainty of the identity of the doublets, however this methodology was outside the scope of this thesis. However, the following evidence for the doublet indeed being separate FKBP isoforms.

a) The anti-FKBP antibody (Ab126) was used throughout this study, which has been conclusively shown to identify both isoforms in mouse SR (Zissimopoulos et al., 2012).

b) Using Co-IP of crude SR from sheep heart, two FKBP bands were detected, which migrate almost identically to recombinant FKBP12 and FKBP12.6, respectively (Dr. N. A. Beard, University of Canberra).

c) Dissociation of the lower FKBP band was significantly higher than the upper band in all failing hearts tested (Figure 4.12). This is more indicative of a different protein isoform with a different affinity for the RyR2, than for a modified version of the same isoform.

Figure 4.12B shows that there is less association of both FKBP12 and FKBP12.6 to RyR2 from ICM and EDMD hearts and that FKBP12 is reduced to a greater extent than FKBP12 ($p<0.02$). (Again, there was no significant difference between the results from ICM and ICM trabecule preparations, $p=0.7$). However, there was no significant differences in association of either FKBP isoform between CF and healthy hearts ($p>0.5$).

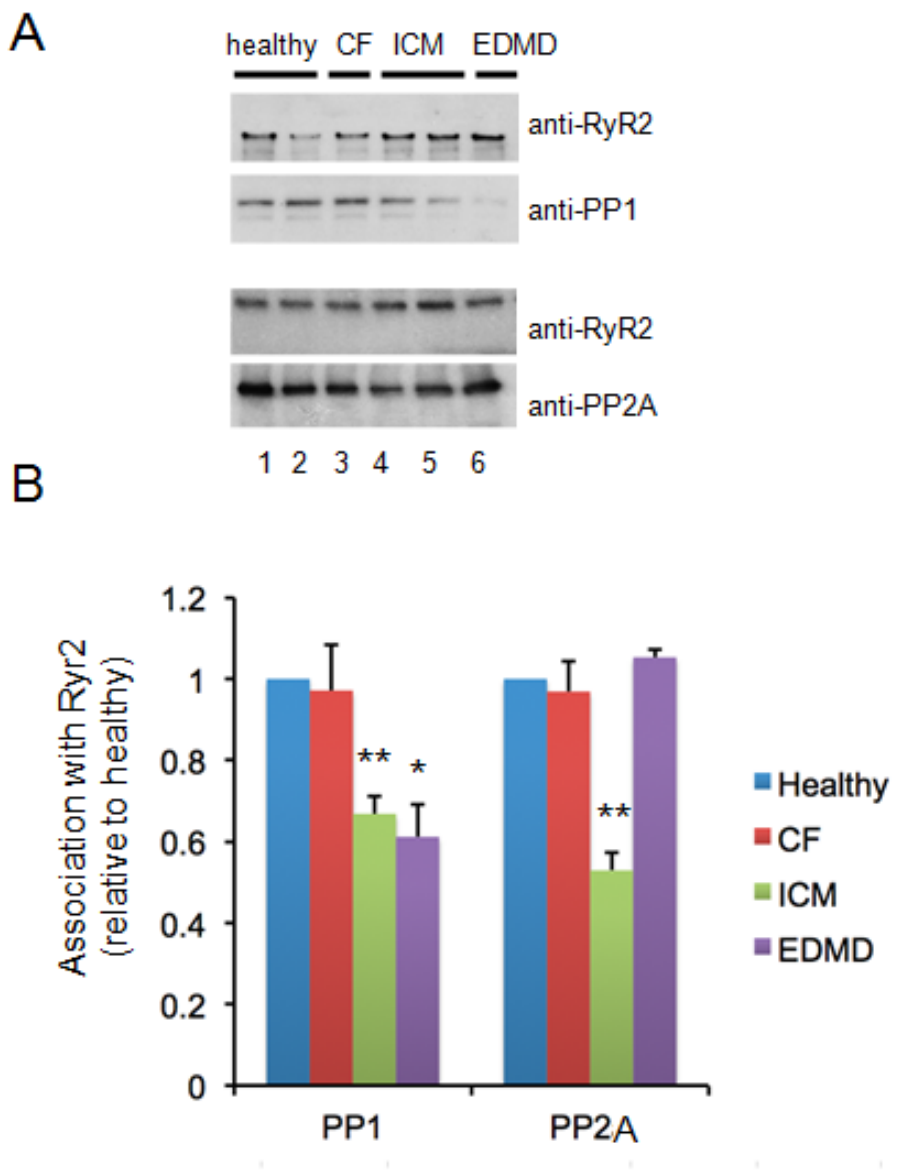

Figure 4.11: Reduced PP1 and PP2a association with RyR2s from failing human heart. (**A**) & (**B**) show RyR2 co-immunoprecipitation (co-IP) of healthy, CF and failing human hearts. (**A**) Following separation of proteins via SDS Page (4-15% bis:acrylamide) and Western Blot, Co-IP samples were probed with antibodies for RyR2, PP1 and PP2a (**B**) Relative association of PP1, PP2A with RyR2. Band densities of target proteins were normalised to RyR2s in each lane and expressed relative to the densities calculated in healthy heart. Data show as mean ± SEM (n = 6 from healthy, 3 from CF, 6 from ICM and 5 from EDMD). Asterisks (*) denote a significant difference in relative protein expression compared with healthy human ventricle (* $p<0.05$, ** $p<0.01$).

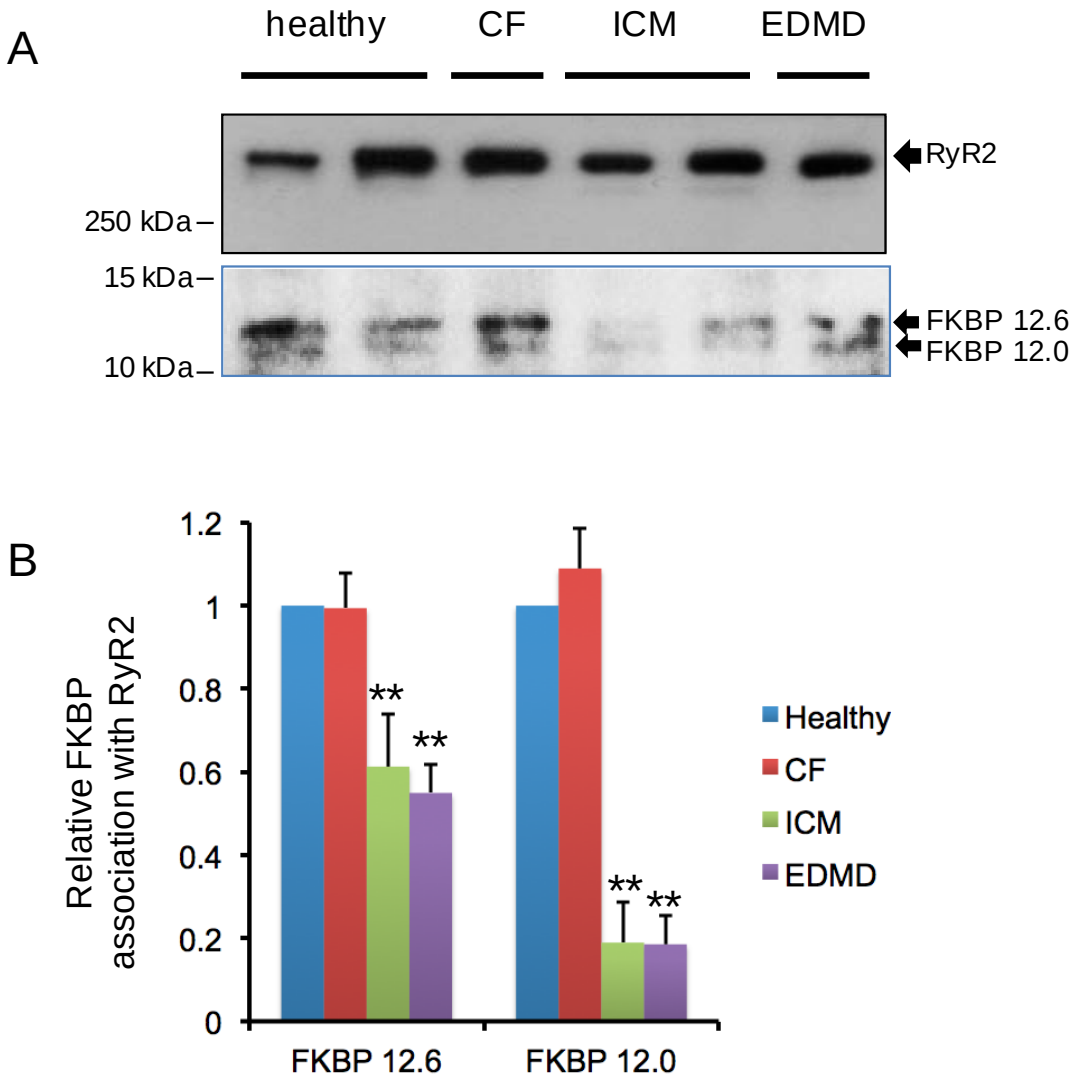

Figure 4.12. Reduced FKBP association with RyR2 from failing human heart. (**A**) RyR2 co-immunoprecipitation (co-IP) of healthy hearts and of failing ventricular SR from human ex-transplant hearts from two patients diagnosed with ischemic cardiomyopathy (ICM) and a cardiomyopathy associated with Emery Dreifuss Muscular Dystrophy (EDMD). Precipitates were separated on 18% bis:acrylamide and Western Blot with an antibody to RyR2 and an antibody which detects the two FKBP isoforms with different affinities, allowing visualization of FKBP12 and FKBP12.6. FKBP12.6 indicated by black arrowheads. **(B)** Relative association of FKBP isoforms with RyR2. Band densities of target proteins are normalized to RyR2 in each lane and expressed relative to the densities calculated in healthy heart. Data show as mean ± SEM (n = 7 from healthy, 4 from CF, 6 from ICM and 7 from EDMD). Asterisks (*) denote a significant difference in relative protein expression compared with healthy human ventricle (* $p<0.05$, ** $p<0.01$).

4.4 Discussion

This study provides the most detailed examination so far of RyR2 gating, its regulation by intracellular Ca^{2+} and Mg^{2+} and its macromolecular structural properties. Previous studies have produced a very restricted view of RyR2 regulation. Single channel recordings of RyR2 isolated from failing human hearts (Holmberg and Williams 1992) with several myopathies including ICM and IDC and healthy hearts (Wehrens, Lehnart et al. 2004) demonstrated apparently normal activation by cytoplasmic Ca^{2+} suggesting that heart remodelling in HF had no effect on RyR2 function. Jiang and his colleagues (Jiang, Lokuta et al. 2002) also reached the same conclusion based on the finding that the open probability of RyR2 from healthy hearts in systolic (5 μM) cytoplasmic Ca^{2+} were no different to that observed in failing hearts with DCM and ICM. However, Marks and colleagues (Marx, Reiken et al. 2000) did find differences between RyRs taken from healthy and failing hearts at diastolic levels of cytoplasmic Ca^{2+} (50 nM). This study substantially expands on previous reports of Ca^{2+} regulation on RyR2 from healthy and failing human hearts but in a limited number of cases (1 CF, 1 EDMD and 2 ICM). The data from the four healthy donor hearts revealed no significant differences between these groups in the Ca^{2+} and Mg^{2+} regulation of their RyRs indicating that RyR2 from these hearts were representative of those from healthy hearts in general (Figure 3.1). Our results also show that the function and macromolecular structure of RyR2 from individual cases of CF and HF were different to that seen in all healthy hearts (*e.g.* Figure 4.2). A clear limitation of using one or two cases of each type of cardiomyopathy is that it is not possible to establish if the differences seen are representative of CF or HF in general. However, it is encouraging to see that Marx *et al.* (Marx, Reiken et al. 2000) found similar types of RyR2 activity as reported here. They found that 95% of RyR2 from healthy hearts were inactive under these conditions whereas only 30% of RyR2 from failing hearts were inactive with half of the active ones showing full activity (*i.e.* P_o ~1); behaviour not seen at all in RyR2 from healthy hearts.

I found substantial changes in the function of RyRs in CF and failing hearts whereas structural changes were only detected in failing hearts. The finding that RyRs in failing heart had a 12% lower conductance than those from healthy heart, even if their gating appeared the same as healthy hearts, suggests that the reduction of RyR2 conductance in

HF occurs before changes in RyR gating in the progression of HF. The fact that RyR2 conductances are even lower in channels that exhibit altered gating suggests that the conductance decrease becomes more pronounced as HF progresses. A second type of behaviour that was never observed in channels from healthy hearts characterised by lower conductance than seen with normally gated channels along with long open times and multiple conductance levels (Figure 4.1). Unfortunately, no control was used during the experiments to show the characteristic modification of the RyR2 channel by ryanodine and ruthenium red. However, similar observation has been shown in single channel recordings of RyR2 from failing hearts in human (Marx, Reiken et al. 2000). The fact that there were relatively more RyRs with higher P_o in CF heart indicates that high RyRs in the heart have undergone some form of remodelling as a consequence of pulmonary stress.

4.4.1 RyR2 complex remodelling in HF

Western blots were used to probe the composition of the RyR2 complex that was isolated from healthy, CF and failing human hearts. Our biochemical investigations showed no changes in RyR2 macromolecular complex or phosphorylation status in CF compared to healthy. However, other factors such as oxidation or/and nitrosylation in RyR2 from CF heart can't be ruled out at this stage. RyR2 showed higher phosphorylation at S^{2808} and S^{2814} in failing hearts, which implies that both PKA and CaMKII pathways play a role in hyperphosphorylating RyR2. There is much disparity in the literature on the level or degree of phosphorylation of serine residues 2808, 2814 and 2030 in healthy heart and controversy exists over whether or not any or all of these residues are hyperphosphorylated in failing heart (Bers, Eisner et al. 2003; Dulhunty, Beard et al. 2007). In healthy and ICM hearts there were no significant differences in expression of NCX, CSQ2, triadin-1 and junctin. RyRs from EDMD heart showed reduction in CSQ2 and triadin-1. CSQ2 acts as Ca^{2+} buffer and controls RyR2 open probability in a luminal Ca^{2+} dependent manner via interactions with triadin-1 and junctin (Gyorke, Hester et al. 2004; Terentyev, Viatchenko-Karpinski et al. 2007). At low luminal Ca^{2+} concentration CSQ2 prevents RyR2 activation by binding tightly to triadin and junctin. This inhibition is relieved by binding of Ca^{2+} to CSQ2, and as Ca^{2+}

rises (Gyorke, Hester et al. 2004) the binding disrupts the interaction of CSQ2 to triadin and junctin thereby removing the inhibitory effect of CSQ2 on RyR2. Therefore, reduced expression of CSQ2 might cause the increase in RyR2 sensitivity to luminal Ca^{2+} observed in EDMD. Consistent with the previous findings (Go, Moschella et al. 1995), RyR2 expression was reduced in ICM and EDMD hearts. Jiang *et.al.* have shown a 30 ± 5 % reduction in SERCA2a levels in HF (combined from ICM and DCM hearts) (Jiang, Lokuta et al. 2002). I also detected a decrease in SERCA2a levels in ICM heart but not in EDMD.

Reduction in the amount of bound FKBP12.6 and phosphatase (PP1, PP2A) in the RyR2 complex has been reported in human HF (Marx, Reiken et al. 2000). This study showed a reduction in the expression of PP1 and PP2A in ICM hearts, while EDMD heart showed a reduction in PP1 only. These findings are consistent with the proposal that reduction in PP1 and PP2A levels in the RyR2 macromolecular complex (Marx, Reiken et al. 2000; Yano, Ono et al. 2000) rather than increased PKA activity are responsible for the RyR2 hyperphosphorylation and the formation of "leaky" channels (Marks 2003). It has been proposed that loss of FKBP12.6 from RyR2 increases diastolic Ca^{2+} leak (Marx, Reiken et al. 2000; Yano, Ono et al. 2000), while binding of FKBP12.6 to the channel minimizes Ca^{2+} release from the SR during diastole (Wehrens, Lehnart et al. 2003). Surprisingly, this work showed that both FKBP12 and FKBP12.6 are dissociated from RyR2 in failing hearts and FKBP12 is reduced to a greater extent than FKBP12.6. Sitsapesan and co-workers (Galfre, Pitt et al. 2012) showed that FKBP12.6 lowered RyR2 P_o by antagonising the activating effects of FKBP12. They also proposed that increases in the FKBP12/FKBP12.6 ratio contribute towards a higher RyR2 P_o, 'leaky' RyR2 channels and Ca^{2+} -dependent arrhythmias. The reduction in the FKBP12/FKBP12.6 ratio seen in failing hearts in this thesis, on its own, should lead to a loss of RyR2 activity which is opposite to what is seen in my single channel studies. Moreover, loss of FKBP12.6 should not make a significant difference to RyR2 activity because only a minority of RyR2 actually bind to this molecule (Guo, Cornea et al. 2010). Therefore, it is likely that there are other factors such as RyR2 oxidation and hyperphosphorylation that cause the observed increase in RyR2 activity in failing hearts.

4.4.2 Mechanisms for RyR2 variability

RyRs from healthy hearts exhibited channel to channel variation in activity, which could not be attributed to systematic differences in RyR2 properties from different hearts (Figure 3.1). The scatter seen here in P_o (Figure 4.3A) is consistent with other single channel studies of RyR2 from human (Jiang, Lokuta et al. 2002) and sheep (Laver, Roden et al. 1995; Copello, Barg et al. 1997). The reason for the scatter in RyR2 gating is not yet clear. Individual RyRs may exhibit different degrees of post-translational modifications that would influence their gating activity. It has been reported that RyR2 activity is increased by phosphorylation (Marx, Reiken et al. 2000; Shen 2006; Li, Imtiaz et al. 2013). RyR2 activity can be altered by modification of approximately 84 thiols and 100 cysteine residues per subunit (Xu, Eu et al. 1998), which are susceptible to modulation by redox modifications, including disulfide crosslinking, S-nitrosylation, and S-glutathionylation (Sun, Xin et al. 2001). Since variations in phosphorylation and oxidation of key amino acids cause changes in RyR activity, and that it is almost certain that different RyRs in the cell possess different post-translational modifications, it is reasonable to expect that the variations shown in the bilayer experiments reflect the natural variation in RyR2 gating in the cell. Moreover, individual RyRs macromolecular complexes may differ in their complement of co-proteins that would also contribute to channel to channel variation. For example, FRET assays of fluorescent labelled FKBP in permeablised cardiomyocytes indicated that only 10-20% of all RyRs in the cell are complexed with FKBP12.6 (Guo, Cornea et al. 2010).

However, RyR2 from CF, ICM and EDMD hearts showed greater scatter than those from healthy hearts (Figure 4.3). Distributions of P_o are consistent with two populations of RyRs, a normal group and an aberrant group. This is based on the bimodal distributions of individual RyRs in which there is a standard distribution centred at 3 s^{-1} and a tail at higher values. The standard distribution of opening rates among healthy and failing hearts are centred about similar levels but their relative weighting in the total distributions vary. In healthy heart, the standard distribution comprises 92% of the RyRs whereas in failing hearts this component has only 84% of the RyRs from ICM hearts, 50% from EDMD and none from ICM trabecule. Our results are consistent with previous single channel recordings from failing hearts in human (post- & pre-Left

Ventricular Assistance Device implantation) and in dog that showed two types of channel behaviour at diastolic conditions (Marx, Reiken et al. 2000). They found that 70% of channels from failing heart were high activity outliers compared to healthy heart with 8%, levels not dissimilar to ones reported here. In this study, the differences in the proportion of high activity RyRs between HF types may be due to which part of the heart the tissues were taken (*e.g.* ventricle *vs.* trabecule) and/or due to heart to heart variations in the progression of myopathies.

The heterogeneity seen in RyRs from failing hearts types may reflect heterogeneity in structural remodelling of the SR and t-tubular systems recently observed in failing hearts. Using confocal imaging, Cannell and his co-workers (Crossman, Ruygrok et al. 2011) found structural remodelling of the SR and t-tubular systems and loss of dyad junctions in HF. Together with my results one could propose that the high activity group of RyRs come from these remodelled regions. As yet, there is not a good understanding of how RyRs could be remodelled in these regions. Recently, it was found that a loss of dyads occurs in response to excessive Ca^{2+} release that activates calpains, which cleave junctophilin to separate the t-tubule and SR membrane. These calpains are known to degrade RyRs (Pedrozo, Sanchez et al. 2010) and this may lead to the observed loss of Ca^{2+}/Mg^{2+} regulation of RyR2. However, there was no evidence for increased degradation in RyR2 from failing hearts in the Western blot experiments (RyRs degradation is measured by the presence of a breakdown fragment at 400 kDa in addition to the 560 kDa band, Figure 4.10A-C). The relative intensities of these bands were similar from failing and healthy hearts (*c.f.* Figure 4.10A-C).

4.4.3 Ca^{2+}/ Mg^{2+} regulation of RyR2 from failing hearts

Given that Mg^{2+} is a strong inhibitor of RyR2 (Laver and Honen 2008) that plays an important role in moderating SR Ca^{2+} release during diastole, I measured RyRs inhibition by luminal and cytoplasmic Mg^{2+} in failing hearts. The two populations of RyRs mentioned above showed different sensitivities to luminal and cytoplasmic Mg^{2+}. The group that showed higher open probability exhibited less sensitivity to inhibition by cytoplasmic and luminal Mg^{2+}. Interestingly, the high P_o group showed substantial

differences in the inhibition by Mg^{2+} between failing hearts types Figure 4.7). RyRs from the ICM failing heart showed less sensitivity to luminal Mg^{2+} than cytoplasmic Mg^{2+} inhibition, whereas RyRs from the EDMD failing heart showed less sensitivity to both. These differences in function might reflect the differences seen in the remodeling of the RyR2 complex. For example, differences in phosphorylation of S^{2808} between ICM & EDMD (Figure 4.10, ICM exhibited higher phosphorylation) or RyR association with PP2a (Figure 4.11, PP2A less associated from ICM but not from EDMD; p=0.0001). As RyR2 is remodelled (hyperphosphorylation and oxidation) in HF it would be expected that Mg^{2+} sensitivity is affected (Hain, Onoue et al. 1995; Donoso, Aracena et al. 2000).

My results show that differences in the activity of RyR2 between healthy and failing hearts depended on the experimental conditions. RyR2 from failing hearts showed higher activity than healthy hearts at diastolic Ca^{2+} (100 nM) but no significant difference at systolic Ca^{2+} (10 μM; Figure 4.4, p=0.58) These findings reconcile the apparently conflicting findings from two groups where Marks and colleagues (Marx, Reiken et al. 2000) detected high activity channels in HF using diastolic Ca^{2+} (50 nM) whereas Jiang and colleagues (Jiang, Lokuta et al. 2002) found no difference in RyR2 activity at systolic Ca^{2+} (5 μM).

The changes in Ca^{2+} and Mg^{2+} regulation seen in RyR2 from failing hearts suggests that during diastole, a large fraction of RyRs (50% from EDMD and 16% from ICM) become highly active in HF. These RyR2 should be more strongly activated at diastolic cytoplasmic [Ca^{2+}] and have much less inhibition by intracellular Mg^{2+}. Given the role of Mg^{2+} in preventing Ca^{2+} release during diastole, low inhibitory effect of Mg^{2+} on these RyRs should contribute to excessive Ca^{2+} release in HF and this would tend to deplete SR Ca^{2+} store. These RyRs showed 10 to 100-fold less inhibition by cytoplasmic Mg^{2+} (Figure 4.5B) and 10-fold by luminal Mg^{2+} (Figure 4.6B). The question that could arise here is: how the heart can function with such a large fraction of RyRs being totally unregulated. If all cells in the heart had this percentage of their channels as high activity channels, it would be hard to see how Ca^{2+} stores could maintain a usable Ca^{2+} load. However, if these remodelled channels were all located in localised regions of the cell,

as indicated by confocal microscopy (see above), it would only be these regions that fail to exhibit ECC and muscle contraction. Myocyte contraction could be produced by healthy regions of the cell.

Overall, I found that the mean properties of RyR showed very little variation between different healthy hearts. RyR from failing hearts showed considerably greater variation within hearts and between hearts consistent with differences in RyR2 phosphorylation or association of co-proteins in the RyR2 complex. The degree of HF induced changes in RyR2 activity depended on the experimental conditions (activity increased under diastolic conditions but not under systolic conditions). CF channels showed increases in activity similar to HF but with no apparent changes in phosphorylation or the association of co proteins in the RyR2 macromolecular complex. These results suggest that CF hearts are at an early stage of progression to HF where the nature of the RyR2 remodelling is not yet known.

Chapter 5- Inhibition of RYR2 from healthy and failing human hearts by calmodulin (CaM)

5.1 Introduction

The RyR2 is a macromolecular complex comprising a Ca^{2+} channel and many other accessory proteins such as calmodulin (CaM) that regulate channel activity. CaM influences RyR2 mediated Ca^{2+} release by a direct interaction (binding) to the channel and by phosphorylation of the RyR2 through CaMKII (Ai, Curran et al. 2005). Binding of CaM (~ 50-100 nM free [CaM] in the cell) (Maier, Ziolo et al. 2006; Guo, Fruen et al. 2011) to canine RyR2s partially inhibits calcium release in cardiomyocytes due to its ability to inhibit RyR2 channel opening (Xu and Meissner 2004; Guo, Zhang et al. 2006). 99% of the total intracellular CaM (6 μM) is bound to cell proteins (Maier, Ziolo et al. 2006; Guo, Fruen et al. 2011). Same effect of 100 nM CaM has been shown recently using sheep RyR2 (Hwang, Nitu et al. 2014). The inhibition is seen as a decrease in RyR2 opening frequency and mean open time in lipid bilayers (IC_{50} of 100 nM) (Xu and Meissner 2004) and a decrease in Ca^{2+} spark frequency in permeabilized myocytes (IC_{50} of 100 nM) (Guo, Zhang et al. 2006). However, Sigalas *et al.* show that the physiological level of CaM (50-100 nM) causes an increase in RyR2 P_o from sheep cardiac cells (Sigalas, Bent et al. 2009; Sigalas, Mayo-Martin et al. 2009). As yet no one has examined the effect of CaM on human RyR2s activity.

CaM is a 148 amino acid protein arranged in two globular heads each of which is composed of 2 binding EF-hands (Black, Tikunova et al. 2000). The Ca^{2+}-free calmodulin is named apocalmodulin (apoCaM), whilst the Ca^{2+}-bound calmodulin is named Ca^{2+}/calmodulin (CaCaM, four Ca^{2+} bound). A fluorescence-resonance-energy-transfer (FRET) detection of CaM binding to the cardiac RyR2, based on cryo-electron microscopy, showed that the effects of CaM on RyR2 are mediated via binding to a single binding domain comprising of amino acid residues 3581–3612 and 4261–4286 (corresponding to 3614–3643 and 4302–4328 in RyR1) (Huang, Liu et al. 2013). Using metabolically ^{35}S-labeled CaM, Meissner and his co-worker have shown that each RyR2 subunit can bind with a binding affinity of 5.5 ± 2.2 nM in the presence of 100 μM Ca^{2+} (*i.e.*, CaCaM) and 54 ± 34 nM in presence of ≤10 nM Ca^{2+} (*i.e.*, ApoCaM) (Balshaw, Xu et al. 2001; Balshaw, Yamaguchi et al. 2002). CaCaM and ApoCaM bind to and dissociate from RyR2s on a time scale of seconds to minutes (Tripathy, Xu et al. 1995).

During the process of RyR2 isolation from the heart and its incorporation into lipid bilayers, the macromolecular complex stays mostly intact (Marks, Marx et al. 2002) except for CaM which can dissociate from the RyR2 complex in minutes (Xu and Meissner 2004). Most single channel studies do not include this important regulatory molecule in the RyR2 complex, whereas in the cell, CaM is abundant and is associated with the RyR. By incorporating CaM back into the RyR2 complex, this work will obtain a more accurate picture of the function of RyR2 in the cell.

Dysregulation of RyR2 by CaM has been linked to cardiac arrhythmia in HF and inherited syndromes. Meissner and co-workers have shown that substitutions within a core CaM binding sequence which disrupts CaM binding to RyR2, results in severe cardiac hypertrophy and early death in mutant mice (Yamaguchi, Takahashi et al. 2007). Previous studies have found that mutations in CaM can impair CaM binding to or cause aberrant CaM regulation of the RyR2, thereby increasing the RyR2 channel opening rate and spontaneous Ca^{2+} release (Xu, Yano et al. 2010). Recent genetic studies have identified CaM mutations in human genetic arrhythmia syndromes (*e.g.*, Catecholaminergic Polymorphic Ventricular Tachycardia (CPVT) and Long QT) that cause severe ventricular arrhythmia and sudden cardiac death (Nyegaard, Overgaard et al. 2012; Crotti, Johnson et al. 2013) indicating that CaM is important in maintaining normal heart function and development. It has also been shown that CaM binding to RyR2s can be reduced in heart failure (HF) (Ono, Yano et al. 2010). Several recent studies have shown that a reduction in CaM binding to RyR2s lead to HF in mice (Yamaguchi, Takahashi et al. 2007; Hino, Yano et al. 2012; Yamaguchi, Chakraborty et al. 2013) and that reinstating proper CaM binding to RyR2s from failing paced-dog hearts restores normal RyR2 channel function (Hino, Yano et al. 2012). Accordingly, it appears that decreased CaM binding to RyR2 plays a key role in the pathogenesis of HF. It has been suggested that abnormal RyR2 gating is the major causative factor for cardiac dysfunction, lethal arrhythmia and remodelling in HF (Yano, Yamamoto et al. 2005). Thus, it is possible that progression of HF results from depression of RyR2 activity associated with the loss of CaM binding. However, RyR2 remodelling in HF also includes changes in RyR2 phosphorylation, nitrosylation and oxidation (Marx, Reiken et al. 2000) as well as loss of regulatory coproteins such as FKBP12.6 and PP1 (Xu, Eu et al. 1998; Ide, Tsutsui et al. 1999). To date, it is not clear whether CaM will

have the same effect on remodelled RyRs as it does on the normal RyR complex. The previous finding here that RyR2 gating is altered in failing hearts (see chapter 4), suggests that HF alters Ca^{2+} dynamics by changing the regulation by intracellular ions and that this occurs as a result of changes in the way the RyR2 complexes with other intracellular proteins. Recently, Bers and his co-workers have examined the effect of CaM on human RyR2 from healthy and failing hearts. They found that CaM binds to RyR2 with high affinity (CaM is bound to >70% of RyR2 monomers), while in HF RyR2 shows decreased CaM affinity. This study has also shown that binding of CaM to RyR2s from mice cardiomyocytes inhibits SR Ca^{2+}release. CaM dissociation from RyR2 can cause severe ventricular arrhythmia (Yang, Guo et al. 2014). To date, there have not been any studies that have investigated the effect of CaM on the gating of human RyR2s and how it may be affected by RyR2 remodeling in failing hearts.

5.2 Materials and methods

5.2.1 Human heart tissue & single-channel measurements

RyR2s were isolated from healthy and ischemic cardiomyopathy human hearts as described previously for sheep RyRs (Laver, Roden et al. 1995). Human tissues were obtained with approval from the Ethics Committee of the University of Newcastle Australia (See section 2.1& Table 2.1.).

RyR2s were incorporated into lipid bilayers and channel gating was measured at -40 mV by single channel recordings in the presence of cytoplasmic ATP (2 mM), Ca^{2+}, (0.1 or 3 μM) and varying concentrations of CaM (nM: 20, 50, 100, 200 and 500). CaM was added and removed from the RyR2 complex by using a local perfusion method as shown in Figure 2.4. Luminal solutions contained 250 mM Cs and 0.1 mM Ca^{2+}. Bath solutions were buffered to pH 7.4 using 10 mM TES (See sections 2.2 & 2.3).

5.2.2 In-vitro Phosphorylation of the RyR2 channel

Using the local perfusion method, the phosphorylation state of the RyR2 in the bilayer could be altered by applying PKA and its substrates to the cytoplasmic bath. In two experiments, incubations were carried out by replacing the recording solution for 2 or 10 minutes (see above) with a *cis* solution containing PKA (20 μg), 1 mM Mg^{2+}, 3 μM Ca^{2+} and 2 mM ATP. Following this, the same channel was recorded again using the same recording solutions. An alternative method of phosphorylation employed in two other experiments was to incubate RyRs with exogenous PKA in PKA buffer containing (mM): 50 Tris-HCl (pH 7.4), 10 MgCl2, 2 ATP, 1 cAMP, 10 NaF and 0.25 g/ml PKA (Sigma Aldrich) for 5 minutes at 30 ^{o}C prior to incorporation into the bilayer.

5.3 Results

5.3.1 CaM inhibits RyR2s from failing human heart

The rate of CaM association and dissociation was measured by applying and removing CaM using a perfusion apparatus and monitoring single channel activity (Figure 5.1). The addition of CaM (500 nM at 3 μM Ca^{2+}) to the cytoplasmic bath caused a reduction in open probability of RyR2 from failing human heart (ICM, Figure 5.1). This change occurred within the time taken for solution exchange by the perfusion system (2-5 s depending on perfusion rate) and was mediated by a decrease in the channel open time and increase in the channel mean closed time (Figure 5.2). Upon washout of CaM, RyR2 activity recovered within ~30 s (Figure 5.1) suggesting that CaM dissociation from the RyR occurred over this time period.

The effect of various concentrations of CaM on RyR2 activity is shown in Figure 5.3. Figure 5.3A shows a representative trace where the addition of 500 nM CaM reduced RyR P_o. A diary plot of RyR2 P_o during addition of various [CaM] is shown in Figure 5.3B. At the beginning of the record (450 s after the commencement of the experiment), 100 nM CaM was applied to a single RyR2 channel and the P_o declined from 0.8 to 0.3. Washing off CaM (at 600 s) returned the P_o to its previous levels after which 500 nM CaM was added (at 750 s), followed by solutions containing 200 nM and 500 nM CaM. The level of CaM inhibition at 100 and 200 nM was similar to that seen at 500 nM. The CaM dose-response of RyR2 activity is shown in Figure 5.4 where it can be seen that CaM causes a maximum of 60% to 80% inhibition of RyR2 at 100 nM CaM.

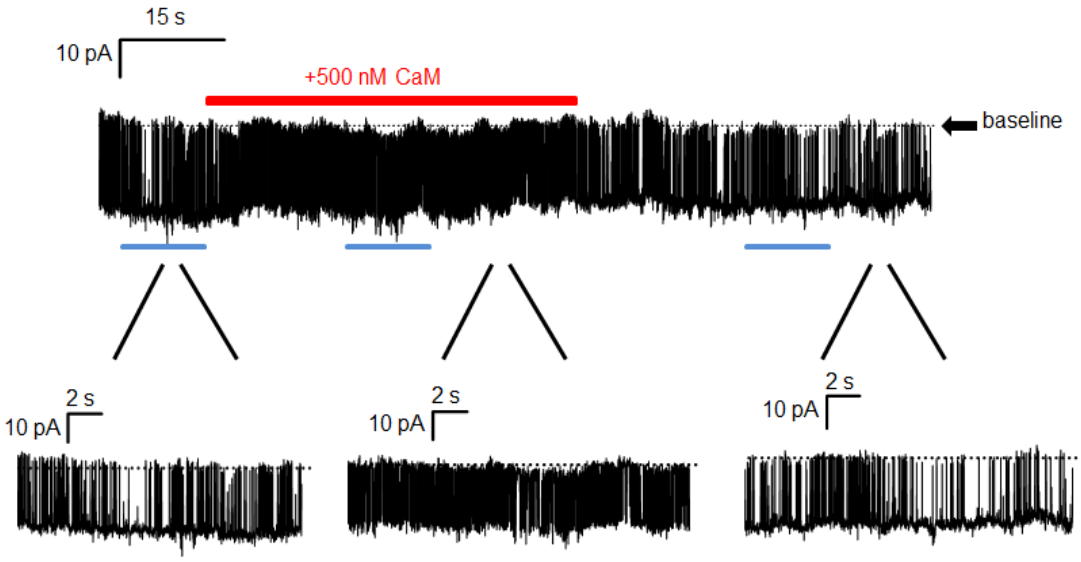

Figure 5.1: CaM effect on single RyR2 recording at 3 µM cytoplasmic Ca^{2+}. RyR2s from the left ventricle of a failing with ischemic cardiomyopathy (ICM) exposed to 500 nM CaM for the period indicated by the red bar. Channel openings are downward current jumps from the baseline (arrow and dashed lines). Channel recordings were taken in the presence of 0.1 mM luminal Ca^{2+} and 2 mM ATP in the cytoplasm at -40 mV. Expanded traces at the bottom taken from sections of the top trace are indicated by blue bars.

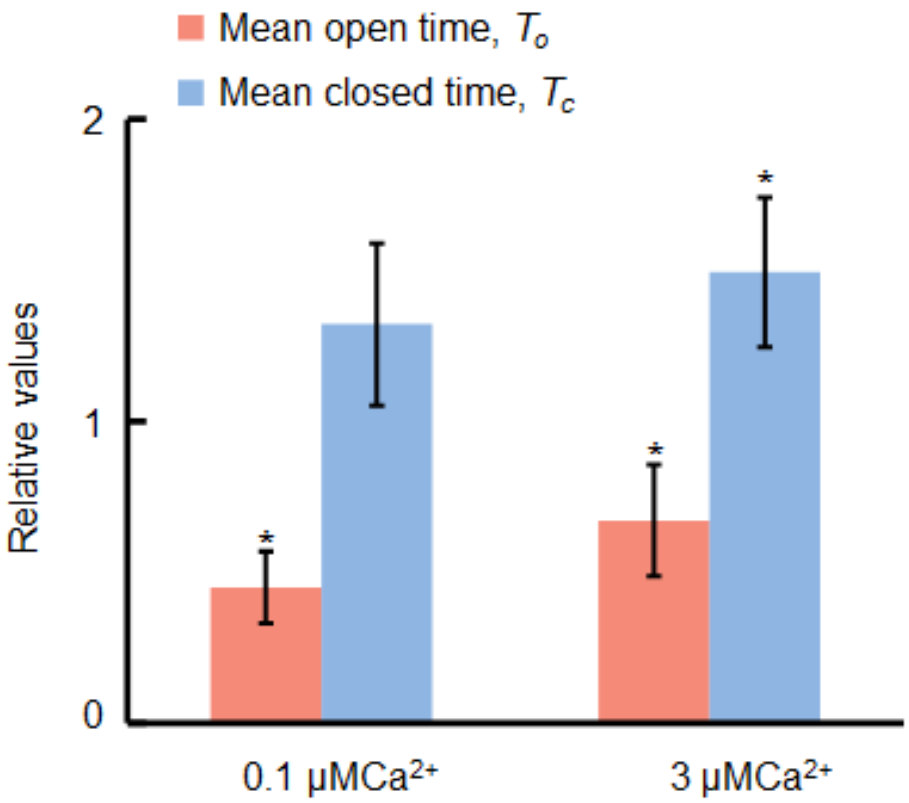

Figure 5.2: Relative CaM effect on RyR2 T_o and T_c at 0.1 and 3 μM cytoplasmic Ca^{2+}. RyR2 T_o and T_c in the presence of 500 nM CaM relative to that in the absence of CaM. Channel recordings at -40 mV for RyR2 from ICM heart were taken in the presence of 0.1 mM luminal Ca^{2+} and 2 mM ATP in the cytoplasm. Data are shown as the mean ± sem (n = 5 at 0.1 μM cytoplasmic Ca^{2+} and 10 at 3 μM cytoplasmic Ca^{2+}). Asterisks (*) denote a significant difference in relative values compared to that in the absence of CaM (* $p<0.05$, ** $p<0.01$).

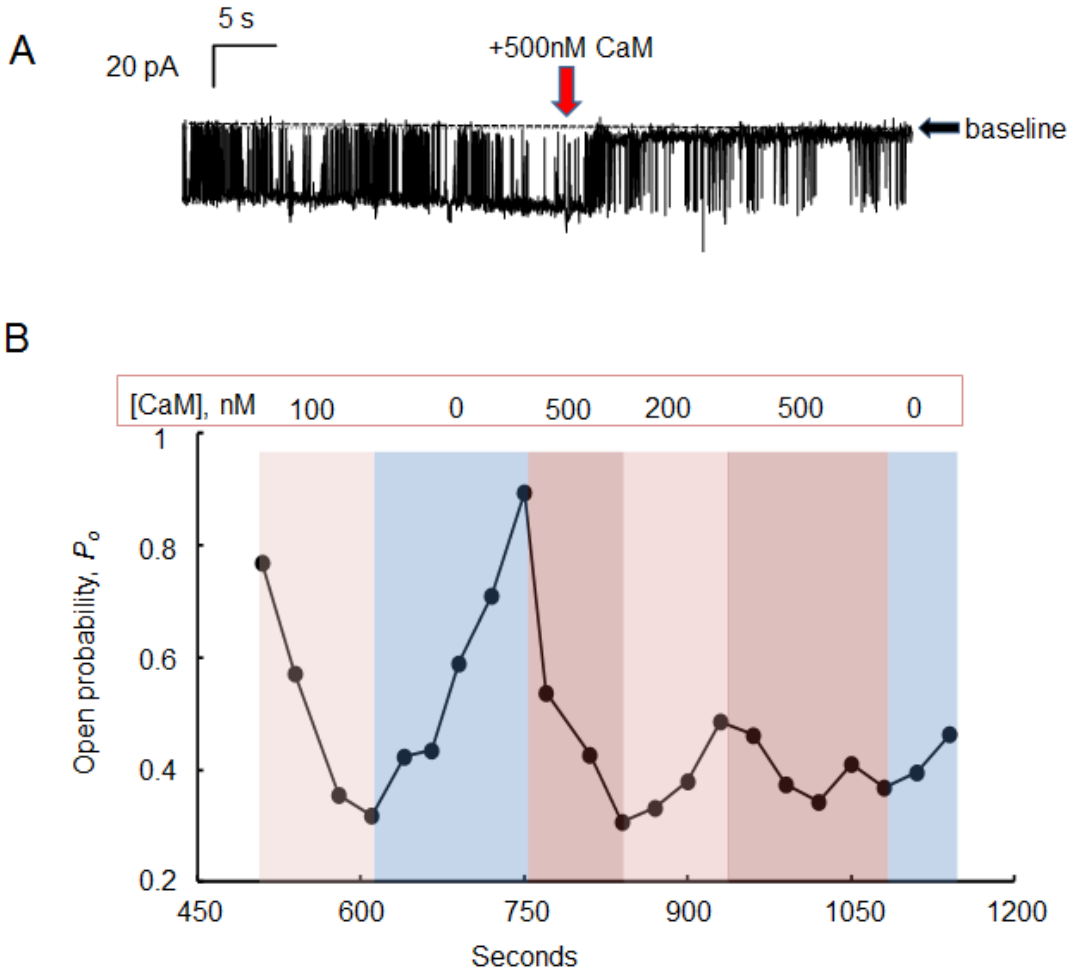

Figure 5.3: CaM effect on single RyR2 from failing human heart at 3 µM cytoplasmic Ca^{2+}. (A) Single channel recordings for RyR2 from ICM failing heart before and after CaM addition that occurred at 750 s after the beginning of the experiment. Channel openings appear as downward current jumps from the baseline (black arrow and dashed line). Channel activity was recorded at -40 mV in the presence of 0.1 mM luminal Ca^{2+} and 2 mM ATP in the cytoplasm. **(B)** The full time-course of RyR P_o exposed to various CaM concentrations from the experiment shown in part A.

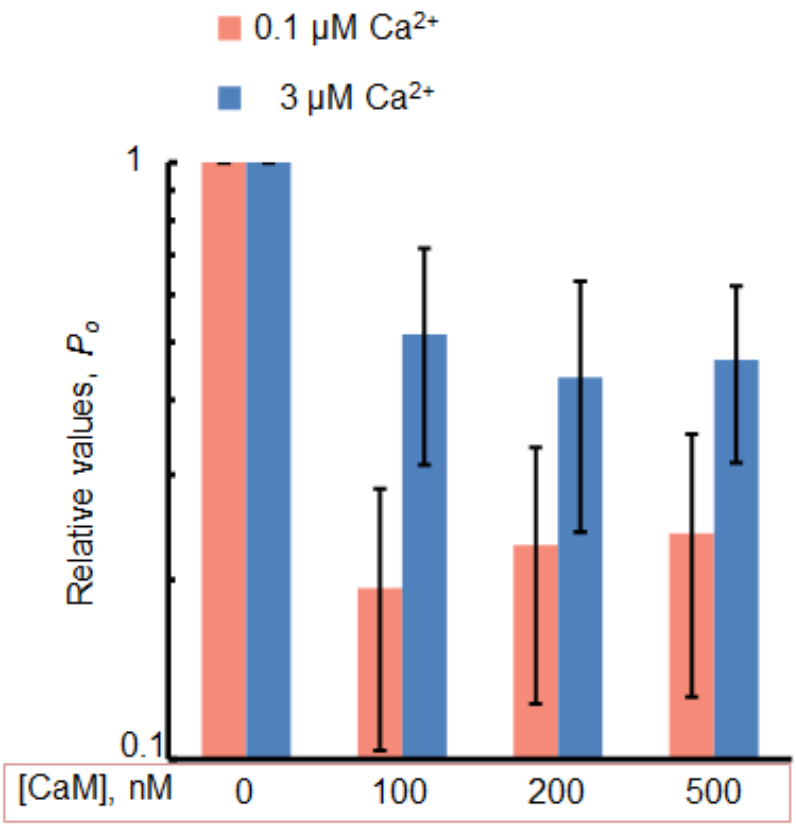

Figure 5.4: Relative effect of CaM dose-response on RyR2 from failing human hearts at 0.1 and 3 μM cytoplasmic Ca^{2+}. RyR2 P_o in the presence of various concentrations of CaM (100, 200 and 500 nM) relative to that in the absence of CaM. Channel activity was recorded at -40 mV for RyR2s from ICM heart were taken in the presence of 0.1 mM luminal Ca^{2+} and 2 mM ATP in the cytoplasm.. Data are shown as the mean ± sem (n = 3 at 0.1 μM cytoplasmic Ca^{2+} and n = 2 at 3 μM cytoplasmic Ca^{2+}).

5.3.2 CaM had no effect on RyR2s from healthy human heart

The inhibitory effect of CaM on RyR2 from healthy human heart was also measured in this study (Figure 5.5). Surprisingly, RyR2s from healthy human heart were not affected by the addition of 500 nM CaM (Figure 5.5A & B), a level ~ 5-fold higher than the physiological CaM concentration.

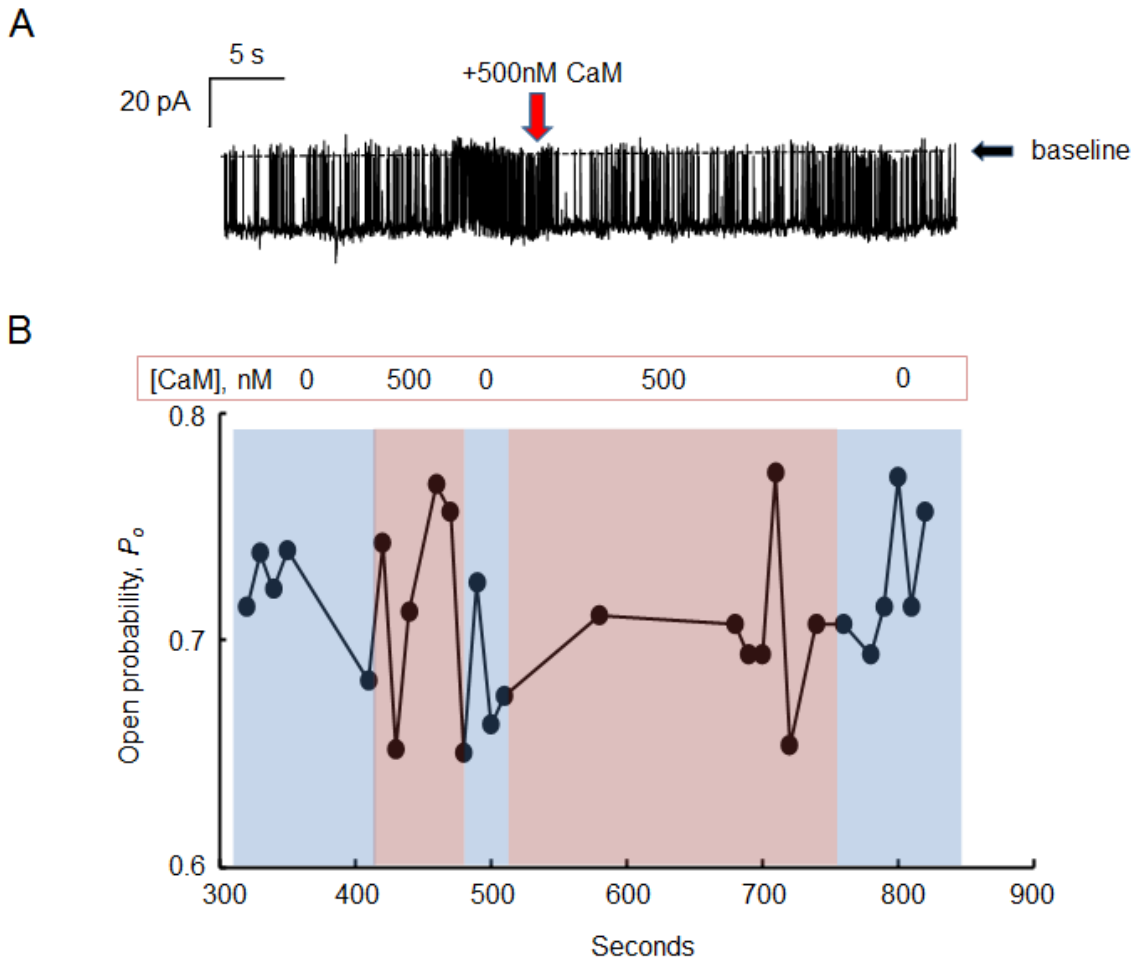

Figure 5.5: CaM effect on single RyR2 from healthy human heart in 3 µM cytoplasmic Ca^{2+}. (A) Single channel recordings for RyR2 before and after CaM addition at 400 s after the beginning of the experiment. Channel openings are downward current jumps from the baseline (black arrow and dashed line). Channel activity was recorded at -40 mV in the presence of 0.1 mM luminal Ca^{2+} and 2 mM ATP in the cytoplasm. **(B)** Time-course of RyR P_o exposed to periods of 0 and 500 nM CaM.

5.3.3 CaM inhibition of human RyR2 is potentiated by phosphorylation

It was considered a possibility that the different responses of healthy and failing heart to CaM were due to the increased phosphorylation of the RyR2 observed in failing hearts (see Figure 4.10). To test this hypothesis, the effect of 500 nM CaM was measured on RyR2s from healthy heart before and after phosphorylation by PKA. This was achieved using two experimental approaches (see Section 5.2.2). Figure 5.6 shows the diary plot of one of two experiments where a single channel in the bilayer was exposed to PKA and substrates for 2 minutes via the perfusion system. PKA incubation caused an increase in RyR2 activity followed by a substantial reduction in RyR2 activity caused by the addition of 500 nM CaM. A similar CaM-induced reduction in RyR2 activity was seen in both experiments. A simpler, non-paired method of measuring the effect of phosphorylation was to measure the effect of CaM on RyR2s from healthy heart that were incubated with exogenous PKA prior to incorporation into the bilayer. Figure 5.7 shows one of two such experiments. RyR2s that were pre-incubated with PKA prior to fusion with lipid bilayers, had a P_o very close to 1 (Figure 5.7A & B). The addition of 500 nM CaM caused a clear change in RyR2 activity (Figure 5.7A) even though it only produced minor changes in P_o. However, CaM did produce a substantial reduction in T_o which is shown in Figure 5.7C. Thus, the average P_o from all four experiments showed that RyR2 pre-treated with PKA were inhibited upon the addition of CaM (Figure 5.8, blue bars).

The summary of data for healthy and failing hearts is shown in Figure 5.8 where it can be seen that the addition of 500 nM CaM to the cytoplasmic bath caused a reduction in RyR2 P_o from healthy (treated with PKA) and failing human hearts. This reduction is mediated primarily by changes in both mean open and closed times.

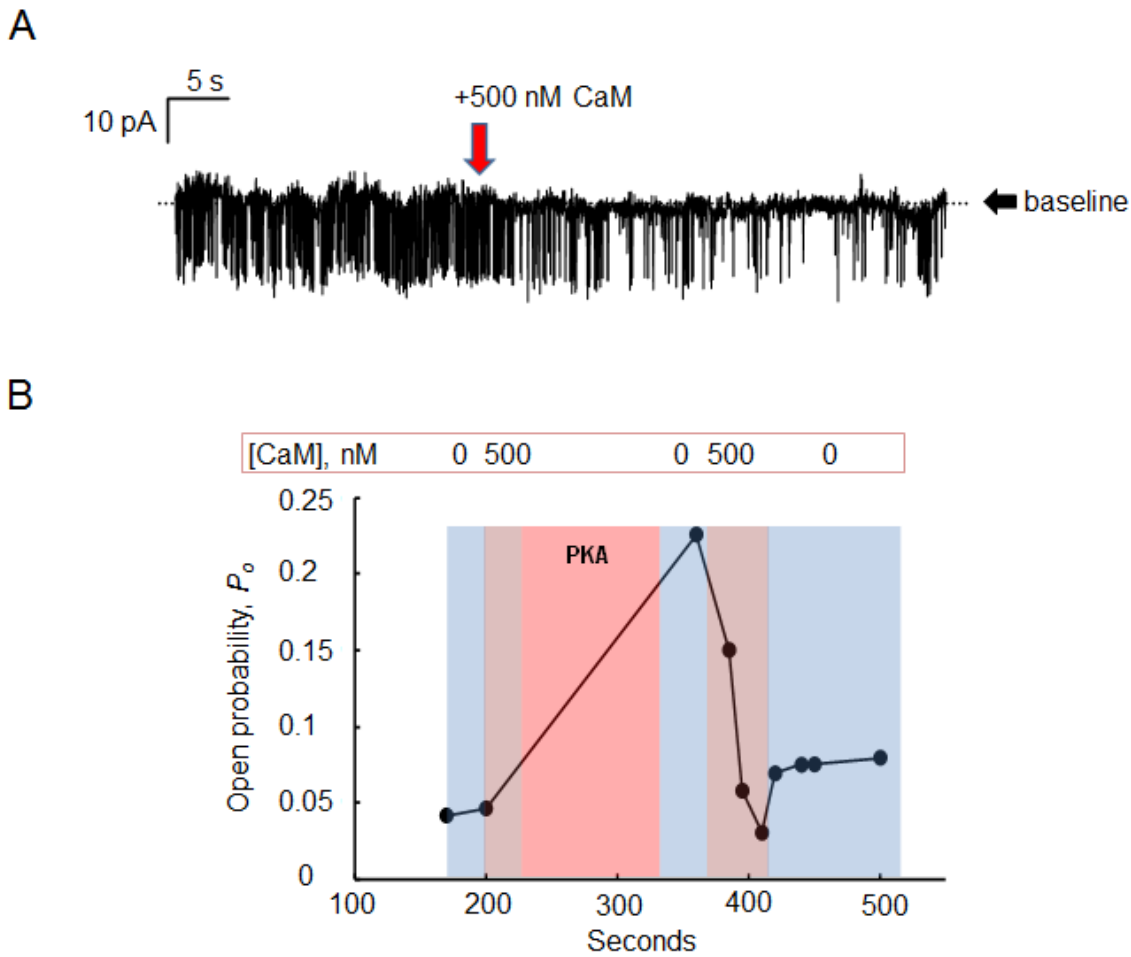

Figure 5.6: CaM effect on RyR2s from healthy human heart pre-treated with PKA. **(A)** Single channel recordings of RyR2s that were phosphorylated after adding PKA and its substrate to the cytoplasmic bath at 220 s, for 2 mins from the beginning of the experiment. Channel recordings were taken before and after the addition of CaM at 370 s after the beginning of the experiment. Channel openings are downward current jumps from the baseline (black arrow and dashed line). Channel activity at -40 mV was recorded in 3 µM cytoplasmic Ca^{2+} and 0.1 mM luminal Ca^{2+} in the presence of 2 mM ATP in the cytoplasm. **(B)** Time-course of RyR P_o exposed to CaM before and after PKA addition to the cytoplasmic bath.

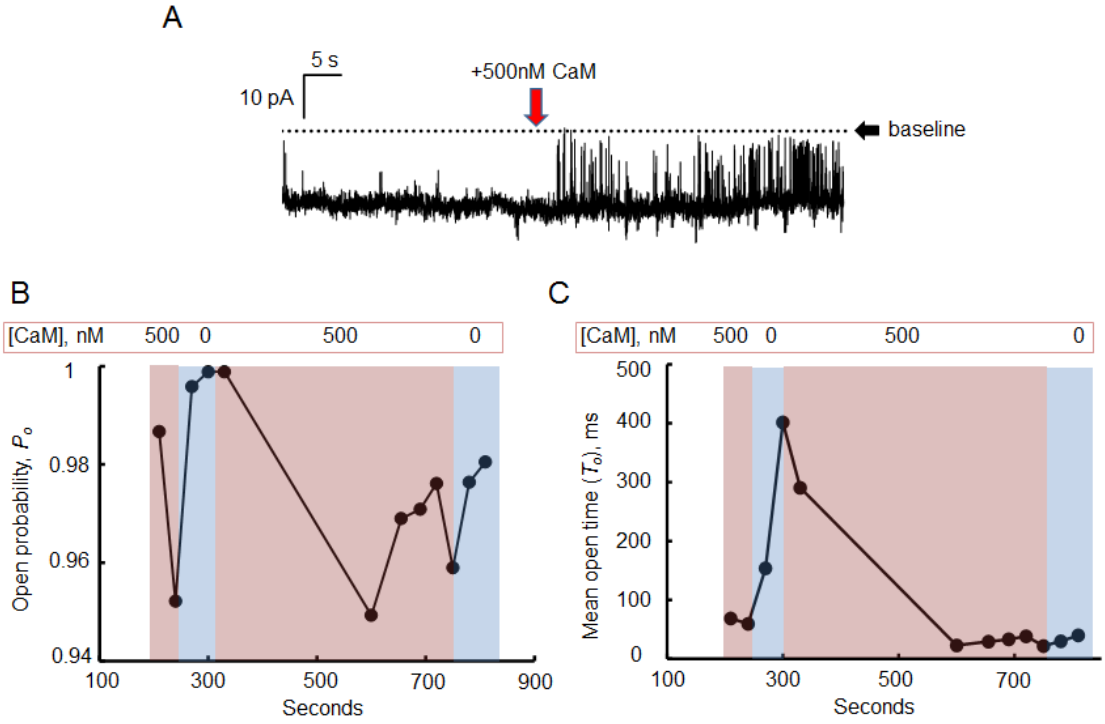

Figure 5.7: CaM effect on RyR2s from healthy human heart incubated with PKA. (A) Single channel recordings for RyR2s that were phosphorylated by pre- incubation with PKA and its substrate for 5 min at 30 ^{o}C prior to incorporation into the bilayer. Channel recordings were taken before and after CaM addition that occurred at 300 s after the beginning of the experiment. Channel openings are downward current jumps from the baseline (black arrow and dashed line). Channel activity at -40 mV was recorded in 3 µM cytoplasmic Ca^{2+} and 0.1 mM luminal Ca^{2+} in the presence of 2 mM ATP in the cytoplasm **(B)** Time-course of RyR P_o exposed to CaM after incubation with PKA. **(C)** Time-course of RyR T_o exposed to CaM after incubation with PKA.

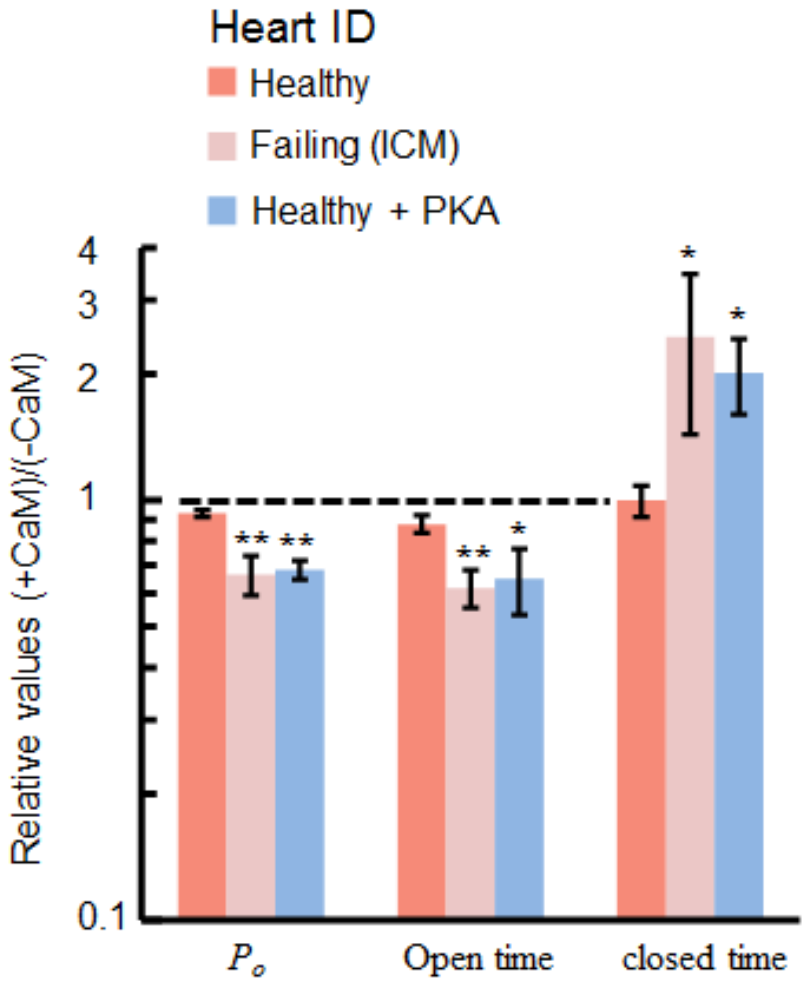

Figure 5.8: Relative CaM effect on RyR2s from healthy and failing human hearts in 3 µM cytoplasmic Ca^{2+}. RyR2s were isolated from four healthy human hearts and from the left ventricle of a failing heart with ischemic cardiomyopathy (ICM). Channel recordings were made in the presence of 0.1 mM luminal Ca^{2+} and 2 mM ATP in the cytoplasm at -40 mV. Data are shown as mean ± sem (n = 6-8 from healthy, 10 from ICM and 4-6 from healthy + PKA). Asterisks (*) denote a significant difference in relative values compared with healthy human heart (* $p<0.05$, ** $p<0.01$).

5.4 Discussion

These bilayer experiments present the first determination of the effects of CaM on RyR2s isolated from healthy and failing human hearts. Single channel recordings showed that CaM has a much stronger inhibitory effect on RyR2s from failing hearts with ischemic cardiomyopathy than RyR2s from healthy hearts. The data also indicate that the effect of CaM binding to RyR2s depends on the RyR being hyperphosphorylated which has important implications to RyR regulation during adrenergic stimulation and HF where phosphorylation is increased.

A previous study found that modulation of RyR2s from canine heart by CaM is affected by Ca^{2+} concentration where different mechanisms were seen at low and high Ca^{2+} (Xu and Meissner 2004). At < 10 μM cytosolic Ca^{2+}, CaM reduced the RyR2 P_o by decreasing the mean open times and by increasing mean close times, whereas at higher cytosolic [Ca^{2+}] (≥ 10 μM), CaM was less effective in reducing channel activity by decreasing mean open times without affecting mean closed times (Xu and Meissner 2004). In the studies here, analyses of single-channel recordings from failing human heart showed that in 0.1 and 3 μM cytosolic Ca^{2+}, CaM decreased channel P_o by decreasing the mean open times and by increasing mean closed times which is consistent with the above findings by Xu *et al.* (Figures 5.2 & 5.8).

The results here have shown a strong inhibitory effect of CaM on RyR2 activity from failing human heart, suggesting that CaM could serve a protective role in HF by reducing diastolic Ca^{2+} leak. Previous findings have shown that a proper CaM binding to RyR2s from paced-dog failing hearts, stabilizes channel function and restores normal Ca^{2+} handling and contractile function in HF (Hino, Yano et al. 2012). However, several studies showed that CaM binding to failing heart is reduced by 50% which would act against such a protective mechanism (Ono, Yano et al. 2010; Hino, Yano et al. 2012). The mechanism by which CaM binding is reduced in HF is related to inter-domain interactions in the RyR2. Disrupting RyR2 inter-domain interaction by exposing RyR2 to inter-domain disrupting peptide (DPc10) caused a marked decline in CaM binding to RyR2s (Yamamoto and Ikemoto 2002; Xu, Yano et al. 2010). In the failing heart RyR2

oxidation is known to disrupt interdomain interactions in the RyR2 channel (Belevych, Terentyev et al. ; Mochizuki, Yano et al. 2007; Gyorke and Carnes 2008) and this may have a role in reducing CaM binding to RyR2. Furthermore, Meissner and his co-workers have shown that CaM binding affinity to RyR2s is reduced in the presence of oxidizing conditions (Balshaw, Xu et al. 2001). Together, these findings highlight the importance of CaM in the RyR2 complex in failing hearts.

RyR2 from healthy human heart showed very little or no inhibitory effect of the addition of CaM. Binding of CaM to RyR2 from healthy human heart with high affinity (Yang, Guo et al. 2014) indicates that the lack of effect of CaM on healthy human RyRs is due to lack of action of the bound CaM. Pilot experiments where healthy human RyR2s were incubated with PKA to simulate RyR2 phosphorylation that occurs during HF, indicated that phosphorylation of the RyR2 markedly increased the inhibiting effect of CaM on RyR2 from healthy hearts. These results indicate that the effect of CaM binding to RyR2 depends on the RyR being hyperphosphorylated. Therefore, it would be expected that intracellular CaM acts to attenuate the amplification of Ca^{2+} release which occurs with acute phosphorylation during adrenergic stimulation, as well as during chronic phosphorylation that occurs in HF.

Reduction of CaM binding to RyR2s seems to play a critical role in the pathogenesis of aberrant Ca^{2+} release in failing hearts which may be more critical than FKBP12.6 in regulating RyR2 channels in human HF. It has been argued that FKBP12.6 binding to the RyR2 has an important role in minimizing Ca^{2+} release during diastole (Wehrens, Lehnart et al. 2003). However, the role of FKBP12.6 in RyR2 modulation remains highly controversial. Moreover, it has been shown that the quantity of FKBP12.6 is much lower than that of RyR2s and therefore only a small portion of RyR2 molecules (about 15%) can be bound to FKBP12.6 (Guo, Cornea et al. 2010). On the other hand, the free CaM concentration in the cell (~ 50-100 nM, (Maier, Ziolo et al. 2006; Guo, Fruen et al. 2011)), by far exceeds the RyR2 affinity for CaM (K_d 30-100 nM, (Guo, Fruen et al. 2011)) so that nearly all RyR2s will have CaM bound to them.

Chapter 6-General Discussion

6.1 Key findings and hypothesis

Calcium release through RyR2s is the key determinant of cardiac contraction and rhythm. The aim of this research project was to understand how RyR2s in the heart are remodelled during the progression of HF and how this contributes to aberrant calcium signalling in the cell. This is an important issue because approximately 50% of people with HF die from arrhythmias due to aberrant calcium signalling long before their heart muscle actually fails. The fundamental role of RyR2s in Ca^{2+} regulation in healthy and failing hearts is well recognised but poorly understood. A key aspect of this project was access to available human heart tissue, both failing and healthy. RyR2 activity from healthy and failing human hearts was measured using single channel recordings in artificial lipid bilayers. The experiments tested the hypothesis that heart failure alters Ca^{2+} dynamics by changing its regulation by intracellular [Ca^{2+}] and [Mg^{2+}] and that this occurs as a result of changes in the way the RyR2 complexes with other intracellular proteins.

6.1.1 Relevance of animal RyRs to human RyRs.

Tissue from healthy human hearts recently made available through my collaborators, Dr Molenaar at the University of Queensland and Dr dos Remedios at the University of Sydney, enabled the first measurements of the regulation of calcium release channels from healthy human heart to be reported here. Healthy human hearts were obtained from four patients of different ages, sex and cause of death. It has been shown that the cardiovascular effects of FKBP12.6 may be different depending on sex (Xin, Senbonmatsu et al. 2002). Given that FKBP12.6 has a key role in regulation of RyR2 activity (Ahern, Junankar et al. 1994; Kaftan, Marks et al. 1996; Marx, Reiken et al. 2000; Galfre, Pitt et al. 2012), it is quite possible that RyR2 properties differ in males and females. A recent study has shown that the adrenergic tone of rat hearts affect the activity of RyRs isolated from these hearts when incorporated into artificial lipid bilayers (Li, Imtiaz et al. 2013). Therefore it is possible that excessive adrenergic stimulation just before death could alter RyR activity in healthy hearts. However, data from the four donor hearts revealed no significant differences between these groups in the Ca^{2+} and Mg^{2+} regulation of their RyRs. Therefore, it is unlikely that donor

variations had an important influence on RyR2 function. Using a similar argument, it is also unlikely that these donor variations had an effect on differences in association of either FKBP isoform and the level of phosphorylation of RyR2 at S^{2814}, S^{2808} between healthy human hearts

A detailed analysis of the regulation of healthy human RyR2s by intracellular Ca^{2+} and Mg^{2+} (Chapter 3) showed that human RyR2s displayed the same regulation by cytoplasmic Ca^{2+}/ Mg^{2+} as seen in rat and sheep (Figure 3.6A&C). However, RyR2 sensitivity to luminal Ca^{2+} and Mg^{2+} varied between species and RyR2 from human hearts were less sensitive to inhibition by luminal Mg^{2+} compared to that seen in sheep and rat RyR2s. The latter findings suggest that the proportion of Ca^{2+} release from the SR during EC coupling is higher in human hearts and more affected by luminal Ca^{2+} than in rat and sheep hearts.

Under systolic conditions in presence of 1 mM Mg^{2+}, RyR2s from human and sheep hearts have similar gating properties whereas, RyR2s from rat heart are 3-fold less sensitive to activation by cytoplasmic Ca^{2+} (Figure 3.7A). Computer simulations of SR Ca^{2+} release within a 3D model of the cardiac dyad demonstrate that this difference in Ca^{2+} sensitivity leads to substantial differences between species in the triggering and termination of localised Ca^{2+} sparks (Cannell, Kong et al. 2013). The activity of the RyR2 at diastolic cytoplasmic [Ca^{2+}] shows a dependency on store load that differs between species and is most likely to produce corresponding differences in the store load dependence of Ca^{2+} spark frequency. Thus, differences in RyR2 regulation by Ca^{2+} and Mg^{2+} are likely to contribute to E-C coupling differences between species.

In addition, the contribution that CaM makes to the functioning of the RyR2 complex in healthy hearts was examined. CaM has been shown elsewhere to be critical for normal cardiac function and altered CaM binding may contribute to defects in SR Ca^{2+} release in arrhythmias and HF (Guo, Fruen et al. 2011). The data presented here indicate that the addition of CaM had very little or no effect on RYR2s activity from healthy human heart (n=4), whereas, previously published studies (including from this laboratory) have shown that CaM inhibits RyR2 activity from sheep (30% inhibition

(Hwang, Nitu et al. 2014)**)** and dog (80% inhibition (Balshaw, Xu et al. 2001; Xu and Meissner 2004)) and both are commonly used models for RyR2 function in HF (Balshaw, Xu et al. 2001; Xu and Meissner 2004; Hwang, Nitu et al. 2014). Therefore, it is apparent that CaM can regulate RyR2 activity from different species in various ways. In terms of CaM regulation of RyR2s, one could propose that animal models may not be accurate models for RyR2 function in humans.

The molecular mechanism for the differences between CaM effects on RyR2 from different species is not yet clear. They could arise from differences in the amino acid sequences of the RyR2s or species-specific posttranslational modifications. For example, the adrenergic tone of rat hearts is known to affect the activity of isolated RyRs when incorporated into artificial lipid bilayers (Li, Imtiaz et al. 2013). This thesis has further demonstrated that the action of CaM depended on the phosphorylation state of the RyR2 in that its phosphorylation markedly increased the inhibiting effect of CaM on RyR2s from healthy hearts. Therefore, it is possible that variations in adrenergic tone between species could underlie the different RyR2 properties from sheep, rat and human.

The lack of effect of CaM on human RyR2s raises questions as to whether CaM has any role in the function of healthy heart. However, the importance of CaM in maintaining normal heart function is underscored by mutations in CaM that are known to cause CPVT. CPVT in humans results from increased RyR2 channel openings and spontaneous Ca^{2+} release (Watanabe and Knollmann 2011; Hwang, Nitu et al. 2014). Interestingly, CPVT is a ventricular tachycardia that occurs during periods of adrenergic stimulation, *i.e.*, at times when the phosphorylation of RyR2 is elevated and where CaM does indeed cause inhibition of the RyR2. Thus, it is possible that CaM normally blunts the adrenergic stimulation of RyR2 activity during periods of stress and exercise. Lack of a CaM effect could cause excess adrenergic stimulation and arrhythmia. To date there have not been any studies investigating the binding of CaM to human RyRs. Hence, it is not clear whether the lack of effect of CaM on human RyRs is due to lack of binding or lack of action of the bound CaM.

6.1.2 Are animal heart models good for failing human heart?

Experimental animal models of HF are often needed to address specific questions not easily answered in patients. However, one of the main problems researching in this area is that animal models of HF (rat in particular) do not match the human condition (*e.g* differences in myocardial function that could present in animal models compared to human heart, (Bers 1991)).

Previous studies have shown striking differences in the calcium release units (CRUs) among different cardiac muscle preparations. Differences in the number of RyR2 molecules in CRUs have been reported between cardiac muscle preparations from different species. Species with faster heart rate exhibit greater numbers of RyRs within the dyadic cleft (Soeller, Crossman et al. 2007). Bers and co-workers (Bers and Stiffel 1993; Bers 2001) have reported variation in the RyR2 to DHPR ratio (ranging from 4-10 times) between rabbit, guinea pig, rat, and ferret. Bassani *et al.* have also shown species-dependent differences in cellular relaxation mechanisms (Ca^{2+} removal from the cytosol) during E-C coupling (Bassani, Bassani et al. 1994). These differences are believed to underlie species-specific differences in the proportion of Ca^{2+} entering the cell and Ca^{2+} emanating from the SR during EC coupling (Bers 2001). In this thesis, species-dependent differences in the regulation of RyR2 by intracellular Ca^{2+} and Mg^{2+} have also been clearly demonstrated.

Moreover, it has been shown that CaM differentially regulated RyR2 channel activity from different species (see section 6.1.1). Importantly, it was found that the regulatory action of CaM depends on the phosphorylation state of the RyR2 that increases during adrenergic stimulation as well as in HF (chronic phosphorylation). Other studies have shown that the adrenergic pathway that accelerates relaxation of cardiac myocytes in humans, differs to that which occurs in other mammals (Kaumann, Sanders et al. 1996; Zheng, Zhu et al. 2005; Molenaar, Savarimuthu et al. 2007). Therefore, it is possible that variations occur in the adrenergic pathway between species. Given the importance of adrenergic stimulation in RyR2 regulation in healthy and failing hearts (i.e. RyR2 regulation by accessory proteins like kinases, phosphatases, CaM and FKBP12.6) and

the potential importance of Ca^{2+} and Mg^{2+} regulation of RyR2s, one could propose that animal models may not be accurate models for failing human heart.

6.1.3 Do different forms of HF exhibit variations in RyR2 remodelling?

The functional and structural properties of RyR2s from failing hearts exhibited heart to heart variations between failing heart types. RyRs from failing hearts showed differences in the proportion of high channel activity between HF types (15% of the RyRs from ICM hearts and 50% from EDMD, Figure 4.3B). Moreover, differences in the sensitivity to luminal and cytoplasmic Mg^{2+} inhibition by RyRs with high channel activity was also observed between failing hearts (Figure 4.7). RyRs from failing hearts also showed differences in structure between HF types. RyR2s from ICM hearts exhibited less association of phosphatases (PP1 and PP2A) and a reduction in the expression level of SERCA2a, whereas EDMD heart showed reduction in the expression of CSQ2 and Triadin-1 and exhibited less association of PP1 only- (Figures 4.9 & 4.11). These differences may indicate heart to heart variations in the progression of myopathy and differences in structural remodelling in dyad junctions among failing hearts.

Insufficient statistical power to confirm that RyR2 exhibits functional and structural changes among failing heart types was the main limitation in this study. Another one or two types of failing hearts are needed with increasing the n value of each heart to study RyR2 function. Western Blots are needed to probe for associated changes in the RyR2 complex.

6.1.4 Has RyR2 from CF heart undergone remodelling?

An interesting finding was that RyR2s from a donor who died of cystic fibrosis showed functional changes similar to those seen with HF. Initially, this heart sample was included among our healthy heart group since the heart was designated for transplant but no suitable recipient was found on the day of explant. However, as the study progressed, it became clear that RyR2 function from this heart differed from those obtained from four other hearts donated by healthy accident victims. This finding suggested that a high percentage of RyRs in this heart had undergone some form of remodelling perhaps as a consequence of pulmonary stress (early stage of progression to HF).

The biochemical investigations failed to show any changes (which may have a role in RyRs remodelling in CF heart) in the association of co-proteins in the RyR2 macromolecular complex or phosphorylation status in CF compared to healthy hearts. However, it cannot be ruled out that there could be changes by other factors such as oxidation or/and nitrosylation in RyR2 from CF heart. As yet the nature of the RyR2 remodelling is not clear.

A limitation of this study was that there were insufficient numbers of CF hearts to confirm that the RyR2 generally undergoes remodelling in CF hearts. Another one or two more CF hearts are needed to complete this study of RyR2 function and to carry out Western Blots to probe for associated changes in the RyR2 complex.

6.2 Future directions

6.2.1 Test the hypothesis that regulation of RyR2 by CaM is potentiated by adrenergic stimulation or RyR2 remodeling in HF.

The finding that phosphorylation of RyR2s markedly increases the inhibiting effect of CaM on RyR2 from healthy hearts has some intriguing implications for the importance of CaM in adrenergic-induced sudden cardiac death, since during adrenergic stimulation

RyR2 phosphorylation is increased. In order to determine the effects of CaM on RyR2 isolated from adrenergically-stimulated hearts or hearts subjected to cardiac remodeling during HF, the effect of CaM on the activity of RyR2 isolated from hearts that were subjected to adrenergic stress compared to RyR2s from non-stressed hearts would need to be measured. For these experiments it is impractical to use human hearts so one would use a rat model for adrenergic stimulation. The data presented here already indicates that CaM has a much stronger inhibitory effect on RyR2s from human hearts with ischemic cardiomyopathy than RyRs from healthy human hearts. One could examine CaM effects on RyR2s remodeled by other types of HF to see if altered CaM effects are due to altered RyR2 phosphorylation of RyR2 by altering the RyR2 phosphorylation state of healthy and remodeled RyR2 that have been pre-incubated with PKA or PP1 (phosphorylation status will be confirmed using Western Blot).

The cause of RyR2 channel dysfunction in HF is highly controversial and may involve many mechanisms. It has been proposed that RyR2 remodelling in HF involves a defective inter-domain interaction in response to oxidation associated with RyR2 hyperphosphorylation (Oda, Yano et al. 2005; Yano, Okuda et al. 2005). It has been shown that disrupting the RyR2 inter-domain interaction by exposing RyR2s to the inter-domain disrupting peptide (DPc10) caused a marked decline in CaM binding to RyR2s (Yamamoto and Ikemoto 2002). Furthermore, Meissner and his co-workers have shown that, using dog heart RyR2s, the oxidizing conditions stimulated by glutathione (GSSG), reduced the RyR2 binding affinity to CaM (Balshaw, Xu et al. 2001). In the failing heart, disruption of inter-domain interactions in RyR2s by oxidation (Belevych, Terentyev et al. ; Mochizuki, Yano et al. 2007; Gyorke and Carnes 2008) may have a role in reducing CaM binding to the RyR2. Therefore, it will also test whether oxidation of healthy human RyR2s alters CaM regulation by measuring this at various redox potentials using a range of GSH/GSSG ratios, or by incubation of RyR2s from healthy human hearts with H_2O_2. These experiments may help to define how CaM contributes to altered SR Ca^{2+} release that occurs in failing hearts. As yet, it is not clear to what extent the action of CaM on RyR2 activity is influenced by adrenergic stimulation and weakened inter-domain interactions and HF remodeling.

6.2.2 Role of FKBP12.6 in HF.

It has been proposed that loss of FKBP12.6 from RyR2 increases diastolic Ca^{2+} leak (contributing towards a higher RyR2 open probability) (Marx, Reiken et al. 2000; Yano, Ono et al. 2000), whilst binding of FKBP12.6 to the channel minimizes Ca^{2+} release from the SR during diastole (Wehrens, Lehnart et al. 2003). However, the role of FKBP12.6 in RyR2 modulation remains highly controversial. It has been suggested that loss of FKBP12.6 should not make a significant difference to RyR2 activity because only a minority of RyR2s actually bind this molecule (about 15%) (Guo, Cornea et al. 2010).

It has been shown that alteration in FKBP12/FKBP12.6 ratio contributes towards a higher RyR2 open probability, *i.e.*, 'leaky' RyR2 channels (Galfre, Pitt et al. 2012). Sitsapesan and coworkers (Galfre, Pitt et al. 2012) found that FKBP12 is a RyR2 activator and that FKBP12.6 could lower RyR2 P_o by antagonising the activating effects of FKBP12. My data showed that in heart failure there was a 3-fold larger reduction in FKBP12 (RyR2 activator) than in FKBP12.6 (RyR2 inhibitor; Figure 4.12), which, on its own, should lead to a loss of RyR2 activity. However, the effect of HF in single channel studies presented here showed an opposite effect. Therefore, either the relative inhibition by FKBP12.6 outweighs activation by FKBP12 or other factors such as RyR2 oxidation or hyperphosphorylation may have caused the observed increase in RyR2 activity in failing hearts. In order to examine the effect of FKBP12/FKBP12.6 dissociation from RyR2 and its contribution to HF progression, one could remove the FKBP12/FKBP12.6 associated with the RyR2s from healthy and failing human hearts by incubation of the SR vesicles with rapamycin (10 uM) at 37 ^{o}C for 15 min as described by Timerman *et al.* (Timerman, Ogunbumni et al. 1993; Timerman, Wiederrecht et al. 1995). The amount of FKBP remaining associated with SR vesicles could be visualized using IP and Western Blot (see sections 4.2.4 & 4.2.5). The SR vesicles containing FKBP-depleted RyR2s isolated from healthy and failing human hearts would be incorporated into planar lipid bilayers. Single channel recordings of RyR2 stripped of ~ 100% of FKBP could be compared with RyR2s from native SR to examine the effects of these ligands on RyR2 function.

The possibility of restoring healthy RyR2 function in vitro by the exogenous addition of the accessory protein FKBP12.6 to RyR2s from failing human hearts in the bilayer could also be tested. The composition of the RyR complex could be manipulated in artificial membranes whilst simultaneously measuring functional changes in the RyR2 by using single channel recordings. An alternative method would be to incubate RyRs with exogenous FKBP12.6 for 15 hrs at 4 ^{o}C prior to incorporation into the bilayer (the binding would be confirmed using IP and Western blot) (Galfre, Pitt et al. 2012). The results of these experiments may reveal the ways in which the effects of the RyR2 complex degradation can be partially reversed and whether FKBP12.6 dissociation from the RyR2 alters RyR2 function as seen in HF.

Reference

Ahern, G. P., P. R. Junankar, et al. (1994). "Single channel activity of the ryanodine receptor calcium release channel is modulated by FK-506." FEBS Lett. 352: 369-374.

Ai, X., J. W. Curran, et al. (2005). "Ca2+/calmodulin-dependent protein kinase modulates cardiac ryanodine receptor phosphorylation and sarcoplasmic reticulum Ca2+ leak in heart failure." Circ Res 97(12): 1314-1322.

Ai, X., J. W. Curran, et al. (2005). "Ca^{2+}/calmodulin-dependent protein kinase modulates cardiac ryanodine receptor phosphorylation and sarcoplasmic reticulum Ca^{2+} leak in heart failure." Circ. Res. 97(12): 1314-1322.

Anderson, J. L., E. M. Gilbert, et al. (1989). "Prevention of symptomatic recurrences of paroxysmal atrial fibrillation in patients initially tolerating antiarrhythmic therapy. A multicenter, double-blind, crossover study of flecainide and placebo with transtelephonic monitoring. Flecainide Supraventricular Tachycardia Study Group." Circulation 80(6): 1557-1570.

Apostolakis, S., M. Oeff, et al. (2013). "Flecainide acetate for the treatment of atrial and ventricular arrhythmias." Expert Opin Pharmacother 14(3): 347-357.

Azibani, F., A. Muchir, et al. (2014). "Striated muscle laminopathies." Semin Cell Dev Biol.

Balog, E. M., B. R. Fruen, et al. (2001). "Divergent effects of the malignant hyperthermia-susceptible arg(615)cys mutation on the Ca^{2+} and Mg^{2+} dependence of the RyR1." Biophys J 81(4): 2050-2058.

Balshaw, D. M., L. Xu, et al. (2001). "Calmodulin binding and inhibition of cardiac muscle calcium release channel (ryanodine receptor)." J. Biol. Chem. 276(23): 20144-20153.

Balshaw, D. M., N. Yamaguchi, et al. (2002). "Modulation of intracellular calcium-release channels by calmodulin." J Membr Biol 185(1): 1-8.

Barbuti, A. and D. DiFrancesco (2008). "Control of cardiac rate by "funny" channels in health and disease." Ann N Y Acad Sci 1123: 213-223.

Bassani, J. W., R. A. Bassani, et al. (1994). "Relaxation in rabbit and rat cardiac cells: species-dependent differences in cellular mechanisms." J Physiol 476(2): 279-293.

Beard, N. A., D. R. Laver, et al. (2004). "Calsequestrin and the calcium release channel of skeletal and cardiac muscle." Prog. Biophys. Mol. Biol. 85(1): 33-69.

Belevych, A. E., D. Terentyev, et al. "The relationship between arrhythmogenesis and impaired contractility in heart failure: role of altered ryanodine receptor function." Cardiovasc Res 90(3): 493-502.

Bell, J. R., C. L. Curl, et al. (2012). "Ca2+/calmodulin-dependent protein kinase inhibition suppresses post-ischemic arrhythmogenesis and mediates sinus bradycardic recovery in reperfusion." Int J Cardiol 159(2): 112-118.

Benkusky, N. A., C. S. Weber, et al. (2007). "Intact beta-adrenergic response and unmodified progression toward heart failure in mice with genetic ablation of a major protein kinase A phosphorylation site in the cardiac ryanodine receptor." Circ Res 101(8): 819-829.

Berridge, M. J. (1997). "Elementary and global aspects of calcium signalling." J Physiol 499 (Pt 2): 291-306.

Bers, D. M. (1991). Excitation-contraction coupling and contractile force. Developments in cardiovascular medicine. Control of cardiac contraction by SR-Ca release and sarcolemmal-Ca fluxes. D. M. Bers. Dordrecht, Boston, London, Kluver. 122: 149-170.

Bers, D. M. (2001). Excitation-contraction coupling and cardiac contractile force. Dordrecht, Kluwer Academic Publications.

Bers, D. M. (2001). Excitation-contraction coupling and cardiac contractile force. Boston, Kluwer Academic Publishers,.

Bers, D. M. (2002). "Calcium and cardiac rhythms: physiological and pathophysiological." Circ Res 90(1): 14-17.
Bers, D. M. (2002). "Cardiac excitation-contraction coupling." Nature 415(6868): 198-205.
Bers, D. M. (2004). "Macromolecular complexes regulating cardiac ryanodine receptor function." Journal of Molecular and Cellular Cardiology 37: 417-429.
Bers, D. M. (2006). "Altered cardiac myocyte Ca regulation in heart failure." Physiology (Bethesda) 21: 380-387.
Bers, D. M. (2006). "Cardiac ryanodine receptor phosphorylation: target sites and functional consequences." Biochem J 396(1): e1-3.
Bers, D. M., D. A. Eisner, et al. (2003). "Sarcoplasmic reticulum Ca^{2+} and heart failure: Roles of diastolic leak and Ca^{2+} transport." Circ Res 93(6): 487-490.
Bers, D. M., D. A. Eisner, et al. (2003). "Sarcoplasmic reticulum Ca^{2+} and heart failure: roles of diastolic leak and Ca^{2+} transport." Circ. Res. 93(6): 487-490.
Bers, D. M. and T. Guo (2005). "Calcium signaling in cardiac ventricular myocytes." Ann N Y Acad Sci 1047: 86-98.
Bers, D. M. and V. M. Stiffel (1993). "Ratio of ryanodine to dihydropyridine receptors in cardiac and skeletal muscle and implications for E-C coupling." Am J Physiol 264(6 Pt 1): C1587-1593.
Bhogal, M. S. and J. Colyer (1998). "Depletion of Ca2+ from the sarcoplasmic reticulum of cardiac muscle prompts phosphorylation of phospholamban to stimulate store refilling." Proc Natl Acad Sci U S A 95(4): 1484-1489.
Bialer, M. G., N. L. McDaniel, et al. (1991). "Progression of cardiac disease in Emery-Dreifuss muscular dystrophy." Clin Cardiol 14(5): 411-416.
Black, D. J., S. B. Tikunova, et al. (2000). "Acid pairs increase the N-terminal Ca2+ affinity of CaM by increasing the rate of Ca2+ association." Biochemistry 39(45): 13831-13837.
Braunwald, E. and C. A. Chidsey (1965). "The adrenergic nervous system in the control of the normal and failing heart." Proc R Soc Med 58(12): 1063-1066.
Bright-Thomas, R. J. and A. K. Webb (2002). "The heart in cystic fibrosis." J R Soc Med 95 Suppl 41: 2-10.
Brilliantes, A.-M. B., K. Ondrias, et al. (1994). "Stabilization of calcium release channel (ryanodine receptor) function by FK506-binding protein." Cell 77: 513-523.
Bristow, M. R., R. Ginsburg, et al. (1982). "Decreased catecholamine sensitivity and beta-adrenergic-receptor density in failing human hearts." N Engl J Med 307(4): 205-211.
Brochet, D. X., D. Yang, et al. (2005). "Ca2+ blinks: rapid nanoscopic store calcium signaling." Proc Natl Acad Sci U S A 102(8): 3099-3104.
Brodde, O. E. (1991). "Beta 1- and beta 2-adrenoceptors in the human heart: properties, function, and alterations in chronic heart failure." Pharmacol Rev 43(2): 203-242.
Brodde, O. E. and K. Leineweber (2004). "Autonomic receptor systems in the failing and aging human heart: similarities and differences." Eur J Pharmacol 500(1-3): 167-176.
Brodde, O. E. and M. C. Michel (1999). "Adrenergic and muscarinic receptors in the human heart." Pharmacol Rev 51(4): 651-690.
Bronstein, J. M., D. B. Farber, et al. (1993). "Regulation of type-II calmodulin kinase: functional implications." Brain Res Brain Res Rev 18(1): 135-147.
Brooks, S. P. and K. B. Storey (1992). "Bound and determined: a computer program for making buffers of defined ion concentrations." Anal Biochem 201(1): 119-126.
Brown, H., R. Kozlowski, et al. (1997). Physiology and pharmacology of the heart. Oxford [England] ; Malden, MA, USA, Blackwell Science.
Brown, S. C., R. J. Piercy, et al. (2008). "Investigating the pathology of Emery-Dreifuss muscular dystrophy." Biochem Soc Trans 36(Pt 6): 1335-1338.

Burghuber, O. C., U. Salzer-Muhar, et al. (1988). "Right ventricular performance and pulmonary haemodynamics in adolescent and adult patients with cystic fibrosis." Eur J Pediatr 148(3): 187-192.

Camus, P., A. Fanton, et al. (2004). "Interstitial lung disease induced by drugs and radiation." Respiration 71(4): 301-326.

Cannell, B. L., C. H. T. Kong, et al. (2013). "Control of sarcoplasmic reticulum Ca^{2+} release by stochastic RyR gating within a 3D model of the cardiac dyad and importance of induction decay for CICR termination." Biophys J 104: 2149-2159.

Cannell, M. B., C. H. Kong, et al. (2013). "Control of sarcoplasmic reticulum Ca2+ release by stochastic RyR gating within a 3D model of the cardiac dyad and importance of induction decay for CICR termination." Biophys J 104(10): 2149-2159.

Caron, M. G. and R. J. Lefkowitz (1993). "Catecholamine receptors: structure, function, and regulation." Recent Prog Horm Res 48: 277-290.

Carter, S., J. Colyer, et al. (2006). "Maximum phosphorylation of the cardiac ryanodine receptor at serine-2809 by protein kinase a produces unique modifications to channel gating and conductance not observed at lower levels of phosphorylation." Circ Res 98(12): 1506-1513.

Chakraborti, S., T. Chakraborti, et al. (2002). "Protective role of magnesium in cardiovascular diseases: a review." Mol Cell Biochem 238(1-2): 163-179.

Chakraborti, S., T. Chakraborti, et al. (2002). "Protective role of magnessium in cardiovascular diseases: A review." Molecular and Cellular Biochemistry 238: 163-179.

Chandler, N., O. Aslanidi, et al. (2011). "Computer three-dimensional anatomical reconstruction of the human sinus node and a novel paranodal area." Anat Rec (Hoboken) 294(6): 970-979.

Chen, X., V. Piacentino, 3rd, et al. (2002). "L-type Ca2+ channel density and regulation are altered in failing human ventricular myocytes and recover after support with mechanical assist devices." Circ Res 91(6): 517-524.

Cheng, H., M. Fill, et al. (1995). "Models of Ca2+ release channel adaptation." Science 267: 2009-2010.

Cheng, H., M. R. Lederer, et al. (1996). "Calcium sparks and $[Ca^{2+}]_i$ waves in cardiac myocytes." Am. J. Physiol. 270(1 Pt 1): C148-159.

Cheng, H., M. R. Lederer, et al. (1996). "Calcium sparks and $[Ca^{2+}]_i$ waves in cardiac myocytes." Am J Physiol 270(1 Pt 1): C148-C159.

Cheng, H. and W. J. Lederer (2008). "Calcium sparks." Physiol Rev 88(4): 1491-1545.

Cheng, H., W. J. Lederer, et al. (1993). "Calcium sparks: elementary events underlying excitation-contraction coupling in heart muscle." Science 262(5134): 740-744.

Cheng, Y., I. George, et al. (2007). "Bradycardic therapy improves left ventricular function and remodeling in dogs with coronary embolization-induced chronic heart failure." J Pharmacol Exp Ther 321(2): 469-476.

Ching, L. L., A. J. Williams, et al. (2000). "Evidence for Ca^{2+} activation and inactivation sites on the luminal side of the cardiac ryanodine receptor complex." Circ. Res. 87(3): 201-206.

Chopra, N., T. Yang, et al. (2009). "Ablation of triadin causes loss of cardiac Ca2+ release units, impaired excitation-contraction coupling, and cardiac arrhythmias." Proceedings of the National Academy of Sciences of the United States of America 106(18): 7636-7641.

Choudhary, G. and S. C. Dudley, Jr. (2002). "Heart failure, oxidative stress, and ion channel modulation." Congest Heart Fail 8(3): 148-155.

Cohen, F. S. and W. D. Niles (1993). "Reconstituting channels into planar membranes: a conceptual framework and methods for fusing vesicles to planar bilayer phospholipid membranes." Methods Enzymol. 220: 50-68.

Cohn, J. N., T. B. Levine, et al. (1984). "Plasma norepinephrine as a guide to prognosis in patients with chronic congestive heart failure." N Engl J Med 311(13): 819-823.

Copello, J. A., S. Barg, et al. (1997). "Heterogeneity of Ca^{2+} gating of skeletal muscle and cardiac ryanodine receptors." Biophys. J. 73(1): 141-156.

Coronado, R., S. Kawano, et al. (1992). "Planar bilayer recording of ryanodine receptors of sarcoplasmic reticulum." Methods Enzymol. 207: 699-707.

Crossman, D. J., P. N. Ruygrok, et al. (2011). "Changes in the organization of excitation-contraction coupling structures in failing human heart." PLoS One 6(3): e17901.

Crossman, D. J., P. R. Ruygrok, et al. (2010). "Changes in the organization of excitation-contraction coupling structures in failing human heart." PLoS One 6(3): e17901.

Crotti, L., C. N. Johnson, et al. (2013). "Calmodulin mutations associated with recurrent cardiac arrest in infants." Circulation 127(9): 1009-1017.

Curran, J., M. J. Hinton, et al. (2007). "Beta-adrenergic enhancement of sarcoplasmic reticulum calcium leak in cardiac myocytes is mediated by calcium/calmodulin-dependent protein kinase." Circ. Res. 100(3): 391-398.

Currie, S., C. M. Loughrey, et al. (2004). "Calcium/calmodulin-dependent protein kinase IIdelta associates with the ryanodine receptor complex and regulates channel function in rabbit heart." Biochem J 377(Pt 2): 357-366.

Dash, R., K. F. Frank, et al. (2001). "Gender influences on sarcoplasmic reticulum Ca2+-handling in failing human myocardium." J Mol Cell Cardiol 33(7): 1345-1353.

DiFrancesco, D. (1993). "Pacemaker mechanisms in cardiac tissue." Annu Rev Physiol 55: 455-472.

Donoso, P., P. Aracena, et al. (2000). "Sulfhydryl oxidation overrides Mg(2+) inhibition of calcium-induced calcium release in skeletal muscle triads." Biophys J 79(1): 279-286.

Dulhunty, A. F., N. A. Beard, et al. (2007). "Agonists and antagonists of the cardiac ryanodine receptor: potential therapeutic agents?" Pharmacol. Ther. 113(2): 247-263.

Edman, C. F. and H. Schulman (1994). "Identification and characterization of delta B-CaM kinase and delta C-CaM kinase from rat heart, two new multifunctional Ca2+/calmodulin-dependent protein kinase isoforms." Biochim Biophys Acta 1221(1): 89-101.

Eisner, D. A., H. S. Choi, et al. (2000). "Integrative Analysis of Calcium Cycling in Cardiac Muscle." Circ Res 87(12): 1087-1094.

El-Armouche, A., O. Zolk, et al. (2003). "Inhibitory G-proteins and their role in desensitization of the adenylyl cyclase pathway in heart failure." Cardiovasc Res 60(3): 478-487.

Eschenhagen, T. (2010). "Is ryanodine receptor phosphorylation key to the fight or flight response and heart failure?" J Clin Invest 120(12): 4197-4203.

Feng, W., G. Liu, et al. (2000). "Transmembrane redox sensor of ryanodine receptor complex." J. Biol. Chem. 275: 35902-35907.

Florea, V. G., N. D. Florea, et al. (2000). "Right ventricular dysfunction in adult severe cystic fibrosis." Chest 118(4): 1063-1068.

Franzini-Armstrong, C. and A. O. Jorgensen (1994). "Structure and development of E-C coupling units in skeletal muscle." Annu Rev Physiol 56: 509-534.

Franzini-Armstrong, C. and F. Protasi (1997). "Ryanodine receptors of striated muscles: a complex channel capable of multiple interactions." Physiol. Rev. 77(3): 699-729.

Franzini-Armstrong, C., F. Protasi, et al. (1999). "Shape, size, and distribution of Ca^{2+} release units and couplons in skeletal and cardiac muscles." Biophys J 77(3): 1528-1539.

Frick, K. D., L. Hariharan, et al. "Cost-effectiveness of 2 approaches to managing nasolacrimal duct obstruction in infants: the importance of the spontaneous resolution rate." Arch Ophthalmol 129(5): 603-609.

Galfre, E., S. J. Pitt, et al. (2012). "FKBP12 activates the cardiac ryanodine receptor Ca2+-release channel and is antagonised by FKBP12.6." PLoS One 7(2): e31956.

Gao, Z., M. V. Singh, et al. (2011). "Catecholamine-independent heart rate increases require Ca2+/calmodulin-dependent protein kinase II." Circ Arrhythm Electrophysiol 4(3): 379-387.

Gehrmann, J. and C. I. Berul (2000). "Cardiac electrophysiology in genetically engineered mice." J Cardiovasc Electrophysiol 11(3): 354-368.

George, C. H. (2008). "Sarcoplasmic reticulum Ca^{2+} leak in heart failure: mere observation or functional relevance?" Cardiovasc. Res. 77(2): 302-314.

George, C. H. and F. A. Lai (2007). "Developing new anti-arrhythmics: clues from the molecular basis of cardiac ryanodine receptor (RyR2) Ca2+-release channel dysfunction." Curr Pharm Des 13(31): 3195-3211.

Ginsburg, K. S., C. R. Weber, et al. (1998). "Control of maximum sarcoplasmic reticulum Ca load in intact ferret ventricular myocytes. Effects Of thapsigargin and isoproterenol." J Gen Physiol 111(4): 491-504.

Go, L. O., M. C. Moschella, et al. (1995). "Differential regulation of two types of intracellular calcium release channels during end-stage heart failure." J Clin Invest 95(2): 888-894.

Gong, H., H. Sun, et al. (2002). "Specific beta(2)AR blocker ICI 118,551 actively decreases contraction through a G(i)-coupled form of the beta(2)AR in myocytes from failing human heart." Circulation 105(21): 2497-2503.

Greener, I. D., O. Monfredi, et al. (2011). "Molecular architecture of the human specialised atrioventricular conduction axis." J Mol Cell Cardiol 50(4): 642-651.

Guo, T., R. L. Cornea, et al. (2010). "Kinetics of FKBP12.6 binding to ryanodine receptors in permeabilized cardiac myocytes and effects on Ca sparks." Circ Res 106(11): 1743-1752.

Guo, T., B. R. Fruen, et al. (2011). "FRET detection of calmodulin binding to the cardiac RyR2 calcium release channel." Biophys J 101(9): 2170-2177.

Guo, T., D. Gillespie, et al. (2012). "Ryanodine receptor current amplitude controls Ca2+ sparks in cardiac muscle." Circ Res 111(1): 28-36.

Guo, T., T. Zhang, et al. (2006). "Ca2+/Calmodulin-dependent protein kinase II phosphorylation of ryanodine receptor does affect calcium sparks in mouse ventricular myocytes." Circ Res 99(4): 398-406.

Guo, X., D. Chapman, et al. (2003). "Partial prevention of changes in SR gene expression in congestive heart failure due to myocardial infarction by enalapril or losartan." Mol. Cell Biochem. 254(1-2): 163-172.

Gyorke, I. and S. Gyorke (1998). "Regulation of the cardiac ryanodine receptor channel by luminal Ca^{2+} involves luminal Ca^{2+} sensing sites." Biophys. J. 75(6): 2801-2810.

Gyorke, I., N. Hester, et al. (2004). "The role of calsequestrin, triadin, and junctin in conferring cardiac ryanodine receptor responsiveness to luminal calcium." Biophys. J. 86(4): 2121-2128.

Gyorke, S. and C. Carnes (2008). "Dysregulated sarcoplasmic reticulum calcium release: potential pharmacological target in cardiac disease." Pharmacol Ther 119(3): 340-354.

Gyorke, S., I. Gyorke, et al. (2002). "Regulation of sarcoplasmic reticulum calcium release by luminal calcium in cardiac muscle." Front Biosci 7: d1454-d1463.

Gyorke, S. and D. Terentyev (2008). "Modulation of ryanodine receptor by luminal calcium and accessory proteins in health and cardiac disease." Cardiovasc Res 77(2): 245-255.

Hagemann, D., J. Bohlender, et al. (2001). "Expression of Ca2+/calmodulin-dependent protein kinase II delta-subunit isoforms in rats with hypertensive cardiac hypertrophy." Mol Cell Biochem 220(1-2): 69-76.

Haigney, M. C., S. Wei, et al. (1998). "Loss of cardiac magnesium in experimental heart failure prolongs and destabilizes repolarization in dogs." J. Am. Coll. Cardiol. 31(3): 701-706.

Hain, J., H. Onoue, et al. (1995). "Phosphorylation modulates the function of the calcium release channel of sarcoplasmic reticulum from cardiac muscle." J Biol Chem 270(5): 2074-2081.

Hakamata, Y., J. Nakai, et al. (1992). "Primary structure and distribution of a novel ryanodine receptor/calcium release channel from rabbit brain." FEBS Lett 312(2-3): 229-235.

Harrison, S. M. and D. M. Bers (1987). "The effect of temperature and ionic strength on the apparent Ca- affinity of EGTA and the analogous Ca-chelators BAPTA and dibromo-BAPTA." Biochim. Biophys. Acta 925: 133-143.

Hartzell, H. C. (1988). "Regulation of cardiac ion channels by catecholamines, acetylcholine and second messenger systems." Prog Biophys Mol Biol 52(3): 165-247.

Hasenfuss, G., L. A. Mulieri, et al. (1991). "Energetics of isometric force development in control and volume-overload human myocardium. Comparison with animal species." Circ Res 68(3): 836-846.

Hino, A., M. Yano, et al. (2012). "Enhanced binding of calmodulin to the ryanodine receptor corrects contractile dysfunction in failing hearts." Cardiovascular research 96(3): 433-443.

Hobai, I. A. and B. O'Rourke (2001). "Decreased sarcoplasmic reticulum calcium content is responsible for defective excitation-contraction coupling in canine heart failure." Circulation 103(11): 1577-1584.

Hoch, B., R. Meyer, et al. (1999). "Identification and expression of delta-isoforms of the multifunctional Ca2+/calmodulin-dependent protein kinase in failing and nonfailing human myocardium." Circ Res 84(6): 713-721.

Holmberg, S. R. and A. J. Williams (1992). "The calcium-release channel from cardiac sarcoplasmic reticulum: function in the failing and acutely ischaemic heart." Basic Res Cardiol 87 Suppl 1: 255-268.

Hori, M., S. Sasayama, et al. (2004). "Low-dose carvedilol improves left ventricular function and reduces cardiovascular hospitalization in Japanese patients with chronic heart failure: the Multicenter Carvedilol Heart Failure Dose Assessment (MUCHA) trial." Am Heart J 147(2): 324-330.

Houser, S. R. (2010). "Does protein kinase a-mediated phosphorylation of the cardiac ryanodine receptor play any role in adrenergic regulation of calcium handling in health and disease?" Circ Res 106(11): 1672-1674.

Hu, S. T., Y. F. Shen, et al. "Altered intracellular Ca2+ regulation in chronic rat heart failure." J Physiol Sci 60(2): 85-94.

Hu, S. T., Y. F. Shen, et al. (2010). "Altered intracellular Ca2+ regulation in chronic rat heart failure." J Physiol Sci 60(2): 85-94.

Huang, X., Y. Liu, et al. (2013). "Two potential calmodulin-binding sequences in the ryanodine receptor contribute to a mobile, intra-subunit calmodulin-binding domain." J Cell Sci 126(Pt 19): 4527-4535.

Huertas, M. A. and G. D. Smith (2007). "The dynamics of luminal depletion and the stochastic gating of Ca2+-activated Ca2+ channels and release sites." J Theor Biol 246(2): 332-354.

Hwang, C., A. J. Sinskey, et al. (1992). "Oxidized redox state of glutathione in the endoplasmic reticulum." Science 257(5076): 1496-1502.

Hwang, H. S., F. R. Nitu, et al. (2014). "Divergent regulation of ryanodine receptor 2 calcium release channels by arrhythmogenic human calmodulin missense mutants." Circ Res 114(7): 1114-1124.

Hwang, H. S., F. R. Nitu, et al. (2014). "Divergent Regulation of RyR2 Calcium Release Channels by Arrhythmogenic Human Calmodulin Missense Mutants." Circ Res.

Hymel, L., M. Inui, et al. (1988). "Purified ryanodine receptor of skeletal muscle sarcoplasmic reticulum forms Ca^{2+}-activated oligomeric Ca^{2+} channels in planar bilayers." Proc Natl Acad Sci USA 85: 441-445.

Ide, T., H. Tsutsui, et al. (1999). "Mitochondrial electron transport complex I is a potential source of oxygen free radicals in the failing myocardium." Circ Res 85(4): 357-363.

Ikemoto, N. and T. Yamamoto (2002). "Regulation of calcium release by interdomain interaction within ryanodine receptors." Front. Biosci. 7: d671-683.

Jacobstein, M. D., S. S. Hirschfeld, et al. (1981). "Ventricular interdependence in severe cystic fibrosis. A two-dimensional echocardiographic study." Chest 80(4): 399-404.

Jayaraman, T., A. M. Brillantes, et al. (1992). "FK506 binding protein associated with the calcium release channel (ryanodine receptor)." J. Biol. Chem. 267: 9474-9477.

Jiang, M. T., A. J. Lokuta, et al. (2002). "Abnormal Ca2+ release, but normal ryanodine receptors, in canine and human heart failure." Circ Res 91(11): 1015-1022.

Johnson, G. L., J. F. Kanga, et al. (1991). "Changes in left ventricular diastolic filling patterns by Doppler echocardiography in cystic fibrosis." Chest 99(3): 646-650.

Jones, J. L., D. F. Reynolds, et al. (2005). "Ryanodine receptor binding to FKBP12 is modulated by channel activation state." J Cell Sci 118(Pt 20): 4613-4619.

Jorgensen, A. O. and K. P. Campbell (1984). "Evidence for the presence of calsequestrin in two structurally different regions of myocardial sarcoplasmic reticulum." kkk 98: 1597-1602.

Kaftan, E., A. R. Marks, et al. (1996). "Effects of rapamycin on ryanodine receptor/Ca(2+)-release channels from cardiac muscle." Circ. Res. 78: 990-997.

Kaumann, A., S. Bartel, et al. (1999). "Activation of $beta_2$-adrenergic receptors hastens relaxation and mediates phosphorylation of phospholamban, troponin I, and C-protein in ventricular myocardium from patients with terminal heart failure." Circulation 99(1): 65-72.

Kaumann, A. J., L. Sanders, et al. (1996). "Beta 2-adrenoceptor activation by zinterol causes protein phosphorylation, contractile effects and relaxant effects through a cAMP pathway in human atrium." Mol Cell Biochem 163-164: 113-123.

Kermode, H., A. J. Williams, et al. (1998). "The interactions of ATP, ADP, and inorganic phosphate with the sheep cardiac ryanodine receptor." Biophys. J. 74(3): 1296-1304.

Kilts, J. D., M. A. Gerhardt, et al. (2000). "Beta(2)-adrenergic and several other G protein-coupled receptors in human atrial membranes activate both G(s) and G(i)." Circ Res 87(8): 705-709.

Kinugawa, T., K. Ogino, et al. (1996). "Catecholamines, renin-angiotensin-aldosterone system, and atrial natriuretic peptide at rest and during submaximal exercise in patients with congestive heart failure." Am J Med Sci 312(3): 110-117.

Knollmann, B. C. (2009). "New roles of calsequestrin and triadin in cardiac muscle." J Physiol 587(Pt 13): 3081-3087.

Knollmann, B. C., N. Chopra, et al. (2006). "Casq2 deletion causes sarcoplasmic reticulum volume increase, premature Ca2+ release, and catecholaminergic polymorphic ventricular tachycardia." J Clin Invest 116(9): 2510-2520.

Kobayashi, S., M. Yano, et al. (2009). "Dantrolene, a therapeutic agent for malignant hyperthermia, markedly improves the function of failing cardiomyocytes by

stabilizing interdomain interactions within the ryanodine receptor." J. Am. Coll. Cardiol. 53(21): 1993-2005.

Kobayashi, Y. M., B. A. Alseikhan, et al. (2000). "Localization and characterization of the calsequestrin-binding domain of triadin 1. Evidence for a charged beta-strand in mediating the protein-protein interaction." J. Biol. Chem. 275(23): 17639-17646.

Kobayashi, Y. M. and L. R. Jones (1999). "Identification of triadin 1 as the predominant triadin isoform expressed in mammalian myocardium." J Biol Chem 274(40): 28660-28668.

Koss, K. L. and E. G. Kranias (1996). "Phospholamban: a prominent regulator of myocardial contractility." Circ Res 79(6): 1059-1063.

Krause, S. M. (1991). "Effect of increased free $[Mg^{2+}]_i$ with myocardial stunning on sarcoplasmic reticulum Ca^{2+}-ATPase activity." Am. J. Physiol. 261(1 Pt 2): H229-235.

Kubalova, Z., D. Terentyev, et al. (2005). "Abnormal intrastore calcium signaling in chronic heart failure." Proc Natl Acad Sci U S A 102(39): 14104-14109.

Kushnir, A., M. J. Betzenhauser, et al. "Ryanodine receptor studies using genetically engineered mice." FEBS Lett 584(10): 1956-1965.

Kuzumoto, M., A. Takeuchi, et al. (2008). "Simulation analysis of intracellular Na+ and Cl- homeostasis during beta 1-adrenergic stimulation of cardiac myocyte." Prog Biophys Mol Biol 96(1-3): 171-186.

Laemmli, U. K. (1970). "Cleavage of structural proteins during the assembly of the head of bacteriophage T4." Nature 227(5259): 680-685.

Laver, D. (2001). "The power of single channel recording and analysis: its application to ryanodine receptors in lipid bilayers." Clin. Exp. Pharmacol. Physiol. 28(8): 675-686.

Laver, D. (2009). "Electrical Methods for Determining Surface Charge Density and Electrolyte Composition at the Lipid Bilayer-Solution Interface." Advances in Planar Lipid Bilayers and Liposomes 9: 87-105.

Laver, D. (2010). Regulation of the RyR channel gating by different modulators. In Structure-function of calcium release channels Current Topics in Membranes. I. Serysheva, Elsevier. 66: 69-89.

Laver, D. R. (2005). "Coupled calcium release channels and their regulation by luminal and cytosolic ions." Eur Biophys J 34(5): 359-368.

Laver, D. R. (2007). "Ca^{2+} stores regulate ryanodine receptor Ca^{2+} release channels via luminal and cytosolic Ca^{2+} sites." Biophys J 92(10): 3541-3555.

Laver, D. R. (2007). "Ca^{2+} Stores Regulate Ryanodine Receptor Ca^{2+} Release Channels via Luminal and Cytosolic Ca^{2+} Sites." Biophys. J. 92(10): 3541-3555.

Laver, D. R. (2007). "Ca^{2+} stores regulate ryanodine receptor Ca^{2+} release channels via luminal and cytosolic Ca^{2+} sites." Clinical and Experimental Pharmacology and Physiology 34: 889-896.

Laver, D. R. (2009). "Luminal Ca^{2+} activation of cardiac ryanodine receptors by luminal and cytoplasmic domains." Eur. Biophys. J. 39: 19-26.

Laver, D. R., T. M. Baynes, et al. (1997). "Magnesium inhibition of ryanodine-receptor calcium channels: Evidence for two independent mechanisms." J Memb Biol 156: 213-229.

Laver, D. R., T. M. Baynes, et al. (1997). "Magnesium inhibition of ryanodine-receptor calcium channels: evidence for two independent mechanisms." J. Memb. Biol. 156: 213-229.

Laver, D. R. and B. N. Honen (2008). "Luminal Mg^{2+}, a key factor controlling RYR2-mediated Ca^{2+} release: Cytoplasmic and luminal regulation modeled in a tetrameric channel." J Gen Physiol 132(4): 429-446.

Laver, D. R. and B. N. Honen (2008). "Luminal Mg^{2+}, A Key Factor Controlling RYR2-mediated Ca^{2+} Release: Cytoplasmic and Luminal Regulation Modeled in a Tetrameric Channel." J. Gen. Physiol. 132(4): 429-446.

Laver, D. R., C. H. T. Kong, et al. (2013). "Termination of calcium-induced calcium release by induction decay: An emergent property of stochastic channel gating and molecular scale architecture." Journal of Molecular and Cellular Cardiology 54: 98-100.

Laver, D. R., C. H. T. Kong, et al. (2013). "Termination of calcium-induced calcium release by induction decay: An emergent property of stochastic channel gating and molecular scale architecture." J Molec Cell Cardiol 54: 98-100.

Laver, D. R. and G. D. Lamb (1998). "Inactivation of Ca^{2+} release channels (ryanodine receptors RyR1 and RyR2) with rapid steps in [Ca^{2+}] and voltage." Biophys. J. 74(5): 2352-2364.

Laver, D. R., E. R. O'Neill, et al. (2004). "Luminal Ca^{2+}-regulated Mg^{2+} inhibition of skeletal RyRs reconstituted as isolated channels or coupled clusters." J Gen Physiol 124(6): 741-758.

Laver, D. R., V. J. Owen, et al. (1997). "Reduced inhibitory effect of Mg^{2+} on ryanodine receptor-Ca^{2+} release channels in malignant hyperthermia." Biophys J 73: 1913-1924.

Laver, D. R., L. D. Roden, et al. (1995). "Cytoplasmic Ca^{2+} inhibits the ryanodine receptor from cardiac muscle." J. Memb. Biol. 147(1): 7-22.

Laver, D. R., L. D. Roden, et al. (1995). "Cytoplasmic Ca^{2+} inhibits the ryanodine receptor from cardiac muscle." J Memb Biol 147(1): 7-22.

Laver, D. R. and D. F. van Helden (2011). "Three independent mechanisms contribute to tetracaine inhibition of cardiac calcium release channels." J Mol Cell Cardiol 51(3): 357-369.

Lehnart, S. E., L. S. Maier, et al. (2009). "Abnormalities of calcium metabolism and myocardial contractility depression in the failing heart." Heart Fail Rev 14(4): 213-224.

Lehnart, S. E., X. H. Wehrens, et al. (2004). "Sudden death in familial polymorphic ventricular tachycardia associated with calcium release channel (ryanodine receptor) leak." Circulation 109(25): 3208-3214.

Lehnart, S. E., X. H. Wehrens, et al. (2005). "Defective ryanodine receptor interdomain interactions may contribute to intracellular Ca2+ leak: a novel therapeutic target in heart failure." Circulation 111(25): 3342-3346.

Lehnart, S. E., X. H. Wehrens, et al. (2005). "Phosphodiesterase 4D deficiency in the ryanodine-receptor complex promotes heart failure and arrhythmias." Cell 123(1): 25-35.

Li, J., M. S. Imtiaz, et al. (2013). "Beta-qdrenergic stimulation increases RyR2 activity via intracellular Ca^{2+} and Mg^{2+} regulation." PLoS One 8(3): e58334.

Li, J., M. S. Imtiaz, et al. (2013). "ss-Adrenergic stimulation increases RyR2 activity via intracellular Ca2+ and Mg2+ regulation." PLoS One 8(3): e58334.

Lindner, M., E. Erdmann, et al. (1998). "Calcium content of the sarcoplasmic reticulum in isolated ventricular myocytes from patients with terminal heart failure." J Mol Cell Cardiol 30(4): 743-749.

Ling, H., T. Zhang, et al. (2009). "Requirement for Ca2+/calmodulin-dependent kinase II in the transition from pressure overload-induced cardiac hypertrophy to heart failure in mice." J Clin Invest 119(5): 1230-1240.

Liu, Y., M. Porta, et al. (2010). "Flux regulation of cardiac ryanodine receptor channels." J Gen Physiol 135(1): 15-27.

Lohse, M. J., S. Engelhardt, et al. (2003). "What is the role of beta-adrenergic signaling in heart failure?" Circ Res 93(10): 896-906.

Lokuta, A. J., T. B. Rogers, et al. (1995). "Modulation of cardiac ryanodine receptors of swine and rabbit by a phosphorylation-dephosphorylation mechanism." J. Physiol. (Lond.) 487: 609-622.

Lompre, A. M., J. J. Mercadier, et al. (1981). "Species- and age-dependent changes in the relative amounts of cardiac myosin isoenzymes in mammals." Dev Biol 84(2): 286-290.

Ma, J., M. B. Bhat, et al. (1995). "Rectification of skeletal muscle ryanodine receptor mediated by FK506 binding protein." Biophys. J. 69: 2398-2404.

MacQuaide, N., J. Dempster, et al. (2007). "Measurement and modeling of Ca2+ waves in isolated rabbit ventricular cardiomyocytes." Biophys J 93(7): 2581-2595.

Maier, L. S., T. Zhang, et al. (2003). "Transgenic CaMKIIdeltaC overexpression uniquely alters cardiac myocyte Ca2+ handling: reduced SR Ca2+ load and activated SR Ca2+ release." Circ Res 92(8): 904-911.

Maier, L. S., M. T. Ziolo, et al. (2006). "Dynamic changes in free Ca-calmodulin levels in adult cardiac myocytes." J Mol Cell Cardiol 41(3): 451-458.

Marín-García, J. (2010). "Heart Failure." Springer Science+Business Media DOI 10.1007/978-1-60761-147-9_6, .

Marinov, B. S., R. O. Olojo, et al. (2007). "Non-thiol reagents regulate ryanodine receptor function by redox interactions that modify reactive thiols." Antioxid Redox Signal 9(5): 609-621.

Marks, A. R. (1997). "Intracellular calcium-release channels: regulators of cell life and death." Am J Physiol 272(2 Pt 2): H597-605.

Marks, A. R. (2001). "Ryanodine receptors/calcium release channels in heart failure and sudden cardiac death." J. Mol. Cell. Cardiol. 33(4): 615-624.

Marks, A. R. (2003). "A guide for the perplexed: towards an understanding of the molecular basis of heart failure." Circulation 107(11): 1456-1459.

Marks, A. R., S. O. Marx, et al. (2002). "Regulation of ryanodine receptors via macromolecular complexes: a novel role for leucine/isoleucine zippers." Trends in Cardiovascular Medicine 12(4): 166-170.

Marks, A. R., P. Tempst, et al. (1989). "Molecular cloning and characterization of the ryanodine receptor/junctional channel complex cDNA from skeletal muscle sarcoplasmic reticulum." Proc Natl Acad Sci U S A 86(22): 8683-8687.

Marks, P. W. and F. R. Maxfield (1991). "Preparation of solutions with free calcium concentration in the nanomolar range using 1,2-bis(o-aminophenoxy)ethane-N,N,N',N'-tetraacetic acid." Anal. Biochem. 193(1): 61-71.

Maron, B. J., J. A. Towbin, et al. (2006). "Contemporary definitions and classification of the cardiomyopathies: an American Heart Association Scientific Statement from the Council on Clinical Cardiology, Heart Failure and Transplantation Committee; Quality of Care and Outcomes Research and Functional Genomics and Translational Biology Interdisciplinary Working Groups; and Council on Epidemiology and Prevention." Circulation 113(14): 1807-1816.

Marx, S. O., J. Gaburjakova, et al. (2001). "Coupled gating between cardiac calcium release channels (ryanodine receptors)." Circ. Res. 88(11): 1151-1158.

Marx, S. O., S. Reiken, et al. (2000). "PKA phosphorylation dissociates FKBP12.6 from the calcium release channel (ryanodine receptor): defective regulation in failing hearts." Cell 101(4): 365-376.

McGavin, J. K. and G. M. Keating (2002). "Bisoprolol: a review of its use in chronic heart failure." Drugs 62(18): 2677-2696.

McGrath, K. F., A. Yuki, et al. (2009). "Morphological characteristics of cardiac calcium release units in animals with metabolic and circulatory disorders." J Muscle Res Cell Motil 30(5-6): 225-231.

Meissner, G. (1986). "Ryanodine activation and inhibition of the Ca2+ release channel of sarcoplasmic reticulum." J. Biol. Chem. 261(14): 6300-6306.

Meissner, G. (1986). "Ryanodine activation and inhibition of the Ca^{2+} release channel of sarcoplasmic reticulum." J Biol Chem 261(14): 6300-6306.

Meissner, G. (1994). "Ryanodine receptor/Ca^{2+} release channels and their regulation by endogenous effectors." Annual Reviews in Physiology 56: 485-508.

Meissner, G. (1994). "Ryanodine receptor/Ca2+ release channels and their regulation by endogenous effectors." Annu Rev Physiol 56: 485-508.

Meissner, G. (2002). "Regulation of mammalian ryanodine receptors." Front Biosci 7: d2072-2080.

Meissner, G. and J. S. Henderson (1987). "Rapid calcium release from cardiac sarcoplasmic reticulum vesicles is dependent on Ca^{2+} and is modulated by Mg^{2+}, adenine nucleotide, and calmodulin." J. Biol. Chem. 262: 3065-3073.

Meissner, G., E. Rios, et al. (1997). "Regulation of skeletal muscle Ca2+ release channel (ryanodine receptor) by Ca2+ and monovalent cations and anions." J Biol Chem 272(3): 1628-1638.

Miller, C. and E. Racker (1976). "Ca^{++}-induced fusion of fragmented sarcoplasmic reticulum with artificial planar bilayers." Cell 9: 283-300.

Mitchell, R. D., H. K. Simmerman, et al. (1988). "Ca2+ binding effects on protein conformation and protein interactions of canine cardiac calsequestrin." J. Biol. Chem. 263(3): 1376-1381.

Mochizuki, M., M. Yano, et al. (2007). "Scavenging free radicals by low-dose carvedilol prevents redox-dependent Ca2+ leak via stabilization of ryanodine receptor in heart failure." J Am Coll Cardiol 49(16): 1722-1732.

Mohler, P. J. and X. H. Wehrens (2007). "Mechanisms of human arrhythmia syndromes: abnormal cardiac macromolecular interactions." Physiology (Bethesda) 22: 342-350.

Molenaar, P., S. Bartel, et al. (2000). "Both $beta_2$- and $beta_1$-adrenergic receptors mediate hastened relaxation and phosphorylation of phospholamban and troponin I in ventricular myocardium of Fallot infants, consistent with selective coupling of $beta_2$-adrenergic receptors to G_s-protein." Circulation 102(15): 1814-1821.

Molenaar, P., S. M. Savarimuthu, et al. (2007). "(-)-Adrenaline elicits positive inotropic, lusitropic, and biochemical effects through $beta_2$ -adrenoceptors in human atrial myocardium from nonfailing and failing hearts, consistent with G_s coupling but not with G_i coupling." Naunyn Schmiedebergs Arch. Pharmacol. 375(1): 11-28.

Molenaar, P., S. M. Savarimuthu, et al. (2007). "(-)-Adrenaline elicits positive inotropic, lusitropic, and biochemical effects through beta2 -adrenoceptors in human atrial myocardium from nonfailing and failing hearts, consistent with Gs coupling but not with Gi coupling." Naunyn Schmiedebergs Arch Pharmacol 375(1): 11-28.

Mozaffarian, D., S. D. Anker, et al. (2007). "Prediction of mode of death in heart failure: the Seattle Heart Failure Model." Circulation 116(4): 392-398.

Nakai, J., T. Imagawa, et al. (1990). "Primary structure and functional expression from cDNA of the cardiac ryanodine receptor/calcium release channel." FEBS Lett 271(1-2): 169-177.

Neuss, H. and M. Schlepper (1988). "Long-term efficacy and safety of flecainide for supraventricular tachycardia." Am J Cardiol 62(6): 56D-61D.

Nishi, M., H. Sakagami, et al. (2003). "Coexpression of junctophilin type 3 and type 4 in brain." Brain Res Mol Brain Res 118(1-2): 102-110.

Nyegaard, M., M. T. Overgaard, et al. (2012). "Mutations in calmodulin cause ventricular tachycardia and sudden cardiac death." Am J Hum Genet 91(4): 703-712.

Oda, T., M. Yano, et al. (2005). "Defective regulation of interdomain interactions within the ryanodine receptor plays a key role in the pathogenesis of heart failure." Circulation 111(25): 3400-3410.

Ono, M., M. Yano, et al. (2010). "Dissociation of calmodulin from cardiac ryanodine receptor causes aberrant Ca(2+) release in heart failure." Cardiovascular research 87(4): 609-617.

Packer, M., M. R. Bristow, et al. (1996). "The effect of carvedilol on morbidity and mortality in patients with chronic heart failure. U.S. Carvedilol Heart Failure Study Group." N Engl J Med 334(21): 1349-1355.

Packer, M., A. J. Coats, et al. (2001). "Effect of carvedilol on survival in severe chronic heart failure." N Engl J Med 344(22): 1651-1658.

Park, H., I. Y. Park, et al. (2004). "Comparing skeletal and cardiac calsequestrin structures and their calcium binding: a proposed mechanism for coupled calcium binding and protein polymerization." J Biol Chem 279(17): 18026-18033.

Park, Y. I., E. J. Kim, et al. (2005). "Interaction between Cardiac Calsequestrin and Drugs with Known Cardiotoxicity." Mol Pharmacol 67(1): 97-104.

Pathak, A., F. del Monte, et al. (2005). "Enhancement of cardiac function and suppression of heart failure progression by inhibition of protein phosphatase 1." Circ Res 96(7): 756-766.

Pedrozo, Z., G. Sanchez, et al. (2010). "Calpains and proteasomes mediate degradation of ryanodine receptors in a model of cardiac ischemic reperfusion." Biochimica et biophysica acta 1802(3): 356-362.

Perrin, F. M. and W. Serino (2010). "Ischaemic heart disease--a new issue in cystic fibrosis?" J R Soc Med 103 Suppl 1: S44-48.

Pesenti, S., D. Lauque, et al. (2002). "Diffuse infiltrative lung disease associated with flecainide. Report of two cases." Respiration 69(2): 182-185.

Piacentino, V., 3rd, C. R. Weber, et al. (2003). "Cellular basis of abnormal calcium transients of failing human ventricular myocytes." Circ Res 92(6): 651-658.

Pollock, J., S. M. McFarlane, et al. (2002). "TNF-alpha receptors simultaneously activate Ca2+ mobilisation and stress kinases in cultured sensory neurones." Neuropharmacology 42(1): 93-106.

Poole-Wilson, P. A., K. Swedberg, et al. (2003). "Comparison of carvedilol and metoprolol on clinical outcomes in patients with chronic heart failure in the Carvedilol Or Metoprolol European Trial (COMET): randomised controlled trial." Lancet 362(9377): 7-13.

Radermacher, M., V. Rao, et al. (1994). "Cryo-electron microscopy and three-dimensional reconstruction of the calcium release channel/ryanodine receptor from skeletal muscle." kkk 127: 411-423.

Reiken, S., M. Gaburjakova, et al. (2001). "beta-adrenergic receptor blockers restore cardiac calcium release channel (ryanodine receptor) structure and function in heart failure." Circulation 104(23): 2843-2848.

Reiken, S., M. Gaburjakova, et al. (2003). "Protein kinase A phosphorylation of the cardiac calcium release channel (ryanodine receptor) in normal and failing hearts. Role of phosphatases and response to isoproterenol." J Biol Chem 278(1): 444-453.

Reiken, S., A. Lacampagne, et al. (2003). "PKA phosphorylation activates the calcium release channel (ryanodine receptor) in skeletal muscle: defective regulation in heart failure." J Cell Biol 160(6): 919-928.

Reiken, S., X. H. Wehrens, et al. (2003). "Beta-blockers restore calcium release channel function and improve cardiac muscle performance in human heart failure." Circulation 107(19): 2459-2466.

Respress, J. L., R. J. van Oort, et al. (2012). "Role of RyR2 phosphorylation at S2814 during heart failure progression." Circ Res 110(11): 1474-1483.

Rockman, H. A., W. J. Koch, et al. (2002). "Seven-transmembrane-spanning receptors and heart function." Nature 415(6868): 206-212.

Rodriguez, P., M. S. Bhogal, et al. (2003). "Stoichiometric phosphorylation of cardiac ryanodine receptor on serine 2809 by calmodulin-dependent kinase II and protein kinase A." J. Biol. Chem. 278(40): 38593-38600.

Sag, C. M., D. P. Wadsack, et al. (2009). "Calcium/calmodulin-dependent protein kinase II contributes to cardiac arrhythmogenesis in heart failure." Circ Heart Fail 2(6): 664-675.

Sanders, L., S. Rakovic, et al. (2006). "Fundamental importance of Na+-Ca2+ exchange for the pacemaking mechanism in guinea-pig sino-atrial node." J Physiol 571(Pt 3): 639-649.

Schiefer, A., G. Meissner, et al. (1995). "Ca2+ activation and Ca2+ inactivation of canine reconstituted cardiac sarcoplasmic reticulum Ca(2+)-release channels." J Physiol 489 (Pt 2): 337-348.

Seipel, L., R. R. Abendroth, et al. (1981). "[Electrophysiological effects of the new antiarrhythmic drug flecainide (R 818) in man (author's transl)]." Z Kardiol 70(7): 524-529.

Sellers, Z. M., V. De Arcangelis, et al. (2010). "Cardiomyocytes with disrupted CFTR function require CaMKII and Ca(2+)-activated Cl(-) channel activity to maintain contraction rate." J Physiol 588(Pt 13): 2417-2429.

Sellers, Z. M., A. Kovacs, et al. (2013). "Left ventricular and aortic dysfunction in cystic fibrosis mice." J Cyst Fibros 12(5): 517-524.

Sellers, Z. M., A. P. Naren, et al. (2012). "MRP4 and CFTR in the regulation of cAMP and beta-adrenergic contraction in cardiac myocytes." Eur J Pharmacol 681(1-3): 80-87.

Sewell, T. J., E. Lam, et al. (1994). "Inhibition of calcineurin by a novel FK-506-binding protein." J Biol Chem 269(33): 21094-21102.

Shan, J., M. J. Betzenhauser, et al. (2010). "Role of chronic ryanodine receptor phosphorylation in heart failure and beta-adrenergic receptor blockade in mice." J Clin Invest 120(12): 4375-4387.

Shannon, T. R. and D. M. Bers (1997). "Assessment of intra-SR free [Ca] and buffering in rat heart." Biophys J 73(3): 1524-1531.

Shannon, T. R., K. S. Ginsburg, et al. (2000). "Potentiation of fractional sarcoplasmic reticulum calcium release by total and free intra-sarcoplasmic reticulum calcium concentration." Biophys. J. 78(1): 334-343.

Shannon, T. R., T. Guo, et al. (2003). "Ca2+ scraps: local depletions of free [Ca2+] in cardiac sarcoplasmic reticulum during contractions leave substantial Ca2+ reserve." Circ Res 93(1): 40-45.

Shannon, T. R. and W. Y. Lew (2009). "Diastolic release of calcium from the sarcoplasmic reticulum: a potential target for treating triggered arrhythmias and heart failure." J Am Coll Cardiol 53(21): 2006-2008.

Shannon, T. R., S. M. Pogwizd, et al. (2003). "Elevated sarcoplasmic reticulum Ca2+ leak in intact ventricular myocytes from rabbits in heart failure." Circ Res 93(7): 592-594.

Shen, J. X. (2006). "Isoprenaline enhances local Ca2+ release in cardiac myocytes." Acta Pharmacol Sin 27(7): 927-932.

Shin, J. and J. A. Johnson (2007). "Pharmacogenetics of beta-blockers." Pharmacotherapy 27(6): 874-887.

Sies, H. (1999). "Glutathione and its role in cellular functions." Free Radic Biol Med 27(9-10): 916-921.

Sigalas, C., S. Bent, et al. (2009). "Ca(2+)-calmodulin can activate and inactivate cardiac ryanodine receptors." Br J Pharmacol 156(5): 794-806.

Sigalas, C., M. B. Mayo-Martin, et al. (2009). "Ca2+-calmodulin increases RyR2 open probability yet reduces ryanoid association with RyR2." Biophys J 97(7): 1907-1916.

Sipido, K. R. (2007). "CaM or cAMP: linking beta-adrenergic stimulation to 'leaky' RyRs." Circ Res 100(3): 296-298.

Sitsapesan, R., R. A. P. Montgomery, et al. (1995). "New insights into the gating mechanisms of cardiac ryanodine receptors revealed by rapid changes in ligand concentration." Circ. Res. 77: 765-772.

Sitsapesan, R. and A. J. Williams (1994). "Gating of the native and purified cardiac SR Ca^{2+}-release channels with monovalent cations as permeant species." Biophys J 67: 1484-1494.

Sitsapesan, R. and A. J. Williams (1994). "Regulation of the gating of the sheep cardiac sarcoplasmic reticulum Ca^{2+}-release channel by luminal Ca^{2+}." J. Memb. Biol. 137(3): 215-226.

Sitsapesan, R. and A. J. Williams (1994). "Regulation of the gating of the sheep cardiac sarcoplasmic reticulum Ca^{2+}-release channel by luminal Ca^{2+}." J Memb Biol 137(3): 215-226.

Sitsapesan, R. and A. J. Williams (1994). "Regulation of the gating of the sheep cardiac sarcoplasmic reticulum Ca(2+)-release channel by luminal Ca2+." J. Memb. Biol. 137(3): 215-226.

Sitsapesan, R. and A. J. Williams (1995). "The gating of the sheep skeletal sarcoplasmic reticulum Ca^{2+}-release channel is regulated by luminal Ca^{2+}." J. Memb. Biol. 146: 133-144.

Sitsapesan, R. and A. J. Williams (1997). "Regulation of current flow through ryanodine receptors by luminal Ca^{2+}." J Membr Biol 159(3): 179-185.

Sitsapesan, R. and A. J. Williams (1997). "Regulation of current flow through ryanodine receptors by luminal Ca^{2+}." J. Memb. Biol. 159(3): 179-185.

Smith, J. S., R. Coronado, et al. (1986). "Single channel measurements of the calcium release channel from skeletal muscle sarcoplasmic reticulum. Activation by Ca^{2+} and ATP and modulation by Mg^{2+}." J Gen Physiol 88: 573-588.

Smith, J. S., R. Coronado, et al. (1986). "Single channel measurements of the calcium release channel from skeletal muscle sarcoplasmic reticulum. Activation by Ca^{2+} and ATP and modulation by Mg^{2+}." J. Gen. Physiol. 88: 573-588.

Smith, J. S., T. Imagawa, et al. (1988). "Purified ryanodine receptor from rabbit skeletal muscle is the calcium-release channel of sarcoplasmic reticulum." J Gen Physiol 92(1): 1-26.

Smith, J. S., T. Imagawa, et al. (1988). "Purified ryanodine receptor from rabbit skeletal muscle is the calcium-release channel of sarcoplasmic reticulum." J. Gen. Physiol. 92: 1-26.

Soeller, C. and M. B. Cannell (1997). "Numerical simulation of local calcium movements during L-type calcium channel gating in the cardiac diad." Biophys J 73(1): 97-111.

Soeller, C. and M. B. Cannell (2004). "Analysing cardiac excitation-contraction coupling with mathematical models of local control." Prog Biophys Mol Biol 85(2-3): 141-162.

Soeller, C., D. Crossman, et al. (2007). "Analysis of ryanodine receptor clusters in rat and human cardiac myocytes." Proc Natl Acad Sci USA 104(38): 14958-14963.

Song, L. S., Y. Pi, et al. (2005). "Paradoxical cellular Ca2+ signaling in severe but compensated canine left ventricular hypertrophy." Circ Res 97(5): 457-464.

Song, L. S., E. A. Sobie, et al. (2006). "Orphaned ryanodine receptors in the failing heart." Proc Natl Acad Sci U S A 103(11): 4305-4310.

Sorrentino, V. and P. Volpe (1993). "Ryanodine receptors: how many, where and why?" Trends. Pharmacol. Sci. 14(3): 98-103.

Stange, M., L. Xu, et al. (2003). "Characterization of recombinant skeletal muscle (Ser-2843) and cardiac muscle (Ser-2809) ryanodine receptor phosphorylation mutants." J. Biol. Chem. 278(51): 51693-51702.

Studer, R., H. Reinecke, et al. (1994). "Gene expression of the cardiac Na(+)-Ca2+ exchanger in end-stage human heart failure." Circ Res 75(3): 443-453.

Sun, J., C. Xin, et al. (2001). "Cysteine-3635 is responsible for skeletal muscle ryanodine receptor modulation by NO." Proc. Natl. Acad. Sci. U.S.A. 98(20): 11158-11162.

Swynghedauw, B. (1986). "Developmental and functional adaptation of contractile proteins in cardiac and skeletal muscles." Physiol Rev 66(3): 710-771.

Takeshima, H., S. Komazaki, et al. (2000). "Junctophilins: a novel family of junctional membrane complex proteins." Mol Cell 6(1): 11-22.

Tanaka, H., F. A. Dinenno, et al. (2000). "Aging, habitual exercise, and dynamic arterial compliance." Circulation 102(11): 1270-1275.

Tanaka, M., T. Ozawa, et al. (1986). "Apparent cooperativity of Ca2+ binding associated with crystallization of Ca2+-binding protein from sarcoplasmic reticulum." Arch Biochem Biophys 251(1): 369-378.

Terentyev, D., I. Gyorke, et al. (2008). "Redox modification of ryanodine receptors contributes to sarcoplasmic reticulum Ca2+ leak in chronic heart failure." Circ Res 103(12): 1466-1472.

Terentyev, D., S. Viatchenko-Karpinski, et al. (2007). "Protein protein interactions between triadin and calsequestrin are involved in modulation of sarcoplasmic reticulum calcium release in cardiac myocytes." J Physiol 583(Pt 1): 71-80.

Tijskens, P., L. R. Jones, et al. (2003). "Junctin and calsequestrin overexpression in cardiac muscle: the role of junctin and the synthetic and delivery pathways for the two proteins." J Mol Cell Cardiol 35(8): 961-974.

Timerman, A. P., E. Ogunbumni, et al. (1993). "The calcium release channel of sarcoplasmic reticulum is modulated by FK-506-binding protein. Dissociation and reconstitution of FKBP-12 to the calcium release channel of skeletal muscle sarcoplasmic reticulum." J Biol Chem 268(31): 22992-22999.

Timerman, A. P., H. Onoue, et al. (1996). "Selective binding of FKBP12.6 by the cardiac ryanodine receptor." J Biol Chem 271(34): 20385-20391.

Timerman, A. P., G. Wiederrecht, et al. (1995). "Characterization of an exchange reaction between soluble FKBP-12 and the FKBP.ryanodine receptor complex. Modulation by FKBP mutants deficient in peptidyl-prolyl isomerase activity." J Biol Chem 270(6): 2451-2459.

Tinker, A., A. R. Lindsay, et al. (1992). "A model for ionic conduction in the ryanodine receptor channel of sheep cardiac muscle sarcoplasmic reticulum." J. Gen. Physiol. 100: 495-517.

Tinker, A. and A. J. Williams (1992). "Divalent cation conduction in the ryanodine receptor channel of sheep cardiac muscle sarcoplasmic reticulum." J. Gen. Physiol. 100: 479-493.

Toischer, K., A. G. Rokita, et al. (2010). "Differential cardiac remodeling in preload versus afterload." Circulation 122(10): 993-1003.

Tomaselli, G. F. and D. P. Zipes (2004). "What causes sudden death in heart failure?" Circ. Res. 95(8): 754-763.

Towbin, H., T. Staehelin, et al. (1992). "Electrophoretic transfer of proteins from polyacrylamide gels to nitrocellulose sheets: procedure and some applications. 1979." Biotechnology 24: 145-149.

Tripathy, A. and G. Meissner (1996). "Sarcoplasmic reticulum lumenal Ca^{2+} has access to cytosolic activation and inactivation sites of skeletal muscle Ca^{2+} release channel." Biophys J 70: 2600-2615.

Tripathy, A. and G. Meissner (1996). "Sarcoplasmic reticulum lumenal Ca^{2+} has access to cytosolic activation and inactivation sites of skeletal muscle Ca^{2+} release channel." Biophys. J. 70: 2600-2615.

Tripathy, A., L. Xu, et al. (1995). "Calmodulin activation and inhibition of skeletal muscle Ca^{2+} release channel (ryanodine receptor)." Biophys. J. 69: 106-119.

Tsien, R. Y. (1980). "New calcium indicators and buffers with high selectivity against magnesium and protons: design, synthesis, and properties of prototype structures." Biochemistry 19(11): 2396-2404.

Uchinoumi, H., M. Yano, et al. "Catecholaminergic polymorphic ventricular tachycardia is caused by mutation-linked defective conformational regulation of the ryanodine receptor." Circ Res 106(8): 1413-1424.

Valdivia, H. H., J. H. Kaplan, et al. (1995). "Rapid adaptation of cardiac ryanodine receptors: Modulation by Mg^{2+} and Phosphorylation." Science 267: 1997-2000.

Valverde, R. H., G. G. Tortelote, et al. (2005). "Ca2+/calmodulin-dependent protein kinase II is an essential mediator in the coordinated regulation of electrocyte Ca2+-ATPase by calmodulin and protein kinase A." J Biol Chem 280(34): 30611-30618.

van Oort, R. J., M. D. McCauley, et al. (2010). "Ryanodine receptor phosphorylation by calcium/calmodulin-dependent protein kinase II promotes life-threatening ventricular arrhythmias in mice with heart failure." Circulation 122(25): 2669-2679.

Venetucci, L. A., A. W. Trafford, et al. (2007). "Increasing ryanodine receptor open probability alone does not produce arrhythmogenic calcium waves: threshold sarcoplasmic reticulum calcium content is required." Circ Res 100(1): 105-111.

Vetter, S. W. and E. Leclerc (2003). "Novel aspects of calmodulin target recognition and activation." Eur J Biochem 270(3): 404-414.

Voit, T., O. Krogmann, et al. (1988). "Emery-Dreifuss muscular dystrophy: disease spectrum and differential diagnosis." Neuropediatrics 19(2): 62-71.

Walker, C. A. and F. G. Spinale (1999). "The structure and function of the cardiac myocyte: a review of fundamental concepts." J Thorac Cardiovasc Surg 118(2): 375-382.

Wang, R., W. Chen, et al. (2007). "Localization of an NH(2)-terminal disease-causing mutation hot spot to the "clamp" region in the three-dimensional structure of the cardiac ryanodine receptor." J Biol Chem 282(24): 17785-17793.

Wang, S., W. R. Trumble, et al. (1998). "Crystal structure of calsequestrin from rabbit skeletal muscle sarcoplasmic reticulum." Nat Struct Biol 5(6): 476-483.

Wang, S. Q., M. D. Stern, et al. (2004). "The quantal nature of Ca^{2+} sparks and in situ operation of the ryanodine receptor array in cardiac cells." Proc. Natl. Acad. Sci U S A 101(11): 3979-3984.

Watanabe, H. and B. C. Knollmann (2011). "Mechanism underlying catecholaminergic polymorphic ventricular tachycardia and approaches to therapy." J Electrocardiol 44(6): 650-655.

Wehrens, X. H., S. E. Lehnart, et al. (2003). "FKBP12.6 deficiency and defective calcium release channel (ryanodine receptor) function linked to exercise-induced sudden cardiac death." Cell 113(7): 829-840.

Wehrens, X. H., S. E. Lehnart, et al. (2005). "Intracellular calcium release and cardiac disease." Annu Rev Physiol 67: 69-98.

Wehrens, X. H., S. E. Lehnart, et al. (2005). "Ryanodine receptor-targeted anti-arrhythmic therapy." Ann N Y Acad Sci 1047: 366-375.

Wehrens, X. H., S. E. Lehnart, et al. (2006). "Ryanodine receptor/calcium release channel PKA phosphorylation: a critical mediator of heart failure progression." Proc Natl Acad Sci U S A 103(3): 511-518.

Wehrens, X. H., S. E. Lehnart, et al. (2004). "Protection from cardiac arrhythmia through ryanodine receptor-stabilizing protein calstabin2." Science 304(5668): 292-296.

Wehrens, X. H., S. E. Lehnart, et al. (2004). "Ca^{2+}/calmodulin-dependent protein kinase II phosphorylation regulates the cardiac ryanodine receptor." Circ Res 94(6): e61-70.

Wehrens, X. H., S. E. Lehnart, et al. (2004). "Ca^{2+}/calmodulin-dependent protein kinase II phosphorylation regulates the cardiac ryanodine receptor." Circ Res 94(6): 61-70.

Wei, S. K., J. F. Quigley, et al. (2002). "Cytosolic free magnesium modulates Na/Ca exchange currents in pig myocytes." Cardiovasc Res 53(2): 334-340.

Wei, S. K., J. F. Quigley, et al. (2002). "Cytosolic free magnesium modulates Na/Ca exchange currents in pig myocytes." Cardiovasc. Res. 53(2): 334-340.

Weitzenblum, E. (1994). "The pulmonary circulation and the heart in chronic lung disease." Monaldi Arch Chest Dis 49(3): 231-234.

White, M., F. Yanowitz, et al. (1995). "Role of beta-adrenergic receptor downregulation in the peak exercise response in patients with heart failure due to idiopathic dilated cardiomyopathy." Am J Cardiol 76(17): 1271-1276.

White, R. E. and H. C. Hartzell (1988). "Effects of intracellular free magnesium on calcium current in isolated cardiac myocytes." Science 239(4841 Pt 1): 778-780.

Wier, W. G. (2007). "Gain and cardiac E-C coupling: revisited and revised." Circ Res 101(6): 533-535.

Winkelmann, B. R. and H. Leinberger (1987). "Life-threatening flecainide toxicity. A pharmacodynamic approach." Ann Intern Med 106(6): 807-814.

Witcher, D. R., R. J. Kovacs, et al. (1991). "Unique phosphorylation site on the cardiac ryanodine receptor regulates calcium channel activity." J. Biol. Chem. 266: 11144-11152.

Xiao, B., M. T. Jiang, et al. (2005). "Characterization of a novel PKA phosphorylation site, serine-2030, reveals no PKA hyperphosphorylation of the cardiac ryanodine receptor in canine heart failure." Circ Res 96(8): 847-855.

Xiao, B., C. Sutherland, et al. (2004). "Protein kinase A phosphorylation at serine-2808 of the cardiac Ca2+-release channel (ryanodine receptor) does not dissociate 12.6-kDa FK506-binding protein (FKBP12.6)." Circ Res 94(4): 487-495.

Xiao, B., X. Tian, et al. (2007). "Functional Consequence of Protein Kinase A-dependent Phosphorylation of the Cardiac Ryanodine Receptor: SENSITIZATION OF STORE OVERLOAD-INDUCED Ca2+ RELEASE." J Biol Chem 282(41): 30256-30264.

Xiao, B., G. Zhong, et al. (2006). "Ser-2030, but not Ser-2808, is the major phosphorylation site in cardiac ryanodine receptors responding to protein kinase A activation upon beta-adrenergic stimulation in normal and failing hearts." Biochem. J. 396(1): 7-16.

Xiao, J., X. Tian, et al. (2007). "Removal of FKBP12.6 does not alter the conductance and activation of the cardiac ryanodine receptor or the susceptibility to stress-induced ventricular arrhythmias." J Biol Chem 282(48): 34828-34838.

Xiao, R. P., H. H. Valdivia, et al. (1997). "The immunophilin FK506-binding protein modulates Ca2+ release channel closure in rat heart." J. Physiol. (Lond.) 500: 343-354.

Xin, H. B., T. Senbonmatsu, et al. (2002). "Oestrogen protects FKBP12.6 null mice from cardiac hypertrophy." Nature 416(6878): 334-338.

Xu, L., J. P. Eu, et al. (1998). "Activation of the cardiac calcium release channel (ryanodine receptor) by poly-S-nitrosylation." Science 279(5348): 234-237.

Xu, L., J. P. Eu, et al. (1998). "Activation of the cardiac calcium release channel (ryanodine receptor) by poly-S-nitrosylation." Science 279(5348): 234-237.

Xu, L. and G. Meissner (1998). "Regulation of cardiac muscle Ca^{2+} release channel by sarcoplasmic reticulum lumenal Ca^{2+}." Biophys. J. 75(5): 2302-2312.

Xu, L. and G. Meissner (2004). "Mechanism of calmodulin inhibition of cardiac sarcoplasmic reticulum Ca2+ release channel (ryanodine receptor)." Biophys J 86(2): 797-804.

Xu, L. and G. Meissner (2004). "Mechanism of calmodulin inhibition of cardiac sarcoplasmic reticulum Ca2+ release channel (ryanodine receptor)." Biophys. J. 86(2): 797-804.

Xu, X., M. Yano, et al. (2010). "Defective calmodulin binding to the cardiac ryanodine receptor plays a key role in CPVT-associated channel dysfunction." Biochem Biophys Res Commun 394(3): 660-666.

Yamaguchi, N., A. Chakraborty, et al. (2013). "Cardiac hypertrophy associated with impaired regulation of cardiac ryanodine receptor by calmodulin and S100A1." Am J Physiol Heart Circ Physiol 305(1): H86-94.

Yamaguchi, N. and G. Meissner (2007). "Does Ca2+/calmodulin-dependent protein kinase deltac activate or inhibit the cardiac ryanodine receptor ion channel?" Circ Res 100(3): 293-295.

Yamaguchi, N., N. Takahashi, et al. (2007). "Early cardiac hypertrophy in mice with impaired calmodulin regulation of cardiac muscle Ca release channel." J. Clin. Invest. 117(5): 1344-1353.

Yamamoto, T., R. El-Hayek, et al. (2000). "Postulated role of interdomain interaction within the ryanodine receptor in Ca^{2+} channel regulation." J. Biol. Chem. 275(16): 11618-11625.

Yamamoto, T. and N. Ikemoto (2002). "Peptide probe study of the critical regulatory domain of the cardiac ryanodine receptor." Biochem. Biophys. Res. Commun. 291(4): 1102-1108.

Yamamoto, T., M. Yano, et al. (2008). "Identification of target domains of the cardiac ryanodine receptor to correct channel disorder in failing hearts." Circulation 117(6): 762-772.

Yang, Y., T. Guo, et al. (2014). "Cardiac myocyte Z-line calmodulin is mainly RyR2-bound, and reduction is arrhythmogenic and occurs in heart failure." Circ Res 114(2): 295-306.

Yano, M. (2005). "[Abnormal ryanodine receptor function in heart failure]." Nippon Yakurigaku Zasshi 126(6): 372-376.

Yano, M. (2008). "Ryanodine receptor as a new therapeutic target of heart failure and lethal arrhythmia." Circ J 72(4): 509-514.

Yano, M., S. Kobayashi, et al. (2003). "FKBP12.6-mediated stabilization of calcium-release channel (ryanodine receptor) as a novel therapeutic strategy against heart failure." Circulation 107(3): 477-484.

Yano, M., S. Okuda, et al. (2005). "Correction of defective interdomain interaction within ryanodine receptor by antioxidant is a new therapeutic strategy against heart failure." Circulation 112(23): 3633-3643.

Yano, M., K. Ono, et al. (2000). "Altered stoichiometry of FKBP12.6 versus ryanodine receptor as a cause of abnormal Ca(2+) leak through ryanodine receptor in heart failure." Circulation 102(17): 2131-2136.

Yano, M., T. Yamamoto, et al. (2005). "Abnormal ryanodine receptor function in heart failure." Pharmacology & therapeutics 107(3): 377-391.

Zahradnik, I., S. Gyorke, et al. (2005). "Calcium activation of ryanodine receptor channels--reconciling RyR gating models with tetrameric channel structure." J Gen Physiol 126(5): 515-527.

Zhang, H., C. A. Makarewich, et al. (2012). "Hyperphosphorylation of the cardiac ryanodine receptor at serine 2808 is not involved in cardiac dysfunction after myocardial infarction." Circ Res 110(6): 831-840.

Zheng, M., W. Zhu, et al. (2005). "Emerging concepts and therapeutic implications of beta-adrenergic receptor subtype signaling." Pharmacol Ther 108(3): 257-268.

Zhou, Q., J. Xiao, et al. (2011). "Carvedilol and its new analogs suppress arrhythmogenic store overload-induced Ca2+ release." Nat Med 17(8): 1003-1009.

Zhou, Z. and S. L. Lipsius (1993). "Na(+)-Ca2+ exchange current in latent pacemaker cells isolated from cat right atrium." J Physiol 466: 263-285.

Zima, A. V., E. Bovo, et al. (2010). "Ca^{2+} spark-dependent and -independent sarcoplasmic reticulum Ca^{2+} leak in normal and failing rabbit ventricular myocytes." J. Physiol 588(Pt 23): 4743-4757.

Zima, A. V., E. Bovo, et al. (2010). "Ca(2)+ spark-dependent and -independent sarcoplasmic reticulum Ca(2)+ leak in normal and failing rabbit ventricular myocytes." J Physiol 588(Pt 23): 4743-4757.

Zissimopoulos, S., N. Docrat, et al. (2007). "Redox sensitivity of the ryanodine receptor interaction with FK506-binding protein." J Biol Chem 282(10): 6976-6983.

Zissimopoulos, S., N. Docrat, et al. (2007). "Redox sensitivity of the ryanodine receptor interaction with FK506-binding protein." J Biol Chem.

Zissimopoulos, S., S. Seifan, et al. (2012). "Disparities in the association of the ryanodine receptor and the FK506-binding proteins in mammalian heart." Journal of cell science 125(Pt 7): 1759-1769.